Direct Electrochemical Reduction of Gaseous Carbon Dioxide to Value Added Products: Investigations on Electrocatalysts

Thesis Submitted in Partial Fulfilment of the Requirements

for the Award of the Degree of

DOCTOR OF PHILOSOPHY

by

SURYA SINGH

Centre for the Environment

Indian Institute of Technology Guwahati

Guwahati – 781 039, Assam, India

September 2015

Dedicated to

My Parents,

who sacrificed for every small possession they could have,

for earning their biggest asset – the educated daughters…

Centre for the Environment
Indian Institute of Technology Guwahati
Guwahati – 781 039
Assam, India

DECLARATION

I do hereby declare that the matter embedded in the thesis entitled "**Direct Electrochemical Reduction of Gaseous Carbon Dioxide to Value Added Products: Investigations on Electrocatalysts**" is the result of investigations carried out by me in the Indian Institute of Technology Guwahati, Guwahati – 781 039, Assam, under the supervision of Dr. Anil Verma, Department of Chemical Engineering, IIT Delhi and Dr. Chandan Mukherjee, Department of Chemistry, IIT Guwahati, and is submitted to the Indian Institute of Technology Guwahati, Guwahati – 781 039, Assam, India, for the award of the degree of Doctor of Philosophy.

In keeping with the general practice of reporting scientific observations, due acknowledgements have been given wherever the work described is based on the findings of other investigators.

(Surya Singh)
Roll No. 11615202
Centre for the Environment
Indian Institute of Technology Guwahati
Guwahati – 781 039, Assam
India

Centre for the Environment
Indian Institute of Technology Guwahati
Guwahati – 781 039
Assam, India

CERTIFICATE

It is certified that the work contained in the thesis entitled "**Direct Electrochemical Reduction of Gaseous Carbon Dioxide to Value Added Products: Investigations on Electrocatalysts**", submitted by Ms. Surya Singh, for the award of the degree of Doctor of Philosophy, has been carried out under our supervision and this work has not been submitted elsewhere for the award of any degree.

(Dr. Anil Verma)
Associate Professor
Department of Chemical Engineering
Indian Institute of Technology Delhi
Hauz Khas, New Delhi – 110 016
India

(Dr. Chandan Mukherjee)
Associate Professor
Department of Chemistry
Indian Institute of Technology Guwahati
Guwahati – 781 039, Assam
India

PREFACE

The aim and purpose of this thesis derive their origin from the environmental science and engineering, whereas, the approach to tackle the challenges is a combination of chemical engineering and chemistry. The thesis tries to find the solution for the two major problems of today's world – the increasing CO_2 concentration in the atmosphere, and the reducing conventional fossil fuels. The idea is to use CO_2 itself to convert into fuels using non-conventional energy sources, so that, both the problems can be targeted simultaneously. The thesis explains in detail about the urgency of the problem and accordingly, the investigations have been made to understand and report the various know-how of the process, along with the development of new and effective electrocatalysts for the conversion of CO_2 into fuel kind of products.

The basic knowledge about the current situation of the atmosphere is dealt in chapter 1, along with the details of the process of electrochemical reduction of CO_2 for the production of fuel kind of products. The chapter also discusses the issues which need to be addressed for the successful application of this process.

To understand the present status of the electrochemical reduction of CO_2, a thorough literature survey is carried out emphasizing the use of electrocatalysts and the details are presented in chapter 2. This chapter critically analyzes the various advantages and shortcomings of the already employed electrocatalysts, which helps to focus on the thrust areas which need clarification and know-how where further developments can be done. Based on the literature survey, objective of the present research work is formulated and given at the end of the chapter 2.

Chapter 3 discusses the various experimental procedures, which are common throughout the thesis. The principle of the various characterization techniques, both *ex-situ* and *in-situ*, are discussed along with the procedure to perform them. The chapter also illustrates the developed experimental set-up

and electrochemical reactor to perform the experimental work. The method of calculation of Faradaic efficiency, rate of the reaction, and selectivity is also discussed in detail.

Chapter 4 is dedicated to the results and discussions of the pure metals which have been chosen as the electrocatalysts for the electrochemical reduction of gaseous CO_2. The chapter includes the synthesis and characterization of the pure metal electrocatalysts (cathode), along with the synthesis, treatment, and characterization of the anode and solid polymer electrolyte. The chapter is very important as it also describes about the catalytic activity protocol which is required in light of the various mismatch and confusing results presented by various literature during cyclic voltammetry experiments. In order to clarify and clear the doubts, the protocol was developed and used for the initial screening of the electrocatalysts in all the further chapters. At the end, the chapter generalizes various results and proposes a layout of work for the subsequent chapters.

Based on the results obtained in chapter 4, it is found necessary to treat the various pure metals in some way so that their efficiency can be increased. This is done through the formation of oxides of all the pure metals, which is dealt in chapter 5. The chapter clarifies the reason for the better performance of some of the oxides over their pure metal counterparts. The chapter also covers the comparison of the metal oxides with the metals at the end. However, in cases where the oxides could not be able to improve the performance, a new treatment method is proposed at the end of the chapter.

To have an insight of the science behind the metal complexes, a ligand is synthesized in which metals are incorporated. The syntheses and characterizations of these metal complexes are detailed in chapter 6. These metal complexes are employed as the electrocatalysts and the Faradaic efficiency, and selectivity are calculated for the direct electrochemical reduction of gaseous CO_2. A reaction mechanism is also proposed for the CO_2 reduction process using these metal complexes. At the end of the chapter, the efficiency of the metal complexes is compared with the metals and found to be far better than their pure metal counterparts.

Chapter 7 describes about another class of electrocatalyst *viz.* bimetallic electrocatalyst which is investigated for the CO_2 electroreduction. This was the second attempt to improve the catalytic performance of the cobalt metal using silver metal. The synthesis and relevant characterizations for the bimetallic electrocatalyst are detailed in the chapter. The performance of this bimetallic electrocatalyst is quantified in terms of Faradaic efficiency, reaction rate, and selectivity. The comparison is also made at the end of the chapter to showcase the better performance of the bimetallic electrocatalyst over the pure metal.

All the results in totality are summarized in the chapter 8. The chapter also includes the future scope of work in this field. It will probably help the new researchers to formulate their objectives for working in the field of electrochemical reduction of CO_2 in order to improve the performance of the process upto a next level.

In this thesis, I have attemped to include and refer all the significant literature available, which has been relevant to the work presented here. However, the unrelated scientific reports have not been considered in the thesis. I have tried to shape the thesis in a manner so that it can be proved beneficial for the new researchers in understanding the role of various electrocatalysts in the field of direct electrochemical reduction of gaseous CO_2, and to formulate and design better electrocatalysts for the further progress of dERC.

(Surya Singh)
Centre for the Environment
IIT Guwahati

A word of gratitude

Today, when I look back into my life, it feels that no road is too tough to be walked on. With the guidance and encouragement of elders & well-wishers, and hard work; impossible can also be turned into possible. For every Indian student, studying at IIT is a dream come true and the same for me. As a doctoral student, it was a wonderful but at the same time, a challenging experience to be at IIT Guwahati. But in all these years which have been spent at IITG, lots of people moulded me into a way that I am today. It was nearly impossible to accomplish my doctoral studies without the help and inspiration extended by these personalities.

Although it is always difficult to translate the feelings of regards and reverence into reality, yet it is detectable when I execute my sense of profound respect to my supervisors Dr. Anil Verma and Dr. Chandan Mukherjee, for their sagacious guidance, judicious planning, erudite suggestions, unstinted co-operation, and sustained encouragement during the course of this investigation. I admire their acuity in planning the project and immense ability for reasoning. I am fortunate to work with Dr. Anil Verma as he made me confident enough to pursue a research work in an area which I was not familiar with even a bit. Since the beginning of my research career, he mentored me and always tried to bring out best in me. He made me capable enough to think and discover beyond the usual norms. Besides being an intellectual supervisor, he is also a very nice and humble human being. I truly admire him for his patient attitude in all circumstances and I respect him for inspiring me in these many ways. I feel myself privileged enough for having Dr. Chandan Mukherjee as my co-supervisor. I greatly admire his keen interest in fruitful discussions with students, his punctuality, and his sense of getting perfection in everything. He always helped me in every possible way and has given ample time for the discussions which inculcated in me the ability to explore. I owe a lot more than words at my command can convey.

I feel honoured to express my gratitude to my doctoral committee members, Dr. Vimal Katiyar, Dr. Lal Mohan Kundu, and Dr. Amit Kumar, for their interest in my work and fruitful inputs time to time which helped me a lot to improve. I must thank Prof. Gopal Das, Head of the Centre for the Environment, for encouragement and advices which helped me to keep moving on and accomplish the work in appropriate time. I also thank Prof. Prabirkumar Saha for his help and support during this work. I am highly thankful to the Dean of Students' Affairs, IIT Delhi (Prof. Shyam K. Gupta), for providing me hostel accommodation and other necessary facilities during my academic stay in IIT Delhi.

I am deeply indebted to Prof. Vijay S. Moholkar, Head of the Chemical Engineering Department (IITG), and Prof. Arun Chattopadhyay, Head of the Chemistry Department (IITG), for allowing me to avail various facilities in the respective departments. Help extended by Central Instruments Facility of IIT Guwahati is deeply acknowledged for giving the opportunity to use some of the world class instrumentation facilities. I am also thankful to all the technical and non-technical staff of Centre for the Environment (Dr. Deepmoni Deka, Mr. Partha P. Bakal, Mr. Rupinder Singh, Mr. Rajiv Gogoi), Department of Chemical Engineering (Dr. Lukumoni

Borah, Mr. Prasun Bhattacharjee, Mr. Debajit Borah, Mr. Kaustavmoni Deka), and Department of Chemistry (Dr. Babulal Das) for helping me in all the ways and at all the times.

I sincerely thank my labmates, Dr. Lepakshi Barbora, Dr. Avijit Ghosh, Dr. Leela M. Aeshala, Dr. Rajeev K. Gautam, Dr. Samir Ghorai, Ms. Bedika Phukan, Mr. Manas K. Mondal, Ms. Richa Rakshit, Mr. V. Shyam K. Yadav, Mr. Th. Sudesh K. Raunija, Mr. Divyanshu Arya, and Mr. Karan Malik for sharing their experiences and helping in various lab activities which helped a lot in better understanding of the subject. I would like to express my myriads of inexpressible thanks and immense gratefulness to my friends and well wishers who always supported me and made me cheerful in the moments of despair and dissappointments. Ms. Neelima Tripathi deserves a special mention here for being a nice, loving, and understanding friend. She has always inspired me with her way to approach any difficult situation, and surely, for making every small occasion so special for me that I will cherish those sweet memories throughout my life. I especially thank her for tolerating me even in times of acute frustation, and for being non-interfering, yet the most supportive friend.

I greatly acknowledge IIT Guwahati for the doctoral fellowship. I must acknowledge Department of Science & Technology (DST), Government of India, for the research funding (Principal investigator – Dr. Anil Verma) under its National Program on Carbon Sequestration Research (project grant number DST/IS-STAC/CO_2-SR-139/12(G)).

This long journey would not have completed without the blessings, endless love, and support from my family. I dedicate my every achievement and accomplishment to my father (Sri Amar Singh), my mother (Smt. Geeta Singh), and my elder sister (Dr. Divya Singh). Words are unable to express my feelings for those who nurtured me, loved me, advised me, supported me, tolerated me, sacrificed for me, and prayed for me every single day so that I can live my life happily. I feel myself the luckiest person for having such a lovely family.

Above all I thank the Almighty God, for bestowing me with the wonderful life and appropriate circumstances in which I could flourish and walk through the path of learning. I thank the Supreme Power of the universe for giving me the strength to rise whenever I fell, and ability to learn from my mistakes. I also thank Him for blessing me with a lovely family and showing mercy on me for my mistakes.

(Surya Singh)
Centre for the Environment
IIT Guwahati

ABSTRACT

To find the solution for many of the environmental problems is need of the hour. Therefore, the research community all over the world is taking up environmental challenges with the hope to maintain the sustainability and integrity of the environment for the future generations. To deal with the increasing CO_2 concentration in the atmosphere is one such challenge which needs to be addressed judiciously. Hence, this thesis aims to focus over this subject for the mitigation of CO_2 through its utilization. Electrochemical reduction of CO_2 has been found to be a suitable technology which not only helps in utilization of the CO_2, but at the same time produce such reaction products which have the high calorific value. Thus, these reaction products can be used as fuels, which will also help to combat the problem of decreasing fossil fuel reserves. With this aim, the CO_2 is electrocatalytically reduced and converted into a variety of products.

The thesis begins with the study of a few metals which are chosen to check their reactivity for the direct electrochemical reduction of gaseous CO_2 (dERC). Four metals, namely, Cu, Zn, Ni, and Co are used after their electroplating over the gas diffusion layer. These metals are tested in electrochemical reactor after being characterized through *in-situ* and *ex-situ* methods. The *in-situ* methods involved characterization using cyclic voltammetry. However, it is found that cyclic voltammetry is not able to determine clearly about the activity of the electrocatalysts for CO_2 reduction. Moreover, contradictory literature results are available. Hence, the development of a catalytic activity protocol is undertaken which can help in the screening of the electrocatalysts without undergoing full cell reaction. The protocol is devised with the aim to ease the judgement for the selection of electrocatalysts, since the full cell reaction is too cumbersome and time consuming. Therefore, protocol helps to select useful electrocatalysts from the group of many at the initial stage itself. The *ex-situ* characterizations included XRD, SEM, and EDX techniques. These electroplated metals served the purpose of cathode in the electrochemical reactor. For the anode, Pt/C is deposited

over the gas diffusion layer through spraying technique. Nafion-117 is used as the solid polymer electrolyte, which provides the passage for H^+ ions from anode to cathode. Gaseous CO_2 is directly fed into the reactor at the cathode side, while water is fed at the anode side of the reactor. The electrical energy is supplied to the reactor, *in lieu of* the renewable energy which helps to reduce the CO_2 into variety of products. Not all the chosen metals proved to be very reactive for CO_2 electroreduction, but some metals show the potential to be improved. All the metals resulted in the formation of CH_4 and CO. Cu is found to be quite selective for CH_4 formation while Zn is found to be selective for CO formation. These 4 metals can be arranged in decreasing trend of Faradaic efficiency as Co > Zn > Cu > Ni. Moreover, the Faradaic efficiency is not much appreciable in any of the cases and hence it is necessary to introduce some changes in the physical or chemical form for increasing the Faradaic efficiency of these metals towards dERC. Various means have been tried to improve the performance such as formation of metal oxide, metal complex, and bimetallic electrocatalyst, based on individual merit of these moieties. Metal oxide is chosen because of its basic nature, which will enhance the adsorption of CO_2 (Lewis acid) on the surface. Occupation of more catalytic sites by CO_2 will eventually help in the increased reduction of CO_2. The reason for studying metal complexes is that the redox properties of these moieties help in the efficient transfer of electrons between CO_2 and electrocatalysts. Increased rate of electron transfer leads to the faster kinetics and improved electroreduction of CO_2. As far as bimetallic electrocatalyst is concerned, the aim is to study the effect of the combination of metals for the CO_2 electroreduction.

Metal oxides are synthesized for all the 4 metals – CuO, ZnO, NiO, and Co_3O_4 using suitable methods and characterized using XRD, FTIR, BET, FESEM, and EDX techniques. The results confirmed the physical nature and formation of the synthesized electrocatalysts. *In-situ* characterizations are also carried out using cyclic voltammetry and catalytic activity protocol tests for CuO, ZnO, and Co_3O_4. However, the electrochemical behaviour of NiO is not studied, because no suitable solvent could be found for the preparation of its catalytic ink. The 3 metal oxide electrocatalysts are found to be

suitable for electrochemical reduction of CO_2 which led to their further studies using full electrochemical reactor. As expected, CuO proved to be very efficient electrocatalyst with the Faradaic efficiency of CH_4 formation as 60% at 2 V. CuO also resulted in the formation of CO and C_2H_4. On the other hand, the efficiency of ZnO is also found good but to a lesser extent as compared to CuO. ZnO results in the formation of either CH_4 or CO depending upon applied voltage, with Faradaic efficiency of 18.8% and 10.34%, respectively. An unfavorable feature of ZnO is its unstable nature in CO_2 electroreduction reaction conditions. ZnO gets converted into Zn electrochemically during the reaction and hence it is difficult to assess the overall performance and stability of ZnO for ERC. As far as Co_3O_4 is concerned, it is not better than Co; rather its efficiency is lesser than Co. Total Faradaic efficiency for CO_2 electroreduction using Co_3O_4 is 4.16% at 2 V. The exact reason for its poor performance could not be elucidated, but it can be said that the variable oxidation states in reducing medium may be a reason for the under-performance of this electrocatalyst. Overall, it can be said that the oxides of Cu and Zn have improved the CO_2 electroreduction performance.

The next aim has been the study of metal complexes and hence, salen ligand is synthesized because of its proven efficacy as catalyst in various other reactions. Since, oxide of Ni could not be studied for dERC, Ni is introduced in salen ligand to form Ni salen complex. Further, to explore more about Cu, it is also used to form Cu salen complex. These two metal complexes along with the salen ligand are characterized using FTIR, NMR, HR-MS, elemental analysis, and electrochemical tests (cyclic voltammetry and the protocol). The characterizations confirmed the successful synthesis of metal complexes and their activity towards dERC. The full cell studies show dramatic increase in the Faradaic efficiency of Ni and Cu salen complex as compared to pure Ni and Cu metals. The total Faradaic efficiency for Ni and Cu salen complex is found to be 74% and 25%, respectively. Both hydrocarbons (CH_4, C_2H_4, and C_2H_6) and CO are formed in appropriate quantities. Another striking feature shown by these metal complexes is their ability to reduce the overpotential required in the reaction to a great extent. A total of 0.5 V reduction in overpotential is achieved for both the metal

complexes. Based on the outcome of the study, a reaction mechanism is proposed which states that the interconversion of the oxidation states of the metals introduced plays a major role in the overall mechanism of CO_2 electroreduction. In the metal complexes, metals (Ni and Cu) remain in +2 state. During the CO_2 reduction process, Ni(II) and Cu(II) converts to Ni(I) and Cu(I) species, respectively. These species further bind with CO_2 and lead to its reduction into hydrocarbons and CO. It can be said that the metal complexes proved to be very effective electrocatalysts for CO_2 reduction.

To study the effect of the combination of two metals over the CO_2 electroreduction reaction, a new class of electrocatalyst is synthesized for dERC. The bimetallic electrocatalyst, Co-Ag, is synthesized and characterized using XRD, BET, FESEM, TEM, and EDX techniques. The characterizations indicated that the synthesized electrocatalyst is a mixture of Co and Ag metals. The cyclic voltammetry studies and catalytic activity protocol suggested that the electrocatalyst is able to reduce the CO_2 in electrochemical environment. Product identification and quantification revealed the formation of CH_4, CO, and C_2H_4. The total Faradaic efficiency is found to be 28% at 2 V. The efficiency is found to be improved over the Co metal. Another advantage of bimetals is lowering down of the overpotential, as compared to Co. The peculiar feature of the electrocatalyst is its ability to form the hydrocarbons, as none of the chosen metal was selective to form hydrocarbons in its individual state. The reason of this is attributed to the change in binding energy levels of the involved metals with the intermediate species of the reaction. The altered binding energy levels helped to hold the intermediate species of the reaction upto the appropriate time so that it can react further to form hydrocarbon moieties. The selectivity towards CH_4 formation is found to be 69% at 2.3 V.

Thus, the performance of the metals, metal oxides, metal complexes, and bimetal electrocatalysts is studied for the formation of value added products from direct electrochemical reduction of CO_2.

Keywords: Bimetals; Catalytic activity protocol; Electrocatalysts; Direct electrochemical reduction of CO_2; Metal oxides; Salen metal complexes

CONTENTS

List of Tables

List of Figures

List of Schemes

List of Symbols

A	area (cm^2)
$C°$	concentration of the bulk solution ($mol \cdot L^{-1}$)
D	diffusion coefficient ($cm^2 \cdot s^{-1}$)
d	spacing between two crystal planes (Å)
$E°$	equilibrium potential (V)
F	Faraday constant ($C \cdot mol^{-1}$)
h	hour
i	current density ($mA \cdot cm^{-2}$)
n	number of moles of a particular product (mol)
Q	total charge passed during the experiment (C)
T	temperature (°C)
V	potential or voltage (V)
z	number of moles of electrons required for formation of 1 mole of a reaction product
θ	diffraction angle (°)
λ	wavelength of X-rays (cm)
υ	potential scan rate ($V \cdot s^{-1}$)

List of Abbreviations

AcN	Acetonitrile
ADB	Asian development bank
AR	Assessment report
BET	Brunauer-Emmett-Teller
BMImCl	1-butyl-3-methylimidazolium chloride
Bu_4NPF_6	Tetra(*n*-butyl)ammonium hexafluorophosphate
CA	Chronoamperometry
CCS	Carbon capture and storage
CNG	Compressed natural gas
CO_{ad}	Adsorbed carbon monoxide
CV	Cyclic voltammetry
dERC	Direct electrochemical reduction of CO_2
DMF	Dimethyl formamide
DMSO	Dimethyl sulfoxide
DoE	Department of energy
EDX	Energy dispersive X-ray spectroscopy
EIA	Energy information administration
ERC	Electrochemical reduction of CO_2
ESI-MS	Electrospray ionization mass spectroscopy
ETP	Energy technology perspectives
FCC	Face centered cubic
FESEM	Field emission scanning electron microscope
FID	Flame ionization detector

FTIR	Fourier transform infra-red
GC	Glassy carbon
GDE	Gas diffusion electrode
GDL	Gas diffusion layer
GHG	Greenhouse gases
HCP	Hexagonal closed packed
HER	Hydrogen evolution reaction
HR-MS	High resolution mass spectroscopy
IEA	International energy agency
IEO	International energy outlook
IPCC	Intergovernmental panel on climate change
IUPAC	International union of pure and applied chemistry
LPG	Liquified petroleum gas
LSV	Linear sweep voltammetry
MEA	Membrane electrode assembly
NHE	Normal hydrogen electrode
NMR	Nuclear magnetic resonance
NRC	National research council
OECD	Organization for economic co-operation and development
ppm	Parts per million
ppmv	Parts per million volume
PVA	Polyvinyl alcohol
RHE	Reversible hydrogen electrode
SEM	Scanning electron microscope
SHE	Standard hydrogen electrode

TBAP	Tetrabutylammonium peruthenate
TBAH	Tetra-*n*-butylammoniumhexafluorophosphate
$TBAPF_6$	Tetrabutylammonium hexafluorophosphate
TCD	Thermal conductivity detector
TEM	Transmission electron microscope
XRD	X-ray diffractometer

1

Introduction

1.1 Background

1.2 CO_2 level in the environment

1.3 Methods of CO_2 utilization/conversion

1.4 Electrochemical reduction of CO_2 and associated issues

1.5 Electrocatalysts

Chapter 1

Introduction

Electrochemical reduction of carbon dioxide is an emerging technology aiming to utilize the CO_2, apart from providing value added products. The process is of great importance in the present scenario, where increasing CO_2 concentration and decreasing fossil fuel reserves are unavoidable. This chapter deals with the present state of environment, various methods of CO_2 utilization, and the advantages of electrochemical reduction of CO_2 in dealing with the existing environmental problems. Along with this, the chapter also figures out the challenges encountered in this field and possible approaches to overcome those challenges.

1.1 Background

The environment consists of all living and non-living things occuring naturally on the earth. All living beings are primarily made up of carbon. Apart from living beings, carbon is also a part of the ocean, air, and rocks; thus making its presence in hydrosphere, atmosphere, and lithosphere, respectively. In atmosphere, carbon is present in combined form with oxygen, namely, carbon dioxide. Carbon dioxide is an important long lived gas in the atmosphere. The amount of carbon dioxide present in the atmosphere is very modest, approximately 0.03% (300 ppm). It is a very small fraction of the total carbon inventory; still it makes huge impact over the life of the organisms. This atmospheric CO_2 is taken up by the plants in the process of photosynthesis (Figure 1.1). The natural sources of the CO_2 in the atmosphere are all the respiring organisms on the earth, volcanic eruption emissions, and release from ocean (Figure 1.1). Thus, the inflow and outflow of CO_2 remains maintained in the atmosphere. This natural flow of CO_2 in the environment through various spheres is known as carbon cycle, as shown in figure 1.1.

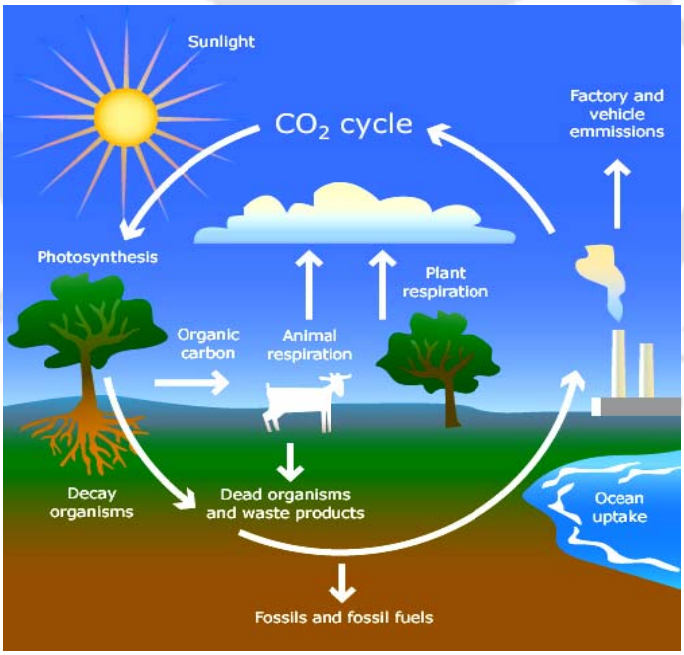

Figure 1.1 Carbon cycle in environment (*http://www.resnet-project.org/ebook/text.php?page=06.07&lang=en*)

However, if there is more inflow of CO_2 into the atmosphere, then it leads to the increased carbon balance in the atmosphere.

At the beginning of human civilization, the CO_2 concentration in the atmosphere was about 275 ppm. This is the concentration to which human civilization is adapted to the most. According to recent researches; the safe level of CO_2 for human civilization is 350 ppm (Hansen *et al.* 2008). However, with the rapid increase in the industrialization and urbanization, the anthropogenic emissions have increased to a great extent. Anthropogenic emissions include burning of fossil fuels, deforestation, industrial activities, transportation, and other activities. These emissions resulted in increased CO_2 in the atmosphere, which has reached much beyond the upper safety limit of 350 ppm, leading to green house effect. This green house effect is responsible for global warming, which ultimately results in climate change.

1.2 CO_2 level in the environment

With the beginning of 18th century, human civilization took a leap towards industrialization and increased the use of energy to a great extent. With the increase in industrial processes, the CO_2 emissions increased and crossed the upper safety limit (350 ppm) in 1985. Now the situation is such that CO_2 concentration has reached around 400 ppm. Figure 1.2 shows the increase in CO_2

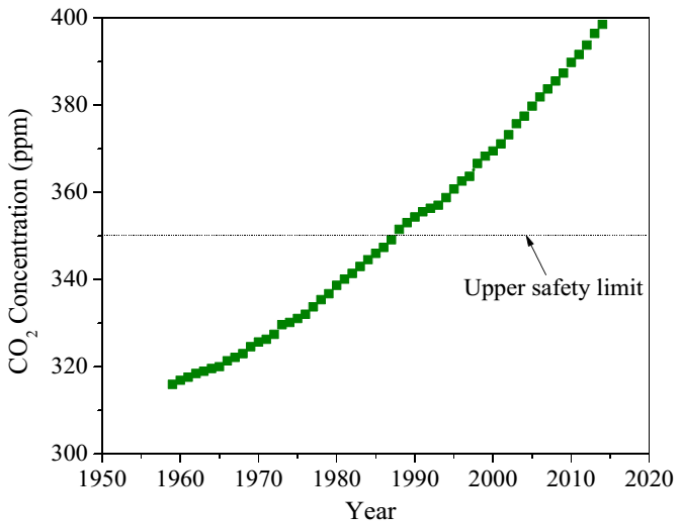

Figure 1.2 Increasing CO_2 levels in atmosphere

concentration since 1959 to 2014, as recorded at Mauna Loa observatory, Hawaii (Tans and Keeling 2015). It can be seen that, the average CO_2 concentration in 2014 was 398.55 ppm, which is far above the safety limit. As per the speculations made by the scientists, this trend will continue to rise in future. Therefore, immediate precautionary measures are required to keep the increasing CO_2 concentration in check.

In 1988, the Intergovernmental Panel on Climate Change (IPCC) recommended a set of targets to reduce anthropogenic emissions of carbon dioxide. The IPCC has issued a report declaring its certainty that human activity is resulting in pollutants that will intensify the greenhouse effect (Houghton *et al.* 1990). Later, in 1992 the Rio Earth Summit made a historic commitment to sustainable development – an economic system that promotes the health of both people and ecosystems. An outcome of this summit was the Kyoto Protocol, which recognized that climate change is a result of greenhouse gases (GHGs) created by human industrial activity. This protocol was adopted with the intension to reduce the greenhouse gases by 5% relative to 1990 levels by 2012. The time period of protocol is over but unfortunately targets could not be achieved. The world is still suffering with the fear of probable increase in temperature and its disastrous outcomes. So, today among the most important and concerning environmental issues, climate change is at the top, followed by increasing energy consumption. Since the industrial revolution began around 1750, human activities have contributed substantially to climate change by adding CO_2 and other heat trapping gases to the atmosphere. The GHGs (as recognized in Kyoto Protocol) are carbon dioxide (CO_2), methane (CH_4), nitrous oxide (N_2O), hydroflourocarbons (HFCs), perflourocarbons (PFCs), and sulphur hexaflouride (SF_6). Atmospheric CO_2 concentrations have been increased by almost 42% since pre-industrial times, from approximately 280 ppmv in the 18^{th} century to 398 ppmv in 2014. Human activities currently release over 30 billion tons of CO_2 into the atmosphere every year (NRC 2010).

Figure 1.3 (a) shows the share of various gases for total anthropogenic greenhouse gas emissions (IPCC 2007). CO_2 is responsible for about 77% of the total greenhouse gas emissions, of which ~57% is directly contributed by the use of fossil fuel in either transport sector or industrial

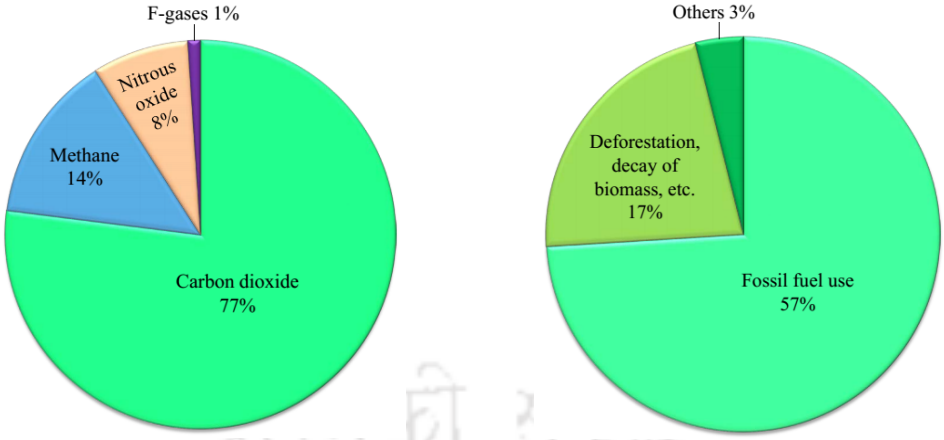

(a) (b)

Figure 1.3 (a) Global greenhouse gas emissions (F-gases include HFCs, PFCs, and SF_6), (b) Contribution of various activities for CO_2 emission

activities and rest ~20% is contributed by other activities (Figure 1.3 b). Unsustainable transportation systems also harm the environment. Transportation is now the fastest growing source of global CO_2 emissions. The transport sector, which is mostly fueled by the conventional non-renewable fossil fuels, contributes significantly in CO_2 emissions and these transport associated CO_2 emissions will be more than double by 2050 according to the Energy Technology Perspectives (IEA 2010).

There is now a growing international consensus that future targets for CO_2 reduction in the post-2012 climate policy framework will not be achieved unless CO_2 contribution from the transport sector, running on conventional fuels, in developing countries is appropriately addressed (Schipper *et al.* 2009). With 1954 million tons of CO_2 released from the consumption and combustion of fossil fuels in 2012, India is ranked 3rd in the world after the China and U.S. (IEA Statistics 2014). India's contribution to world carbon emissions is expected to increase in the coming years due to the rapid pace of urbanization, shift from non-commercial to commercial fuels, increased vehicular usage, and continued use of older and highly inefficient coal fired and fuel power plants (Singh and Singh 2008). The globally increasing CO_2 emission is resulting in

severe, pervasive, and irreversible damage to the environment. Sensing this situation, the recently released fifth assessment report (AR-5) of the IPCC states that the unrestricted use of fossil fuels should be phased out by 2100 if the world has to avoid dangerous climate change (IPCC 2014).

The increased use of transportation vehicles has given rise to another serious threat *viz.* the depletion of conventional fossil fuels. Although, the fossil fuels are renewable and their formation is continued but the rate of formation is far slower than its consumption. Thus, on one side where the world is suffering with the fear of climate change, the fossil fuels (chief energy resource of today's world) depletion has also been identified as a future challenge. The current and predicted world energy consumption is shown in figure 1.4. Over the next 25 years, it is the transportation sector where the demand of liquid fuels will increase more rapidly than in any other end-use sector, with most of the growth projected among the developing non-OECD (Organization for Economic Co-operation and Development) countries (*e.g.* India), while the utilization among the developed OECD countries may remain comparatively unchanged (Figure 1.4). The reason for more growth of energy consumption in non-OECD countries is due to the fact that demands for personal travel increase with the gains in urbanization and personal incomes (International Energy Outlook 2011). Thus it is clear that the energy requirement is continuously increasing and putting a lot of pressure on the conventional energy resources. But since the fossil fuels are limited and

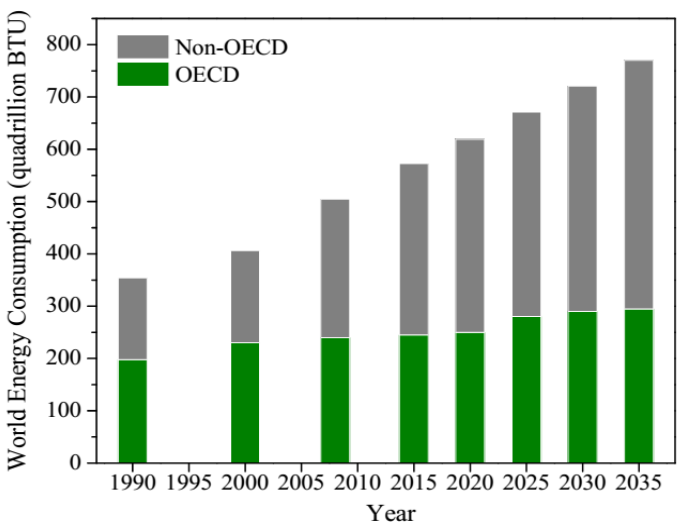

Figure 1.4 World energy consumption

also responsible for environmental issues, alternate energy sources need to be explored for sustainable energy supply.

Thus, dependency on fossil fuels has given rise to two kinds of worries: first, its linked environmental impacts, especially the climate change; and second, the depletion of the finite fossil fuel reserves. In any case, CO_2 emissions and massive use of conventional and limited resources are both sides of the same coin and should be analyzed together. There are 4 possible ways to deal with this problem:

- Decrease in fossil fuel consumption and other activities which result in CO_2 emission: In the longer term, fossil fuel power generation without carbon capture and storage (CCS) technology would need to be phased out almost entirely by 2100 (IPCC 2014).
- Effective use of technologies for reducing CO_2 emission to atmosphere: As per IPCC 5th assessment report, use of renewable energy resources will have to grow from their current 30% share to 80% of the power sector by 2050 to reduce CO_2 emissions (IPCC 2014).
- Capture CO_2 and dump it in geological and/or oceanic reservoirs (CO_2 sequestration)
- Utilize CO_2 by converting it to either fuels or some other value added products, resulting in two-fold advantages:
  - (i) Reduction in CO_2 level, hence minimizing its contribution towards greenhouse effect.
  - (ii) Reducing our dependency over conventional fossil fuels, thus enhancing energy security.

Thus, the last option can help in combating the two most important environmental issues, discussed above.

1.3 Methods of CO_2 utilization/conversion

People have started using CO_2 as a feedstock long time back for its conversion to various industrially important products. CO_2 can be utilized directly as a solvent, working fluid, or in heat transfer. It can also be used after chemical conversion, *e.g.* in Sabatier reaction, in urea formation,

in the formation of sodium salicylate, carbonates, bicarbonates, and many other products (Sakakura *et al.* 2007). The Sabatier and Fischer-Tropsch processes involve the conversion of hydrogen and carbon dioxide into hydrocarbons, which can be used as fuels. Sabatier's reaction scheme shown in equation (1.1) involves the conversion of CO_2 and hydrogen gas into methane and water in presence of Ni catalyst at 300-400°C.

$$CO_2 + 4H_2 \xrightarrow[300\text{-}400\ ^oC]{Ni} CH_4 + 2H_2O \quad (1.1)$$

The Fischer-Tropsch process involves two steps and can also be seen as an alternative process for fuel generation. The first step shown in equation (1.2) is the partial oxidation of coal or natural gas into hydrogen gas and carbon monoxide. The second step, shown in equation (1.3), shows the conversion of synthesis gas (carbon monoxide and hydrogen) into more useful hydrocarbon fuels.

$$2C + 1/2\,O_2 + H_2O \xrightarrow[1073\ ^oC]{Fe} 2CO + H_2 \quad (1.2)$$

$$2nH_2 + nCO \xrightarrow[150\text{-}300\ ^oC]{Fe} C_nH_{2n} + nH_2O \quad (1.3)$$

CO_2 can also be reduced and utilized by using many possible ways such as radiochemical method, chemical reduction by metals, thermochemical method, photochemical method, biochemical method, electrochemical method, and various combinations of these techniques (Scibioh and Viswanathan 2004). Among all these methods, electrochemical method of CO_2 reduction is becoming popular as it offers many advantages:

- value added products such as hydrocarbons, alcohols *etc.* can be obtained,
- reactions can be carried out in ambient temperature and pressure conditions,
- water, a natural resource, can be used as proton source,
- storage of renewable (solar/wind) energy in form of chemicals, if renewable energy is used for carrying out the reactions,
- no harmful emissions in the process,
- no audible pollution, and
- easy scale-up.

1.4 Electrochemical reduction of CO_2 and associated issues

Dealing with the current global energy scenario, electrochemical reduction of CO_2 (ERC) has come up as very promising technology and at the same time challenging too. In recent years, some books and reviews on this topic have also been published (Taniguchi 1989; Sullivan *et al.* 1993). Electrochemical reduction of CO_2 utilizes CO_2 and H_2O as the reactants. Electrochemical reduction of CO_2 may be carried-out in an electrolytic cell as shown in the figure 1.5. The electrical energy (preferably generated from renewable energy sources) is supplied to the reactor to carry out the electrochemical reactions. It can be seen that the electrochemical reduction of CO_2 takes place at cathode resulting in the formation of CH_4 (equation 1.4) and/or other value added products. Moreover, O_2 is produced at anode by the electrochemical oxidation of H_2O as shown in equation (1.5). The overall cell reaction (equation 1.6) is shown for the formation of CH_4 as a representative reaction. The equations show the corresponding standard potential (E°) of the reaction with respect to standard hydrogen electrode (SHE).

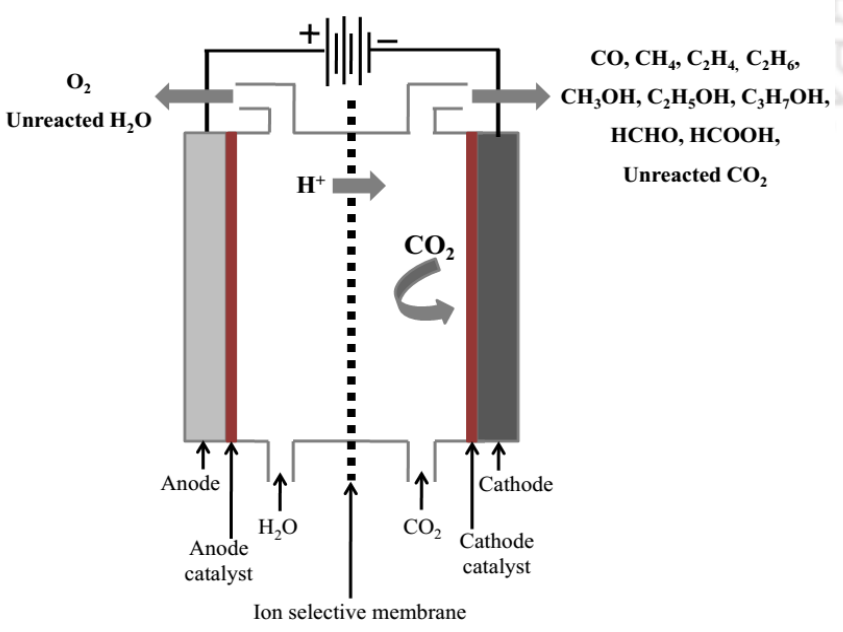

Figure 1.5 Simplified scheme for electrochemical reduction of CO_2

.

$$\text{Cathode: } CO_2 + 8H^+ + 8e^- \rightarrow CH_4 + 2H_2O \quad (E° = 0.17\ V) \quad (1.4)$$

$$\text{Anode: } 4H_2O \rightarrow 8H^+ + 2O_2 + 8e^- \quad (E° = -1.23\ V) \quad (1.5)$$

$$\text{Overall: } CO_2 + 2H_2O \rightarrow CH_4 + 2O_2 \quad (E° = -1.06\ V) \quad (1.6)$$

Electrochemical reduction of CO_2 is carried out either in aqueous or nonaqueous electrolyte solutions saturated with CO_2, or directly as a gas at different metal cathodes. As a result, many products can form. A few important overall reactions are as follows:

$$2CO_2 + H_2O \rightarrow 2CO + O_2 + H_2O \quad E° = -1.33\ V \quad (1.7)$$

$$CO_2 + 2H_2O \rightarrow CH_4 + 2O_2 \quad E° = -1.06\ V \quad (1.8)$$

$$2CO_2 + 3H_2O \rightarrow C_2H_6 + 3.5O_2 \quad E° = -1.085\ V \quad (1.9)$$

$$2CO_2 + 2H_2O \rightarrow C_2H_4 + 3O_2 \quad E° = -1.15\ V \quad (1.10)$$

$$CO_2 + 2H_2O \rightarrow CH_3OH + 1.5O_2 \quad E° = -1.20\ V \quad (1.11)$$

Figure 1.6 shows that the energy density of the products obtained from the ERC (referred as "green fuels") is comparable with the conventional fuels, and therefore these products can also be used as fuels. It may be noted that hydrocarbons and alcohols can alone be used as fuel whereas

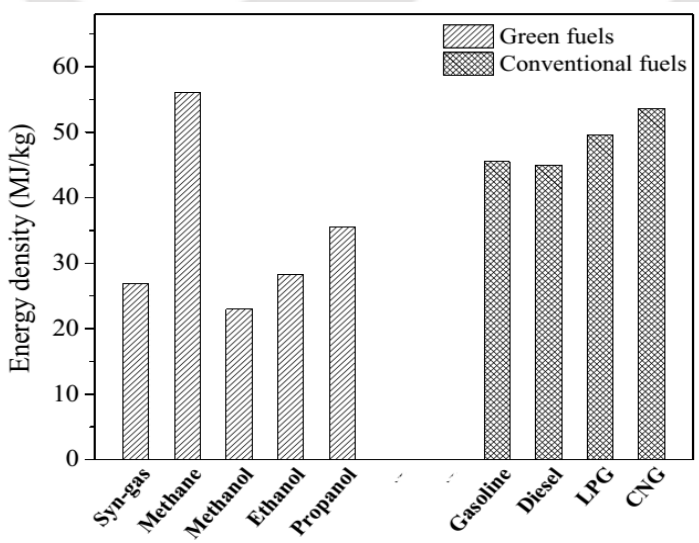

Figure 1.6 Comparison of energy density of the green fuels with the conventional fuels

CO can be used as fuel in the form of synthesis gas (syn-gas) along with H_2, which is a by-product of aqueous ERC. Hence, as an alternative source of energy with an added advantage of mitigating CO_2, the potential of ERC seems to be viable and attractive (Centi *et al.* 2013; Jhong *et al.* 2013; Hu *et al*. 2013).

The research in the field of ERC is continuosly growing and many excellent reviews are also published covering various aspects such as type of reactor for the reaction, electrodes, electrolytes, energy efficiency *etc.* (Scibioh and Viswanathan 2004; Gattrell *et al.* 2006; Jitaru 2007; Hori 2008; Centi and Perathoner 2009; Spinner *et al.* 2012; Costentin *et al.* 2013; Jhong *et al.* 2013; Appel *et al.* 2013; Kim *et al.* 2015). However, with lots of benefits, the process also faces enormous challenges, which are mainly due to the stable nature of CO_2 molecule, concurrent reactions, low product selectivity, mass transfer limitations, and fast deactivation of electrocatalysts.

In the electrochemical reduction of CO_2, the first step is the activation of the stable CO_2 molecule. The carbon atom has double covalent bonds with oxygen atom and the two pairs of electrons are shared between the atoms. The electronegativity of carbon is much less than oxygen (Dean 1999; Lide 2010) still, the CO_2 is a linear molecule, because there are only two electron pairs on the central carbon atom, which are equally shared by two oxygen atoms on both the sides. Due to the linear *sp* hybridized structure, the bond strength of CO_2 is very high (~532 $kJ{\cdot}mol^{-1}$ (Sullivan *et al.* 1993)) thus making it remarkably stable. Therefore, CO_2 needs substantial electrical potential in electrochemical environment to get activated. The activation of CO_2 requires change in its geometry from the linear CO_2 to bent CO_2 anion radical ($\bullet CO_2^-$), which results in a very slow self-exchange rate for the $CO_2/\bullet CO_2^-$ couple, thus making this step rate determining (Schouten *et al.* 2011, Costentin *et al.* 2013). This is the most energy intensive step in the ERC and theoretically requires -1.9 V *vs.* SHE. Therefore, efficient electrocatalysts are required to reduce the activation energy barrier. Another issue of ERC is simultaneous hydrogen evolution reaction at cathode, due to the similar reduction potentials of CO_2 and H_2 in electrochemical environment. This leads to competition between CO_2 electroreduction and hydrogen evolution reaction (HER) during ERC,

which results in significant consumption of supplied energy for HER rather getting used up in the CO_2 electroreduction. Ultimately the current efficiency of the CO_2 electroreduction process is adversely affected. Thus, electrocatalysts are required to make the reaction selective towards ERC. Therefore, to carry out ERC, the issue of electrocatalysts receives the most attention among all other challenges.

1.5 Electrocatalysts

According to IUPAC (1976), "a catalyst is a substance that, being present in small proportions, increases the rate of attainment of chemical equilibrium, without itself undergoing chemical change." Infact, catalyst undergoes transitory changes to catalyze the reaction, and permanent changes which typically lead to the catalyst deactivation. It is well known that a catalyst affects the rate of reaction and thus changes the kinetics of the reaction. Electrocatalyst also does the same thing along with electron transfer. An electrocatalyst participates in an electron transfer reaction at the electrode as well as facilitates the change in the rate of a chemical reaction. Thus any species acting as an electrocatalyst should be efficient in electron transfer as well as in chemical kinetics.

Apart from this, electrocatalysis also differs from usual catalysis as, in electrochemistry, the rate of the reaction depends not only on given system parameters (composition of the catalyst and electrolyte, temperature, state of the catalytic electrode surface), but also on the electrode potential. Thus, in a given system, the potential can be varied by a few tenths of a volt; while as a result, the reaction rate will change by several orders of magnitude. Electrocatalysts are also interesting because in electrochemical reactions, the catalyst surface is not only in contact with the reacting species but also with other species (*i.e.* the solvent molecules and the electrolyte ions) which in turn influence the properties of the surface and give rise to special reaction features.

There are two major types of electrocatalysts employed in ERC - homogeneous and heterogeneous electrocatalysts. In homogeneous catalysis, the catalyst particles are dispersed in

the bulk while in heterogeneous catalysis, a film or coating of catalyst particles is deposited on the electrode surface.

1.5.1 Homogeneous electrocatalysts in electrochemical reduction of CO_2

In ERC, the homogeneous electrocatalysts generally refer to transition metal complexes, which help in the electrochemical reduction of CO_2 at cathode to give reduction products. These transition metal complexes are dispersed in the bulk electrolyte. For the reduction of CO_2, the major setback is the inertness of this molecule. Hence the coordination of this inert molecule with transition metals is a promising way to activate it. The coordination lowers the activation energy required in further reactions of CO_2 and in this way enhances the rate of these reactions. In past 20-30 years, many reports of apparently homogeneous electrocatalysts for the reduction of CO_2 have appeared in literature. In most of the cases, it results in 2 electron reduction product *viz.* CO and $HCOO^-$. However, the efficiency reported in these cases is quite high and reaches >80% (Fisher and Eisenberg 1980; Gambarotta *et al.* 1982; Mahmood *et al.* 1987). Thus, the homogeneous electrocatalysts may be good only for conversion of CO_2 into some other products.

1.5.2 Heterogeneous electrocatalysts in electrochemical reduction of CO_2

Using heterogeneous electrocatalysis, however, variety of reaction products have been reported so far including hydrocarbons, alcohols, carbon monoxide, formic acid *etc.* A review was provided in 2001 on the reduction of CO_2 to hydrocarbons at copper electrodes (Sanchez *et al.* 2001). According to this review, the reaction product distribution strongly depends on the conditions in which reaction has been carried out. When used in the aqueous solution, most flat metallic electrodes yielded carbon monoxide and formic acid (Azuma *et al.* 1990; Kaneco *et al.* 2002). Only copper was suitable electrode for the formation of hydrocarbons such as methane and ethylene (Hori *et al.* 1986, 1989, 1995; Yano *et al.* 2004).

Sanchez *et al.* (2001) has summarized the representative results for the electrochemical CO_2 reduction at metal electrodes. The metal electrodes used in electrochemical reduction of CO_2 were divided into different groups based on the nature of the main product:

a. Hydrocarbons and alcohols (Cu)
b. Carbon monoxide (Au, Ag, Zn, Pd, and Ga)
c. Formic acid (Pb, Hg, In, Sn, Bi, Cd, and Tl)
d. Some metals do not exhibit useful catalytic properties under typical reaction conditions *viz.* 1 atm CO_2 partial pressure and 25°C temperature (Pt, Fe, Rh, Ir, and W). However, this situation can change when conditions are modified.
e. Some metals heavily favor hydrogen evolution even if the reaction conditions are modified (Ti, Nb, Ta, Mo, Mn, and Al).

Therefore, the dual purpose of ERC (CO_2 conversion with fuel production) may be better served by the heterogeneous electrocatalysts.

Apart from the metals, various metal oxides, and metal complexes can also be coated over the electrode surface to be used as heterogeneous electrocatalysts. As per the literature reported till date, the heterogeneous electrocatalysts for CO_2 electroreduction can be broadly divided into pure metals, metal oxides, and transition metal complexes. In few cases metal hydrides and metal carbides have also been investigated. An extensive literature survey on these electrocatalysts has been carried out and reported in the next chapter.

References

Appel A.M., Bercaw J.E., Bocarsly A.B., Dobbek H., DuBois D.L., Dupuis M., Ferry J.G., Fujita E., Hille R., Kenis P.J.A., Kerfeld C.A., Morris R.H., Peden C.H.F., Portis A.R., Ragsdale S.W., Rauchfuss T.B., Reek J.N.H., Seefeldt L.C., Thauer R.K., and Waldrop G.L. (2013), Frontiers, opportunities and challenges in biochemical and chemical catalysis of CO_2 fixation, *Chemical Reviews*, 113, 6621-6658.

Azuma M., Hashimoto K., Hiramoto M., Watanabe M., and Sakata T. (1990), Electrochemical reduction of CO_2 on various metal electrodes in low temperature aqueous $KHCO_3$ media, *Journal of Electrochemical Society*, 137(6), 1772-1778.

Centi G. and Perathoner S. (2009), Opportunities and prospects in the chemical recycling of carbon dioxide to fuels, *Catalysis Today*, 148, 191-205.

Centi G., Quadrelli E.A., and Perathoner S. (2013), Catalysis for CO_2 conversion: a key technology for rapid introduction of renewable energy in the value chain of chemical industries, *Energy and Environmental Science*, 6, 1711-1731.

Costentin C., Robert M., and Saveant J.M. (2013), Catalysis of the electrochemical reduction of carbon dioxide, *Chemical Society Reviews*, 42, 2423-2436.

Dean J.A. (1999), Langes's handbook of Chemistry, Table 4.5, 15th ed., McGraw-Hill Inc., Tennessee, ISBN: 0-07-016384-7.

Fisher B. and Eisenberg R. (1980), Electrocatalytic reduction of carbon dioxide by using macrocycles of nickel and cobalt, *Journal of American Chemical Society*, 102, 7361-7363.

Gambarotta S., Arena F., Floriani C., and Zanazzi P.F. (1982), Carbon dioxide fixation: Bifunctional complexes containing acidic and basic sites working as reversible carriers, *Journal of American Chemical Society*, 104, 5082-5092.

Gattrell M., Gupta N., and Co A. (2006), A review of the aqueous electrochemical reduction of CO_2 to hydrocarbons at copper, *Journal of Electroanalytical Chemistry*, 594, 1-19.

Hansen J., Sato M., Kharecha P., Beerling D., Berner R., Masson-Delmotte V., Pagani M., Raymo M., Royer D.L., and Zachos J.C. (2008), Target atmospheric CO_2: Where should humanity aim?, *The Open Atmospheric Science Journal*, 2, 217-231.

Hori Y. (2008), Electrochemical CO_2 reduction on metal electrodes. In: Vayenas *et al.* (ed.) 'Modern Aspects of Electrochemistry No. 42', Ch. 3, Springer, New York, pp. 89-189.

Hori Y., Kikuchi K., Murata A., and Suzuki S. (1986), Production of methane and ethylene in electrochemical reduction of carbon dioxide at copper electrode in aqueous hydrogencarbonate solution, *Chemistry Letters*, 897-898.

Hori Y., Koga O., Yamazaki H., and Matsuo T. (1995), Infrared spectroscopy of adsorbed CO and intermediate species in electrochemical reduction of CO_2 to hydrocarbons on a Cu electrode, *Electrochimica Acta*, 40(16), 2617-2622.

Hori Y., Murata A., and Takahashi R. (1989), Formation of hydrocarbons in the electrochemical reduciton of CO_2 at a copper electrode in aqueous solution, *Journal of Chemical Society, Faraday Transactions*, 85(8), 2309-2326.

Houghton J.T., Jenkins G.J., and Ephraums J.J. (1990), Climate change: The IPCC scientific assessment, Cambridge University Press, NewYork, USA.

Hu B., Guild C., and Suib S.L. (2013), Thermal, electrochemical, and photochemical conversion of CO_2 to fuels and value-added products, *Journal of CO_2 Utilization*, 1, 18-27.

IEA Energy Technology Perspectives (2010), Scenarios and strategies to 2050, OECD/IEA, France.

IEA Statistics (2014), CO_2 emissions from fuel combustion, OECD/IEA, France.

International Energy Outlook Report (2011), U.S. Energy Information Administration, DOE/EIA-0484(2011).

IPCC (2007) Fourth Assessment Report (AR4), IPCC website (http://www.ipcc.ch/).

IPCC (2014) Fifth Assessment Report (AR5), IPCC website (http://www.ipcc.ch/).

Jhong H., Ma S., and Kenis P. (2013), Electrochemical conversion of CO_2 to useful chemicals: Current status, remaining challenges, and future opportunities, *Current Opinion in Chemical Engineering*, 2(2), 191-199.

Jitaru M. (2007), Electrochemical carbon dioxide reduction – Fundamental and applied topics (Review), *Journal of the University of Chemical Technology and Metallurgy*, 42(4), 333-344.

Kaneco S., Hiei N., Xing Y., Katsumata H., Ohnishi H., Suzuki T., and Ohta K. (2002), Electrochemical conversion of carbon dioxide to methane in aqueous $NaHCO_3$ solution at less than 273 K, *Electrochimica Acta*, 48, 51-55.

Kim D., Sakimoto K.K., Hong D., and Yang P. (2015), Artificial photosynthesis for sustainable fuel and chemical production, *Angewandte Chemie International Edition*, 54(11), 3259-3266.

Lide D.R. (2010), CRC Handbook of Chemistry and Physics, 90th ed., Taylor & Francis Group, Florida, USA.

Mahmood M.N., Masheder D., and Harty C.J. (1987), Use of gas-diffusion electrodes for high-rate electrochemical reduction of carbon dioxide. II. Reduction at metal phthalocyanin-impregnated electrodes, *Journal of Applied Electrochemistry*, 17, 1223-1227.

NRC (2010), Advancing the science of climate change, National Research Council, The National Academics Press, Washington DC, USA.

Sakakura T., Choi J.C., and Yasuda H. (2007), Transformation of carbon dioxide, *Chemical Reviews*, 107, 2365-2387.

Sanchez C.M.S., Montiel V., Tryk D.A., Aldaz A., and Fujishima A. (2001), Electrochemical approaches to alleviation of the problem of carbon dioxide accumulation, IUPAC, *Pure and Applied Chemistry*, 73(12), 1917-1927.

Schipper L., Fabian H., and Leather J. (2009), Transport and carbon dioxide emissions: Forecasts, options analysis, and evaluation, ADB Sustainable Development Working Paper Series No. 9, Publication stock no. WPS091261.

Schouten K.J.P., Kwon Y., Ham C.J.M. vander, Qin Z., and Koper M.T.M. (2011), A new mechanism for the selectivity to C_1 and C_2 species in the electrochemical reduction of carbon dioxide on copper electrodes, *Chemical Science*, 2, 1902-1909.

Scibioh M.A. and Viswanathan B. (2004), Electrochemical reduction of carbon dioxide: A status report, *Proceedings of Indian National Science Academy*, 70 A(3), 407-462.

Singh B.R. and Singh O. (2008), A study on sustainable energy sources and its conversion systems towards development of an efficient zero pollution novel air turbine to use as prime-mover to the light vehicle, *ASME Conference Proceedings*, Vol. 8, Paper No. IMECE2008-66803, 371-378.

Spinner N.S., Vega J.A., and Mustain W.E. (2012), Recent progress in the electrochemical conversion and utilization of CO_2, *Catalysis Science & Technology*, 2, 19-28.

Sullivan B.P., Krist K., and Guard H.E. (1993), Electrochemical and electrocatalytic reactions of carbon dioxide, Elsevier, Amsterdam, ISBN: 0-444-88316-9.

Taniguchi I. (1989), Electrochemical and photoelectrochemical reduction of carbon dioxide. In: Bockris *et al*. (ed.) 'Modern Aspects of Electrochemistry No. 20', Ch. 1, Springer, NewYork, pp. 327-400.

Tans P. and Keeling R. (2015), NOAA Earth system research laboratory & Scripps Institution of Observatory, USA, (http://www.esrl.noaa.gov/gmd/ccgg/).

Yano H., Tanaka T., Nakayama M., and Ogura K. (2004), Selective electrochemical reduction of CO_2 to ethylene at a three-phase interface on copper (I) halide-confined Cu-mesh electrodes in acidic solutions of potassium halides, *Journal of Electroanalytical Chemistry*, 565(2), 287-293.

2

Literature review

Chapter 2

Literature review

The issues related to electrochemical reduction of CO_2 have been discussed in the previous chapter. Development of suitable electrocatalysts is inevitable and hence, extensive research work is required for the improvement of electrocatalysts. Therefore, thorough study of literature is carried out to know the efforts already made in this direction. This chapter provides an exhaustive literature survey in the light of recent developments in electrocatalysts for CO_2 reduction. Based on the outcome of the literature survey, the objective of the research work is defined at the end of this chapter.

2.1 Background

In past few decades, many workers have contributed their effort in finding a suitable electrocatalyst for reduction of CO_2. Various types of electrocatalysts have been used, ranging from metals, metal oxides, and metal complexes to metal carbides, metal sulphides, and metal hydrides *etc.* Along with this, many supported electrocatalysts have also been synthesized with intention to increase the activity of electrocatalysts by enhancing the surface area. However, the requirement of large overpotential is still a major challenge to deal with. Although, the use of metal complexes helps to lower down the overpotential upto great extent, but its inability to undergo multi-electron reduction of CO_2 does not make it a preferred choice as far as generation of fuel kind of products is concerned.

It has been seen that along with electrocatalysts, the reaction medium also affects the product distribution upto great extent (Aeshala *et al.* 2012, 2013, 2014, 2015). In aqueous medium, a range of products are formed. Many studies of electrochemical reduction of CO_2 in early years were carried out in aqueous media with metal electrodes of high hydrogen overvoltage such as mercury and lead, in order to reduce hydrogen evolution reaction (HER). However, since the rate of hydrogen evolution reaction is proportional to the proton activity in electrolyte, the hydrogen evolution reaction is a competing reaction with CO_2 reduction. On the other hand, non-aqueous medium has been selected for solubilizing more amount of CO_2. Where, aqueous medium results in several fuel kind of products such as hydrocarbons and alcohols; non-aqueous medium results only in carbon monoxide, formic acid, oxalic acid *etc.* However, non-aqueous medium has the added advantage of high solubility of CO_2 and reduced competitive hydrogen evolution reaction. Moreover, researchers have studied many electrocatalysts in aqueous medium to get fuel kind of products. Hori *et al.* (1985, 1986, 1989, 1995, 2002, 2003) have used copper as the metal electrode in aqueous medium and reported the production of hydrocarbons and olefins, which made the copper a preferred choice as an electrocatalyst for many successive workers. Ikeda *et al.* (1995, 1996) have also tested copper powder, but, over gas diffusion electrodes in order to increase current density and Faradaic efficiency. Frese (1991) reported the production of

methanol at copper oxide surfaces, which was later confirmed by Le *et al*. (2011). Using the same copper electrode, Kaneco *et al.* (1999 a, 1999 b, 2006) tried to investigate the effect of supporting electrolytes in methanol media and reported the production of ethylene. Apart from copper, several other metals like cobalt (Behar *et al.* 1998), platinum (Hara *et al.* 1995 a), lead (Kaneco *et al.* 1998 a; Guerra *et al.* 2012), mercury (Hori and Suzuki 1982; Haynes and Sawyer 1967), molybdenum (Summers *et al.* 1986), tin (Prakash *et al.* 2013), ruthenium complexes *etc.* have also been used. Hara *et al.* (1995 b) conducted the study in high pressure conditions using various electrodes and suggested that large current densities can be obtained at high pressures.

As per the literature reported till date, the electrocatalysts for CO_2 electroreduction can be divided mainly into pure metals, metal oxides, and transition metal complexes. In a few cases, metal hydrides, metal sulphides, and metal carbides have also been investigated. Many of the pure metals have been tested for ERC but the problem of fast deactivation and non-selectivity for the fuel products have led to the investigation of other substitutes. Metal oxides have always been quite interesting, the reason being the soft acidic nature of the CO_2 molecule. This fact depicts that the presence of strong basicity phases such as oxides can enhance the CO_2 adsorption capacity on the surface, which will eventually increase the CO_2 reduction. The most attractive aspect of metals and metal oxides is their capability to form hydrocarbons and alcohols, which is somewhat unusual with metal complexes as these are mostly selective towards CO formation by utilizing two electron transfer process. For multi-electron transfer products (*viz.* hydrocarbons and alcohols), CO_2 requires some sort of stabilization of the metal-carbon (M-C) bond and/or ability of the electrocatalyst to accommodate multiple electrons, so that the rate of electroreduction is much greater than M-C bond dissociation. However, metal complexes are well known for lowering down the activation energy barrier for the first electron transfer process as they allow their reasonable optimization due to the well designed adaptations of either ligand or the central metal atom.

Hence, for fuel quality products, most of the literature discuss about the metals, metal oxides, and metal complexes. A brief account of the different types of electrocatalysts used in the field of ERC is described in following sections.

2.2 Metal electrocatalysts

A number of metal electrocatalysts have been investigated for ERC to form the potential fuel kind of products. Therefore, these metal electrocatalysts are discussed with special reference to the fuels.

Carbon monoxide, hydrocarbons such as CH_4, and alcohols are the preferred products in ERC, when the aim is to synthesize fuel kind of products. CO is considered as fuel because it can be used as syn-gas when mixed with H_2. Noble metals like Ag and Au serve as efficient electrocatalysts for CO formation from CO_2 with Faradaic efficiency as high as 61-90% for Ag and 81-93% for Au at potentials -1.45 V and -1.14 V *vs.* SHE, respectively (Hori *et al.* 1985; Hara *et al.* 1995 b; Kaneco *et al.* 1998 b, 1998 c). However, large scale utilization of these noble metals is not acceptable due to their high cost. Therefore, Hori *et al.* (1990) worked on Cd modified Cu electrodes and reported the enhanced production of CO. In this case, the generation of hydrocarbons was decreased upto a great extent while CO formation was increased. It was shown that CO formation started to increase while hydrocarbons became suppressed as the amount of deposited Cd on copper was increased. The same group again reported the enhanced current efficiency of CO on Cd modified Ni electrodes with simultaneous decrease in H_2 generation upto a great extent. However, apart from CO and H_2, $HCOO^-$ generation also took place, so the selectivity as well as Faradaic efficiency was distributed. These results suggest that Cd is selective towards CO production (Murata and Hori 1991). However, considering its adverse environmental impacts, Cd may not be acceptable. Azuma *et al.* (1990) reported the production of CO on pure Ni electrodes with 21% Faradaic efficiency at 0°C. CO formation was also found using Pd metal electrocatalyst, however, the Faradaic efficiency was quite low (~12%) along with high H_2

production. Hoshi *et al.* (1995, 1996, 1997, 2000) carried out ERC on Pt and Pt group metals which led to the production of CO in aqueous solution.

Many of the workers also reported cyclic voltammograms to determine activity of the metal electrocatalysts in aqueous medium having dissolved CO_2 in ambient conditions (Kaneco *et al.* 1998 c; Ohta *et al.* 1998; Lee and Tak 2001; Le *et al.* 2011). In almost all the cases, the voltammograms obtained in CO_2 saturated medium is compared with the voltammograms obtained in a medium devoid of CO_2. On comparison, if the current density using the metal electrocatalyst is found more in CO_2 saturated medium, then such an electrocatalyst is considered to be favoring CO_2 reduction and *vice-versa*. However, the higher current density in CO_2 medium does not always guarantee that the electrocatalyst is favoring CO_2 reduction because the increased current density may be due to the increased hydrogen evolution reaction (HER) (Hori 2003). Moreover, pH of the electrolyte medium changes after solubilizing CO_2 into the electrolyte, which inturn assists the HER. Another discrepancy has also been observed that sometimes, in spite of less current density obtained in medium having dissolved CO_2 (in comparison to the current density obtained in medium devoid of CO_2); the electrocatalyst results in product formation (Kaneco *et al.* 1998 b; Shuang *et al.* 2006). Thus, it is difficult to ascertain about the electrocatalytic activity solely on the basis of cyclic voltammograms and hence, full cell reactions followed by product identification are mandatory. Moreover, it makes this process quite cumbersome.

Hara *et al.* (1995 b) performed the electroreduction of CO_2 in 0.1 M aqueous $KHCO_3$ medium at ambient temperature and high pressure (30 atm), considering the fact that high pressure enhances the CO_2 solubility in aqueous medium. It was deduced that electrochemical reduction of CO_2 to CO with high Faradaic efficiency can be achieved at high pressure. It was found that Ag and Au were the most selective for CO formation, followed by Rh, Zn, and Pd *etc*. On the other hand, the metals like Pb, Ti, Ta, and W were found to be the least selective for the CO formation at high pressure. Hori *et al.* (1994) also demonstrated the CO selectivity over various metal electrodes in ambient conditions and reported the order as Au > Ag > Zn > Pd > Ga > Cd > Sn > In > Cu in

Table 2.1 Studies on electroreduction of carbon dioxide using metal electrocatalysts during 2005-2015

Cathode electrocatalyst	Electrolyte	Experimental parameters	Main Products (Faradaic efficiency, %)	References
Cu mesocrystals	0.1 M $KHCO_3$	0.99 V *vs.* RHE	CH_4 (1.5), C_2H_4 (27.2)	Chen *et al.* (2015)
Cu nanocubes	0.1 M $KHCO_3$	0.60 V *vs.* RHE	C_2H_4	Roberts *et al.* (2015)
Ag	BMImCl + 20 wt% H_2O	25°C, 1 atm	CO (> 99)	Zhou *et al.* (2014)
Sn	$KHCO_3$	25°C, 1 atm, pH = 6.98	$HCOO^-$ (91)	Lv *et al.* (2014)
Sn/GDE	$NaHCO_3$	1.6 V *vs.* NHE, 25°C, pH = 8.3	$HCOO^-$ (70)	Prakash *et al.* (2013)
Bi/GC	CH_3CN	25°C, 1 atm	CO (95)	DiMeglio and Rosenthal (2013)
Pb	0.45 M $KHCO_3$ + KCl	10.5 $mA{\cdot}cm^{-2}$, 25°C, 1 atm	$HCOO^-$ (57)	Guerra *et al.* (2012)
Fe	0.5 M H_2SO_4	25°C, 1 atm	CH_4, HCHO, C_2H_6, C_2H_5OH	Perez-Rodriguez *et al.* (2011)
In	$NaHCO_3$	40 $mA{\cdot}cm^{-2}$, pH = 8	$HCOO^-$ (45)	Narayanan *et al.* (2011)
Cu mesh	$KHCO_3$	25°C, 1 atm	CH_4 (19.4), C_2H_4 (18.7)	Goncalves *et al.* (2010)
Cu	0.5 M KH_2PO_4	25°C, 1 atm	HCOOH (6), CO (40), HCs (30)	Ikeda *et al.* (2009)
Pb	NaOH	2.5 $mA{\cdot}cm^{-2}$, 21°C, pH = 8.5	$HCOO^-$ (70)	Innocent *et al.* (2009)
Pb	K_2HPO_4	25°C, 1 atm , pH = 7	$HCOO^-$ (93)	Subramanian *et al.* (2007)
Cu-Ni	$KHCO_3$ in water + methanol (8:2)	-5°C	HCOOH (13), CO (4), HCs (26)	Kaneco *et al.* (2007)
Sn (granulated)	0.5 M $KHCO_3$ + 2 M KCl	60 $mA{\cdot}cm^{-2}$, 18°C, 1 atm, pH = 7.5	$HCOO^-$ (91)	Li and Oloman (2007)
Cu mesh (Sn coated)	0.45 M $KHCO_3$ + 1 M KCl	130 $mA{\cdot}cm^{-2}$, 26°C, 1.4 atm	$HCOO^-$ (86)	Li and Oloman (2006)
Zn	Methanol + NaOH + Cu particles	-30°C	HCOOH (7), CO (60), CH_4 (12)	Kaneco *et al.* (2006)
Ni	0.5 M $KHCO_3$	25°C, 1 atm	HCOOH (29), CO (1.7)	Shuang *et al.* (2006)
Cu	0.45 M $KHCO_3$	22 $mA{\cdot}cm^{-2}$, 25°C	$HCOO^-$ (86)	Hori *et al.* (2005)

aqueous media. Thus, Ag and Au were found to be the best candidates for CO formation in both the ambient as well as high pressure conditions. As far as other metals are concerned, it was found that the reduction of CO_2 to CO at Zn electrode is not very consistent and Faradaic efficiency ranges from 3% to 63.3% at potential of -1.56 V *vs.* SHE in ambient conditions, the reason for which is unknown. Sn and In are very less selective for CO having Faradaic efficiency of only 2.4 – 4.1% and 0.9 – 2.2%, respectively. Over the Cu, Faradaic efficiency ranges from 1.5 – 3.1% at -1.4 V *vs.* SHE in ambient conditions (Hori *et al.* 1985). Recently, DiMeglio and Rosenthal (2013) reported the use of Bi as an efficient electrocatalyst for CO production in ionic liquid with Faradaic efficiency as high as 95% at -1.71 V *vs.* SHE. Bi is nontoxic and hence environment friendly despite being extremely cheap. Therefore, it might be a good replacement of Ag and Au for CO production. Table 2.1 compiles the performance of metal electrocatalysts for CO_2 electroreduction, studied in recent years.

Hydrocarbons (especially methane) have always been the choice as fuels. Having energy density of 56 $MJ \cdot kg^{-1}$, methane is a quite suitable fuel from the environmental safety point of view due to its low CO_2 emissions compared to other fossil fuels. Methane as well as other hydrocarbons formation using ERC was studied by many workers and most of them reported the use of Cu as an electrocatalyst. Hori *et al.* (1985, 1986, 1989, 1994, 2002) have shown that copper electrocatalyzes the CO_2 towards selective formation of CH_4 and other hydrocarbons. In this case, the Faradaic efficiency of hydrocarbon formation was reported upto 60% in 0.1 M $KHCO_3$ electrolyte using current density of 5 $mA \cdot cm^{-2}$ in ambient conditions. CO and alcohol formation were also found along with the hydrocarbons. Dewulf and Bard (1988) and Cook *et al.* (1988) investigated the gas phase reduction of CO_2 using Cu metal and solid polymer electrolyte (Nafion). Cu was deposited over the ion exchange membrane (Nafion) by electroless plating method. This system resulted in the formation of CH_4 and C_2H_4 as the major products. Similar kind of assembly has also been designed by Komatsu *et al.* (1995) with electroless plating of Cu over Nafion membrane. C_2H_4 was formed as the major product with Faradaic efficiency of 9% in gas phase ERC. CH_4 and CO were also formed in minor quantities.

The electrocatalytic activity of Cu for hydrocarbon formation depends upon several factors, such as temperature, pressure, type of electrodes *etc*. Hori *et al.* (1986) found the inverse relationship between Faradaic efficiency and temperature for methane formation over Cu, with Faradaic efficiency as high as 65% at 0°C while approaching 0% at 40°C. In contrast to this, the formation of ethylene and CO was found to be increasing on raising the temperature which can be seen in the Table 2.2. The reason for the higher yield of methane at low temperature was reported due to the presence of longer lived intermediates. The effect of pressure on the activity of copper was also studied and it was found that increase in pressure opposes the hydrocarbon formation. However, in this case ethane was formed in trace amount, which was absent in ambient pressure conditions (Hara *et al.* 1995 b). The comparison of Faradaic efficiencies at ambient conditions and high pressure conditions shows that high pressure results in decreased HCs generation while increased CO production (Table 2.2). Some workers reported that use of gas diffusion electrodes (GDEs) in place of foil electrode increases the surface contact between the electrode/catalyst and CO_2, resulting in enhanced Faradaic efficiency (Mahmood *et al.* 1987 a; Ikeda *et al.* 1995;

Table 2.2 Faradaic efficiency of products in different conditions using Cu electrocatalyst

Products	**Faradaic efficiency of products on Cu electrode (%)**							
	Cu foil[a] 25°C, 1 atm	Cu foil[b] Temperature variable, 1 atm					Cu foil[c] 25°C, 30 atm	Cu GDE[d] 25°C, 1 atm
		0°C	10°C	20°C	30°C	40°C		
CO	2	0.4	1	2	5	7	20.1	40
CH_4	29.4	65	58	50	16	5	9.95	12
C_2H_6	–	–	–	–	–	–	0.06	–
C_2H_4	30.1	2.5	7.5	10	15	20	3.74	18.2
Alcohols	9.9	–	–	–	–	–	–	5.4

[a] $KHCO_3$ solution (0.1 M) at -1.41 V *vs.* SHE (Hori *et al.* 1989)

[b] $KHCO_3$ solution (1 M) at -1.33 to -1.39 V *vs.* SHE (Hori *et al.* 1986)

[c] $KHCO_3$ solution (0.1 M) at -1.44 V *vs.* SHE (Hara *et al.* 1995 b)

[d] K_2SO_4 solution (0.5 M) at -1.25 V *vs.* SHE (Ikeda *et al.* 1995)

Aeshala *et al.* 2012; Prakash *et al.* 2013). Effect of GDE was also investigated over the activity of Cu and in this case the overall reduction of CO_2 was found to be increased over GDE in contrast to foil electrodes. The current density on the Cu loaded GDE was found almost two orders of magnitude higher than that on the Cu foil electrode (Ikeda *et al.* 1995). However, the methane formation over GDE was decreased as compared to foil electrodes.

Other workers showed that the applied potential can also change the selectivity and product distribution upto a great extent. As the applied potential becomes more negative, the formation of hydrocarbons takes place while at less negative potentials, CO prevails (Noda *et al.* 1989). Moreover, surface properties of metal like roughness and purity are also important parameters for determining the methane formation as it affects the adsorption characteristics of the electrode. The smooth surface gets poisoned very soon, whereas rough surface maintains the catalytic activity for longer duration (Kyriacou and Anagnostopoulos 1992). Even the method of pretreatment of the electrode surface, affects the product distribution over Cu upto a great extent. While the untreated Cu results in increased CO formation with time, the electrolytically treated Cu remains stable with time towards deactivation and continues to produce hydrocarbons (Terunuma *et al.* 1997). On the other hand, the air oxidized Cu electrode preferentially produces H_2 with very little methane production (Terunuma *et al.* 1997). In addition, the crystal structure of the electrocatalyst plays an important role as the selectivity for an individual reaction may depend on the atomic configuration of the electrode surface. It was found that the rate of methane formation in CO_2 saturated 0.5 M $KHCO_3$ is highest in Cu (111), followed by Cu (110) and Cu (100) (Hori *et al.* 2002, 2003).

Though, literature shows that Cu is the most widely used electrocatalyst for HC formation but the problem of deactivation of copper electrode limits its continuous use in a reaction. Hori *et al.* (2005) investigated the deactivation and reported that the impurities (especially Fe^{+2} and Zn^{+2}) present in the electrolyte are the major contaminants. It was suggested that these impurities can be removed by the pre-electrolysis of the electrolyte solution. However, this view is questioned by Ogura (2013) because Yano *et al.* (2004) showed that by increasing the concentration of

electrolyte, the product formation (C_2H_4) increases. Thus, the increased concentration of the (heavy) metal impurities due to increased electrolyte concentration indicates that the heavy metal impurity does not poison Cu electrocatalyst. Other workers have pointed out that it is an adsorbate of unknown composition over the copper cathode that causes poisoning (Friebe *et al.* 1997; Yano *et al.* 2007) and the deactivation caused by such an adsorbate can be overcome by pulse mode electrolysis. Lee and Tak (2001) also suggested that the cause of copper poisoning may be the adsorption of some species such as graphite, originating from CO_{ad} on the Cu surface, and in this case too, the pulse modulation helps.

Frese and Leach (1985) studied the methane formation over Ru electrode in acidic medium, using 0.1 N H_2SO_4 electrolyte and found that activity of Ru was affected by the pH, temperature, electrolyte purity *etc.* The current density was less and electrode instability was an issue. Kudo *et al.* (1993) reported the hydrocarbon formation over Ni electrode using 0.1 M $KHCO_3$ electrolyte in ambient as well as in high pressure (60 atm) conditions. It was found that high pressure conditions enhance the formation of hydrocarbons with decreased H_2 evolution. The same phenomena was also observed by Hara *et al.* (1995 b) using Pt loaded gas diffusion electrodes at 30 atm pressure, where Faradaic efficiency for methane formation reached upto 35% at current density of 900 $mA \cdot cm^{-2}$. A little amount of ethane and ethylene formation was also found (Hara *et al.* 1995 b). Over Pd and Cd electrodes with 0.1 M $KHCO_3$ electrolyte, Faradaic efficiency for CH_4 was found to be 2.9% and 1.3%, respectively (Hori *et al.* 1994). Sn and Pb electrodes also produced scanty amount of methane with Faradaic efficiency of 0.2% for both the metals (Hori *et al.* 1985). Figure 2.1 shows the comparison of the Faradaic efficiencies of different metal electrocatalysts for hydrocarbon formation (Kudo *et al.* 1993; Hori *et al.* 1985, 1994, 1989; Frese and Leach 1985).

Summarizing all these studies, it can be said that there is plenty of information over the metal electrocatalysts in aqueous medium. As of now, Ag and Au were found to be efficient electrocatalysts for CO formation while, Cu is the only metal to catalyze ERC for hydrocarbons formation efficiently in aqueous medium. Although some of the studies have been undertaken for

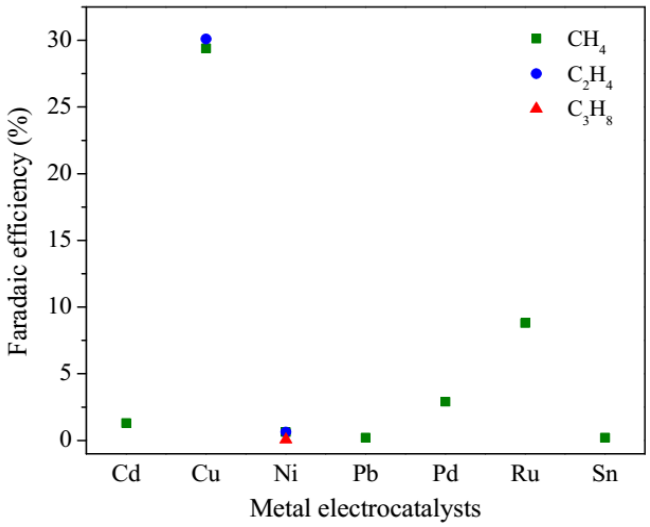

Figure 2.1 Faradaic efficiency of metal electrocatalysts for hydrocarbon formation

direct electrochemical reduction of gaseous CO_2 (DeWulf and Bard 1988; Komatsu *et al.* 1995; Centi *et al.* 2007; Machunda *et al.* 2010), a majority involved only the aqueous phase CO_2 reduction.

2.3 Metal oxide electrocatalysts

Apart from the usage of pure metals, the literature over electrochemical reduction of CO_2 also reveals the use of metal oxides in ERC (Frese 1991; Bandi and Kuhne 1992; Ikeda *et al.* 1993; Popic *et al.* 1997; Li and Kanan 2012). The reason for choosing metal oxides has been their basic nature as described earlier, which enhances the adsorption capacity of the electrocatalyst for the acidic CO_2. In some of the cases, the metal oxides have also been found to be active for longer duration than their unoxidized counterpart. Therefore, metal oxides have been the subject of interest for many of the workers.

The highest attention is paid on copper due to its selectivity mainly towards HCs and upto some extent for alcohols formation too. However, due to its fast deactivation, the desired efficiency could not be achieved till now. Therefore, it was suggested that change in the surface structure may impart some stability. In view of this, many workers have tried cuprous oxide (Cu_2O) in

place of metallic copper surfaces. It was reported that Cu_2O exhibited high Faradaic efficiency for CO_2 reduction at considerable low overpotential. Many reports suggest the use of Cu_2O (Le *et al.* 2011; Keerthiga *et al.* 2012; Aeshala *et al.* 2013) as the major benefit is its good resistivity towards deactivation. It is due to the surface changes caused by the oxidation of Cu, which does not allow for the graphite adsorption (Lee and Tak 2001). It is also said that Cu_2O enables easy formation of $\bullet CO_2^-$ intermediate and decreases H^+ reduction (Li and Kanan 2012), which makes Cu_2O to yield hydrocarbons for longer duration with better Faradaic efficiency.

Table 2.3 shows the comparison of pure Cu electrocatalyst with their corresponding metal oxide (Cu_2O) for ERC. It can be seen in the table that Cu_2O shows higher overall Faradaic efficiency for the electroreduction of CO_2. The use of Cu_2O increases the CO and methanol formation substantially as compared to Cu as an electrocatalyst. Methanol production was reported over Cu_2O surfaces by Le *et al.* (2011). It was found that methanol Faradaic efficiency upto 38% can be achieved over electroplated Cu_2O surface. Where Cu(0) electrodes favor the formation of only hydrocarbons, it was proposed that Cu(I) species plays a selective role towards methanol

Table 2.3 Comparison of catalytic activity of Cu and Cu_2O

Products	**Cu**[a]		**Cu_2O**[b]	
	Potential, V *vs.* SHE	Faradaic efficiency, %	Potential, V *vs.* SHE	Faradaic efficiency, %
CO	-1.41	2	-0.35	40
CH_4	-1.41	29.4	-	-
C_2H_6	-	-	-0.95	10
C_2H_4	-1.41	30.1	-	5
CH_3OH	-	-	-0.86	38
C_2H_5OH	-1.41	6.9	-	-
C_3H_7OH	-1.41	3	-	-

[a] $KHCO_3$ solution (0.1 M) (Hori *et al.* 1989)

[b] $NaHCO_3$ solution (0.5 M) for CO and HCs (Li and Kanan 2012); $KHCO_3$ solution (0.5M) for alcohols (Le *et al.* 2011)

formation by offering more stability to intermediates and enabling formation of H_3CO adsorbates. Moreover, the required electrical potential was also found lower in case of Cu_2O. It was observed that Cu_2O was stable upto 7 hours as compared to Cu, which was deactivated within 1 hour (Lee and Tak 2001; Li and Kanan 2012). It may be noted that the Faradaic efficiency for hydrocarbons formation was reduced when metal oxide was used (Li and Kanan 2012). However, the exact cause of the higher activity of Cu_2O and its reduced tendency towards deactivation is not yet established. It can be hypothesized that somehow oxide surfaces reduce the competitive HER, which inturn results in increased activity towards CO_2 reduction. The Faradaic efficiency towards CO formation increases significantly for Cu_2O as compared to Cu (Table 2.3), which may be due to the formation of highly dispersed Cu nanoclusters as a result of oxide reduction of Cu surface, over which CO formation prevails (Tsai *et al.* 2012). It is also reported that the HER prevails over oxophilic sites (Koper 2013); so it might happen that Cu_2O provides lesser oxophilic sites than pure copper. This may provide an explanation for the better electrocatalytic activity of cuprous oxide surfaces than pure Cu metal. Moreover, the changes introduced in terms of defects over the metal surface after oxide formation can also be a probable reason for the better activity towards ERC.

Andrews *et al.* (2013) reported the production of hydrocarbons and alcohols using single crystal $(10\bar{1}0)$ ZnO electrodes decorated with Cu nanoclusters. The combination of Cu and ZnO produces CO, methane, ethylene, methanol, ethanol, and trace levels of propanol. Faradaic efficiencies of ZnO/Cu electrodes were found similar relative to Cu electrodes with the exception of alcohols where selectivity was improved. Metal oxide surfaces of Ru were also investigated for alcohol production. Many workers have carried out ERC using Ru and RuO_2 (Frese and Leach 1985; Popic *et al.* 1997). However, it has been seen that the activity of RuO_2 was inferior as compared to Ru. The performance of RuO_2 over Ru shows decreased Faradaic efficiency for alcohols. The deactivation is not reported in this case, but high overpotential of RuO_2, limits its use in place of Ru.

Bandi (1990) reported the work over conductive metal oxides and use of surface adatoms in ERC. Various conductive metal oxide mixtures were used and it was found that RuO_2 + TiO_2 [35+65 mole%] and RuO_2 + Co_3O_4 + SnO_2 + TiO_2 [20+10+8+62 mole%] show high Faradaic efficiencies for methanol production in the solution of 0.2 M Na_2SO_4 (pH = 4) saturated with CO_2. Later, ERC was carried out in CO_2 saturated $KHCO_3$ solution at pH 4-7 over RuO_2 + TiO_2 electrodes but only a small amount of CO_2 reduction could be achieved. However, when electrodeposited Cu was added over RuO_2 + TiO_2 electrodes, the Faradaic efficiency of methanol formation was increased upto 30% (Bandi and Kuhne 1992). Popic *et al.* (1997) also discussed the production of methanol using surface adatoms. The Ru surface was modified by adding adatom of Cu and Cd and the reaction was carried out in 0.5 M $NaHCO_3$ at a potential of -0.56 V *vs.* SHE, which resulted in the production of methanol with efficiencies of 17%, 41%, and 38% after 480 min. of electroreduction using RuO_2, RuO_2/Cu, and RuO_2/Cd electrodes, respectively. It was found that surface modification with little amount of metals having high hydrogen overvoltage diminishes the hydrogen evolution reaction and inturn enhances the efficiency of CO_2 reduction. Surface structure of adatoms also plays an important role as shown by Qu *et al.* (2005) who reported the formation of methanol over Pt electrodes modified by RuO_2/TiO_2 composite nanotubes and RuO_2/TiO_2 composite nanoparticles. They found that Pt electrode modified by the RuO_2/TiO_2 nanotubes based composites resulted in more efficient formation of methanol (Faradaic efficiency 61%) compared to RuO_2/TiO_2 nanoparticle based composites (Faradaic efficiency 40%), however, the reason is not enunciated. Table 2.4 summarizes the performance of metal oxide electrocatalysts for the reduction of CO_2 dissolved in a medium.

Table 2.4 Studies on electroreduction of carbon dioxide using metal oxide electrocatalysts during 2005-2015

Cathode electrocatalyst	Electrolyte	Experimental parameters	Main Products (Faradaic efficiency, %)	References
Cu_2O films	0.1 M $KHCO_3$	-0.99 V *vs.* RHE, 25°C, 1 atm	C_2H_4 (34-39), C_2H_5OH (9-16), CH_4 (<1)	Ren *et al.* (2015)
$Ir_{0.8}Ru_{0.2}$-oxide on flat Ti surface	0.4 M Briton Robinson buffer solution (pH 5.82)	4°C & 22°C, 1atm	C_2H_5OH (96 at 4°C & 85 at 22°C)	Ullah *et al.* (2015)
Gd_2O_3 nanoparticles/GC	0.1 M TBAH/CH_3CN	25°C, 1 atm	CO	Behnamfar (2015)
CuO nanoparticles	0.2 M KI	1.5 V *vs.* SHE	C_2H_5OH (35) C_3H_7OH (5)	Chi *et al.* (2014)
Cu (core)/CuO (shell)	1 M $KHCO_3$	25°C, 1 atm	CO (23), HCOOH (20), CH_3OH (1-3)	Lan *et al.* (2014)
γ-Ti_3O_5	-	1-2.5 V	CO (7), HCOOH (10)	Sharma *et al.* (2014)
ZnO decorated with Cu nanoclusters	0.1 M $KHCO_3$	-1.203 V *vs.* SHE	CO (5.4), CH_4 (1.8), C_2H_4 (10), CH_3OH (2.8), C_2H_5OH (10), $HCOO^-$ (8)	Andrews *et al.* (2013)
Cu from thick Cu_2O films	0.5 M $NaHCO_3$	$Q \geq \sim 5$ C·cm^{-2}	CO (45), HCOOH (33), C_2H_4(5), C_2H_6 (10)	Li and Kanan (2012)
Surface oxidized Cu	0.5 M KCl	25°C	C_2H_6 (27)	Keerthiga *et al.* (2012)
Electrodeposited Cu_2O	$KHCO_3$	25°C, pH = 7.6	CH_3OH (38)	Le *et al.* (2011)
Cu_2O/Zn disk	KOH/methanol	-30°C, pH = 7.5	CH_4 (7.5), C_2H_4 (6.8)	Ohya *et al.* (2009)
Cu plate/Cu_2O	$KHCO_3$	25°C, 1 atm	C_2H_4 (22)/C_2H_4 (28)	Yano and Yamasaki (2008)
Pt with RuO_2/TiO_2 composites	0.5 M $NaHCO_3$	25°C, 1 atm	CH_3OH (60.5)	Qu *et al.* (2005)

2.4 Metal complex electrocatalysts

Metal complexes are also tried for the electrochemical reduction of carbon dioxide. The benefit with metal complexes is that these can be designed by suitable ligand and central metal atom, and hence can be tailored accordingly. Detailed review over the application of metal complex electrocatalysts in ERC is provided by Benson *et al.* (2009) and Inglis *et al.* (2012).

A number of transition metal complexes have been reported, however, these were selective for the CO formation (Tezuka *et al.* 1982; Gambarotta *et al.* 1982; Beley *et al.* 1984, 1986; Mahmood *et al.* 1987 b; Ishida *et al.* 1987; Collin *et al.* 1988; Bruce *et al.* 1988, 1992; Hammouche *et al.* 1991; Bhugan *et al.* 1996; Grodkowski *et al.* 2002; Issacs *et al.* 2003; Laitar *et al.* 2005; Raebiger *et al.* 2006). A stable CO_2 adduct to a transition metal was reported as $[Co(salen)(CO_2)M]^+$ (M = Li, Na, K, Cs) by Gambraotta *et al.* (1982). Phthalocyanin complexes of Co were also proved to be very active towards the ERC for CO generation (Lieber and Lewis 1984). The Co phthalocyanin complex reduced easily and thus CO_2 transformation could be carried out at low overpotential values with faster rates. Hawecker *et al.* (1984) reported selective and sustained CO production in DMF:H_2O (9:1) solution using bipyridine ligands at low potential. Tetra-aza-macrocyclic complexes of Co and Ni are interesting in the sense that the product ratio of CO/H_2 obtained was 1:1 or 2:1, which can be used as syn-gas, after proper modulation (Fisher and Eisenberg 1980). Simon-Manso and Kubiak (2005) reported the use of dinuclear Ni complexes for the formation of CO. Phosphine ligands are also reported for ERC, the first being $Rh(dppe)_2Cl$ (dppe = 1,2-bis(diphenylphosphino)ethane) complex, reported in 1984 by Slater and Wagenknecht. However, it resulted only in the formation of formate and no CO was observed. Later, phosphine ligands of Pd complex were studied and it resulted in the formation of CO in acidic solutions. It is important to note here that basicity/redox potential of the phosphine ligands is crucial for the formation of CO as more negative redox potential results in the formation of H_2 (DuBois *et al.* 1991; DuBois 1997; Raebiger *et al.* 2006).

Table 2.5 Studies on electroreduction of carbon dioxide using metal complex electrocatalysts during 2005-2015

Cathode electrocatalyst	**Electrolyte**	**Experimental parameters**	**Main Products (Faradaic efficiency, %)**	**References**
$[Re(CO)_3\{\alpha,\alpha'$-Diimine-(4-piperidinyl-1,8-naphthalimide)$\}Cl]$ complex	0.1M $TBAPF_6$ with external H^+ sources (CH_3OH, CF_3CH_2OH)	25°C, 1 atm	CO (68-92)	Franco *et al.* (2015)
Multimetallic porphyrin and polyoxotungstate modified electrodes	DMF	25°C, 1 atm	CO, HCOOH, CH_3OH	Garcia *et al.* (2014)
N,N´-ethylenebis(acetylacetoniminato) complex of Ni and Cu	AcN/ DMF/ DMSO + 0.1 M Bu_4NPF_6	25±2°C	$C_2O_4^{-2}$	Udugala-Ganehenege *et al.* (2014)
Ag modified with 3,5-diamino-1,2,4-triazole (DAT)	1 M KOH	25°C	CO	Schmitt and Gewirth (2014)
Diazine bridged dinuclear Re complex	$TBAPF_6$	25°C	-NA-	Valenti *et al.* (2014)
Ni/Co-terpyridine complex	0.1 M TBAP in DMF-H_2O	25°C, 1 atm	CO (38-76)	Elgrishi *et al.* (2014)
Pyridinium ($pyrH^+$) ion	*N*-methyl pyridinium ion	25°C	CH_3OH (30)	Yan *et al.* (2013)
N-based organometallic silver	1 M KOH	25°C, 1 atm	CO (85)	Tornow *et al.* (2012)
Cu complex of [*N*-(2-mercaptopropyl)-*N,N*-bis(2-pyridylmethyl)amine]	Acetonitrile	25°C	$C_2O_4^{-2}$	Angamuthu *et al.* (2010)
Bimetallic Pd complex	DMF	1.04 V *vs.* NHE	CO (80)	Raebiger *et al.* (2006)
Carbene supported copper (I) boryl	Deuterated benzene	25°C, 1 atm	CO	Laitar *et al.* (2005)
Dinuclear Ni complex	Acetonitrile	25°C, 1 atm	CO	Simon-Manso and Kubiak (2005)

Metal complexes do not seem to be very effective for hydrocarbon and alcohol formation possibly because the contact time of the CO_2 with the catalyst is limited and metal-carbon bond gets dissociated quickly and thus multi-electron transfer mechanism gets hindered. Furuya and Matsui (1989) and Magdesieva *et al.* (2002) reported the formation of CH_4 using Cu, Ga and Ti phthalocyanins. Seshadri *et al.* (1994) reported pyridinium ion for methanol production as a novel homogeneous electrocatalyst and Faradaic efficiency of CH_3OH formation was achieved upto 30%. Labeling studies with $^{13}CO_2$ was used to verify the formation of $^{13}CH_3OH$. Later, Yan *et al.* (2013) reported the mechanism of this reaction in which the inner-sphere reduction of pyridinium took place to form a surface hydride. The noticeable attributes of the system were the low overpotential and stability for ~19 hours, which is rare for CO_2 electroreduction systems. Garcia *et al.* (2014) studied the multimetallic porphyrins/polyoxotungstate modified multilayer ITO electrodes for the ERC. Three different metal ions *viz.* Mn(III), Ni(II), and Zn(II), were investigated and formation of CO (3.85×10^{-2} mM) was found when ITO was modified with Ni(II) metal ion at the centre of the porphyrin. However, Mn(III) and Zn(II) metal ions modified ITO electrode resulted in the formation of methanol. The different metal centres in the electrodes were found to be responsible for the activity and selectivity of the electrodes. Strong binding of Mn(III) atoms with the anion (polyoxotungstate) help to produce maximum coverage over the electrode surface, thus resulting in the highest activity. Moreover, it has also been reported that the non-homogeneous film of porphyrins resulted in the random distribution of active sites, which were responsible for the varied electrocatalytic behaviour of the synthesized electrodes. These recent researches prove that hydrocarbons and alcohol formation is also possible using the metal complexes with proper modulation in the metal and ligand moiety. Thus, there is immense scope in the field of metal complexes also to produce fuel kind of products. Table 2.5 summarizes the performance of metal complex electrocatalysts for the reduction of CO_2 dissolved in a medium.

2.5 Metal carbide, metal sulphide, and metal hydride electrocatalysts

Metal carbide, metal sulphide, and metal hydride are not studied well as compared to metals, metal oxides, and metal complexes. Carbides of group V elements (*e.g.* V, Nb, and Ta) have been

investigated for their electrocatalytic activity in ERC by Yotsuhashi *et al.* (2012) and production of CO, CH_4, C_2H_4, and C_2H_6 was reported at low overvoltages. However, when carbides of metals other than group V (*e.g.* Mo, Ti) were tested, then only hydrogen evolution could be observed for which no plausible reason was given. There is no other reported work over metal carbides, as of now. Molybdenum disulphide has been chosen by Asadi *et al.* (2014) to investigate CO_2 electroreduction. Very interesting results were found using first principle modelling, which reveals that the molybdenum-terminated edges of MoS_2 are mainly responsible for its catalytic performance due to their metallic character and high *d*-electron density. Pugh *et al.* (1991) investigated the key steps in ERC for the insertion of CO_2 into metal-hydride (M-H) bond. Studies were carried out for Ru bipyridine complex *cis*-$[Ru(bpy)_2(CO)H]^+$, which acted as a catalyst for ERC and resulted in the formation of CO. The insertion of CO_2 into the Ru-H bond was preceeded by the bipyridinium based reduction of *cis*-$[Ru(bpy)_2(CO)H]^+$. The second step was the re-formation of the metal-hydride bond by the reduction of water. Late transition metal hydrides were also found to reduce CO_2, where trialkylboranes play a key role (Miller *et al.* 2011). It is supposed that the chemistry involves assistance of trialkylborane which forms a formate-borane adduct thus favouring the CO_2 reduction, however further investigation is still going on.

2.6 Summary of literature review

The discussion over electrocatalysts for the formation of fuel kind of products using electrochemical reduction of CO_2 reveals that there are enough possibilities for CO, hydrocarbons, and alcohol product formation. However, still there are various challenges to overcome for the development of this process. The major obstacle is to minimize the competitive hydrogen evolution reaction which is one of the important causes for the under-performance of CO_2 reduction. It has also been seen in the literature that in many of the cases, cyclic voltammetry gives erroneous results, which makes the conclusion unpredictable about the activity of an electrocatalyst. It is difficult to predict the behaviour of the electrocatalysts for the ERC, based on only CV results. This discrepancy also needs to be overcome. Another need is to improve the selectivity of the catalysts for such products which can be directly used as fuels (*e.g.*

hydrocarbons and alcohols). In spite of the significant efforts made for enhancing the Faradaic efficiency, there is scope for further improvement. Energy consumption for carrying out the process needs to be minimized and it requires the development of electrocatalysts which can work at low overpotential. To overcome the high overpotential issues, the use of metal complexes can be advocated. Apart from this, if the metal complexes are tuned in an efficient way, they can also result in hydrocarbon formation along with the CO. To further explore the process, designing of new class of electrocatalysts is essential. In this direction, combined effect of two or three metals can be studied, because combination of metals results in some of the unique properties which can not be obtained with single metals. Further, it has been seen in most of the literature that CO_2 reduction has been performed after dissolving it in the aqueous/non-aqueous medium. However, the reports over direct reduction of gaseous CO_2 are scanty. For the large-scale practical application, direct reduction of gaseous CO_2 is essential. In the light of all these facts, the objective of this research work has been formulated, as discussed in the subsequent section.

2.7 Research objectives

Based on the literature survey, it can be said that there is need to investigate the electrocatalysts for the production of fuel kind of products in gas phase ERC *viz.* direct electrochemical reduction of gaseous CO_2 (dERC). Moreover, the technical know-how of the dERC needs to be explored. Further, lack of any specific method for shortlisting the electrocatalysts among the group of many for dERC, demands the formulation of a suitable method. Therefore, the major **aim of the thesis is to develop suitable electrocatalysts to improve the efficiency of the direct electrochemical reduction of gaseous CO_2 (dERC) at low overpotential along with production of fuel kind of products**. The development of a suitable method for the preliminary selection of electrocatalysts was also attemped. To achieve these aims, at the first step, a protocol was developed for the quick selection of electrocatalysts. As the second objective, four metals were studied to access their performance in the gas-phase CO_2 reduction. Further, some of these metals were modified with the formation of metal oxides. Some of the selected metals were also modified by incorporating into the ligand and formation of metal complexes. To improve the efficiency further, and to see

the combined effect of two metals over dERC, bimetallic system was also studied. The various investigations which were carried out to accomplish the objective are given as follows:

I. Development of catalytic activity protocol for electrochemical reduction of CO_2

A catalytic activity protocol was developed and validated for the quick selection of useful electrocatalysts. The protocol also enabled the comparison among various electrocatalysts, based on their performance for CO_2 electroreduction.

II. Investigations to elucidate the performance of metal electrocatalysts for gas-phase electrochemical reduction of CO_2

Four metals, Cu, Zn, Ni, and Co were selected and studied for dERC. For full cell reaction, the metals were electroplated over suitable substrate and analyzed. The developed electrodes (cathodes) were characterized using X-ray diffraction (XRD), energy dispersive X-ray spectroscopy (EDX), scanning electron microscopy (SEM), and electrochemical tests. These metal electrodes were studied for direct gas phase electroreduction of CO_2.

III. Development of metal oxides for dERC to improve the performance

Oxides of Cu, Zn, Ni, and Co were synthesized *viz.* CuO, ZnO, NiO, and Co_3O_4. These metal oxides were characterized using X-ray diffraction (XRD), energy dispersive X-ray spectroscopy (EDX), BET surface area studies, Fourier transform infrared (FTIR) spectroscopy, field emission scanning electron microscopy (FESEM), and electrochemical tests. The developed metal oxides were studied thoroughly in full cell reactions and their performances were compared with the metals.

IV. Development of metal complexes using salen ligand for lowering the overpotential of the dERC and to improve the performance further

The salen ligand and corresponding metal complexes of Cu and Ni were synthesized. The metal complexes were thoroughly characterized using Fourier transform infrared (FTIR) spectroscopy,

nuclear magnetic resonance (NMR) spectroscopy, high resolution mass spectroscopy (HR-MS), elemental (CHN) analysis, and electrochemical tests. The metal complexes were studied in full cell to estimate their efficiency, selectivity, and overpotential requirement. Based on the reaction products, probable mechanism was also elucidated for dERC.

V. Development of a bimetallic electrocatalyst to study the effect of combination of metals over dERC

To see the combined effect of two metals in the dERC, bimetallic electrocatalyst was developed. It was characterized using X-ray diffraction (XRD), energy dispersive X-ray spectroscopy (EDX), BET surface area studies, field emission scanning electron microscopy (FESEM), transmission electron microscopy (TEM), and electrochemical tests and further tested in full cell reaction.

Next chapter provides the details over the experimental set-up used for the direct electrochemical reduction of gaseous CO_2. Various general techniques and methods used to carry out these works are also elaborated in chapter 3. Moreover, the techniques particular to specific electrocatalysts are detailed in the relevant chapters.

References

Aeshala L.M., Rahman S.U., and Verma A. (2012), Effect of solid polymer electrolyte on electrochemical reduction of CO_2, *Separation and Purification Technology*, 94, 131-137.

Aeshala L.M., Uppaluri R.G., and Verma A. (2013), Effect of cationic and anionic solid polymer electrolyte on direct electrochemical reduction of gaseous CO_2 to fuel, *Journal of CO_2 Utilization*, 3-4, 49-55.

Aeshala L.M., Uppaluri R.G., and Verma A. (2014), Electrochemical conversion of CO_2 to fuels: Tuning of reaction zone using suitable functional group in solid polymer electrolyte, *Physical Chemistry Chemical Physics*, 16, 17588-17594.

Aeshala L.M. and Verma A. (2015), Amines as reaction environment regulator for CO_2 reduction to CH_4, *Macromolecular Symposia*, Accepted.

Andrews E., Ren M., Wang F., Zhang Z., Sprunger P., Kurtz R., and Flake J. (2013), Electrochemical reduction of CO_2 at Cu nanocluster/$(10\bar{1}0)$ ZnO electrodes, *Journal of the Electrochemical Society*, 160(11), H841-H846.

Angamuthu R., Byers P., Lutz M., Spek A.L., and Bouwman E. (2010), Electrocatalytic CO_2 conversion to oxalate by a copper complex, *Science*, 327, 313-315.

Asadi M., Kumar B., Behranginia A., Rosen B.A., Baskin A., Repnin N., Pisasale D., Phillips P., Zhu W., Haasch R., Klie R.F., Kral P., Abiade J., and Salehi-Khojin A. (2014), Robust carbon dioxide reduction on molybdenum disulphide edges, *Nature Communications*, 5, 4470-4477.

Azuma M., Hashimoto K., Hiramoto M., Watanabe M., and Sakata T. (1990), Electrochemical reduction of carbon dioxide on various metal electrodes in low temperature aqueous $KHCO_3$ media, *Journal of Electrochemical Society*, 137(6), 1772-1778.

Bandi A. (1990), Electrochemical reduction of carbon dioxide on conductive metallic oxides, *Journal of the Electrochemical Society*, 137(7), 2157-2160.

Bandi A. and Kuhne H.M. (1992), Electrochemical reduction of carbon dioxide in water: Analysis of reaction mechanism on ruthenium-titanium-oxide, *Journal of the Electrochemical Society*, 139(6), 1605-1610.

Behar D., Dhanasekaran T., Neta P., Hosten C.M., Ejeh D., Hambright P., and Fujita E. (1998), Cobalt porphyrin catalyzed reduction of CO_2. Radiation, chemical, photochemical, and electrochemical studies, *Journal of Physical Chemistry*, 102, 2870-2877.

Behnamfar M.T. (2015), Preparation of Gd_2O_3 nanoparticles from a new precursor and their catalytic activity for electrochemical reduction of CO_2 to CO, *Journal of Particle Science and Technology*, 1, 21-30.

Beley M., Collin J.P., Ruppert R., and Sauvage J.P. (1984), Nickel(II)-cyclam: an extremely selective electrocatalyst for reduction of CO_2 in water, *Chemical Communications*, 19, 1315-1316.

Beley M., Collin J.P., Ruppert R., and Sauvage J.P. (1986), Electrocatalytic reduction of CO_2 by Ni Cyclam^{2+} in water: Study of the factors affecting the efficiency and the selectivity of the process, *Journal of American Chemical Society*, 108, 7461-7467.

Benson E.E., Kubiak C.P., Sathrum A.J., and Smieja J.M. (2009), Electrocatalytic and homogeneous approaches to conversion of CO_2 to liquid fuels, *Chemical Society Reviews*, 38, 89-99.

Bhugun I., Lexa D., and Saveant J.M. (1996), Catalysis of the electrochemical reduction of carbon dioxide by iron(0) porphyrins: Synergistic effect of weak Bronsted acids, *Journal of American Chemical Society*, 118, 1769-1776.

Bruce M.R.M., Megehee E., Sullivan B.P., Thorp H.H., O'Toole T.R., Downard A., and Meyer T.J. (1988), Electrocatalytic reduction of CO_2 by associative activation, *Organometallics*, 7, 238-240.

Bruce M.R.M., Megehee E., Sullivan B.P., Thorp H.H., O'Toole T.R., Downard A., Pugh J.R., and Meyer T.J. (1992), Electrocatalytic reduction of carbon dioxide based on 2,2'-bipyridyl complexes of Osmium, *Inorganic Chemistry*, 31, 4864-4873.

Centi G., Perathoner S., Wine G., and Gangeri M. (2007), Electrocatalytic conversion of CO_2 to long carbon-chain hydrocarbons, *Green Chemistry*, 9, 671-678.

Chen C.S., Handoko A.D., Wan J.H., Ma L., Ren D., and Yeo B.S. (2015), Stable and selective electrochemical reduction of carbon dioxide to ethylene on copper mesocrystals, *Catalysis Science & Technology*, 5, 161-168.

Chi D., Yang H., Du Y., Lv T., Sui G., Wang H., and Lu J. (2014), Morphology controlled CuO nanoparticles for electroreduction of CO_2 to ethanol, *RSC Advances*, 4, 37329-37332.

Collin J.P., Jouaiti A., and Sauvage J.P. (1988), Electrocatalytic properties of $Ni(cyclam)^{2+}$ and $Ni_2(biscyclam)^{4+}$ with respect to CO_2 and H_2O reduction, *Inorganic Chemistry*, 27, 1986-1990.

Cook R.L., MacDuff R.C., and Sammells A.F. (1988), Ambient temperature gas phase CO_2 reduction to hydrocarbons at solid polymer electrolyte cells, *Journal of the Electrochemical Society*, 135, 1470-1471.

DeWulf D.W. and Bard A.J. (1988), The electrochemical reduction of CO_2 to CH_4 and C_2H_4 at Cu/Nafion electrodes (solid polymer electrolyte structures), *Catalysis Letters*, 1, 73-80.

DiMeglio J.L. and Rosenthal J. (2013), Selective conversion of CO_2 to CO with high efficiency using an inexpensive Bismuth based electrocatalyst, *Journal of American Chemical Society*, 135, 8798-8801.

DuBois D.L. (1997), Development of transition metal phosphine complexes as electrocatalysts for CO_2 and CO reduction, *Comments on Inorganic Chemistry*, 19(5), 307-325.

DuBois D.L., Miedaner A., and Haltiwanger R.C. (1991), Electrochemical reduction of CO_2 catalyzed by [Pd(triphosphine)(solvent)]$(BF_4)_2$ complexes: Synthetic and mechanistic studies, *Journal of American Chemical Society*, 113(23), 8753 – 8764.

Elgrishi N., Chambers M.B., Artero V., and Fontecave M. (2014), Terpyridine complexes of first row transition metals and electrochemical reduction of CO_2 to CO, *Physical Chemistry Chemical Physics*, 16, 13635-13644.

Fisher B. and Eisenberg R. (1980), Electrocatalytic reduction of carbon dioxide by using macrocycles of nickel and cobalt, *Journal of American Chemical Society*, 102, 7361-7363.

Franco F., Cometto C., Garino C., Minero C., Sordello F., Nervi C., and Gobetto R. (2015), Photo- and electrocatalytic reduction of CO_2 by [$Re(CO)_3${α,α´-Diimine-(4-piperidinyl-1,8-naphthalimide)}Cl] complexes, *European Journal of Inorganic Chemistry*, 296-304.

Frese Jr. K.W. (1991), Electrochemical reduction of CO_2 at intentionally oxidized copper electrodes, *Journal of the Electrochemical Society*, 138(11), 3338-3344.

Frese Jr. K.W. and Leach S. (1985), Electrochemical reduction of carbon dioxide to methane, methanol and CO on Ru electrodes, *Journal of the Electrochemical Society*, 132(1), 259-260.

Friebe P., Bogdanoff P., Alonso-Vante N., and Tributsch H. (1997), A real time mass spectroscopy study of the (electro)chemical factors affecting CO_2 reduction at copper, *Journal of Catalysis*, 168, 374-385.

Furuya N. and Matsui K. (1989), Electroreduction of carbon dioxide on gas-diffusion electrodes modified by metal phthalocyanines, *Journal of Electroanalytical Chemistry and Interfacial Electrochemistry*, 271(1-2), 181-191.

Gambarotta S., Arena F., Floriani C., and Zanazzi F. (1982), Carbon dioxide fixation: Bifunctional complexes containing acidic and basic sites working as reversible carriers, *Journal of American Chemical Society*, 104, 5082-5092.

Garcia M., Aguirre M.J., Canzi G., Kubiak C.P., Ohlbaum M., and Isaacs M. (2014), Electro and photoelectrochemical reduction of carbon dioxide on multimetallic porphyrins/polyoxotungstate modified electrodes, *Electrochimica Acta*, 115, 146-154.

Goncalves M.R., Gomes A., Condeco J., Fernandes R., Pardal T., Sequeira C.A.C., and Branco J.B. (2010), Selective electrochemical conversion of CO_2 to C_2 hydrocarbons, *Energy Conversion and Management*, 51, 30-32.

Grodkowski J., Neta P., Fujita E., Mahammed A., Simkhovich L., and Gross Z. (2002), Reduction of cobalt and iron corroles and catalyzed reduction of CO_2, *Journal of Physical Chemistry A*, 106, 4772-4778.

Guerra M., Quintanilla S., and Irabien A. (2012), Conversion of carbon dioxide into formate using a continuous electrochemical reduction process in a lead cathode, *Chemical Engineering Journal*, 207-208, 278-284.

Hammouche M., Lexa D., Momenteau M., and Saveant J.M. (1991), Chemical catalysis of electrochemical reactions. Homogeneous catalysis of the electrochemical reduction of carbon dioxide by iron("0") porphyrins. Role of the addition of magnesium cations, *Journal of American Chemical Society*, 113, 8455-8466.

Hara K., Kudo A., Sakata T., and Watanabe M. (1995 a), High efficiency electrochemical reduction of carbon dioxide under high pressure on a gas diffusion electrode containing Pt catalysts, *Journal of the Electrochemical Society*, 142(4), L57-L59.

Hara K., Kudo A., and Sakata T. (1995 b), Electrochemical reduction of carbon dioxide under high pressure on various electrodes in an aqueous electrolyte, *Journal of Electroanalytical Chemistry*, 391, 141-147.

Hawecker J., Lehn J.M., and Ziessel R. (1984), Electrocatalytic reduction of carbon dioxide mediated by $Re(bipy)(CO)_3Cl$ (bipy = 2,2'-bipyridine), *Journal of Chemical Society, Chemical Communications*, 6, 328-330.

Haynes L. and Sawyer D.T. (1967), Electrochemistry of CO_2 in dimethyl sulfoxide at gold and mercury electrodes, *Analytical Chemistry*, 39(3), 332-338.

Hori Y. and Suzuki S. (1982), Electrolytic reduction of carbon dioxide at mercury electrode in aqueous solution, *Bulletin of Chemical Society of Japan*, 55(3), 660-665.

Hori Y., Kikuchi K., and Suzuki S. (1985), Production of CO and CH_4 in electrochemical reduction of CO_2 at metal electrodes in aqueous hydrogencarbonate solution, *Chemistry Letters*, 1695-1698.

Hori Y., Kikuchi K., Murata A., and Suzuki S. (1986), Production of methane and ethylene in electrochemical reduction of carbon dioxide at copper electrode in aqueous hydrogencarbonate solution, *Chemistry Letters*, 897-898.

Hori Y., Koga O., Yamazaki H., and Matsuo T. (1995), Infrared spectroscopy of adsorbed CO and intermediate species in electrochemical reduction of CO_2 to hydrocarbons on a Cu electrode, *Electrochimica Acta*, 40, 2617-2622.

Hori Y., Konishi H., Futamura T., Murata A., Koga O., Sakurai H., and Oguma K. (2005), "Deactivation of copper electrode" in electrochemical reduction of CO_2, *Electrochimica Acta*, 50, 5354-5369.

Hori Y., Murata A., and Ito S. (1990), Enhanced evolution of CO and suppressed formation of hydrocarbons in electroreduction of CO_2 at a copper electrode modified with cadmium, *Chemistry Letters*, 1231-1234.

Hori Y., Murata A., and Takahashi R. (1989), Formation of hydrocarbons in the electrochemical reduction of carbon dioxide at a copper electrode in aqueous solution, *Journal of Chemical Society, Faraday Transactions 1*, 85(8), 2309-2326.

Hori Y., Takahashi I., Koga O., and Hoshi N. (2002), Selective formation of C_2 compounds from electrochemical reduction of CO_2 at a series of copper single crystal electrodes, *Journal of Physical Chemistry B*, 106, 15-17.

Hori Y., Takahashi I., Koga O., and Hoshi N. (2003), Electrochemical reduction of CO_2 at various series of copper single crystal electrodes, *Journal of Molecular Catalysis A: Chemical*, 199, 39-47.

Hori Y., Wakebe H., Tsukamoto T., and Koga O. (1994), Electrocatalytic process of CO selectivity in electrochemical reduction of CO_2 at metal electrodes in aqueous media, *Electrochimica Acta*, 39(11-12), 1833-1839.

Hori Y. (2003), CO_2 reduction, catalyzed by metal electrodes, In Vielstich *et al.* (ed.) 'Electrocatalysis, Handbook of fuel cells', Vol. 2, Ch. 48, John Wiley & Sons, England, pp. 720-732.

Hoshi N. and Hori Y. (2000), Electrochemical reduction of carbon dioxide at a series of platinum single crystal electrodes, *Electrochimica Acta*, 45, 4263-4270.

Hoshi N., Ito H., Suzuki T., and Hori Y. (1995), CO_2 reduction on Rh single crystal electrodes and the structural effect, *Journal of Electroanalytical Chemistry*, 395, 309-312.

Hoshi N., Suzuki T., and Hori Y. (1996), Step density dependence of CO_2 reduction rate on Pt(S)-[n(111) × (111)] single crystal electrodes, *Electrochimica Acta*, 41(10), 1647-1653.

Hoshi N., Suzuki T., and Hori Y. (1997), Catalytic activity of CO_2 reduction on Pt single crystal electrodes: Pt(S)-[n(111) × (111)], Pt(S)-[n(111) × (100)], Pt(S)-[n(100) × (111)], *Journal of Physical Chemistry B*, 101, 8520-8524.

Ikeda S., Ito T., Azuma K., Ito K., and Noda H. (1995), Electrochemical mass reduction of carbon dioxide using Cu loaded gas diffusion electrodes. I. Preparation of electrode and reduction products, *Denki Kagaku*, 63(4), 303-309.

Ikeda S., Ito T., Azuma K., Nishi N., Ito K., and Noda H. (1996), Electrochemical mass reduction of carbon dioxide using Cu-loaded gas diffusion electrodes. II. Proposal of reaction mechanism, *Denki Kagaku*, 64(1), 69-75.

Ikeda S., Ito K., and Noda H. (2009), Electrochemical reduction of carbon dioxide using gas diffusion electrodes loaded with fine catalysts, *American Institute of Physics Conference Proceedings*, 1136, 108-113.

Ikeda S., Tomita Y., Hattori A., Ito K., Noda H., and Sakai M. (1993), Selective ethanol formation by electrochemical reduction of carbon dioxide on electrodes comprised of the mixtures of copper and zinc oxides, *Denki Kagaku*, 61(7), 807-809.

Inglis J.L., MacLean B.J., Pryce M.T., and Vos J.G. (2012), Electrocatalytic pathways towards sustainable fuel production from water and CO_2, *Coordination Chemistry Reviews*, 256, 2571-2600.

Innocent B., Liaigre D., Pasquier D., Ropital F., Leger J.M., and Kokoh K.B. (2009), Electroreduction of carbon dioxide to formate on lead electrode in aqueous medium, *Journal of Applied Electrochemistry*, 39, 227-232.

Isaacs M., Canales J.C., Riquelme A., Lucero M., Aguirre M.J., and Costamagna J. (2003), Contribution of the ligand to the electroreduction of CO_2 catalyzed by a cobalt(II)macrocyclic complex, *Journal of Coordination Chemistry*, 56(14), 1193-1201.

Ishida H., Tanaka K., and Tanaka T. (1987), Electrochemical CO_2 reduction catalyzed by $[Ru(bpy)_2(CO)_2]^{2+}$ and $[Ru(bpy)_2(CO)Cl)^{+}$. The effect of pH on the formation of CO and $HCOO^-$, *Organometallics*, 6, 181-186.

Kaneco S., Iiba K., Ohta K., Mizuno T., and Saji A. (1998 b), Electrochemical reduction of CO_2 at an Ag electrode in KOH-methanol at low temperature, *Electrochimica Acta*, 44, 573-578.

Kaneco S., Iiba K., Ohta K., and Mizuno T. (1999 a), Electrochemical reduction of carbon dioxide on copper in methanol with various potassium supporting electrolytes at low temperature, *Journal of Solid State Electrochemistry*, 3, 424-428.

Kaneco S., Iiba K., Ohta K., Mizuno T., and Saji A. (1998 c), Electrochemical reduction of CO_2 on Au in KOH + methanol at low temperature, *Journal of Electroanalytical Chemistry*, 441, 215-220.

Kaneco S., Iiba K., Suzuki S., Ohta K., and Mizuno T. (1999 b), Electrochemical reduction of carbon dioxide to hydrocarbons with high Faradaic efficiency in LiOH/methanol, *Journal of Physical Chemistry B*, 103, 7456-7460.

Kaneco S., Iwao R., Iiba K., Ohta K., and Mizuno T. (1998 a), Electrochemical conversion of carbon dioxide to formic acid on Pb in KOH/methanol electrolyte at ambient temperature and pressure, *Energy*, 23(12), 1107-1112.

Kaneco S., Sakaguchi Y., Katsumata H., Suzuki T., and Ohta K. (2007), Cu deposited nickel electrode for the electrochemical conversion of CO_2 in water/methanol mixture media, *Bulletin of Catalysis Society of India*, 6, 74-82.

Kaneco S., Ueno Y., Katsumata H., Suzuki T., and Ohta K. (2006), Electrochemical reduction of CO_2 in copper particle suspended methanol, *Chemical Engineering Journal*, 119, 107-112.

Keerthiga G., Viswanathan B., Pulikottil C.A., and Chetty R. (2012), Electrochemical reduction of carbon dioxide at surface oxidized copper electrodes, *Bonfring International Journal of Industrial Engineering and Management Science*, 2(1), 41-43.

Komatsu S., Tanaka M., Okumura A., and Kungi A. (1995), Preparation of Cu-solid polymer electrolyte composite electrodes and application to gas-phase electrochemical reduction of CO_2, *Electrochimica Acta*, 40, 745-753.

Koper M.T.M. (2013), Hydrogen electrocatalysis – A basic solution, *Nature Chemistry*, 5, 255-256.

Kudo A., Nakagawa S., Tsuneto A., and Sakata T. (1993), Electrochemical reduction of high pressure CO_2 on Ni electrodes, *Journal of Electrochemical Society*, 140(6), 1541-1545.

Kyriacou G. and Anagnostopoulos A. (1992), Electroreduction of CO_2 on differently prepared copper electrodes. The influence of electrode treatment on the current efficiencies, *Journal of Electroanalytical Chemistry*, 322, 233-246.

Laitar D.S., Muller P., and Sadighi J.P. (2005), Efficient homogeneous catalysis in the reduction of CO_2 to CO, *Journal of American Chemical Society*, 127, 17196-17197.

Lan Y., Gai C., Kenis P.J.A., and Lu J. (2014), Electrochemical reduction of carbon dioxide on Cu/CuO core/shell catalysts, *ChemElectroChem*, 1(9), 1577-1582.

Lee J. and Tak Y. (2001), Electrocatalytic activity of Cu electrode in electroreduction of CO_2, *Electrochimica Acta*, 46, 3015-3022.

Le M., Ren M., Zhang Z., Sprunger P.T., Kurtz R.L., and Flake J.C. (2011), Electrochemical reduction of CO_2 to CH_3OH at copper oxide surfaces, *Journal of the Electrochemical Society*, 158(5), E45-E49.

Li C.W. and Kanan M.W. (2012), CO_2 reduction at low overpotential on Cu electrodes resulting from the reduction of thick Cu_2O films, *Journal of the American Chemical Society*, 134, 7231-7234.

Li H. and Oloman C. (2006), Development of a continuous reactor for the electroreduction of carbon dioxide to formate – Part 1: Process variables, *Journal of Applied Electrochemistry*, 36, 1105-1115.

Li H. and Oloman C. (2007), Development of a continuous reactor for the electroreduction of carbon dioxide to formate – Part 2: Scale-up, *Journal of Applied Electrochemistry*, 37, 1107-1117.

Lieber C.M. and Lewis N.S. (1984), Catalytic reduction of CO_2 at carbon electrodes modified with cobalt phthalocyanin, *Journal of American Chemical Society*, 106, 5033-5034.

Lv W., Zhang R., Gao P., and Lei L. (2014), Studies on the Faradaic efficiency for electrochemical reduction of carbon dioxide to formate on tin electrode, *Journal of Power Sources*, 253, 276-281.

Machunda R.L., Lee J.G., and Lee J. (2010), Microstructural surface changes of electrodeposited Pb on gas diffusion electrode during electroreduction of gas-phase CO_2, *Surface and Interface Analysis*, 42, 564-567.

Magdesieva T.V., Zhukov I.V., Kravchuk D.N., Semenikhin O.A., Tomilova L.G., and Butin K.P. (2002), Electrocatalytic CO_2 reduction in methanol catalyzed by mono-, di-, and electropolymerized phthalocyanin complexes, *Russian Chemical Bulletin, International Edition*, 51(5), 805-812.

Mahmood M.N., Masheder D., and Harty C.J. (1987 a), Use of gas-diffusion electrodes for high rate electrochemical reduction of carbon dioxide. I. Reduction at lead, indium- and tin-impregnated electrodes, *Journal of Applied Electrochemistry*, 17, 1159-1170.

Mahmood M.N., Masheder D., and Harty C.J. (1987 b), Use of gas-diffusion electrodes for high rate electrochemical reduction of carbon dioxide. II. Reduction at metal phthalocyanine-impregnated electrodes, *Journal of Applied Electrochemistry*, 17, 1223-1227.

Miller A.J.M., Labinger J.A., and Bercaw J.E. (2011), Trialkylborane assisted CO_2 reduction by late transition metal hydrides, *Organometallics*, 30, 4308-4314.

Murata A. and Hori Y. (1991), Electrochemical reduction of CO_2 to CO at Ni electrodes modified with Cd, *Chemistry Letters*, 181-184.

Narayanan S.R., Haines B., Soler J., and Valdez T.I. (2011), Electrochemical conversion of carbon dioxide to formate in alkaline polymer electrolyte membtane cells, *Journal of Electrochemical Society*, 158, A167-A173.

Noda H., Ikeda S., Oda Y., and Ito K. (1989), Potential dependencies of the products on electrochemical reduction of carbon dioxide at copper electrode, *Chemistry Letters*, 18(2), 289-292.

Ogura K. (2013), Electrochemical reduction of carbon dioxide to ethylene: Mechanistic approach, *Journal of CO_2 Utilization*, 1, 43-49.

Ohta K., Kawamoto M., Mizuno T., and Lowy D.A. (1998), Electrochemical reduction of carbon dioxide in methanol at ambient temperature and pressure, *Journal of Applied Electrochemistry*, 28, 717-724.

Ohya S., Kaneco S., Katsumata H., Suzuki T., and Ohta K. (2009), Electrochemical reduction of CO_2 in methanol with aid of CuO and Cu_2O, *Catalysis Today*, 148, 329-334.

Perez-Rodriguez S., Garcia G., Calvillo L., Celorrio V., Pastor E., and Lazaro J. (2011), Carbon supported Fe catalysts for CO_2 electroreduction to high added value products: A DEMS study: Effect of the functionalization of the support, *International Journal of Electrochemistry*, Article Id 249804, doi:10.4061/2011/249804.

Popic J.P., Avramov-Ivic M.L., and Vukovic N.B. (1997), Reduction of carbon dioxide on ruthenium oxide and modified ruthenium oxide electrodes in 0.5 M $NaHCO_3$, *Journal of Electroanalytical Chemistry*, 421, 105-110.

Prakash G.K.S., Viva F.A., and Olah G.A. (2013), Electrochemical reduction of CO_2 over Sn-Nafion® coated electrode for a fuel-cell-like device, *Journal of Power Sources*, 223, 68-73.

Pugh J.R., Bruce M.R.M., Sullivan B.P., and Meyer T.J. (1991), Formation of metal-hydride bond and the insertion of CO_2. Key steps in the electrocatalytic reduction of carbon dioxide to formate anion, *Inorganic Chemistry*, 30(1), 86-91.

Qu J., Zhang X., Wang Y., and Xie C. (2005), Electrochemical reduction of CO_2 on RuO_2/TiO_2 nanotubes composite modified Pt electrode, *Electrochimica Acta*, 50, 3576-3580.

Raebiger J.W., Turner J.W., Noll B.C., Curtis C.J., Miedaner A., Cox B., and DuBois D.L. (2006), Electrochemical reduction of CO_2 to CO catalyzed by a bimetallic palladium complex, *Organometallics*, 25, 3345-3351.

Ren D., Deng Y., Handoko A.D., Chen C.S., Malkhandi S., and Yeo B.S. (2015), Selective electrochemical reduction of carbon dioxide to ethylene and ethanol on copper(I) oxide catalysts, *ACS Catalysis*, 5, 2814-2821.

Roberts F.S., Kuhl K.P., and Nilsson A. (2015), High selectivity for ethylene from carbon dioxide reduction over copper nanocube electrocatalysts, *Angewandte Chemie*, 127(17), 5268-5271.

Schmitt K.G. and Gewirth A.A. (2014), *In situ* surface-enhanced Raman spectroscopy of the electrochemical reduction of carbon dioxide on silver with 3,5-diamino-1,2,4-triazole, *The Journal of Physical Chemistry C*, 118, 17567-17576.

Seshadri G., Lin C., and Bocarsly A.B. (1994), A new homogeneous electrocatalyst for the reduction of carbon dioxide to methanol at low overpotential, *Journal of Electroanalytical Chemistry*, 372(1-2), 145-150.

Sharma P.P., Ke F.S., and Zhou X.D. (2014), The role of nonstoichiometry on the electrocatalytic properties of $TiO_{2-\delta}$ towards the conversion of carbon dioxide to fuels, *ECS Transactions*, 61(1), 331-339.

Shuang S., Zhiqiao H., Jiexu Y., and Jianmeng C. (2006), Preliminary study on electrochemical reduction of carbon dioxide on nickel and platinum electrodes, *High Technology Letters*, 12(3), 333-336.

Simon-Manso E. and Kubiak C.P. (2005), Dinuclear nickel complexes as catalysts for electrochemical reduction of carbon dioxide, *Organometallics*, 24, 96-102.

Slater S. and Wagenknecht J.H. (1984), Electrochemical reduction of carbon dioxide catalyzed by $Rh(diphos)_2Cl$, *Journal of American Chemical Society*, 106(18), 5367-5368.

Subramanian K., Asokan K., Jeevarathinam D., and Chandrasekaran M. (2007), Electrochemical membrane reactor for the reduction of carbon dioxide to formate, *Journal of Applied Electrochemistry*, 37, 255-260.

Summers D.P., Leach S., and Frese Jr. K.W. (1986), The electrochemical reduction of aqueous carbon dioxide to methanol at molybdenum electrodes with low overpotentials, *Journal of Electroanalytical Chemistry*, 205, 219-232.

Terunuma Y., Saitoh A., and Momose Y. (1997), Relationship between hydrocarbon production in the electrochemical reduction of CO_2 and the characteristics of the Cu electrode, *Journal of Electroanalytical Chemistry*, 434, 69-75.

Tezuka M., Yajima T., and Tsuchiya A. (1982), Electroreduction of carbon dioxide catalyzed by iron sulfur clusters $[Fe_4S_4(SR)_4]^{2-}$, *Journal of American Chemical Society*, 104, 6834-6836.

Tornow C.E., Thorson M.R., Ma S., Gewirth A.A., and Kenis P.J.A. (2012), Nitrogen-based catalysts for the electrochemical reduction of CO_2 to CO, *Journal of American Chemical Society*, 134, 19520-19523.

Tsai C.C., Bugayong J., and Griffin G.L. (2012), Role of surface oxide layer during CO_2 reduction at copper electrodes, *Materials Research Society Symposium Proceedings*, 1446, 59-64.

Udugala-Ganehenege M.Y., Dissanayake N.M., Liu Y., Bond A.M., and Zhang J. (2014), Electrochemistry of nickel(II) and copper(II) *N,N´*-ethylenebis(acetylacetoniminato) complexes and their electrocatalytic activity for reduction of carbon dioxide and carboxylic acid protons, *Transition Metal Chemistry*, 39, 819-830.

Ullah N., Ali I., Jansen M., and Omanovic S. (2015), Electrochemical reduction of CO_2 in an aqueous electrolyte employing an iridium/ruthenium oxide electrode, *The Canadian Journal of Chemical Engineering*, 93, 55-62.

Valenti G., Panigati M., Boni A., D'Alfonso G., Paolucci F., and Prodi L. (2014), Diazine bridged dinuclear rhenium complex: New molecular material for the CO_2 conversion, *Inorganica Chimica Acta*, 417, 270-273.

Yan Y., Zeitler E.L., Gu J., Hu Y., and Bocarsly A.B. (2013), Electrochemistry of aqueous pyridinium: Exploration of a key aspect of electrocatalytic reduction of CO_2 to methanol, *Journal of the American Chemical Society*, 135(38), 14020-14023.

Yano J. and Yamasaki S. (2008), Pulse-mode electrochemical reduction of carbon dioxide using copper and copper oxide electrodes for selective ethylene formation, *Journal of Applied Electrochemistry*, 38, 1721-1726.

Yano H., Tanaka T., Nakayama M., and Ogura K. (2004), Selective electrochemical reduction of CO_2 to ethylene at a three-phase interface on copper(I) halide-confined Cu-mesh electrodes in acidic solutions of potassium halides, *Journal of Electroanalytical Chemistry*, 565, 287-293.

Yano J., Morita T., Shimano K., Nagami Y., and Yamasaki S. (2007), Selective ethylene formation by pulse mode electrochemical reduction of carbon dioxide using copper and copper-oxide electrodes, *Journal of Solid State Electrochemistry*, 11, 554-557.

Yotsuhashi S., Taniguchi R., and Zenitani Y. (2012), Carbon dioxide reduction method, and carbon dioxide reduction catalyst and carbon dioxide reduction device used for the method, US Patent, US2012/0018311 A1.

Zhou F., Liu S., Yang B., Wang P., Alshammari A.S., and Deng Y. (2014), Highly selective electrocatalytic reduction of carbon dioxide to carbon monoxide on silver electrode with aqueous ionic liquids, *Electrochemistry Communications*, 46, 103-106.

3

Experimental

3.1 Background

3.2 Electrocatalyst characterization techniques

3.3 Evaluation of electrocatalyst for CO_2 reduction

3.4 Experimental techniques used in electrochemical studies

3.5 Product analysis and quantification

Chapter 3

Experimental

In this chapter various techniques and methods to accomplish the work are discussed. Experimental methodologies for characterization of the developed electrocatalysts are discussed in the beginning. Later, design of the experimental set-up and electrochemical reactor is illustrated. Various electrochemical techniques used and the product analyses methods are also discussed. Moreover, it may be noted that only common experimental techniques are discussed in this chapter, while, the synthesis of electrocatalysts and specific characterization techniques along with the materials are discussed in the relevant chapters.

3.1 Background

Characterization of a material refers to the broad and general process by which a material's structure, and physical and (electro)chemical properties are probed and measured. The synthesized electrocatalysts need to be characterized to ascertain right synthesis. Apart from the physical (*ex-situ*) characterizations, electrochemical (*in-situ*) characterizations are also must for an electrocatalyst.

3.2 Electrocatalyst characterization techniques

The synthesized electrocatalysts were characterized using *ex-situ* characterization techniques *viz.* X-ray diffraction (XRD) studies, Fourier transform infrared (FTIR) spectroscopy, Brunauer-Emmett-Teller (BET) surface area analysis, scanning electron microscopy (SEM), field emission scanning electron microscopy (FESEM), transmission electron microscopy (TEM), energy dispersive X-ray spectroscopy (EDX), nuclear magnetic resonance (NMR) spectroscopy, high resolution mass spectrometry (HR-MS), and elemental analysis. After the characterization by *ex-situ* methods, the electrocatalysts were further analyzed in electrochemical environment for *in-situ* studies which include linear sweep voltammetry (LSV), cyclic voltammetry (CV), and chronoamperometry (CA).

3.2.1 X-ray diffraction (XRD)

X-ray diffraction is an effective method for determining crystal structure of materials. It is a rapid analytical technique primarily used for phase identification of a crystalline material and can provide information on unit cells. The material to be analyzed is finely ground, homogenized, and average bulk composition is determined. X-ray diffraction results from the constructive interference between X-rays and electrons of the sample material. The X-rays are produced using a cathode ray tube. These X-rays are filtered to produce monochromatic radiation and collimated to concentrate before directing towards the sample. Constructive interference is produced when the conditions satisfy Bragg's law according to equation (3.1).

$$n\lambda = 2d \sin\theta \quad (3.1)$$

where, λ is the wavelength, d is the spacing between the two crystal planes, and θ is the Bragg's angle, which is the angle between incident and reflected beam.

These diffracted X-rays are then detected, processed and counted. Diffraction peaks are converted to *d*-spacing, which allows identification of the substance because each substance has a set of unique *d*-spacings. Usually this is carried out by comparison of *d*-spacings with standard reference patterns.

X-ray diffraction (XRD) analysis of the electrocatalysts and electrodes was carried out in an advanced X-ray diffractometer (make: Brucker, model: D8 Advance). The powdered electrocatalysts were kept in the sample holder, which was fixed in the XRD analyzer. The radiation produced by X-ray guns was the monochromatic Cu-Kα radiation. Operated at approximately 40 kV and 40 mA, the wavelength of Cu-Kα radiation is 1.54 Å. The XRD gun was swept in different ranges for the different samples with scan speed of 1 s·step^{-1}.

3.2.2 Fourier transform infrared (FTIR) spectroscopy

In FTIR spectroscopy, IR radiation is passed through a sample. Some amount of the infrared radiation is absorbed by the sample while some amount of it is passed through (transmitted). This results in a spectrum, which represents the molecular absorption and transmission by the sample. Each molecular structure produces a unique infrared spectrum, same as of fingerprint hence also called as 'molecular fingerprint'.

To get the spectrum, sample is prepared by grinding approximately 1-3 mg of solid sample with approximately 350 mg of infrared-inert matrix material *viz.* KBr (FTIR grade). Before use, KBr should be dried overnight at 110°C to remove any trace of moisture. Since, there is need of a relative scale for the absorption intensity; a background spectrum must be created with only KBr (without

sample) in the beam. This background spectrum is compared with the spectrum obtained with the sample, and thus percent transmittance is produced.

The FTIR spectra of electrocatalysts were obtained in a Fourier transform infrared (FTIR) spectrometer (make: Shimadzu, model: IR Affinity-1) to identify the various functional groups present in the sample. The transmission spectra of the electrocatalysts were recorded in the spectral range of 400-4000 cm^{-1}.

3.2.3 BET surface area analysis

The surface area of the synthesized electrocatalysts was determined using Brunauer-Emmett-Teller (BET) gas adsorption method. This gas adsorption method is based on the physical adsorption of a gas (inert) on the surface of the solid (electrocatalyst). Physical adsorption results from relatively weak vander Waals force which develops due to dipole-dipole interaction between the adsorbate gas molecules and adsorbent surface (test sample). The amount of adsorbate gas corresponding to a monomolecular layer on the surface is calculated to evaluate the surface area of the sample.

The samples were characterized in BET surface area analyzer (make: Beckman Coulter, model: SA 3100) using N_2 gas. Approximately, 0.3 to 0.5 g of powder was placed in a test tube and allowed to degas for 2 hours at 150°C in flowing nitrogen. This removes contaminants such as water vapor and adsorbed gases from the sample. The sample was then weighed under air-tight conditions, after which it was inserted into the analysis port for further analysis at liquid nitrogen temperature.

3.2.4 Scanning electron microscopy (SEM)

SEM is used very effectively for analyzing surface morphology of solid materials. This microscopy uses a focused beam of high energy electrons to generate a variety of signals at the surface of solid samples. The signals produced are derived from the interactions between electrons and sample. The

signals generated during analysis produce a three-dimensional image and render information about the external morphology of the sample.

In SEM, a beam of highly energetic electrons (primary electrons) is directed towards a sample. These electrons collide with the sample and give rise to secondary electrons, back scattered electrons, as well as X-rays. For imaging samples, secondary electrons and backscattered electrons are commonly used. There is no volume loss in the sample during analysis, and hence the same material can be used to generate images repeatedly. Hence, SEM is termed as non-destructive analytical technique.

Surface morphologies of the electrodes and membrane (*viz.* electrolyte) used in the study were evaluated using scanning electron microscope (make: Leo, model: 1430vp), which was able to magnify the samples in the wide range of 10X to 10 kX. The electrode sample was mounted over the stub using conductive carbon tape and analyzed. The membrane sample was subjected to gold coating before mounting over the stub for making it electrically conductive.

3.2.5 Field emission scanning electron microscopy (FESEM)

Field emission scanning electron microscopy is the more developed version of conventional SEM, where a field emission cathode in the electron gun of a SEM provides narrower and high electron energy beam. This helps to improve the resolution and image quality.

Surface morphologies of the electrocatalysts synthesized for the study were evaluated using field emission scanning electron microscope (make: Zeiss, model: Sigma). This FESEM is able to magnify the samples in higher than 10kX range. The electrocatalysts were dispersed in appropriate solvents and sonicated till completely homogenized dispersion was obtained. A drop of the solution was put over the glass slide covered with aluminium foil and dried in oven. The glass slide was then kept over the stub in field emission scanning electron microscope using conductive carbon tape and analyzed.

3.2.6 Transmission electron microscopy (TEM)

Transmission electron microscopy is another technique to analyze the morphological details of a specimen. The basic difference between SEM (or FESEM) and TEM is that SEM is based on scattered electrons while TEM is based on transmitted electrons. In SEM, back scattered electrons, secondary electrons, and characteristic X-rays generated after the collision with the sample, produce 3-dimensional images, while in TEM, the transmitted electrons from the samples are utilized to produce two-dimensional images. As the electrons need to pass through the samples in TEM, the specimen has to be thin enough to transmit electrons (*i.e.* electronically transparent). TEM provides higher resolution than SEM and is able to analyze the sample at nano level.

The morphology and size of electrocatalysts were analyzed in transmission electron microscope (make: JEOL, model: JEM 2100). The samples were dispersed ultrasonically in appropriate solvent for 30 min for TEM analysis. The homogenously dispersed sample was put over 300 mesh size copper grid using micropipette. The sample kept over the grid was then placed in a Petridish and dried in vacuum oven to remove the volatile contents. Thereafter, the grid having sample was mounted in the single axis tilt sample holder to insert into TEM column for analysis.

3.2.7 Energy dispersive X-ray spectroscopy (EDX)

Energy dispersive X-ray spectroscopy is a qualitative and quantitative non-destructive X-ray microanalytical technique, which provides information about the chemical composition of the samples having elements with atomic number (z) > 3. In EDX spectroscopy, an electron beam is focussed on the sample in either a scanning electron microscope (SEM) or transmission electron microscope (TEM). The electrons from the primary beam penetrate the sample and interact with the atoms of the sample. After interaction, the X-rays are detected by an energy dispersive detector and signal is displayed as spectrum of intensity *vs.* X-ray energy.

The sample does not require any special preparation for EDX analysis. It is done in the same way as in case of SEM or TEM analysis. The EDX spectra of the electrocatalysts were obtained using scanning electron microscope (make: Leo, model: 1430vp) and transmission electron microscope (make: JEOL, model: JEM 2100).

3.2.8 Nuclear magnetic resonance (NMR) spectroscopy

Nuclear magnetic resonance (NMR) spectroscopy is an analytical technique used extensively for determining the structure of organic compounds. It is concerned with the magnetic properties of certain nuclei. NMR is based on the principle that many nuclei have spin and all nuclei are electrically charged. A spinning charge generates a magnetic field and the resulting spin-magnet has a magnetic moment proportional to the spin. So, if an external magnetic field is applied, then two spin states come into the picture. The magnetic moment of the lower energy state gets aligned with the external magnetic field while that of the higher energy state opposes the external magnetic field. The energy difference between the two spin states is very small and depends on the applied external magnetic field. However, this energy difference increases with increase in the external magnetic field. Hence, for NMR spectroscopy, strong magnetic fields are required. This energy difference is responsible for the energy transfer between the base energy level and higher energy level of the nucleus. The energy transfer takes place at a specific wavelength corresponding to the range of radio frequency. The same range of frequency is emitted when the spin comes back to its base energy. Thus, if the signal produced in the sample being analyzed, matches with the signal of a certain nuclei then it helps in the identification. Most commonly, the nuclei used in this spectroscopy are hydrogen-1 (^{1}H) and carbon-13 (^{13}C) both of which possess the fractional spin of 1/2.

For the present work, ^{1}H-NMR has been used. For carrying out the analysis using NMR spectroscopy, the sample is solubilized in a specific solvent. For ^{1}H-NMR spectroscopy, the solvent should not contain any simple hydrogen atoms as they would result in erroneous peaks. Use of $CDCl_3$ as a

solvent serves this purpose as hydrogen atom is replaced by its isotope, deuterium, which possesses sufficient magnetic properties.

For the anaylsis of synthesized ligand, nuclear magnetic resonance spectrometer (make: Varian, model: Mercury plus) has been used. The applied external magnetic field corresponded to the precession frequency of 400 MHz. Small amount of the sample was solubilized in $CDCl_3$ in an NMR tube. The NMR sample tube was inserted into the spinner and positioned using the gold coloured depth gauge. Further, the NMR sample and spinner were inserted into the bore tube and pneumatically lowered into the magnet for the analysis.

3.2.9 High resolution mass spectrometry (HR-MS)

Mass spectrometry is a highly effective analytical technique used to analyze the unknown samples as well as to quantify the materials. In this process, samples are converted to gaseous ions, which are identified by their specific mass to charge ratio with the use of a magnetic field. The basic principle underlying the process is that a charged particle passing through a magnetic field is deflected along a circular path on a radius, which is proportional to the mass to charge ratio of the particles. The first step in the mass spectrometric analysis is the electron ionization of the sample to produce gas phase ions, also known as molecular ions. If the molecular ion is unstable, then it can go for further fragmentation to produce smaller ions. The produced ions are then collimated and accelerated into a magnetic field. The magnetic field helps to separate the ions based on their mass to charge (*m/z*) ratio. The ions having the smallest *m/z* ratio will be deflected the most and *vice-versa*. The most useful information obtained using this analytical technique is the molecular weight of the sample. The sample to be analyzed is injected by solubilizing in an appropriate solvent.

The mass of the synthesized ligand was obtained through the high-resolution mass spectrometer (make: Agilent, model: 6520). The sample was dissolved in acetonitrile and injected using a syringe.

The mobile phase used was a mixture of 0.1% formic acid and acetonitrile. The peaks obtained helped to identify the mass of the sample.

3.2.10 Elemental analysis

Elemental analysis of carbon (C), hydrogen (H), and nitrogen (N), also called as CHN analysis, is very important for organic samples. The CHN analysis is accomplished by combusting the sample in the oxygen atmosphere and the various combustion products such as carbon dioxide, water, and nitric oxide are collected. The combustion products obtained after the reaction are passed through the gas chromatographic system to evaluate the amount of carbon dioxide, water, and nitric oxide present in the sample. Thus, mass of C, H, and N present in the sample can be known. The accurate measurement of the mass of these products helps to identify the composition of an unknown sample. The composition of the compound is usually expressed in terms of weight percent of each element in the compound. The elemental analysis of a compound enables to determine the empirical formula of the compound, using which, the molecular formula can be easily determined as the molecular formula is an integer (*n*) multiple of the empirical formula.

The determination of the mass percentage of CHN elements is based upon the direct weight of the material sampled. Therefore, it becomes mandatory to dry the sample completely and foreign particles (if any) should be removed. Amount of sample required for analysis is approximately 2-3 mg. To find out the elemental formula of the metal complex electrocatalysts, the required amount of the sample was introduced in elemental analyser (make: EuroEA) and amount of various elements was determined in percentage.

3.3 Evaluation of electrocatalyst for CO_2 reduction

The synthesized electrocatalysts were evaluated for their activity towards electrochemical reduction of CO_2 using both half-cell and full cell studies. The different experimental set-up(s) were developed in-house and used for the studies.

3.3.1 Experimental set-up for half-cell studies

The half-cell studies were carried out in a conventional three-electrode system used in electrochemical measurements. The saturated Ag/AgCl was used as a reference electrode and platinum wire was used as a counter electrode. Different synthesized electrocatalysts were used along with gas diffusion layer to fabricate the working electrode having area of 0.5 cm^2. Different electrolytes were used for carrying out the reaction in aqueous and non-aqueous media. The electrolytes were also purged with inert (N_2) and CO_2 gases, depending upon the experiment. The details are discussed in the section 4.3.1.2 and 4.3.1.2.1.

To record the data, potentiostat/galvanostat (make: CH Instruments Inc., USA, model: CHI6008B) was used. As shown in figure 3.1, the potential difference is measured between the working and reference electrodes and the current is measured between the working and counter electrodes.

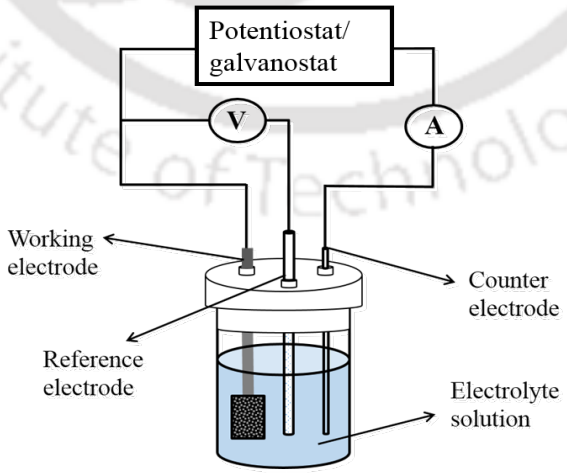

Figure 3.1 Schematic of the half-cell experimental set-up

3.3.2 Experimental set-up for full cell studies

The full cell studies involve a complex set-up of electrochemical reactor, peristaltic pumps, potentiostat/galvanostat, gas chromatography modules, gas distribution system, and liquid-gas separator *etc*. A snapshot of the entire experimental set-up is shown in figure 3.2. For the ease of understanding, the set-up is discussed in the following sub-sections.

3.3.2.1 Electrochemical reactor

The full cell studies were carried out in an indigenously developed electrochemical reactor (Aeshala *et al.* 2012), as shown in figure 3.3. The reactor resembles fuel cell assembly, where the anode and cathode are placed on the opposite sides of an ion exchange membrane. Two graphite plates with properly lined flow channels and ribs were used as end plates to deliver reactants to the electrodes and collect the products from the outlets as shown in the figure 3.3.

Figure 3.2 Snapshot of experimental set-up developed for the study of dERC

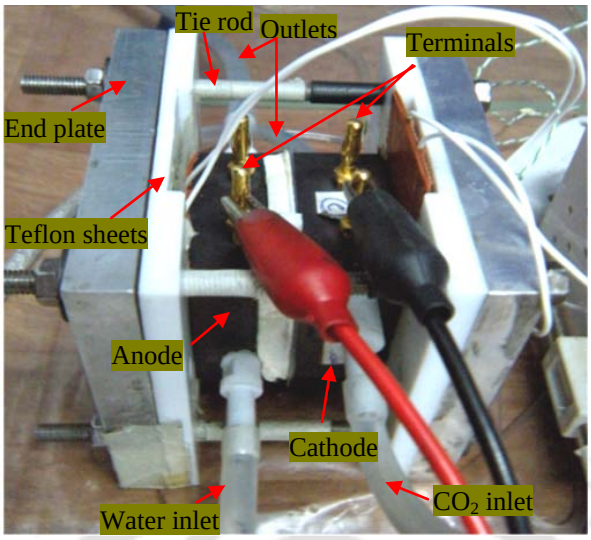

Figure 3.3 Snapshot of the electrochemical reactor

A snapshot of the electrochemical reactor is shown in figure 3.3. Suitable electrical potential was supplied through the gold terminals of the end plates. The electrons produced during the reaction were collected through gold-plated terminal at the anode end plate. Likewise, the electrons which were supplied to the cathode through external circuit were first received by gold-plated terminal at the cathode end plate and then transported to the cathodic reaction sites. The anode and cathode were used after assembling in membrane electrode assembly (MEA). The fabrication of MEA is detailed in section 3.3.2.1.1. The MEA was sandwitched in between the two graphite end plates. The dERC reactor was checked for any leakages and short-circuiting (Aeshala *et al.* 2012).

3.3.2.1.1 Fabrication of membrane electrode assembly (MEA)

A solid polymer electrolyte membrane, Nafion-117 (procured from DuPont, USA) was used as cation exchange membrane for the development of MEA in all the experiments. The Nafion membrane was cut in required size and pre-treated to improve the proton conductivity. The pre-treatment was done as per the standard procedure (Barbora *et al.* 2009). The membrane was first treated in 0.5 M H_2O_2 for 1 h at 80°C. The peroxide treated membrane was then boiled in millipore water for 1 h at 80°C to

remove the remains of peroxide. The third treatment utilized 0.5 M H_2SO_4 solution for an hour at 80°C followed by final cleaning with water same as in second treatment step. The treated membrane was stored in millipore water for further use.

Gas diffusion layer (GDL) or porous carbon paper (GDS 210) from CeTech Co. Ltd., Taiwan was used as the backing layer for anode and cathode electrocatalysts to be used in half-cell or full cell reactions. The anode electrocatalyst used in all the studies was 40 wt% Pt/C (procured from Electrochem Inc., USA). The anode was synthesized by coating the GDL with anode electrocatalyst ink. The anode electrocatalyst ink was prepared by sonicating Pt/C along with 5 wt% Nafion dispersion (DuPont, USA) and iso-propyl alcohol. The amount of Pt/C was taken so as to maintain the catalyst loading of 0.5 $mg \cdot cm^{-2}$ on anode in all the experiments. The homogenized mixture obtained after sonication was sprayed onto the GDL. Nitrogen gas was used as the carrier gas for carrying out spraying. The anode thus obtained was further heat treated in an air oven for approximately 12 h at 100°C to get the anode electrode. The cathode was synthesized either in the similar manner or by electroplating technique, which will be discussed in subsequent chapters. The electrode area in all the full cell studies was $3 \times 3\ cm^2$.

MEA was fabricated by sandwitching the treated membrane between the synthesized electrodes (anode and cathode). Hot pressing was done at appropriate temperature under the pressure of 50 $kg \cdot cm^{-2}$ for 3 min in compression moulding machine. Thereafter, the MEA was cooled to room temperature and installed in the electrochemical reactor. A snapshot of the developed MEA and its schematic is shown in figure 3.4.

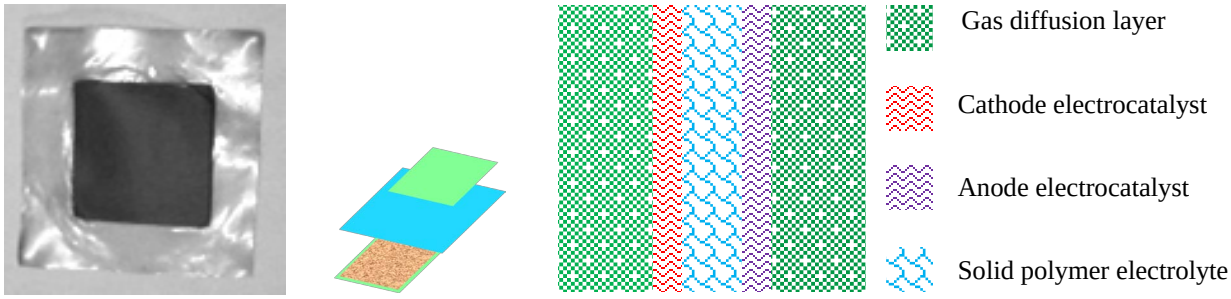

(a) (b)

Figure 3.4 Snapshot of (a) developed MEA, and (b) its various components

3.3.2.2 Performance evaluation of synthesized electrocatalysts for dERC in electrochemical reactor

The developed MEA was kept in between the two graphite plates and the reactor was assembled to check the performance of electrocatalysts for dERC. The schematic of the experimental set-up is shown in figure 3.5. The CO_2 gas (99.995%) was taken from a CO_2 cylinder. The gas was humidified by passing through the humidifier and then allowed to enter in the cathode inlet at the flow rate of 20 $mL \cdot min^{-1}$ which was set by the rotameter. At the anodic end of the electrochemical reactor, deionized water was used as a proton source for the reaction. It was passed to the anode inlet at the flow rate of 1.5 $mL \cdot min^{-1}$ set by the peristaltic pump. To carry out the reaction, an external source of energy was required, and potentiostat/galvanostat served the purpose. The dERC was carried out at different potential values. All the experiments were carried out at 30°C and atmospheric pressure. The anode outlet was connected to vent while the products obtained at the cathode outlet were collected in gas sampling bags for further evaluation in gas chromatograph.

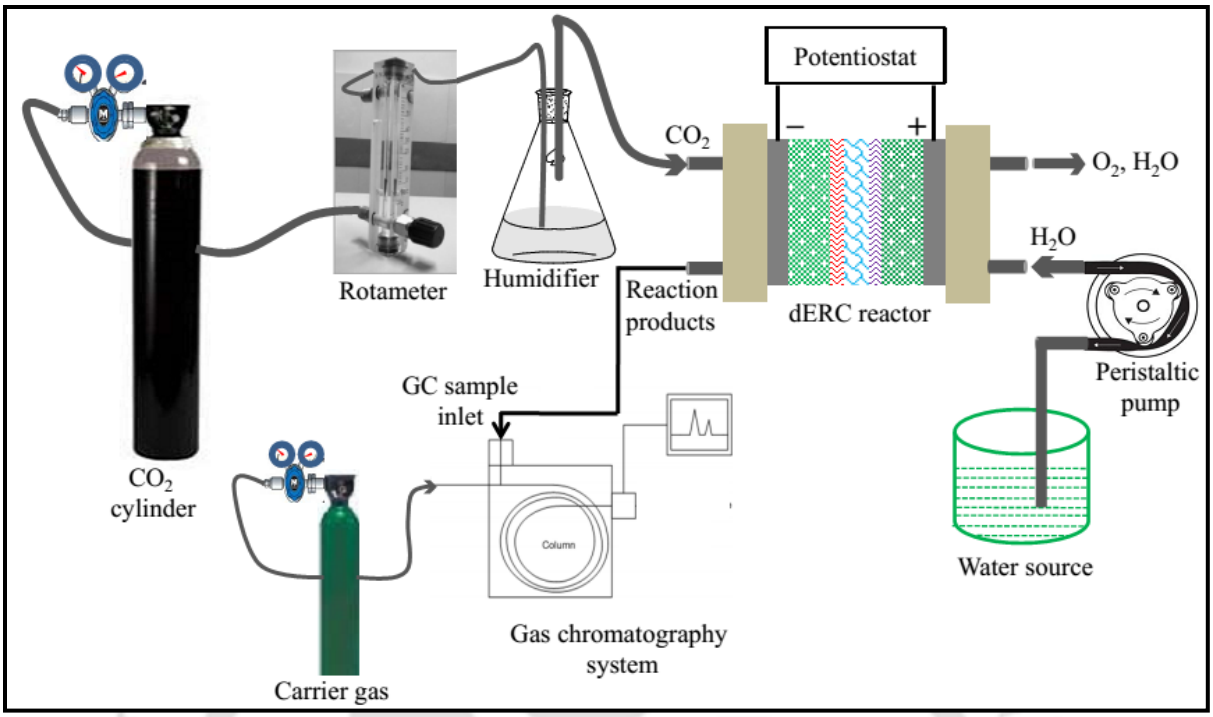

Figure 3.5 Schematic of the experimental set-up

3.3.2.3 Gas chromatography system

The reaction products resulting from the electrochemical reduction of CO_2 in presence of electrocatalysts need to be identified and quantified. Gas chromatographic (GC) technique was used for identification and quantification of reaction products. Gas chromatography requires a mobile phase and a stationary phase. Mobile phase (carrier gas) serves to carry the analyte molecules through the heated column. The mobile phase can be any inert gas, for *e.g.* argon, helium, or nitrogen. The stationary phase consists of a column, which is constructed by packing a tube with column packing material. The material is held in place by sintered metal filters at either end of the tube. The packing material consists of very small support material having very thin coating of liquid solvent of high boiling polymer. A typical gas chromatograph consists of an injection port, a column, carrier gas flow control system, oven, and heaters for maintaining temperature of the injection port and column.

The sample to be analyzed is introduced in the injection port, where it gets vapourized and moves along with the carrier gas. As the gas sample moves through the column (stationary phase), the components of the sample interact with the stationary phase and depending upon the strength of interaction, various components may take longer or shorter time to elute through the column. Usually, the components with lower boiling points move slower than the components with higher boiling points. The time taken by a component to elute from the column is called as the retention time. Strong interaction leads to longer retention time and *vice-versa*. The time at which this separation occurs is dependent on the temperature, length of the column, and flow of the carrier gas. After elution, the different components are identified by the various detectors located at the end of the column.

For analyzing the product samples, the gas chromatograph used in the present study comprised of a packed column (Carbosieve S-II, 3.05 m, 1/8 in., 2.1 mm) along with thermal conductivity detector (TCD), methanizer, and flame ionization detector (FID). The carrier gas used was argon. Thermal conductivity detector is generally used to detect both organic and inorganic compounds. It is based on the change in thermal conductivity of the carrier gas when another compound is present. In the present system, TCD was used primarily for the detection and quantification of the H_2 and CO_2. Methanizer is a system which converts CO and CO_2 to CH_4 for better identification. Moreover, this CH_4 does not interfere with the CH_4 obtained directly from the dERC reactor because the later eluted from the column before the CH_4 from methanizer. After passing through TCD and methanizer, the gas sample (along with carrier gas) enters FID. The detection in FID is generally used to detect organic compounds, as it works by passing the sample through a hydrogen flame and measuring the ions produced while burning the compounds of the sample. In the present study, FID was used for the detection of hydrocarbons (CH_4, C_2H_4, C_2H_6). Thus, after injection of the gas sample in the injection port, it moves along with carrier gas through column, TCD, methanizer, and FID such that detection of H_2, CO_2, CO, and hydrocarbons takes place. Quantification of the products was carried out using calibration curves of the known concentration of standard samples.

3.4 Experimental techniques used in electrochemical studies

The various techniques used for the study were linear sweep voltammetry (LSV), cyclic voltammetry (CV), and chronoamperometry (CA).

3.4.1 Linear sweep voltammetry (LSV)

Linear sweep voltammetry is a potential sweep technique in which a fixed potential range is employed and the voltage is ramped from a lower limit to an upper limit at a particular rate as shown in figure 3.6 (a). The resulting current-potential curve is known as linear sweep voltammogram (LSV). It provides useful information about the rate of electrochemical reactions as a function of the potential. The time taken to sweep the range can be altered by changing the potential scan rate. The applied potential is usually varied linearly with time, therefore the scan rate is defined as the slope ($V \cdot s^{-1}$).

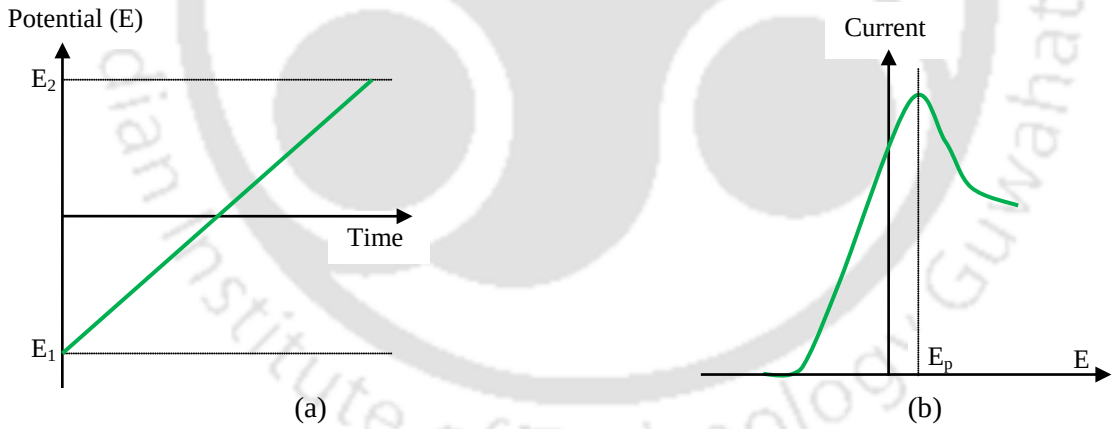

Figure 3.6 Linear sweep voltammetry experiment (a) the potential-time profile applied during experiment (E_1 is the lower limit and E_2 is the upper limit), and (b) the corresponding linear sweep voltammogram showing current response due to change in potential (E_p represents peak potential)

3.4.2 Cyclic voltammetry (CV)

Cyclic voltammetry (CV) is another useful technique to investigate the electrochemical behaviour of a system. In this technique, the potential applied between the electrodes is ramped between low and high values as in case of LSV, however, when the voltage attains a certain maximum value, the potential is reversed back to initial position (Figure 3.7 a). The current response measured during this process is usually normalised to the surface area of the electrodes and represented as the current density. The peak obtained in the cyclic voltammogram is characteristic of the electrode reaction taking place. The peak width and height for the reaction under investigation depends upon the scan rate, concentration of the electrolyte, and the type of electrode used.

The redox reaction taking place in the solution can be expressed as $O + ne^- \leftrightarrow R$, where O and R are the oxidized and reduced species in a redox couple, respectively. When the electron transfer rate in both forward and reverse directions is equal, the reaction is said to be reversible with the separation between anodic and cathodic peak of approximately $59/n$ mV at 25°C, where n is the number of

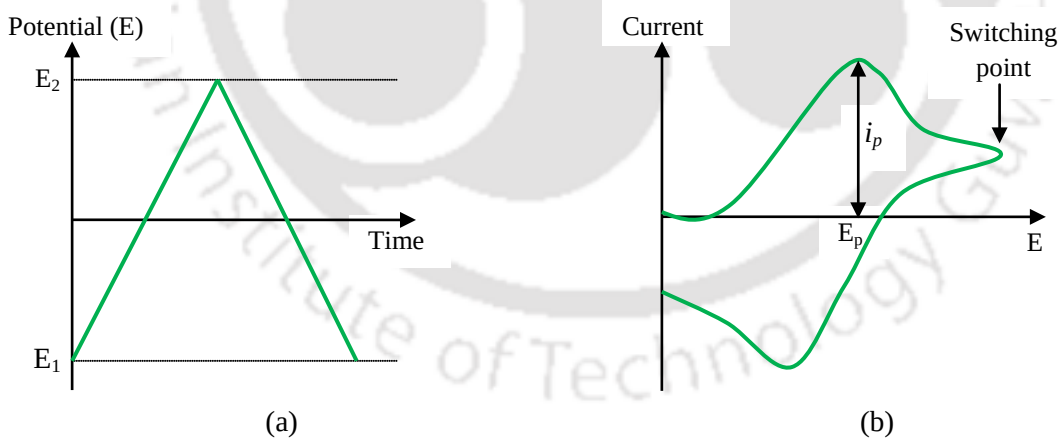

Figure 3.7 Cyclic voltammetry experiment (a) the potential-time profile applied during experiment (E_1 is the lower limit and E_2 is the upper limit) and (b) the corresponding response of the current due to potential sweep (i_p represents peak current and E_p represents peak potential)

electrons transferred during the oxidation or reduction process. In such a system, E_p is independent of the scan rate. Further, for a charge transfer process under the reversible conditions, the peak current density, I_p, is given by the following equation

$$I_p = 2.75\times10^5 n^{3/2} D^{1/2} C^o \upsilon^{1/2} \quad (3.2)$$

where, I_p is the current density at the peak maxima ($A\cdot cm^{-2}$), n is the number of moles of a particular product, D is the diffusion coefficient ($cm^2\cdot s^{-1}$), C^o is the concentration of the bulk solution ($mol\cdot L^{-1}$), and υ is the potential scan rate ($V\cdot s^{-1}$).

It is evident from this reaction that peak height should increase with the scan rate as the peak current density is proportional to the square root of the scan rate. Another important parameter in CV analysis is the half wave potential $E_{1/2}$, which is related to the peak potential as $E_p = E_{1/2} - 1.1RT/nF$ (F represents Faraday constant).

Under irreversible conditions, when the rate of the backward reaction is negligible, then reaction is represented as $O + ne^- \rightarrow R$. In such a case, system does not remain in equilibrium and hence E_p is dependent on the scan rate.

3.4.3 Chronoamperometry (CA)

Chronoamperometry (CA) is a square wave pulsed voltammetric technique in which a fixed potential is applied and the current is measured as a function of time. The current response of the experiment is a composite of the double-layer charging current and Faradaic current. The Faradaic current is due to the electron transfer reaction with an electroactive species. The double layer charging current or the capacitive current decays at a rapid rate as an exponential function of time for diffusion controlled reaction. This current is significant only during the initial period (a few milliseconds).

In the present work, CA was used to study the pulse mode electrolysis for dERC. The total charge (calculated by integrating the current-time curve) measured during the reaction corresponds to the

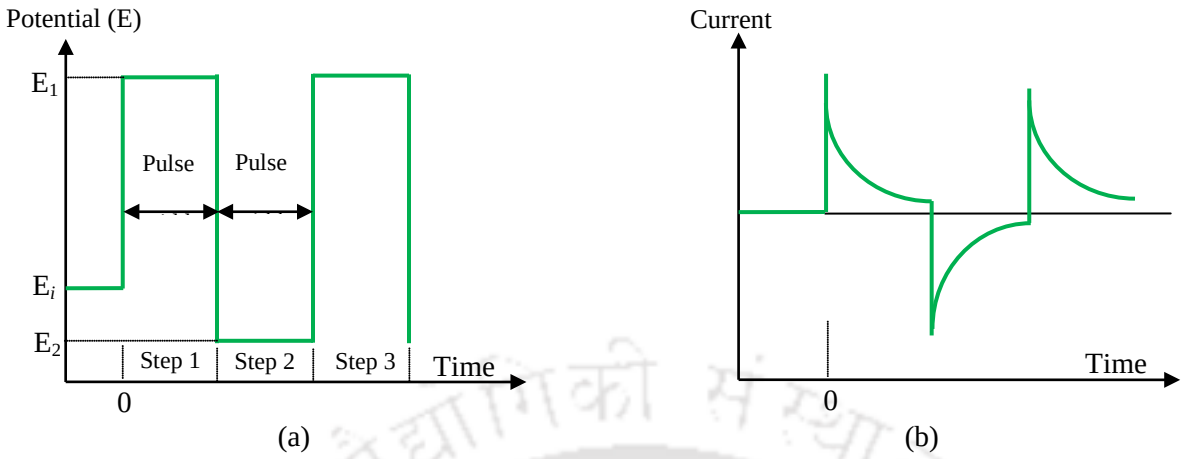

Figure 3.8 Chronoamperometry experiment (a) the potential-time profile applied during experiment (E_i is the initial potential value, and E_1 and E_2 are the points of interest), and (b) the corresponding response of the current with time due to change in potential

electrons used in the CO_2 reduction reactions and thus it is proportional to the amount of the products formed.

In the experiments performed, an initial potential (E_i) was given as shown in figure 3.8. When the experiment is started, the cell is held at this initial potential for a number of seconds, defined as quiet time. After the completion of the quiet time, the potential is instantaneously changed to the potential value of interest (E_1) (Figure 3.8). The current time response is recorded at this potential value for a specific time *viz.* pulse width. After this, the potential is instantaneously changed to another potential value of interest (E_2) and again the current time response is recorded for the given pulse width. This cycle continues for the given number of steps. In the experiments, the applied potential value is always higher than the equilibrium potential of the CO_2 reduction reactions. The difference between the applied potential and the equilibrium potential of the reaction represents the overpotential which may be due to any one of the activation polarization, concentration polarization, ohmic polarization,

or the combination of these. After completion of the reaction, charge is calculated by integrating the current time response. The charge calculated is used for the determination of Faradaic efficiency.

It is to be noted that the CO_2 reduction is a cathodic reaction; hence all the electrochemical experiments have been carried out in cathodic range (-ve potential values). However, for the simplicity and ease of understanding, all the potential and current values have been plotted with positive sign in entire thesis, unless stated otherwise.

3.5 Product analysis and quantification

For the complete understanding of the activity of electrocatalysts, products obtained after full cell reaction have to be quantified. Quantification is done for the products obtained in 1 h of the reaction. The efficiency of the electrocatalyst is represented in terms of Faradaic efficiency, rate of the reaction, and selectivity. To represent the efficiency in such a way, there is need to know the amount of the products formed and the electrical charge utilized to carry out the respective reaction. Gas chromatography analysis provides information about the amount of the products formed and the chronoamperometric experiments results in the quantification of electrical charge utilized.

3.5.1 Faradaic efficiency

Faradaic efficiency, also called as Faradaic yield or current efficiency helps to determine the efficacy of the charge transfer for a particular reaction. The Faradaic efficiency was calculated by determining the charge passed to produce a particular product (of total CO_2 conversion) with respect to total charge passed during the experiment (Kuhl *et al.* 2012). The formula is shown in equation (3.3).

$$\text{Faradaic efficiency} = \frac{n \times F \times z}{Q} \qquad (3.3)$$

where, n = number of moles of particular product (mol)

F = Faraday constant ($C \cdot mol^{-1}$)

z = number of electrons involved for 1 mole of particular product

Q = total charge passed during the experiment (C)

3.5.2 Rate of the reaction

Rate of the reaction for the formation of various products using synthesized electrocatalysts was calculated at the potential value, where the cumulative formation of all the products was found highest. Reaction rate was calculated as the ratio of the amount of the products formed to the amount of the electrocatalyst used, in unit time, represented in units of $g\cdot(g\cdot h^{-1})^{-1}$ (Cao *et al.* 1988).

3.5.3 Selectivity

Selectivity is defined as the amount of desired product to the amount of total CO_2 reduction products obtained (based on the carbon content) during reaction (Ogura *et al.* 2004). The formula of selectivity calculation for the formation of CH_4, CO, and C_2H_4 is represented in equations 3.4 to 3.6,

$$\text{Selectivity of } CH_4 = \frac{n_{CH_4}}{n_{CH_4} + n_{CO} + 2n_{C_2H_4}} \quad (3.4)$$

$$\text{Selectivity of CO} = \frac{n_{CO}}{n_{CH_4} + n_{CO} + 2n_{C_2H_4}} \quad (3.5)$$

$$\text{Selectivity of } C_2H_4 = \frac{2n_{C_2H_4}}{n_{CH_4} + n_{CO} + 2n_{C_2H_4}} \quad (3.6)$$

where, n = number of moles of a particular product (mol).

References

Aeshala L.M., Rahman S.U., and Verma A. (2012), Effect of solid polymer electrolyte on electrochemical reduction of CO_2, *Separation and Purification Technology*, 94, 131-137.

Barbora L., Acharya S., and Verma A. (2009), Synthesis and *ex-situ* characterization of Nafion/TiO_2 composite membranes for direct ethanol fuel cell, *Macromolecular Symposia*, 277, 177-189.

Cao R., Pan W.X., and Griffin G.L. (1988), Direct synthesis of higher alcohols using bimetallic copper/cobalt catalysts, *Langmuir*, 4, 1108-1112.

Kuhl K.P., Cave E.R., Abram D.N., and Jaramillo T.F. (2012), New insights into the electrochemical reduction of carbon dioxide on metallic copper surfaces, *Energy and Environmental Science*, 5, 7050-7059.

Ogura K., Yano H., and Tanaka T. (2004), Selective formation of ethylene from CO_2 by catalytic electrolysis at a three phase interface, *Catalysis Today*, 98, 515-521.

4

Performance of metal electrocatalysts for dERC

Chapter 4

Performance of metal electrocatalysts for dERC

Electrochemical reduction of carbon dioxide requires the usage of efficient electrocatalysts for better performance. This chapter discusses the performance of four metal electrocatalysts for the direct electrochemical reduction of gaseous CO_2. Based on the performance of the metals, attempts will be made to improve these metals and reported in later chapters. This chapter also explains about the need for the catalyst activity protocol. The protocol was developed and validated. Thus, this chapter will explore the possibilities of achieving better Faradaic efficiency by bringing out various changes in metals in various forms along with a suitable protocol for electrocatalyst activity.

4.1 Background

In the electrochemical reduction of carbon dioxide (ERC), electrocatalysts play the most important role. Usually, the metal electrocatalysts have been used for the ERC in aqueous and/or non-aqueous media. However, relatively very few studies are available for direct gas phase electroreduction of CO_2 (dERC) using metal electrocatalysts. Therefore, gas diffusion electrodes using metal electrocatalysts have been fabricated, characterized, and tested for the electrochemical reduction of gaseous CO_2. However, the half-cell studies were conducted by the usual method in which CO_2 is dissolved in a solution for the electrochemical characterization.

To understand the behaviour of metal electrocatalysts, four *d*-block metals *viz.* Cu, Zn, Ni, and Co from the first row of transition series were selected. The selection was made on the basis of various parameters such as, performance of metals towards ERC as studied in literature, inefficiency of metals towards hydrogen evolution reaction (HER) which is a competitive reaction for ERC, the cost effectiveness, and their safeguard towards environment. According to literature survey, copper is the most suitable metal for efficient reduction of aqueous CO_2 in view of the production of hydrocarbons. Therefore, Cu is chosen to see its effectiveness for gaseous CO_2 reduction. Zn is the metal which shows very low exchange current density towards H_2, therefore it might help in increasing the efficiency of ERC by reducing the competitive hydrogen evolution reaction. Co and Ni have been chosen as these metals are under-studied in ERC in their unmodified state. Based on the performance of selected metals, further strategies will be formulated for enhancing the efficiency of dERC.

4.2 Experimental

4.2.1 Materials

Electroplated catalyst on the gas diffusion layer was used in the study. $CuSO_4 \cdot 5H_2O$, $ZnCl_2$, $NiSO_4 \cdot 6H_2O$, $CoSO_4 \cdot 7H_2O$, H_2SO_4, H_3BO_3, and sodium dodecyl sulphate (SDS) were procured from

Merck and used without any further purification. Pt/C (40 wt% Pt) was purchased from ElectroChem, Inc. USA. Nafion membrane (Nafion-117) and Nafion dispersion (5 wt%) were procured from DuPont, USA.

4.2.2 Methods

4.2.2.1 Development of cathode

Electroplating method was adopted for developing cathodes using electroplating bath of the respective metals. To carry out the process, direct current (D.C.) source was used. The gas diffusion layer (GDL) was cleaned prior to plating process using dil. H_2SO_4 solution to remove any dirt or contaminants. Excess water of the GDL was dried and then it was covered with Teflon tape on one side to allow the plating only on single surface. The GDL, as cathode, was then immersed in the electroplating bath. The anode for the electroplating process was a bar of the metal, for which the plating was being carried out at cathode. Suitable composition of plating baths and plating conditions were used for different metals, as shown in Table 4.1. For copper electroplating, Cu electroplating solution was prepared using aqueous solution of 0.2 M $CuSO_4 \cdot 5H_2O$. A few drops of H_2SO_4 were added in the $CuSO_4$ solution to lower down the pH in the range of 3-4. Plating was carried out at room temperature. The copper bar and gas diffusion layer were used as anode and cathode, respectively and 1 V potential was applied between them. Aqueous solution of $ZnCl_2$ (0.5 M) was used with KCl as the additive for carrying out zinc plating. The plating has been carried out at room temperature. The optimum pH for Zn electroplating lies between 5-6 (Zeng *et al*. 2012). Watts electroplating solution of Ni was used for the electroplating of Ni. The solution consisted of 0.1 M aqueous solution of $NiSO_4 \cdot 6H_2O$ as the Ni source. Along with this, H_3BO_3 was used as pH buffer. Since the Ni cathode gets corroded quickly after its exposure to atmosphere, sodium dodecyl sulphate (SDS), an anionic surfactant, was also added in the electroplating bath to avoid corrosion (Guo *et al.* 2002). The optimum pH of Ni electroplating bath lies in between 4-5 (Pierozynski 2012; Hua *et al.*

Table 4.1 Electroplating conditions for the metal electrocatalysts

Properties	Cu	Zn	Ni	Co
Metal source	$CuSO_4 \cdot 5H_2O$	$ZnCl_2$	$NiSO_4 \cdot 6H_2O$	$CoSO_4 \cdot 7H_2O$
Plating solution	0.2 M $CuSO_4 \cdot 5H_2O$	0.5 M $ZnCl_2$	0.1 M $NiSO_4 \cdot 6H_2O$	0.1 M $CoSO_4 \cdot 7H_2O$
Additives	H_2SO_4	KCl	H_3BO_3, SDS, H_2SO_4	H_3BO_3
Temperature	Ambient	Ambient	40°C	40°C
pH	3-4	5-6	4-5	3
Anode	Cu metal	Zn metal	Ni metal	Co metal

2012), which was achieved by adding H_2SO_4. The plating process was carried out at 40°C while continuously stirring the plating solution and Ni metal was used as anode. In order to fabricate Co cathode, the electroplating bath consisted of 0.1 M aqueous solution of $CoSO_4 \cdot 7H_2O$ as cobalt source and H_3BO_3 as stabilizer. H_3BO_3 helps to minimize local pH rise which may be caused by the simultaneously occuring hydrogen evolution reaction. The electrodeposition was carried out at 40°C while stirring the electroplating solution continuously to maintain the constant concentration of electrolyte. The pH of the bath was optimized (pH = 3) before the electrodeposition (Caffarena *et al.* 2006; Santos *et al.* 2007; Santos *et al.* 2009). The electrodeposition of all the metals on the gas diffusion layer was carried out for the time upto attaining the metal loading of 2 $mg \cdot cm^{-2}$.

4.2.2.2 Development of anode

Anode for dERC reactor was prepared by coating Pt/C powder over the GDL. Pt/C (40 wt% Pt) and Nafion dispersion (5 wt% Nafion) were mixed with appropriate amount of iso-propyl alcohol and sonicated to get the anode electrocatalyst ink. The ink was sprayed over the gas diffusion layer using spraying technique and dried overnight at 100°C to get the anode.

4.2.2.3 Preparation of membrane electrode assembly (MEA)

The cation exchange membrane (Nafion-117) was treated using the standard procedure as discussed in section 3.3.2.1.1. The membrane electrode assembly was prepared by sandwitching the Nafion membrane in between anode and cathode at 110°C and 50 $kg \cdot cm^{-2}$ pressure as discussed in section 3.3.2.1.1.

4.2.2.4 Electrochemical tests

The half-cell studies were conducted in conventional three-electrode cell assembly using Ag/AgCl as reference electrode and Pt wire as counter electrode. The working electrode was prepared using electroplating technique with 2 $mg \cdot cm^{-2}$ loading over the gas diffusion layer as discussed earlier in section 4.2.2.1. The voltammetric tests were carried out in suitable electrolytes at the scan rate of 10 $mV \cdot s^{-1}$. In all the half-cell studies, the potential is reported with respect to standard hydrogen electrode (SHE), unless stated otherwise. The full cell studies were carried out in an electrochemical reactor, using the experimental set-up as described in section 3.3.2.1 and 3.3.2.2, respectively. The experiment was conducted using chronoamperometry technique (pulse width 5 s) at 6 different electrode potentials and the reaction products were collected at the cathode outlet and analyzed by GC. The electrochemical experiments were carried out at 30°C and at atmospheric pressure.

4.3 Results and discussion

4.3.1 Characterization of electroplated cathode

4.3.1.1 Physical characterizations

The electroplated cathodes were characterized using XRD, SEM, and EDX techniques.

4.3.1.1.1 XRD studies

The X-ray diffractogram of the Cu, Zn, Ni, and Co electrodes are shown in figures 4.1 to 4.4. The XRD pattern of Cu cathode reveals significant peaks at 43.45°, 50.66°, and 74.31° representing Cu(111), Cu(200), and Cu(220) crystal planes, respectively. This crystal structure belongs to face centered cubic (FCC) structure (Figure 4.1). The XRD pattern of Zn shows significant peaks at 38.03°, 39.16°, 43.43°, 54.44°, 70.27°, and 70.90° corresponding to (002), (100), (101), (102), (103), and (110) crystal planes. The electrodeposited zinc represents the hexagonal closed packed (HCP) structure (Figure 4.2). XRD pattern of Ni is showing the characteristic peaks at 44.49°, 51.63°, 77.48°, 93.03°, 96.84° corresponding to (111), (200), (220), (311), and (222) planes, thus representing face centered cubic (FCC) structure (Figure 4.3). Cobalt shows hexagonal closed packed (HCP) structure with peaks appearing at 41.74°, 44.53°, and 48.75° which represent (100), (002), and (101) crystal planes (Figure 4.4).

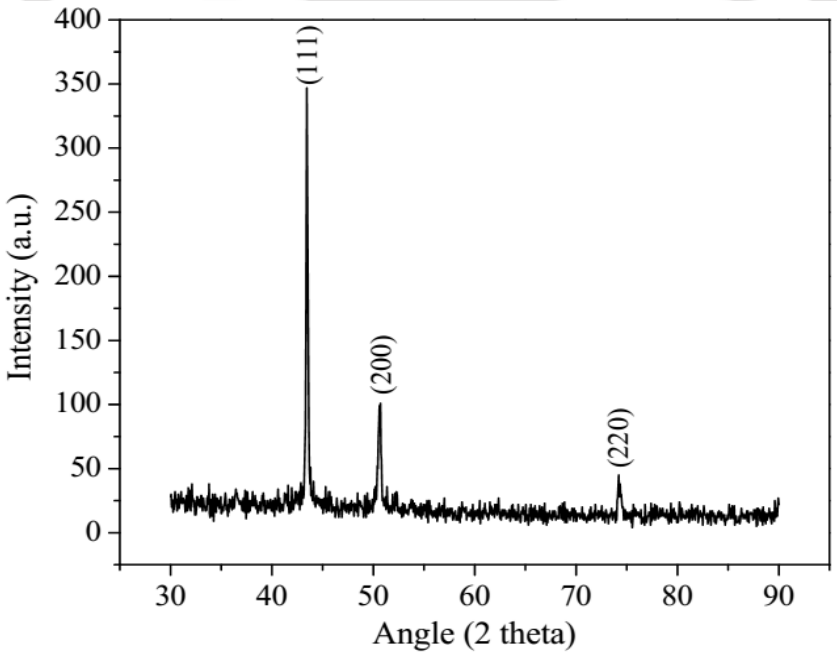

Figure 4.1 XRD pattern of electroplated Cu electrode

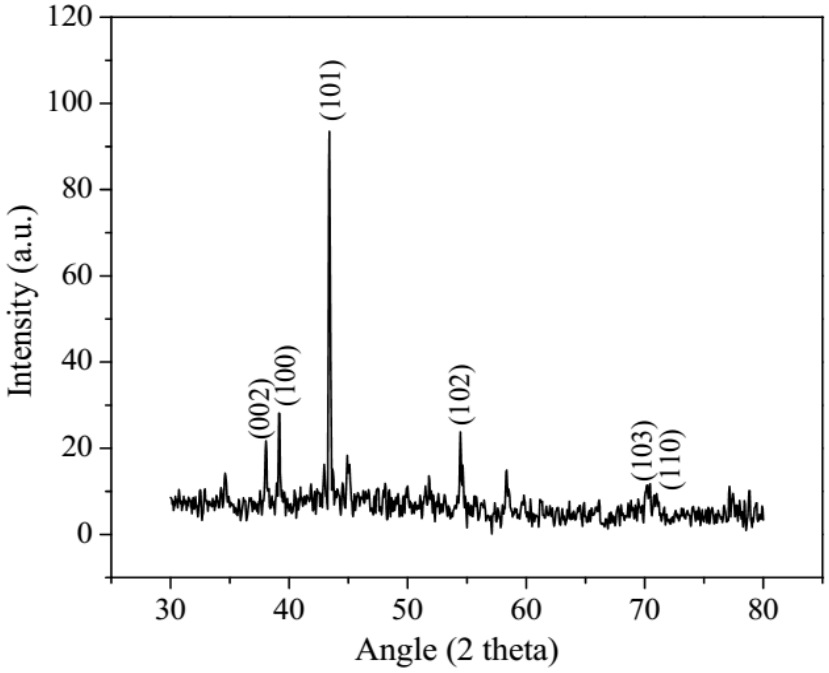

Figure 4.2 XRD pattern of electroplated Zn electrode

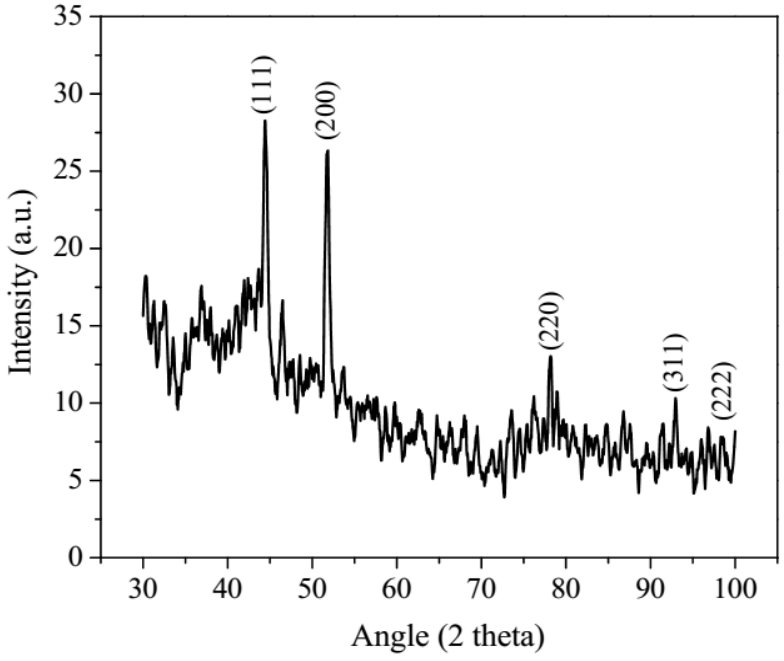

Figure 4.3 XRD pattern of electroplated Ni electrode

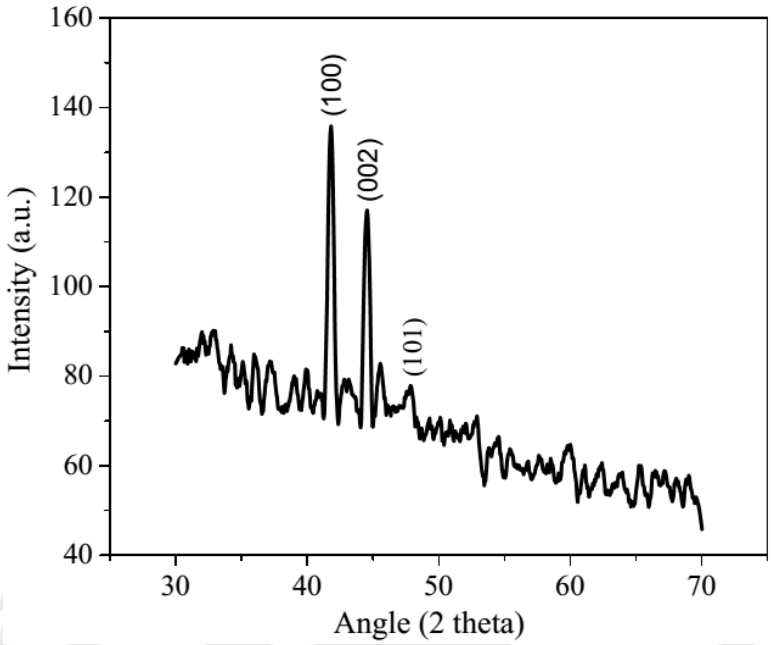

Figure 4.4 XRD pattern of electroplated Co electrode

4.3.1.1.2 SEM studies

The scanning electron microscopic studies of the 4 cathodes, namely Cu, Zn, Ni, and Co were carried out to determine the deposition of metal particles over the gas diffusion layer. Electrodes play the most vital role in the performance of electrochemical system. For the efficient conversion of CO_2 to products, it would be better to have more coverage of electrocatalyst on to and through the gas diffusion layer instead of dense electrocatalyst coating only on to the electrode surface. Therefore, the electroplating was optimized in such a way that desired electrocatalyst loading and surface porosity can be maintained. The SEM image of pure gas diffusion layer is shown in figure 4.5. It can be observed that gas diffusion layer is composed of compressed carbon fibers, which enclose sufficient porosity between them.

The SEM images in figures 4.6 to 4.9 clearly show that the electrocatalyst was uniformly electroplated on to the GDL and the surface porosity was maintained. The SEM image of copper electroplated cathode is shown in figure 4.6. The carbon fibers appear to be completely coated with

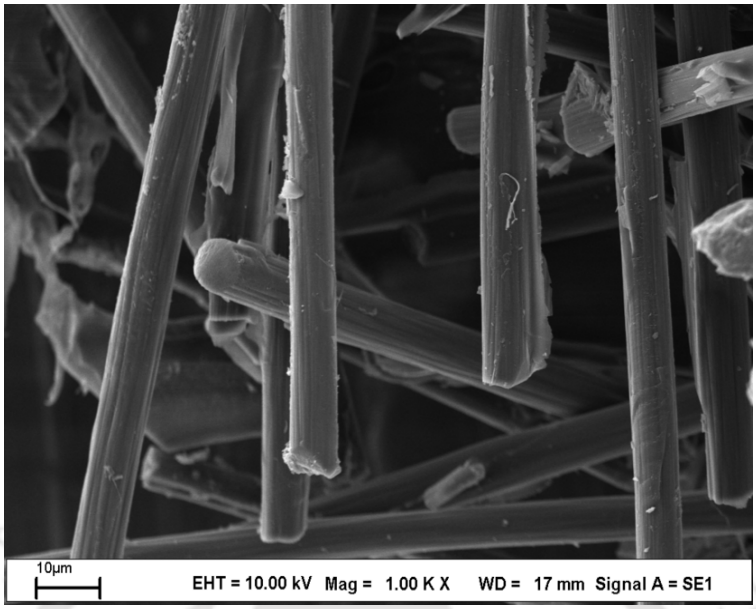

Figure 4.5 SEM image of gas diffusion layer (GDL)

Cu without affecting the porosity. The inset picture also clearly shows the coated carbon fibers. The electroplating has been done to get the electrocatalyst (Cu) loading of 2 mg·cm^{-2}. The loading was calculated using Faraday's law of electrolysis. Practically, ~5 min were required to get 2 mg·cm^{-2} loading of Cu (Aeshala *et al.* 2012). Similarly, figure 4.7 shows the Zn electroplated gas diffusion layer where, all the carbon fibers appear to be coated with zinc. The inset picture (figure 4.7) clearly shows the formation of hexagonal crystals of Zn. In case of nickel (Figure 4.8), more or less uniform electrodeposition is seen over the carbon fibers. Also, the Ni deposits seem to be adhered over the fibers along the length as well as along the diameter. The inset (Figure 4.8) shows the close view of Ni deposits. The electrodeposition of cobalt over the gas diffusion layer is not as smooth as in case of other metal electrodes. The image shows agglomerated particles over some of the carbon fibers along with the fine grained deposition over the other carbon fibers. A few of the carbon fibers also remain uncoated. Such agglomeration may result due to the simultaneous hydrogen evolution going on along with the cobalt electrodeposition process. Excess generation of hydrogen bubbles might have disturbed the deposition of the ions on the carbon fibres, instead rendered the ions to get

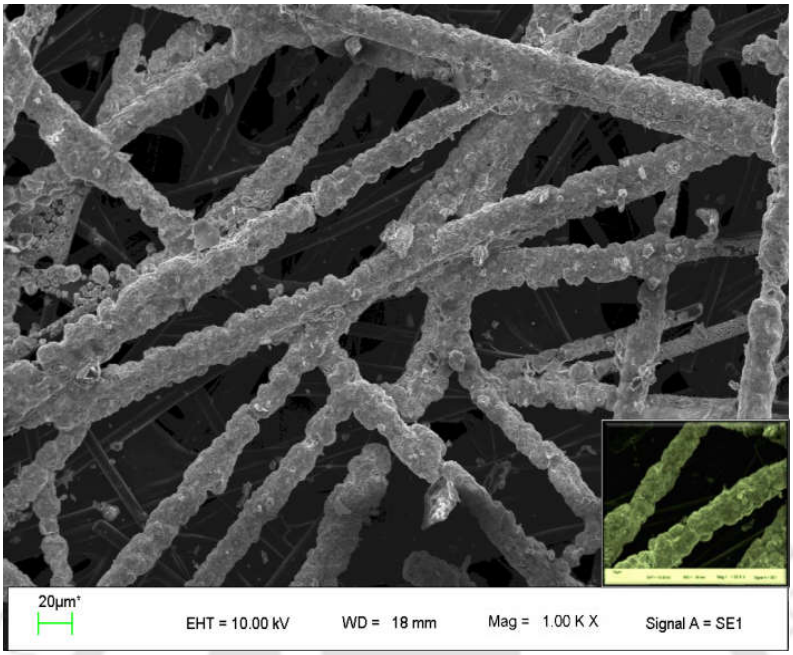

Figure 4.6 SEM image of Cu electrode

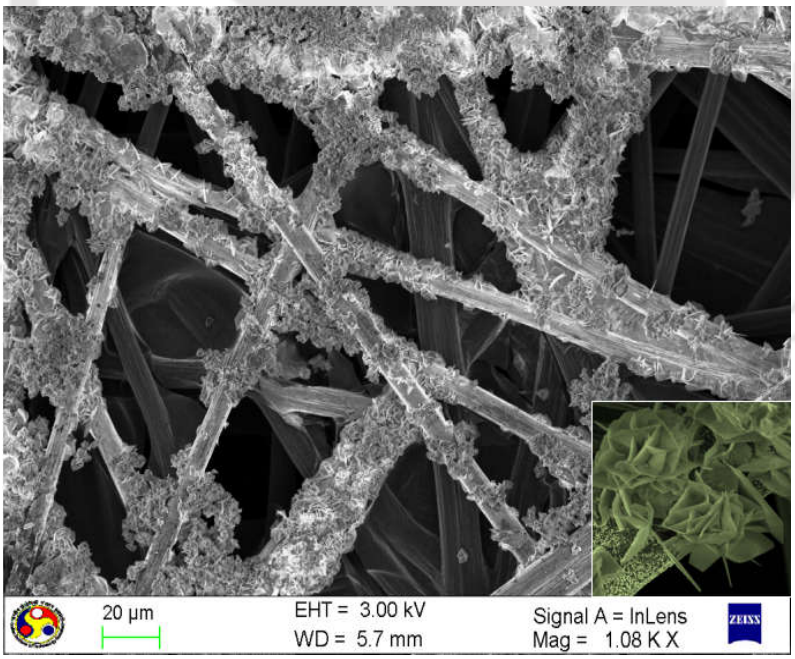

Figure 4.7 SEM image of Zn electrode

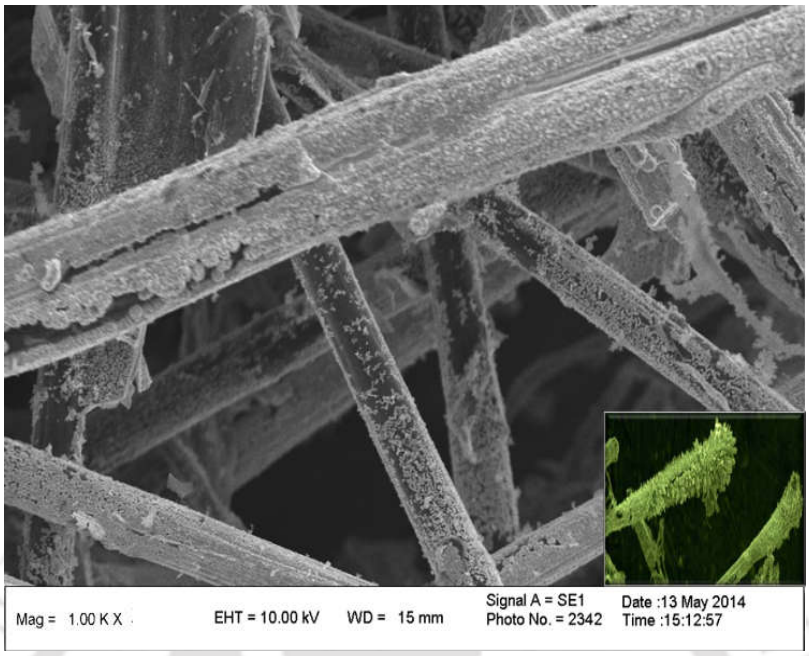

Figure 4.8 SEM image of Ni electrode

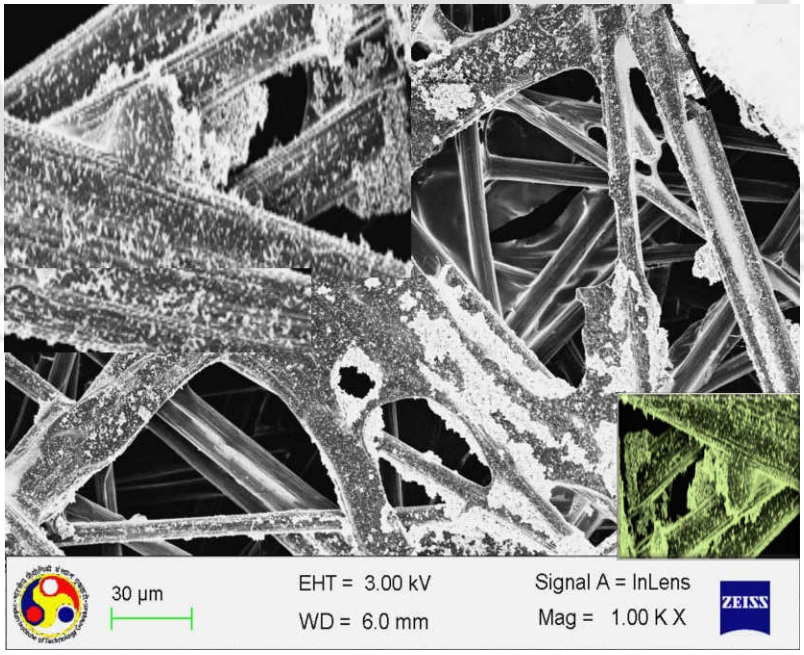

Figure 4.9 SEM image of Co electrode

deposited on the metal, resulting in agglomerates at some of the places while absence of coating at other places (Figure 4.9).

4.3.1.1.3 EDX studies

EDX studies were carried out to confirm the presence of elements electroplated over gas diffusion layer. EDX spectra of all the electroplated cathodes are shown in figure 4.10. The EDX spectra show that the metals are coated on to the gas diffusion layer and hardly have any impurity.

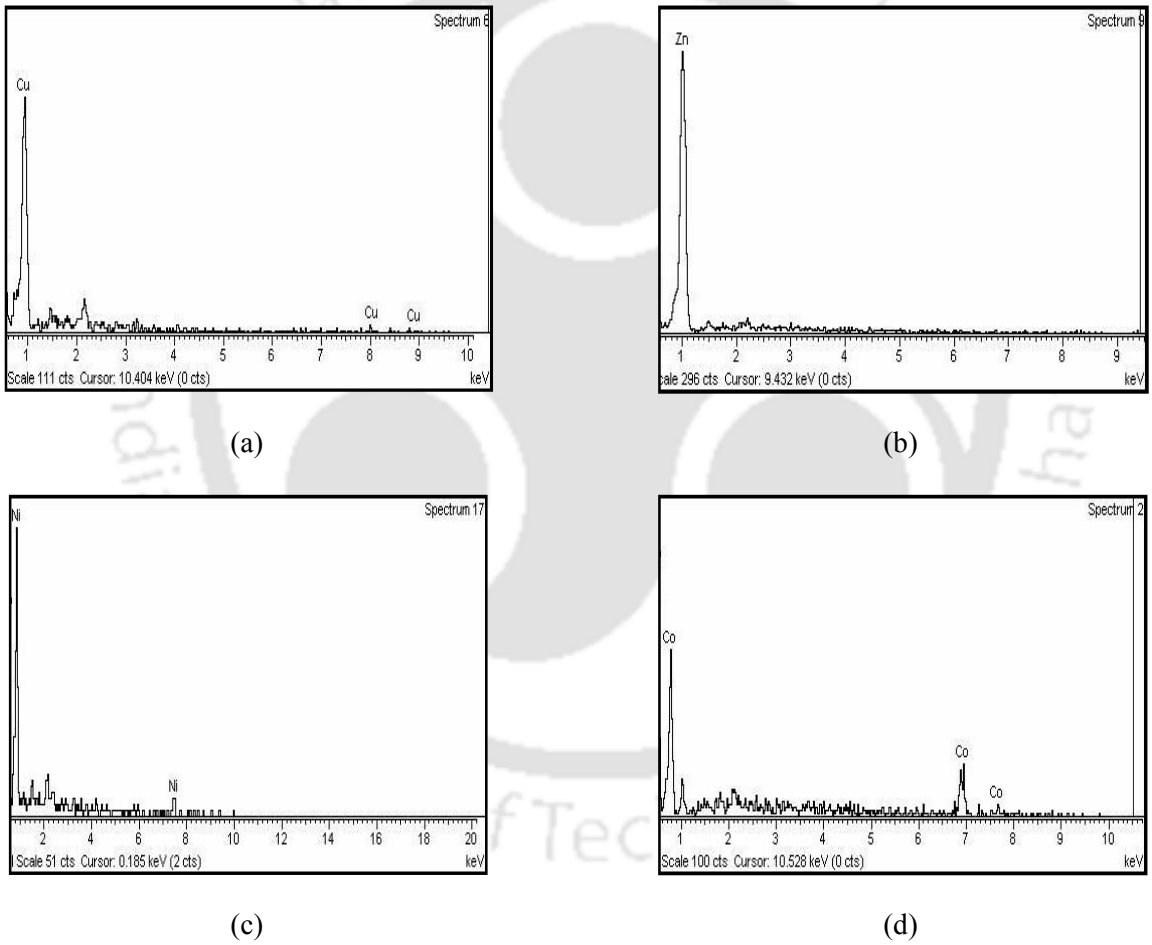

Figure 4.10 EDX spectra of electrodeposited cathode (a) Cu, (b) Zn, (c) Ni, and (d) Co

4.3.1.2 Electrochemical characterizations

The electroplated cathodes need to be characterized electrochemically to judge their efficacy in electrochemical environment before their use in dERC reactor for the product formation. Therefore, the 4 cathodes (Cu, Zn, Ni, and Co) were characterized in half-cell through the conventional 3-electrode test.

4.3.1.2.1 Cyclic Voltammetry

The cyclic voltammtery (CV) tests for the 4 cathodes have been done in a manner described in section 3.3.1, and represented in figures 4.11 to 4.14. CV was conducted in aqueous medium *viz.* 0.5 M $KHCO_3$ solution, saturated with N_2 or CO_2 gases, to compare the voltammograms in inert and CO_2 environments, respectively. The pH of the saturated solution with N_2 and CO_2 was 8.5 and 7.5, respectively. Figure 4.11 shows the cyclic voltammogram of Cu in inert (N_2) and CO_2 atmosphere. It can be seen that appreciable amount of current density was observed in both the environments. The onset potential (the potential at which 0.1 $mA \cdot cm^{-2}$ current density is observed) for Cu electrocatalyst was found to be 1.13 V. The current density in inert atmosphere is due to the reduction of H^+ resulting in the generation of H_2. However, the current density in CO_2 atmosphere is due to both H_2 generation and CO_2 reduction. It can be seen that current density oberseved in CO_2 atmosphere is significantly more as compared to current density observed in inert atmosphere for Cu electrocatalyst. This depicts that Cu is catalyzing the CO_2 reduction reaction resulting in higher current density in CO_2 atmosphere. However, same is not the case with the CV of Zn (Figure 4.12), where the current density in both the atmosphere is almost same. Thus, in such a case, performance of electrocatalyst for CO_2 reduction can not be determined.

Moreover, the CV of Zn shows some other interesting features. Two significant peaks can be observed at 1.38 V and 0.2 V, which are due to the dissolution of Zn in aqueous medium and not due

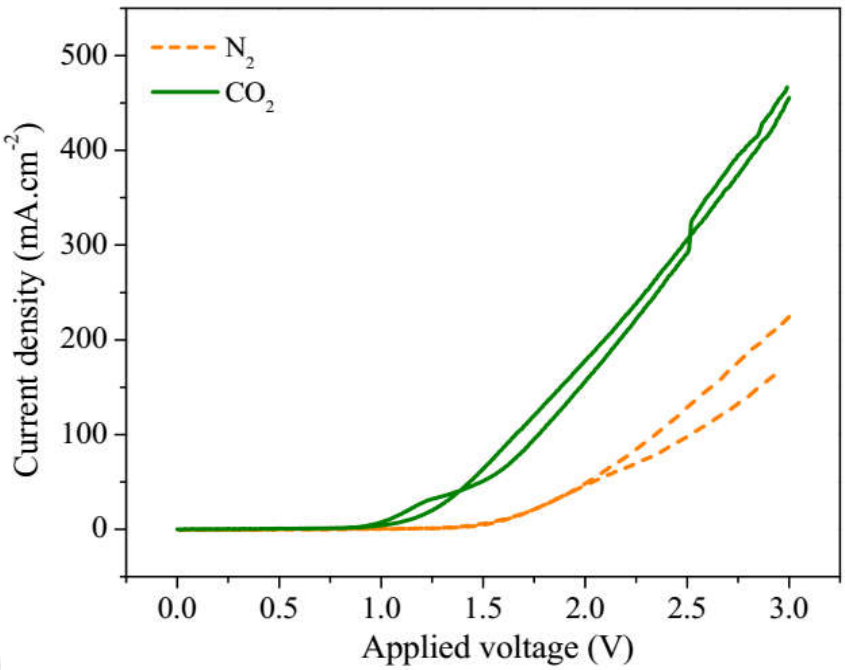

Figure 4.11 Cyclic voltammograms of Cu in N_2 (broken line), and CO_2 (solid line) atmosphere

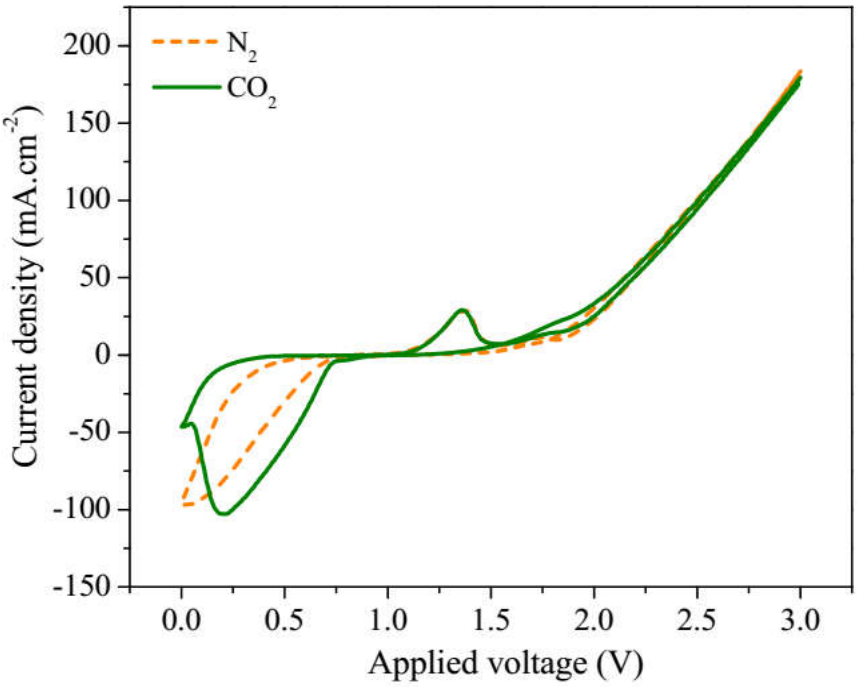

Figure 4.12 Cyclic voltammograms of Zn in N_2 (broken line), and CO_2 (solid line) atmosphere

to CO_2 reduction. Zinc is not stable in aqueous system and easily results in the formation of hydroxides. This notion was supported by the fact that deposition of white precipitate was observed after the completion of cyclic voltammogram. Further, the peaks are present in both inert and CO_2 atmosphere, hence it excludes the possibility that peaks can be due to the CO_2 reduction. Although, the peak position slightly differs in both the environments but that may be due to the introduction of CO_2. The onset potential was not determined in case of Zn as it would not serve any purpose owing to its unstable behaviour and inability to provide any information regarding CO_2 reduction. The cyclic voltammogram of Ni is shown in figure 4.13. For Ni, the onset potential was found to be ~1.13 V. It can also be seen that the current density in CO_2 atmosphere is less as compared to the current density in inert atmosphere. The same trend was also observed in the CV of Co (Figure 4.14) where onset potential was 0.95 V. This observation might lead to misinterpretation that Ni and Co are not able to reduce CO_2. However, without undergoing full cell reactions, any such inference can not be drawn. Therefore, the increase or decrease of current density in CO_2 atmosphere as compared to N_2

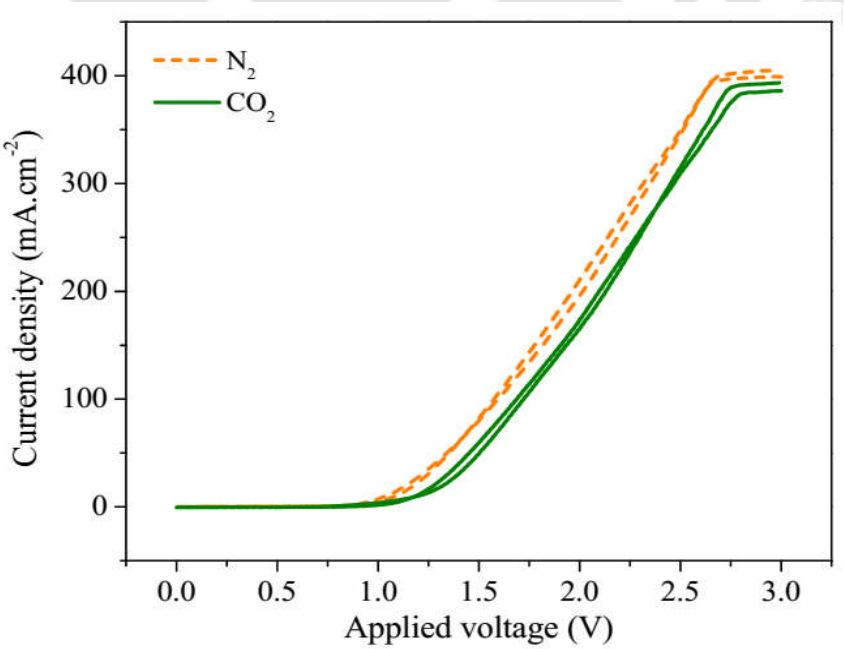

Figure 4.13 Cyclic voltammograms of Ni in N_2 (broken line), and CO_2 (solid line) atmosphere

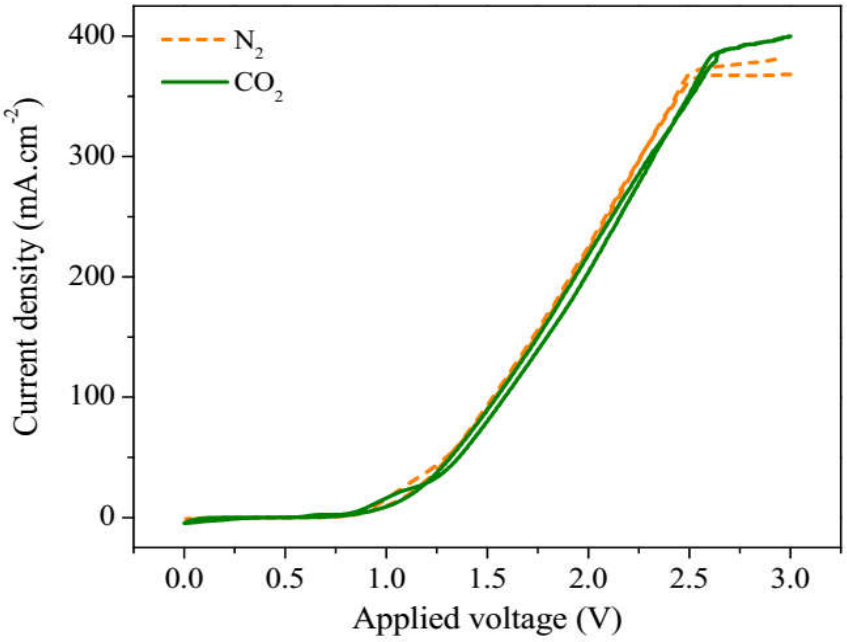

Figure 4.14 Cyclic voltammograms of Co in N_2 (broken line), and CO_2 (solid line) atmosphere

atmosphere, does not give any clear idea regarding the efficacy of electrocatalysts. The cyclic voltammetry results for all the four metals are summarized in Table 4.2.

Table 4.2 Summary of the results obtained after cyclic voltammetry

Metals	**Change in current density as compared to N_2 saturated solution**	**First hand inference based on CV results**
Cu	Current density increased in presence of CO_2	Electrocatalyst is active for ERC
Zn	No significant change was observed in current density in presence of CO_2	Prediction about activity is not possible
Ni	Current density decreased in presence of CO_2	Electrocatalyst has negative effect for ERC or HER
Co	Current density decreased in presence of CO_2	Electrocatalyst has negative effect for ERC or HER

Since, the electrochemical reduction of CO_2 involves complex multi-electron transfer reactions; it becomes difficult to determine the electrocatalytic activity based on the change in current density obtained in presence and absence of CO_2. It can be seen in Table 4.2 that on the basis of CV results, it is difficult to infer about the electrocatalytic activity of metals. One of the main hurdles in evaluating the electrocatalytic activity is the concurrent reduction of H^+/H_2O to H_2 along with the reduction of CO_2, the reduction potential of former being in close proximity to reduction potential of CO_2 to valuable products. Therefore, the simultaneous hydrogen evolution reaction (HER) during CO_2 electroreduction limits the evaluation of the electrocatalyst in the CV. Further, it provides erroneous results sufficient to bewilder the evaluation process, as can be seen in Table 4.2.

These problems may be addressed by selection and evaluation of suitable electrocatalyst using a method, which may help in initial screening of the electrocatalysts for ERC without being affected by HER. Moreover, the method should not be dependent on the identification of the reaction products as it would help to make the process quick. There was no suitable method, as of now, to screen the electrocatalysts from the group of many. The only reported method for *in-situ* characterization of electrocatalysts is cyclic voltammetry, where the current density difference in the inert gas and CO_2 saturated electrolyte helps to determine the electrocatalytic activity for ERC, as discussed above. However, the higher current density in CO_2 atmosphere does not always guarantee that the electrocatalyst is favoring CO_2 reduction because the increased current density may be due to the increased HER (Hori 2003). Moreover, pH of the electrolyte medium changes after solubilizing CO_2 into the electrolyte, which inturn assists the HER. However, this method may mislead as sometimes the current density obtained in a CO_2 saturated electrolyte is lower than the current density in inert gas saturated electrolyte even if the electrocatalyst is active for the CO_2 electroreduction, as seen in case of Ni and Co. This issue has also been reported earlier in case of Pt (Shuang *et al.* 2006) and Ag (Kaneco *et al.* 1998). However, no literature is clearly providing any means to characterize the electrocatalyst, before the full-cell studies. Hence a novel protocol is developed for screening the

electrocatalysts towards the CO_2 electroreduction using half-cell study (Singh *et al.* 2015 a). The protocol provides an easy, inexpensive, and reliable method for quick screening of any electrocatalyst for the ERC. Further, the protocol also helps to make a tentative comparison among the electrocatalysts tested.

4.3.1.2.2 Catalytic activity protocol development

Electrocatalyst alters the rate of any chemical or electrochemical reaction. Moreover, in case of electrochemical reaction the current density is directly related to the rate of reaction. Therefore, the proposed protocol is based on the current density difference determinations in presence and absence of the electrocatalyst.

Figure 4.15 is showing the proposed protocol in which it is shown that the activity of any selected electrocatalyst needs to undergo three tests in three different electrolytic media ($KHCO_3$, KOH, and DMF). It may be noted that generally, the ERC is conducted by saturating the CO_2 in 0.5 M $KHCO_3$ aqueous solution. The reason to use $KHCO_3$ is that in the presence of K^+, the hydrogen evolution is least among all alkali metals (Murata and Hori 1991). Moreover, with HCO_3^- the cathodic reduction of CO_2 proceeds more efficiently, since solubility of HCO_3^- is much higher than CO_2 in aqueous solution (Hori and Suzuki 1983). The willingness towards carrying out reduction in aqueous medium lies in the fact that it provides more valuable products in terms of calorific value (hydrocarbons, alcohols *etc.*) as compared to CO_2 reduction in non aqueous medium, where mostly oxalate, formate, and glycolates are formed (Scibioh and Viswanathan 2004). Therefore, in the 1st test the gaseous CO_2 was bubbled in aqueous 0.5 M $KHCO_3$ solution. The pH of the CO_2 saturated solution was found to be 7.5. Linear sweep voltammetry (LSV) was conducted in presence as well as in absence of the electrocatalyst. If by using the electrocatalyst, the current density decrease or remain same then it may indicate that the electrocatalyst is not active for ERC particularly in aqueous medium. Thus the electrocatalyst needs to be tested further in non-aqueous solution (3rd test) for its activity towards

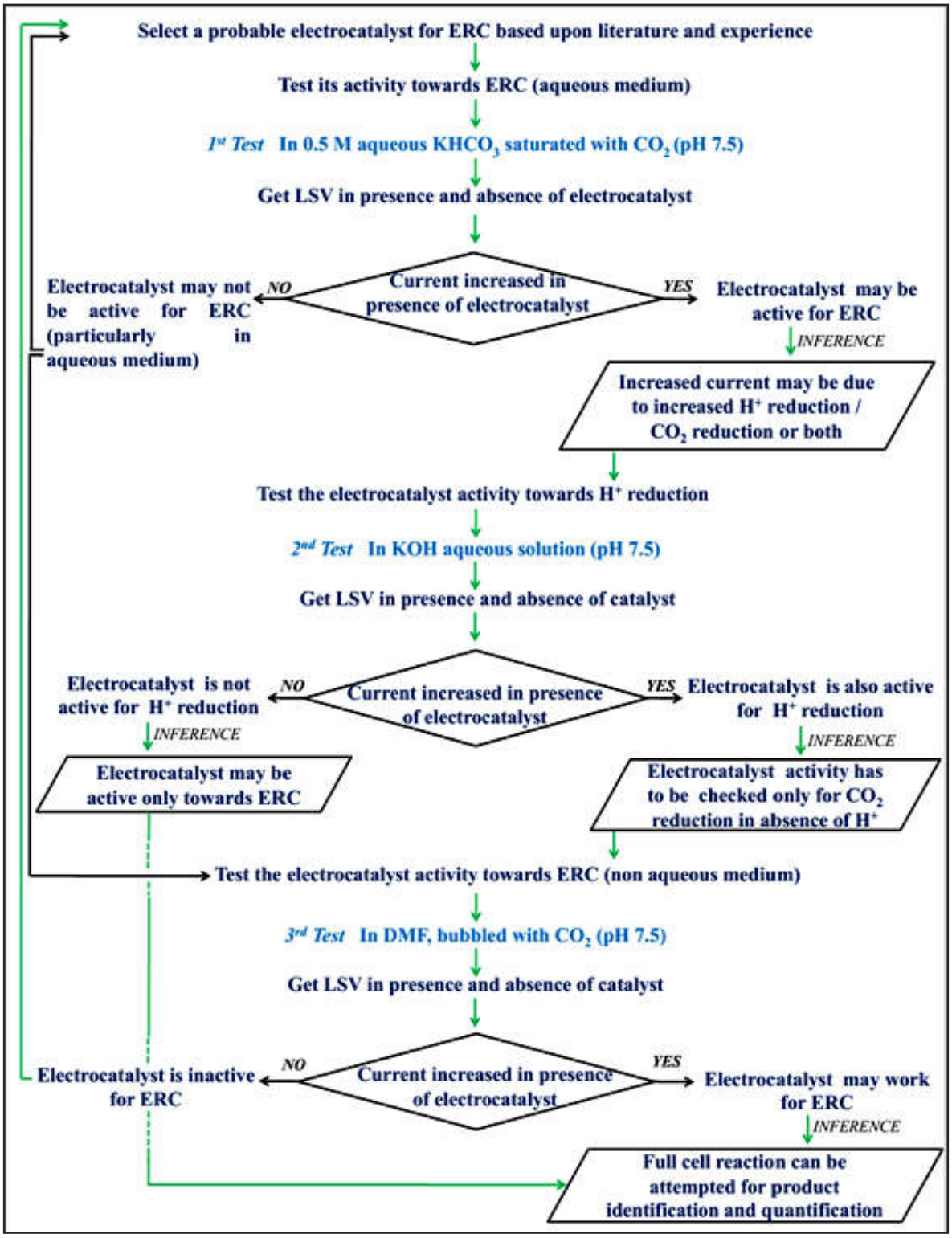

Figure 4.15 The proposed protocol (Singh *et al.* 2015 a)

ERC, where no free protons (H^+) or OH^- are present for the HER. However, if increased current density is shown in the 1st test then it would indicate the activity of the electrocatalyst towards ERC. Since, this test is conducted in aqueous medium, there is enough possibility of H^+ reduction and hence the increased current density may also correspond to HER or for both the HER and CO_2 reduction reactions. Now, to access whether the increased current density was due to HER, 2nd test was conducted. In 2nd test, the electrodes (with and without the electrocatalyst) were used in aqueous KOH solution keeping same pH (*i.e.* 7.5) as in 1st test while CO_2 was not bubbled in the solution. Thus the 2nd test was used to check the catalytic behavior of electrocatalyst towards H_2 generation only. If the electrocatalyst is not active (no increase in current density) for HER then it may be a good electrocatalyst for ERC and may be screened for full electrochemical cell reaction. However, higher current density using electrocatalyst shows the catalytic activity towards HER and thus it is important to further analyze the selected electrocatalyst in 3rd test to check its activity specifically for ERC. In the 3rd test, CO_2 was dissolved in DMF and electrode was used with and without the electrocatalyst. The significant thing to note is that the same pH was maintained in all the tests to avoid any favor to HER. However, the reason for choosing pH 7.5 was that ERC is always favorable in slightly basic medium as at this pH the HER is least active (Hori 2008). It may be noted that the current density produced in 3 different tests may not be compared amongst themselves, as the electrical conductivities of the 3 solutions were different ($mS \cdot cm^{-1}$ in case of $KHCO_3$ and KOH, while $\mu S \cdot cm^{-1}$ in case of DMF), which ultimately affects the current density generated. However, the current density can be compared among the different electrocatalysts in a single test.

4.3.1.2.2.1 Validation of the proposed protocol

To validate the developed protocol, the metal electrocatalysts were tested using the developed protocol. As per the protocol, 1st test needs to be conducted in aqueous medium (0.5 M $KHCO_3$) saturated with CO_2. Hence, linear sweep voltammogram (LSV) was plotted using gas diffusion layer (GDL) without any catalyst. Further, GDL with metal electrocatalysts (Cu, Zn, Ni, or Co) was used to

plot voltammograms. The comparison of voltammograms in presence of metal electrocatalysts and GDL is shown in figure 4.16. It can be clearly observed that all the metal electrodes resulted in significantly higher current density as compared to GDL. This depicts that metal electrocatalysts are able to reduce the electroactive species present in the system. However, there are two electroactive species (CO_2 and H^+) present in the aqueous system. Hence, the increased current density observed can be due to either one or both the species. It is mandatory, therefore, to determine the cause of increased current density in the 1st test. For this purpose, 2nd test (as per the protocol) was conducted to see the behaviour of metal electrocatalysts towards the H^+ reduction. No increment in current density using metal electrocatalysts as compared to GDL in this test would confirm that the increased current density in 1st test was due to CO_2 reduction. The results for the 2nd test are shown in figure 4.17. Remarkably, all the metal electrocatalysts are active for H_2 production, the most active being

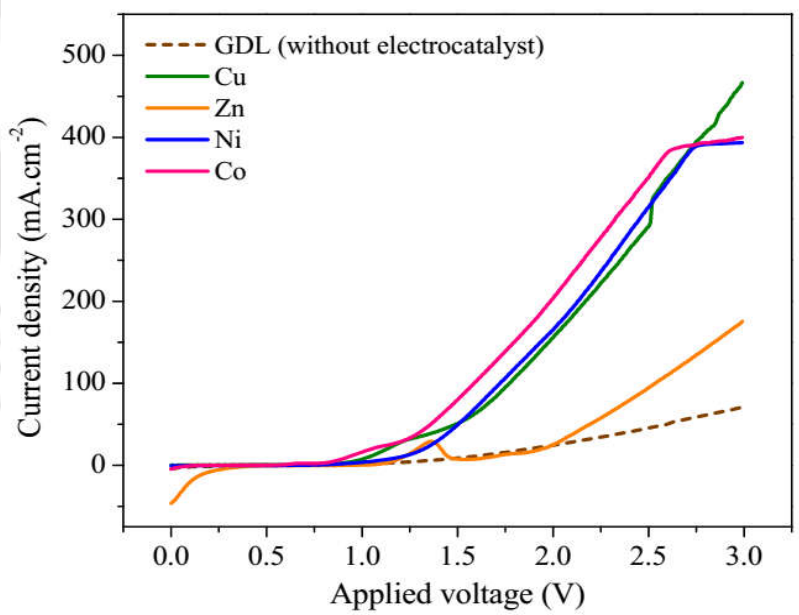

Figure 4.16 Comparison of electrocatalytic activity of electroplated metals on GDL (solid lines), and only GDL (broken line) for the 1st test as per the catalytic activity protocol

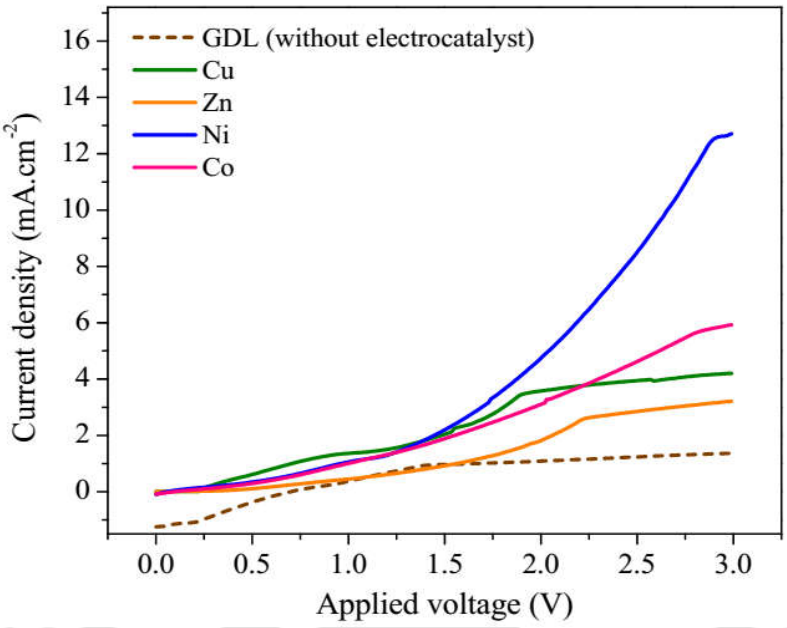

Figure 4.17 Comparison of electrocatalytic activity of electroplated metals on GDL (solid lines), and only GDL (broken line) for the 2nd test as per the catalytic activity protocol

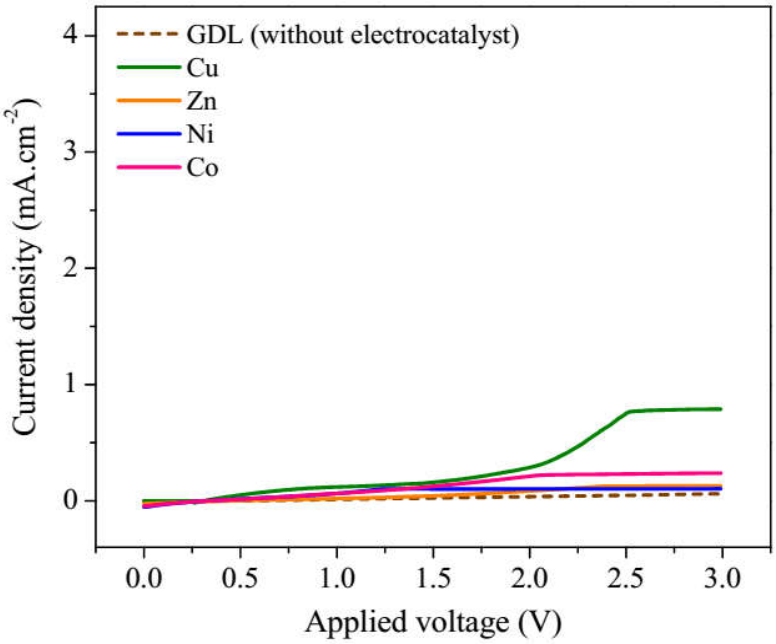

Figure 4.18 Comparison of electrocatalytic activity of electroplated metals on GDL (solid lines), and only GDL (broken line) for the 3rd test as per the catalytic activity protocol

the Ni, followed by Co, Cu, and Zn. This result confirms that the current density observed in 1st test was due to both CO_2 reduction as well as H_2 generation. Therefore, the activity of metal electrocatalysts has to be tested in such a medium where there should not be any interference due to H_2 formation. 3rd test of the protocol address this issue. In 3rd test, reaction is carried out in non-aqueous medium (DMF), bubbled with CO_2. In this test, CO_2 was bubbled only upto the extent to get the same pH as in 1st test. Voltammograms were again obtained in presence and absence of electrocatalysts and compared. The results obtained in 3rd test are shown in figure 4.18. It can be seen that the current density for all the metal electrocatalysts was higher than the current density produced in case of only gas diffusion layer (in absence of electrocatalyst). Since in non-aqueous medium, apart from CO_2, there was no electroactive species present in the system, hence the current density produced can be solely attributed to the reduction of CO_2. Thus, this test confirms the electrocatalytic activity of metal electrocatalysts towards CO_2 reduction and hence, these metals can be used in the full cell reactions for the further studies. It is to be noted that the current densities produced in the three different tests, described above, can not be compared amongst themselves, as the electrical conductivities of the 3 solutions were different ($mS \cdot cm^{-1}$ in case of $KHCO_3$ and KOH, while $\mu S \cdot cm^{-1}$ in case of DMF), which ultimately affect the current density produced. However, the current density can be compared among the different electrocatalysts in a single test (Singh *et al.* 2015 a). It is also noticeable in figure 4.18 that, there is no increment in current density after 2.5 V in case of Cu and 2 V in case of Co and Ni. Moreover, on comparing the corresponding current densitites in figure 4.16 and 4.18, it can be seen that the magnitude of current density is significantly low in case of figure 4.18. In case of CO_2 saturated aqueous system (figure 4.16), a significant amount of current density was due to the reduction of H^+ into hydrogen gas at the cathode apart from CO_2 reduction. In case of DMF (figure 4.18), however, the CO_2 was bubbled only upto a certain level to maintain the pH instead of CO_2 saturation in DMF. Moreover, the electroreduction might not be completed due to absence of other reactants to combine with the reduced or activated CO_2. In turn, the low level of CO_2 in the electrolyte along with increased mass transport resistance and scarcity of co-reactant reduces

the current density, which does not increase even with the increase in the applied voltage. Apart from other reasons, the difference (in the order of 10^3) in electrical conductivities of the media ($mS \cdot cm^{-1}$ in case of $KHCO_3$, while $\mu S \cdot cm^{-1}$ in case of DMF) also affect the performance. Another important observation is the absence of any peak in Zn voltammogram in DMF (3rd test). Thus, it further supports the fact that the peaks observed in the cyclic voltammogram of Zn in aqueous medium (Figure 4.12) were due to dissolution of Zn itself in presence of H_2O.

The developed protocol and its validation, makes clear that all the chosen metal electrocatalysts are active for CO_2 reduction. Table 4.3 shows the comparison of the results obtained after the CV test and protocol test. The protocol qualitatively helps to overcome the confusion arisen after the CV tests for the Zn, Ni, and Co electrocatalysts. These results also validate the developed protocol and hence it will be used as the primary *in-situ* characterization technique for all the electrocatalysts discussed in the forthcoming chapters.

4.3.2 Characterization of anode

Characterization of Pt/C deposited anode is also important as it is also equally involved in the overall process of dERC. The SEM image of the Pt/C anode is shown in figure 4.19. The morphology of the

Table 4.3 Comparison of activities (qualitative) of the catalysts based on the CV and the protocol

Metals	CV method	Proposed protocol
Cu	Active	Active
Zn	Difficult to predict	Active
Ni	Inactive	Active
Co	Inactive	Active

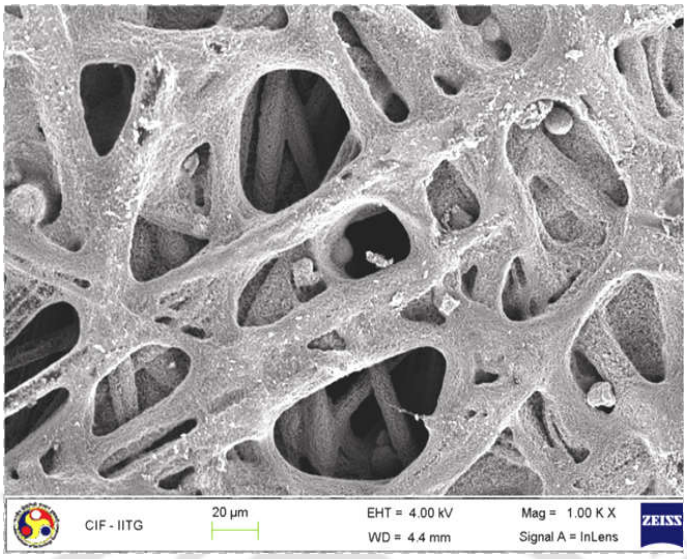

Figure 4.19 SEM image of Pt/C

anode shows the porous structure for the transport of water from one surface (uncoated, not shown here) to another (coated) surface. Although the porosity gets reduced after spraying the Pt/C as compared to pure gas diffusion layer (Figure 4.5), but it is still enough to transport water through it.

4.3.3 Characterization of solid polymer electrolyte (Nafion-117)

The solid polymer electrolyte is another important constituent of electrochemical cell. Commercially available cation exchange membrane, Nafion-117 was used for the present work. XRD pattern of the Nafion is shown in figure 4.20. The Nafion shows a broad peak at 14°-18° which can be deconvoluted into two peaks. These two peaks can be assigned to amorphous (2θ = 16°) and crystalline (2θ = 17.5°) scattering from the polycarbon chains of Nafion (Barbora *et al.* 2010). The SEM image of Nafion, shown in Figure 4.21, appears uniform without any formation of pores and/or cracks. FTIR spectrum of Nafion is shown in figure 4.22. The FTIR spectrum shows 5 major bands *viz.* SO_3- and -SO_3H band, C=O and C-O-C band, C-F band, band representing H_2O bending, and a band for stretching vibration of water. The peaks at 518 cm^{-1} and 633 cm^{-1} for the pure cast Nafion membranes, as shown in figure 4.22, represent SO_3^- group. The band at 718 cm^{-1} can be assigned to

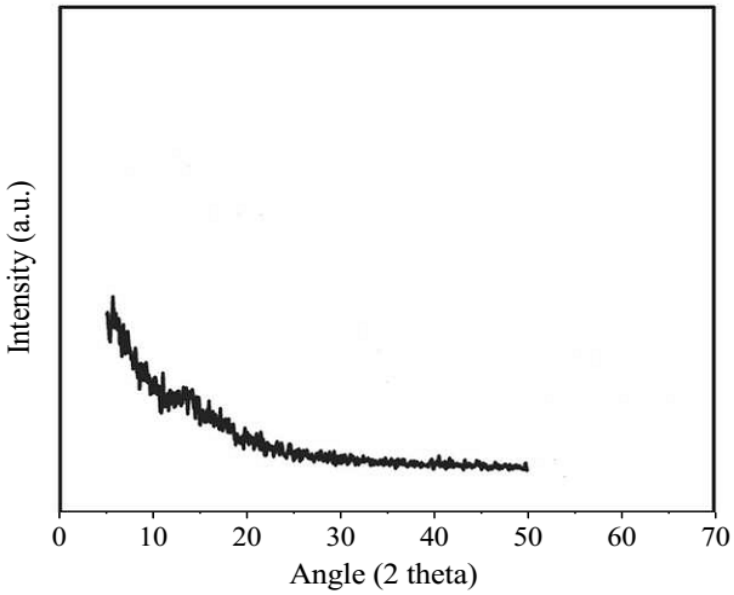

Figure 4.20 XRD pattern of Nafion-117

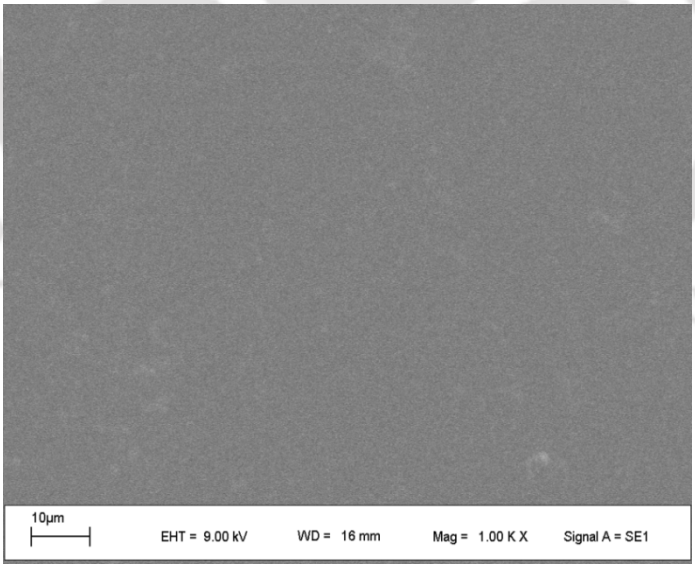

Figure 4.21 SEM image of Nafion-117

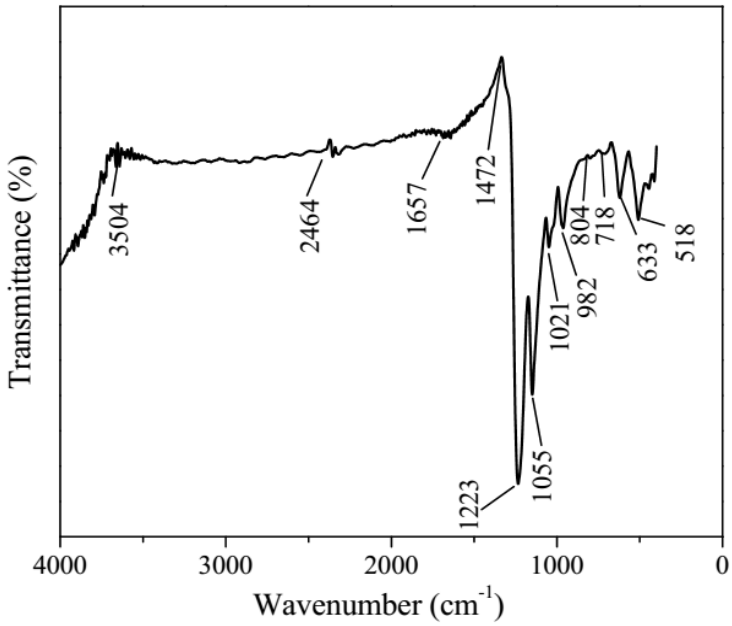

Figure 4.22 FTIR spectrum of Nafion-117

C=O bending (Kumutha and Alias 2006). Peak at 982 cm^{-1} represent vibration of C-O-C bond (Mahreni *et al.* 2009). The stretching vibration of SO_3^- can be seen at 1055 cm^{-1} (Ramani *et al.* 2005). A band for water bending can be seen in the region of 1400-2000 cm^{-1} (Park and Yamazaki 2005) and the peak in the region of 3200 and 3700 cm^{-1} can be assigned to stretching vibration of water molecules (Ludvigsson *et al.* 2000).

4.3.4. dERC studies using metal electrocatalysts

The full cell studies were carried out to examine the preference of the chosen metal electrocatalysts towards CO_2 reduction to form different products and their selectivity. The dERC was carried out in an electrochemical reactor using the experimental set-up as described in section 3.3.2.

4.3.4.1 Copper metal electrocatalyst

The CO_2 gas was fed into the electrochemical reactor and the resulting products were collected and analyzed at different applied voltages ranging from 1.5 to 3 V. Figure 4.23 shows the obtained current density as a function of applied voltage using copper metal electrocatalyst. It can be seen that current density is showing an increasing trend with the applied voltages. With the increasing applied voltages, the supplied electrical charge is consumed by the reacting species at the electrode surface thus resulting in increased current. Current density increases from 5.93 $mA \cdot cm^{-2}$ at 1.5 V to 13 $mA \cdot cm^{-2}$ at 3 V. The current density obtained corresponds to the rate of reaction to form some products and by-products. These reaction products and by-products were quantified and represented in figure 4.24.

Figure 4.24 shows the amount of products formed as a result of dERC. The results are shown for 1 hour of reaction in full thesis, as detailed in section 3.5, unless stated otherwise. It can be seen that CH_4, CO, and H_2 are formed. It is observed that amount of the CO formation is very low as compared to the formation of CH_4. The formation of CH_4 increases from 1.5 V, attains maxima at 2 V and then

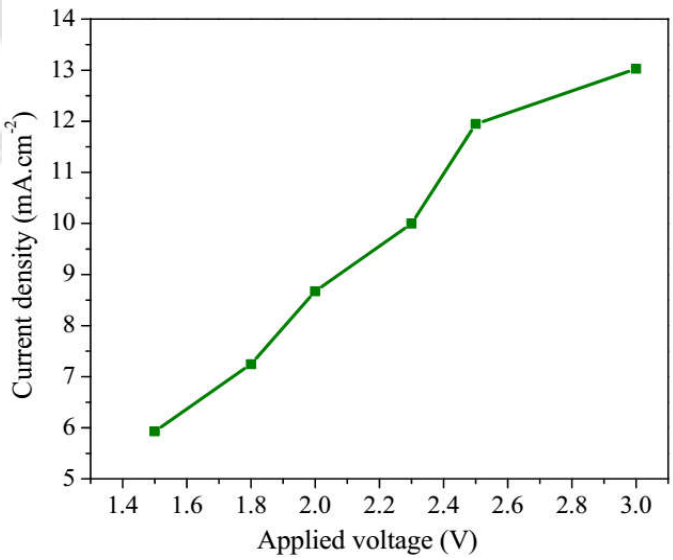

Figure 4.23 Current density as a function of applied voltage using Cu

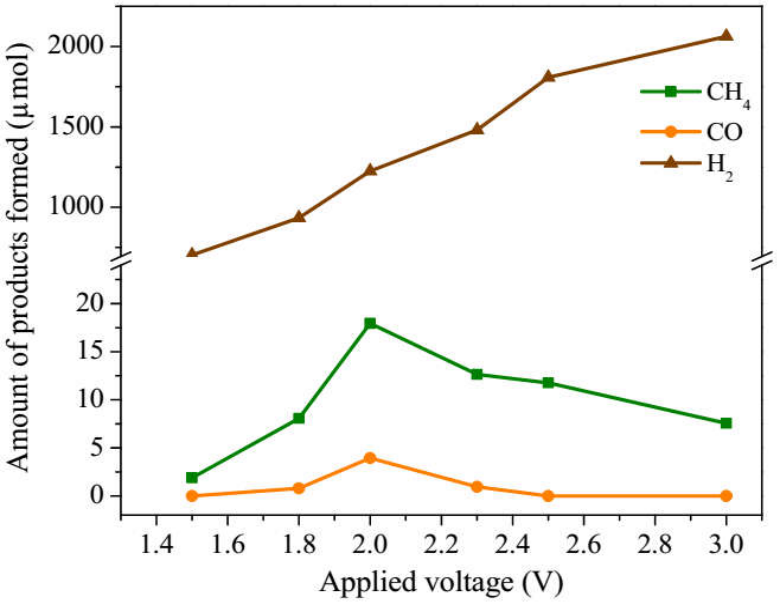

Figure 4.24 Amount of the products formed as a function of applied voltage for electrochemical reduction of CO_2 using Cu

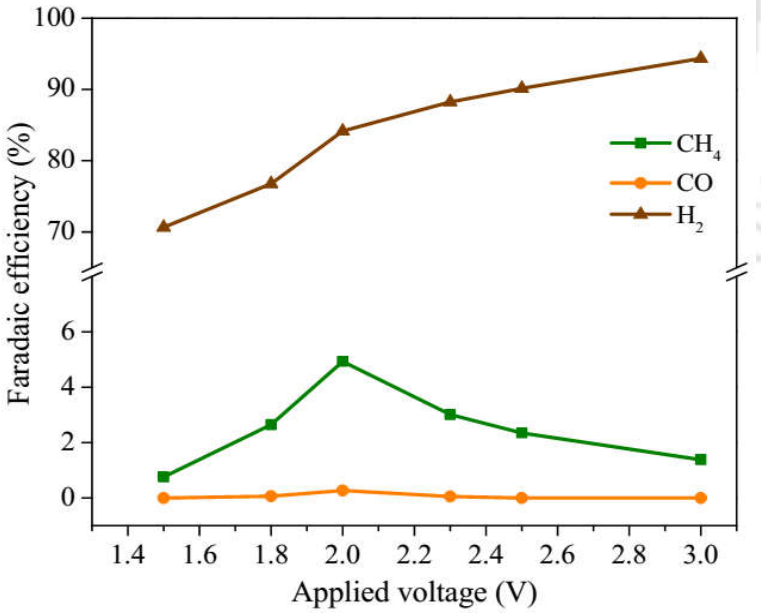

Figure 4.25 Faradaic efficiency as a function of applied voltage for electrochemical reduction of CO_2 using Cu

gradually decreases (Singh *et al.* 2015 b). Similar trend is also shown by the CO. It can be seen in figure 4.24 that amount of the methane formed was 17.94 µmol (at 2 V) and CO formation was 3.94 µmol (2 V). Moreover, hydrogen which is a by-product was increased from 703.78 µmol at 1.5 V to 2063.67 µmol at 3 V (Figure 4.24). This trend shows that most of the supplied energy was consumed for the unwanted H_2 production. H^+ ions are generated from the water oxidation at anode, which passes through the membrane and reduced at cathode. H^+ reduction is a competitive reaction to the CO_2 electroreduction at cathode. The formation of hydrogen increases with increasing applied voltages and this trend shows that Cu is not efficient enough to catalyze CO_2 reduction at the first place *in lieu of* which H_2 formation prevails. The Faradaic efficiency of the products formed is shown in figure 4.25 which is calculated in a manner discussed in section 3.5.1. The Faradaic efficiency is determined for 1 hour duration of product formation as it has been seen that beyond this duration, all the supplied energy gets wasted for the hydrogen (by-product) formation. The Faradaic efficiency follows the same trend as seen in case of the amount of the product formation. The maximum Faradaic efficiency for the CH_4 and CO formation was found at 2 V, *viz.* 4.93% and 0.27%, respectively (Figure 4.25). The low Faradaic efficiency was expected due to the deactivation of Cu electrode (Hori *et al.* 2005; Li and Kanan 2012). Moreover, most of the supplied energy was utilized for the unwanted H_2 production. The exact reason for increased formation of H_2 is not known but it can be postulated that probably higher applied voltages favour the proton and electron transfer, resulting either in more H_2 coverage of electrode surface or Heyrovsky mechanism for H–H bond formation becomes more dominant pathway for hydrogen evolution (Kuhl *et al.* 2012). It was seen in figure 4.23 that current density increases on increasing the applied voltages. This was due to increasing hydrogen formation at higher applied voltages, which is evident in figure 4.24 and 4.25. Thus, increased concentration of H^+ at the cathode surface adversely affects the reduction of CO_2.

4.3.4.2 Zinc metal electrocatalyst

The full cell reactions were also carried out for the zinc cathode. The current density obtained using zinc electrocatalyst is shown in figure 4.26. The current density increases with gradual increase in the applied voltages. The current density increases from 2.89 $mA \cdot cm^{-2}$ at 1.5 V to 14.53 $mA \cdot cm^{-2}$ at 3 V. However, increase in the current density was quicker after 2.3 V. The obtained current density is nothing but the rate of the reaction occuring on the electrode surface. It may be noted that the current density for Zn is higher than Cu electrode for higher applied potential (especially at 3 V). It refers that the reactions (either CO_2 reduction or H_2 formation) taking place at the Zn surface are more at that applied voltage.

In figure 4.27, the amount of the products formed using Zn electrocatalyst is shown with respect to applied voltage. It shows that two products were formed in case of Zn, namely, CH_4 and CO along with the H_2 as a by-product. Moreover, the amount of CO is much higher as compared to CH_4. This is in contrast to the result which was found in case of Cu as an electrocatalyst. Various researchers have

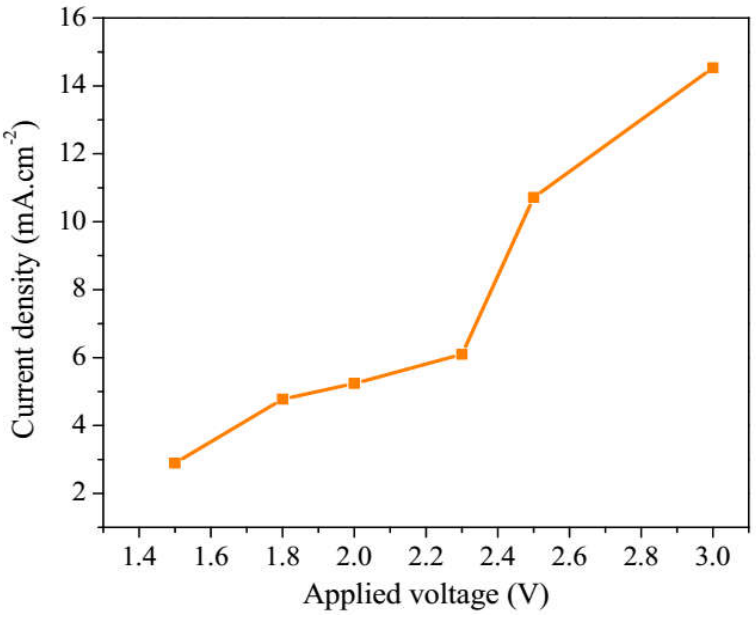

Figure 4.26 Current density as a function of applied voltage using Zn

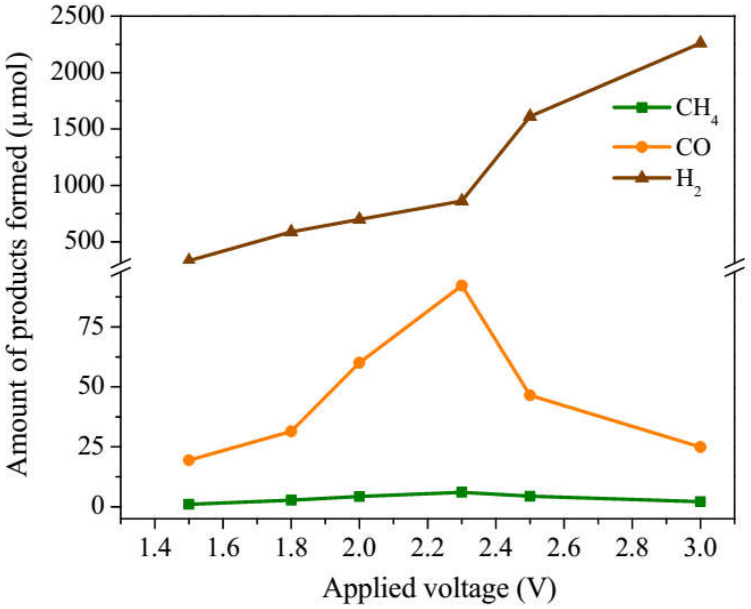

Figure 4.27 Amount of the products formed as a function of applied voltage for electrochemical reduction of CO_2 using Zn

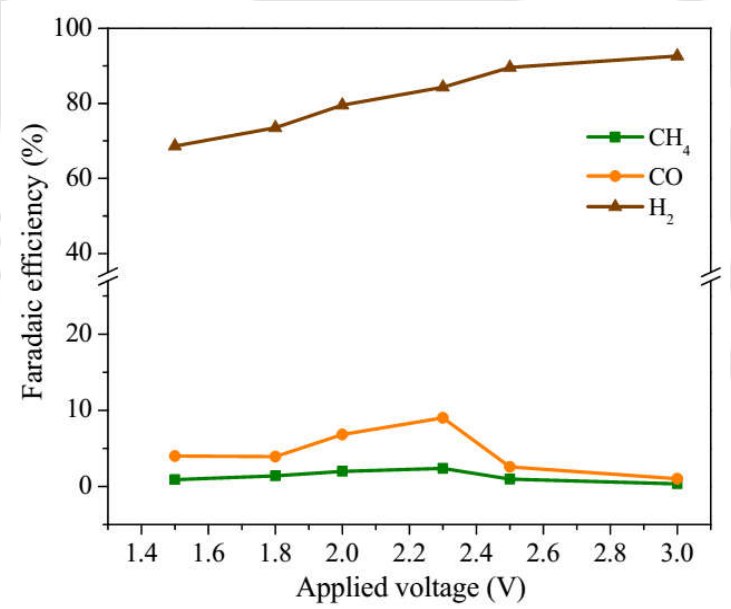

Figure 4.28 Faradaic efficiency as a function of applied voltage for electrochemical reduction of CO_2 using Zn

also found the formation of CO though the CO_2 was dissolved in electrolyte for the ERC (Hori *et al.* 1994; Hara *et al.* 1995). Further, it may be noted that the maximum formation of the products took place at 2.3 V for Zn electrode, whereas, in case of Cu, the maximum amount of product was formed at 2 V. It shows that the Zn electrode has higher overpotential than Cu for the dERC. CO and CH_4 formation was found to be 92.28 µmol and 6.08 µmol, respectively at 2.3 V. It can be seen that at higher applied voltages, the amount of hydrogen formation is quite high and it exceeds the 2063 µmol found in case of Cu. Thus, it can be stated that the higher current density found in case of Zn (as compared to Cu) (Figure 4.26) resulted only in the increased H_2 formation, which is an undesired reaction.

Figure 4.28 shows the Faradaic efficiency of the products formed using Zn metal electrocatalyst. The Faradaic efficiency of CO and CH_4 is ~9% and 2.37 %, respectively at 2.3 V (Figure 4.28). As the applied voltage increases, the amount of CH_4 and CO decreases and hydrogen evolution increases. It follows the same trend as in case of Cu; however, due to more overpotential, the voltage required is more in case of Zn. The total Faradaic efficiency for the CO_2 reduction was found to be 11.37% at 2.3 V, corresponding to the current density of 6.1 $mA \cdot cm^{-2}$. The Faradaic efficiency of H_2 formation was reached upto 92.63% as shown in figure 4.28. It can be said that the product formation using Zn is not very appreciable and the electrocatalyst does not seem to be very active for dERC. The unstable nature of Zn, as discussed in section 4.3.1.2.1, is also responsible for the inferior performance of Zn.

4.3.4.3 Nickel metal electrocatalyst

The current density of Ni for the various applied voltages during dERC is shown in figure 4.29. It is observed that the current density or rate of the reaction increases with increase in the applied voltage for Ni metal electrocatalyst. The increased reaction rate due to the increased current density corresponds to the increased rate of electrical charge being used in the process. The current density

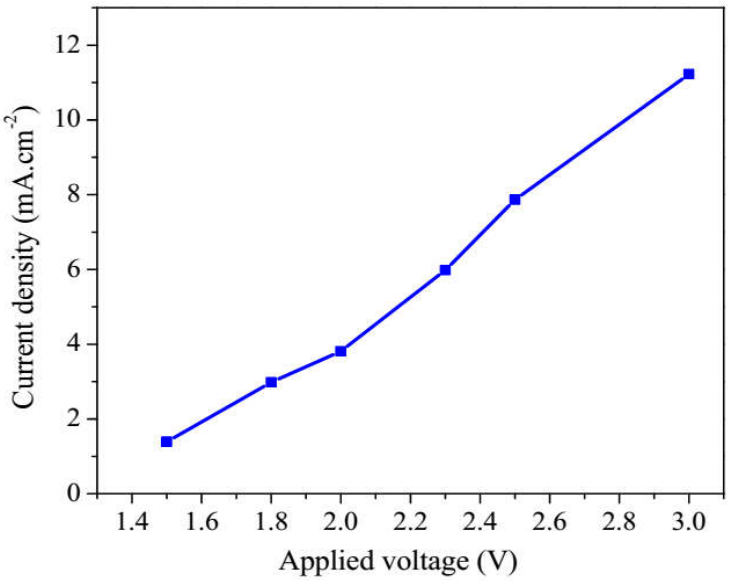

Figure 4.29 Current density as a function of applied voltage using Ni

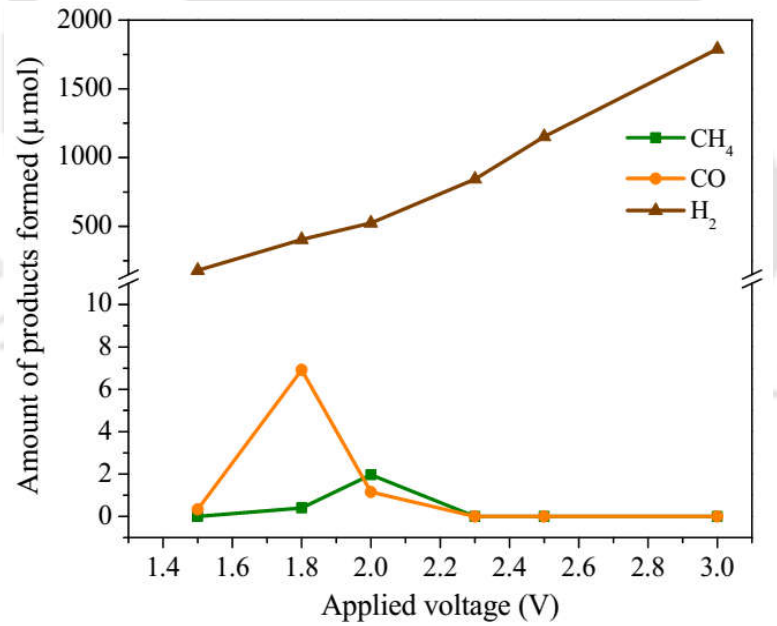

Figure 4.30 Amount of the products formed as a function of applied voltage for electrochemical reduction of CO_2 using Ni

increases from 1.39 $mA \cdot cm^{-2}$ at 1.5 V to 11.22 $mA \cdot cm^{-2}$ at 3 V. It may be noted that the current densities corresponding to various voltages are lower in the case of Ni metal electrocatalyst compared to Cu and Zn. It may refer that the reactions taking place over Ni are in slow pace and may result in less amount of products.

The product distribution as a function of applied voltages for the direct electrochemical reduction of CO_2 using Ni metal electrocatalyst can be seen in figure 4.30. Again, CO was formed as the major product as was seen in case of Zn. Along with CO, CH_4 was also formed in minor quantity along with significant amount of H_2 as a by-product (Singh *et al.* 2015 b). Amount of CO rose sharply from 1.5 V, attained maxima at 1.8 V and then it subsided gradually. Moreover, the formation of CH_4 is highest at 2 V. Amount of hydrogen formed was less as compared to Cu and Zn. The hydrogen evolution increases with increasing voltage and reaches upto 1789 µmol at 3 V. Maximum amount of CO and CH_4 formation was 6.91 µmol and 1.97 µmol, respectively. It shows that Ni is selective for CO formation. Enhanced hydrogen formation with increasing current density shows that at higher voltages H^+ ions occupy most of the active sites over the metal electrocatalysts, leading to inhibition of CO_2 reduction reaction. However, it is to be noted that the overpotential for the CO formation was lowest for Ni electrocatalyst as compared to Cu and Zn. Whereas, Ni poses similar overpotential for CH_4 formation as for Cu but lower overpotential than Zn.

Figure 4.31 shows the Faradaic efficiency of the products obtained in dERC using Ni metal electrocatalyst. At 1.5 V, the formation of both CH_4 and CO is quite meagre. On increasing the voltage, the formation of CO was increased with maximum Faradaic efficiency of 1.38% at 1.8 V. At the same voltage, formation of CH_4 remained meagre with only 0.32% of Faradaic efficiency. However, on further increasing the voltage, the formation of CH_4 reached its maxima with 1.23% Faradaic efficiency at 2 V. After 2 V, the formation of both the products decreased gradually. Faradaic efficiency of these products is a cumulative result of reaction carried out for 1 hour duration. Reaction was not extended beyond 1 hour as the electrocatalyst started to show the exclusive

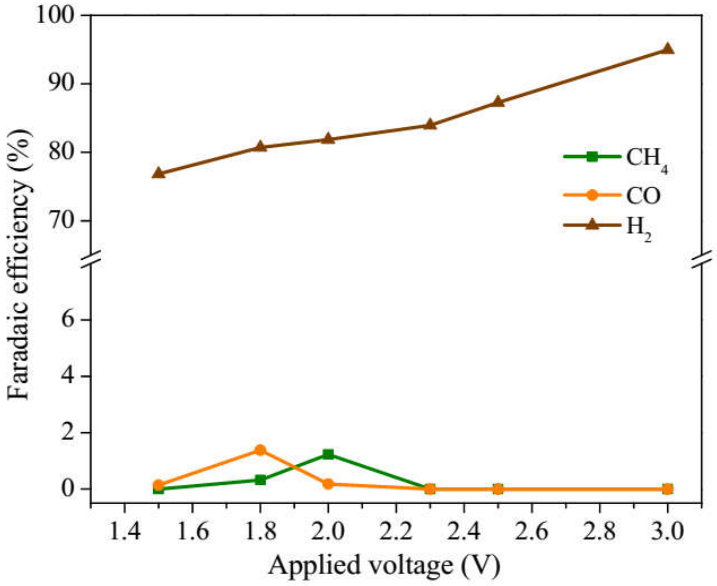

Figure 4.31 Faradaic efficiency as a function of applied voltage for electrochemical reduction of CO_2 using Ni

formation of H_2 after only 40-50 minutes. The Faradaic efficiency of H_2 was found to be 94% at 3 V. One interesting point to note in case of Ni metal electrocatalyst is that, the formation of CO took place at 1.8 V which is the least required voltage as compared to Cu and/or Zn. Thus, overpotential required in case of Ni is less as compared to Cu and Zn (Singh *et al.* 2015 b) but the catalyst is not very active for the dERC.

4.3.4.4 Cobalt metal electrocatalyst

The investigations over Co metal electrocatalyst for electrochemical reduction of CO_2 are shown in figure 4.32. Similar to the cases discussed above, the current density increases with increasing applied voltages in case of Co metal too. More or less, current density increases almost linearly with the applied voltage. It can be seen that the current density at 1.5 V is 0.13 $mA \cdot cm^{-2}$, and then it increases gradually with 6.36 $mA \cdot cm^{-2}$ at 3 V depicting the increase in the rate of the reaction with increasing applied voltage.

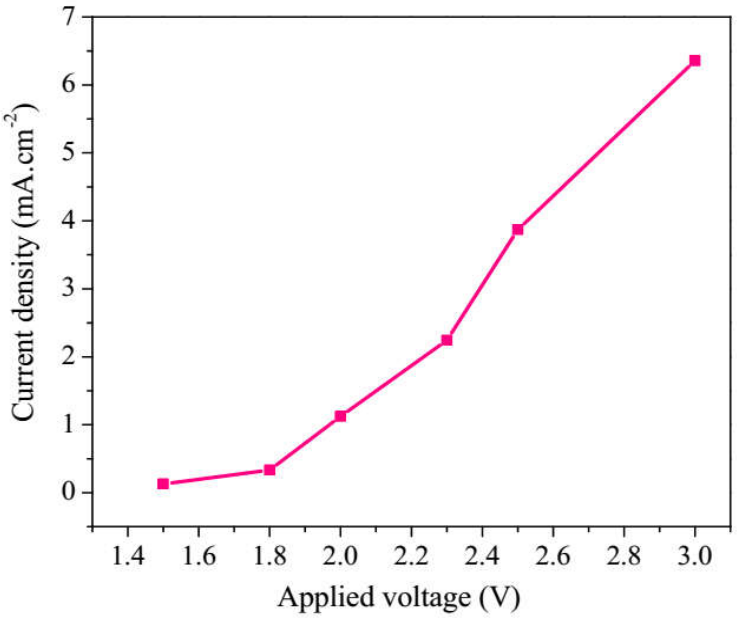

Figure 4.32 Current density as a function of applied voltage using Co

Figure 4.33 shows the product distribution in case of Co metal electrocatalyst as a function of applied voltage. The types of products formed are not different from earlier cases, and again formation of CH_4 and CO was seen. However, similar to Zn and Ni, CO was again the major product in case of Co. Amount of CO was found highest at 2.3 V with 30.86 µmol. CH_4 formation was also found significant and was in highest amount at 2.3 V with 6.21 µmol. On increasing the voltage beyond 2.3 V, the formation of these two products does not increase. Hydrogen formation, as in other cases, goes on increasing with increasing applied voltages and corresponds to increase in current density as seen in figure 4.33. Maximum amount of hydrogen formation was seen at 3 V with 924.66 µmol. However, it may be noted that in case of Co, the hydrogen formation is least among the other three metal electrocatalysts, with surprisingly only ~11 µmol at 1.5 V. Moreover, it can also be concluded that cobalt needs high overpotential as compared to Cu and Ni for the formation of CH_4 and CO.

Figure 4.34 shows the Faradaic efficiency of the products obtained using Co metal electrocatalyst for direct electrochemical reduction of gaseous CO_2. The Faradaic efficiency of the CO is highest at 2.3

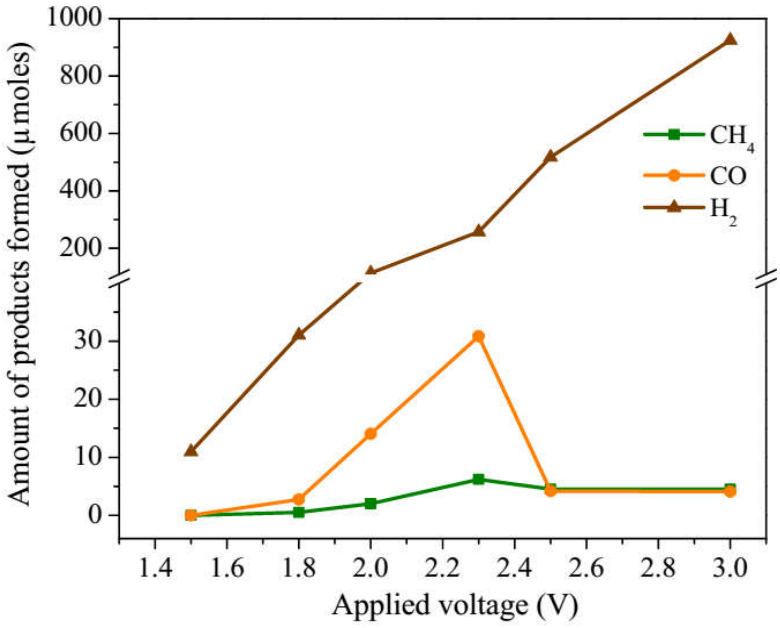

Figure 4.33 Amount of the products formed as a function of applied voltage for electrochemical reduction of CO_2 using Co

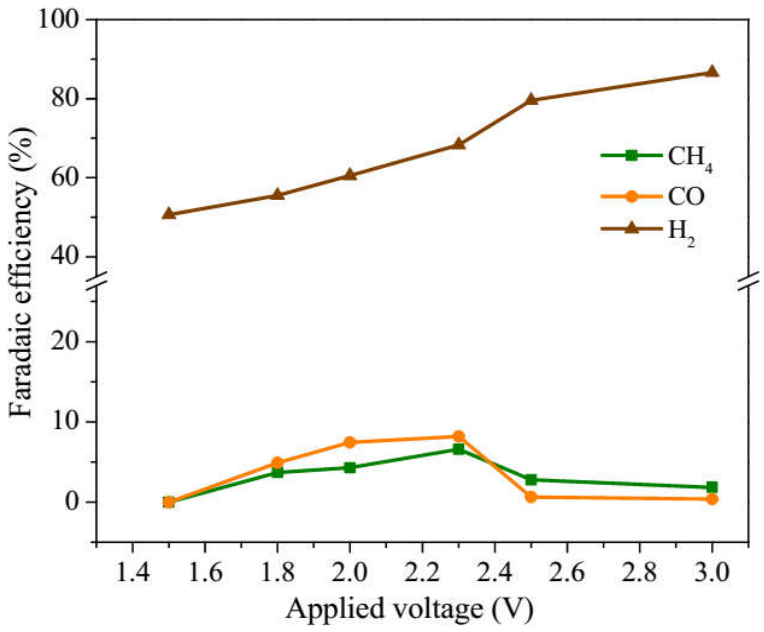

Figure 4.34 Faradaic efficiency as a function of applied voltage for electrochemical reduction of CO_2 using Co

V with 8.19%, while CH_4 is having Faradaic efficiency of 6.59% at the same applied voltage. Faradaic efficiency of H_2 again followed the trend as that of the current density with highest Faradaic efficiency of 86.64% at 3 V. The noticeable fact is the required voltage for the formation of various products. Although significant amount of products formation took place at 2 V, but the maximum Faradaic efficiency could be found only at 2.3 V for both CH_4 and CO, which is quite high voltage.

It can be said that all the tested pure metal electrocatalysts are active for reducing CO_2. The rate of reaction of all the metal electrocatalysts is shown in Table 4.4. The rate of the reaction is calculated at the applied voltage where maximum amount of product formation took place, as discussed in section 3.5.2. It further confirms that chosen metals are actively participating in dERC. However, the Faradaic efficiency of the products is very less. On the other hand, the overpotential required for the reaction is also quite high *esp.* for Zn and Co.

Figures 4.35 to 4.38 show the selectivity patterns of these metals. Based on the selectivity profiles, it can be said that out of the 4 metals studied; only Cu shows the highest selectivity for CH_4 formation. It can be seen in figure 4.35 that CH_4 is selectively formed at all the applied voltages when Cu is used as an electrocatalyst. CO is hardly 20% selective at 2 V. In case of Zn, however, the selectivity trend

Table 4.4 Rate of the reaction of metal electrocatalysts for dERC

Metal electrocatalysts	**Applied voltage (V)**	**Maximum amount of product formed (µmol)**		**Rate of reaction (10^{-3} g·(g·h^{-1})$^{-1}$)**	
		CH_4	**CO**	**CH_4**	**CO**
Ni	1.8	0.40	6.92	0.36	10.76
Cu	2.0	17.94	3.94	15.94	6.13
Zn	2.3	6.08	92.28	5.40	143.54
Co	2.3	6.21	30.86	5.52	48.00

for CH_4 and CO is opposite. In figure 4.36, the selectivity pattern of Zn is shown. CO is predominant product with selectivity more than 90% at all the applied voltages. Thus, it is clear that Cu is selective towards CH_4 formation, while Zn is selective towards CO formation.

The selectivity patterns of Ni and Co are shown in figure 4.37 and 4.38. In contrast to Cu and Zn, Ni and Co show wide variations in the selectivity patterns. In case of Ni (Figure 4.37), CO is predominantly formed at lower applied voltages. As the voltage is increased, the selectivity shifts towards the CH_4 formation. However at higher applied voltages, since no product formation is taking place (Figure 4.30), the selectivity comes out to be zero. The selectivity profile of Co is shown in figure 4.38. In this case the selectivity pattern is similar to Ni, showing selectivity for CO at lower applied voltages, while at higher applied voltages, hydrocarbon formation prevails. Thus, applied voltage plays an important role for determining the selectivity in case of Ni and Co.

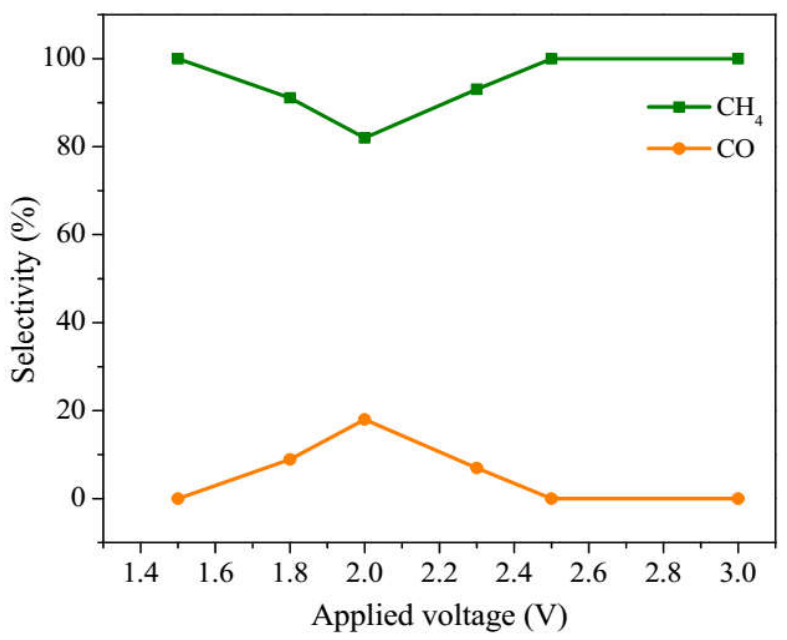

Figure 4.35 Selectivity of products using Cu electrocatalyst for dERC

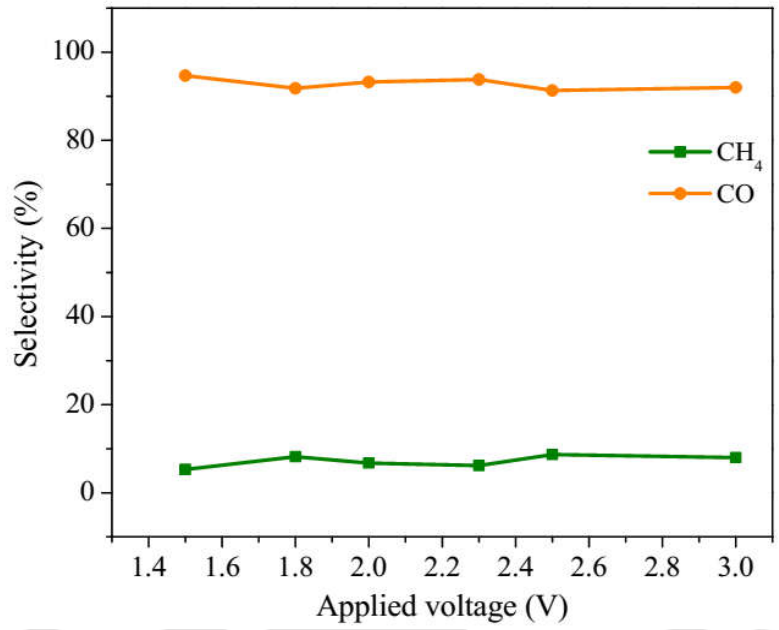

Figure 4.36 Selectivity of products using Zn electrocatalyst for dERC

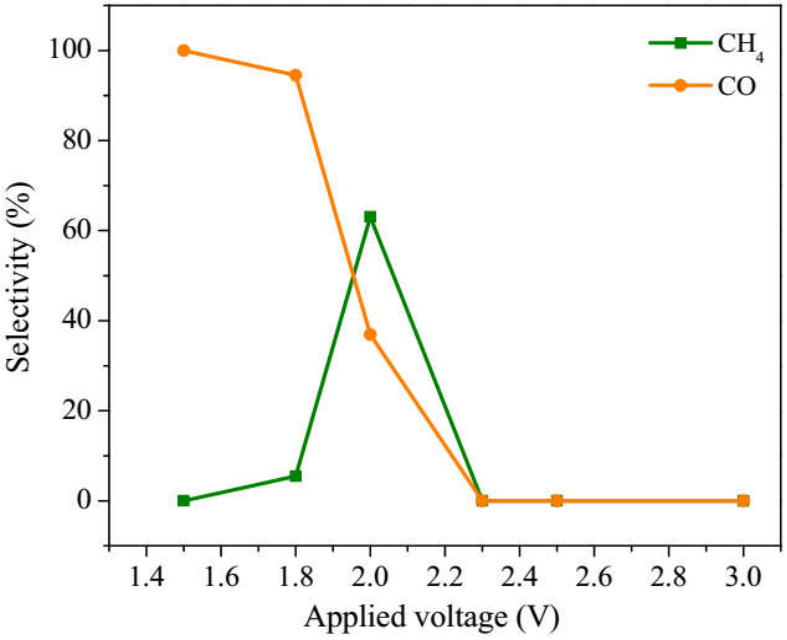

Figure 4.37 Selectivity of products using Ni electrocatalyst for dERC

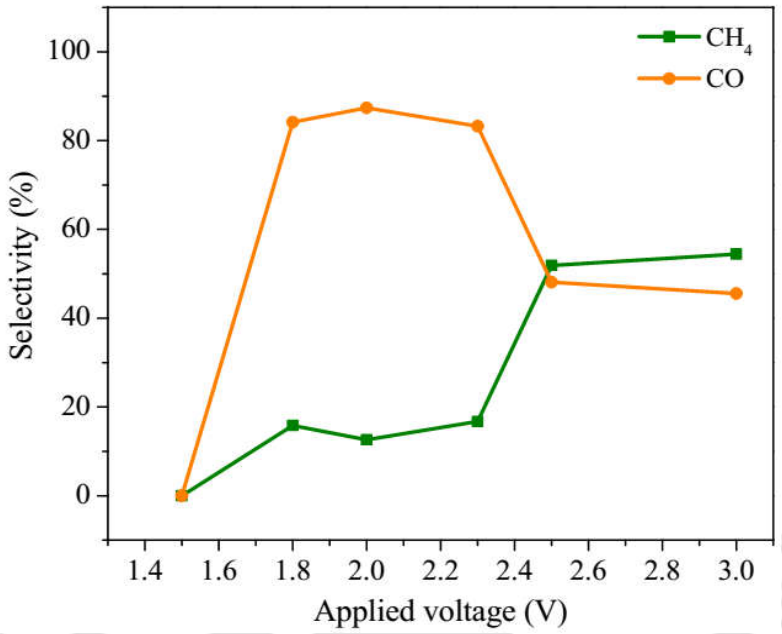

Figure 4.38 Selectivity of products using Co electrocatalyst for dERC

It is observed that the 4 metal electrocatalysts studied for dERC were active. However, the catalytic efficiency of these metals was not appreciable as all the studied electrocatalysts resulted only in the formation of CO and CH_4. Moreover, the energy supplied for the dERC was not fully utilized and resulted in significantly low Faradaic efficiency of < 20% for all the electrocatalysts. Inspite of getting not very encouraging results, the study provides a lot of information and insight as these electrocatalysts were not studied for dERC. It is found that Cu and Ni are good for lowering down the overpotential. Among the 4 metal electrocatalysts, only Cu was found to be selective for hydrocarbon formation. However, it has been seen that the Faradaic efficiency of Cu is less owing to the less conversion of CO_2 into the products. This might be due to the less adsorption of CO_2 on to the metal surface. Further, Zn and Co require high energy for the conversion of CO_2. Although the overpotential required in case of Ni was low, but its efficiency for CO_2 conversion was quite less. To solve these issues, formation of oxides of these metals was attempted, which is discussed in the next chapter.

References

Aeshala L.M., Rahman S.U., and Verma A. (2012), Effect of solid polymer electrolyte on electrochemical reduction of CO_2, *Separation and Purification Technology*, 94, 131-137.

Barbora L., Singh R., Shroti N., and Verma A. (2010), Synthesis and characterization of neodymium oxide modified Nafion membrane for direct alcohol fuel cells, *Materials Chemistry and Physics*, 122, 211-216.

Caffarena V.R., Capitaneo J.L., Simao R.A., and Guimaraes A.P. (2006), Preparation of electrodeposited cobalt nanowires, *Materials Research*, 9(2), 205-208.

Guo R., Liu T., and Wei X. (2002), Effects of SDS and some alcohols on the inhibition efficiency of corrosion for nickel, *Colloids and Surfaces A: Physicochemical and Engineering Aspects*, 209, 37-45.

Hara K., Kudo A., and Sakata T. (1995), Electrochemical reduction of carbon dioxide under high pressure on various electrodes in an aqueous electrolyte, *Journal of Electroanalytical Chemistry*, 391, 141-147.

Hori Y. (2003), CO_2 reduction, catalyzed by metal electrodes, In: Vielstich *et al.* (ed.) 'Electrocatalysis, Handbook of Fuel Cells', Vol. 2, Ch. 48, John Wiley & Sons, England, pp. 720-732.

Hori Y. (2008), Electrochemical CO_2 reduction on metal electrodes, In: Vayenas *et al.* (ed.) 'Modern Aspects of Electrochemistry', No. 42, Ch. 3, Springer, New York, pp. 89-189.

Hori Y., Konishi H., Futamura T., Murata A., Koga O., Sakurai H., and Oguma K. (2005), Deactivation of copper electrode in electrochemical reduction of CO_2, *Electrochimica Acta*, 50, 5354-5369.

Hori Y., Wakebe H., Tsukamoto T., and Koga O. (1994), Electrocatalytic process of CO selectivity in electrochemical reduction of CO_2 at metal electrodes in aqueous media, *Electrochimica Acta*, 39(11/12), 1833-1839.

Hori Y. and Suzuki S. (1983), Electrolytic reduction of bicarbonate ion at mercury electrode, *Journal of Electrochemical Society*, 130(12), 2387-2390.

Hua Z., Liu Y., Yao G., Wang L., Ma J., and Liang L. (2012), Preparation and characterization of nickel-coated carbon fibers by electroplating, *Journal of Materials Engineering and Performance*, 21, 324-330.

Kaneco S., Iiba K., Ohta K., Mizuno T., and Saji A. (1998), Electrochemical reduction of CO_2 at an Ag electrode in KOH-methanol at low temperature, *Electrochimica Acta*, 44, 573-578.

Kuhl K.P., Cave E.R., Abram D.N., and Jaramillo T.F. (2012), New insights into the electrochemical reduction of carbon dioxide on metallic copper surfaces, *Energy and Environmental Science*, 5, 7050-7059.

Kumutha K. and Alias Y. (2006), FTIR spectra of plasticized grafted natural rubber-$LiCF_3SO_3$ electrolytes, *Spectrochimica Acta*, 64, 442-447.

Li C.W. and Kanan M.W. (2012), CO_2 reduction at low overpotential on Cu electrodes resulting from the reduction of thick Cu_2O films, *Journal of the American Chemical Society*, 134, 7231-7234.

Ludvigsson M., Lindgren J., and Tegenfeldt J. (2000), FTIR study of water in cast Nafion films, *Electrochimica Acta*, 45, 2267-2271.

Mahreni A.B., Mohamad A.B., Kadhum A.A.H., Daud W.R.W., and Iyuke S.E. (2009), Nafion/silicon oxide/phosphotungstic acid nanocomposite membrane with enhanced proton conductivity, *Journal of Membrane Science*, 327, 32-40.

Murata A. and Hori Y. (1991), Product selectivity affected by cationic species in electrochemical reduction of CO_2 and CO at a Cu electrode, *Bulletin of Chemical Society of Japan*, 64, 123-127.

Park Y.S. and Yamazaki Y. (2005), Low water uptake content and low water/methanol transport in CP/Nafion hybrid membrane with high non-hydrogen bonding, *Journal of Membrane Science*, 261, 58-66.

Pierozynski B. (2012), Electrodeposition of nickel onto 12K carbon fibre tow in a continuous manner, *Croatica Chemica Acta*, 85(1), 1-8.

Ramani V., Kunz H.R., and Fenton J.M. (2005), Effect of particle size reduction on the conductivity of Nafion/phosphotungstic acid composite membranes, *Journal of Membrane Science*, 266, 110-114.

Santos A., Vojkuvka L., Pallares J., Ferre-Borrull J., and Marsal L.F. (2009), Cobalt and nickel nanopillars on aluminium substrates by direct current electrodeposition process, *Nanoscale Research Letters*, 4, 1021-1028.

Santos J.S., Matos R., Trivinho-Strixino F., and Pereira E.C. (2007), Effect of temperature on Co electrodeposition in the presence of boric acid, *Electrochimica Acta*, 53, 644-649.

Scibioh M.A. and Viswanathan B. (2004), Electrochemical reduction of carbon dioxide: A status report, *Proceedings of Indian National Science Academy*, 70 A(3), 407-462.

Shuang S., Zhiqiao H., Jiexu Y., and Jianmeng C. (2006), Preliminary study on electrochemical reduction of carbon dioxide on nickel and platinum electrodes, *High Technology Letters*, 12(3), 333-336.

Singh S., Mukherjee C., and Verma A. (2015 a), Development of catalytic activity protocol for electrochemical reduction of carbon dioxide to value added products, *Clean Technologies and Environmental Policy*, 17(2), 533-540.

Singh S., Phukan B., Mukherjee C., and Verma A. (2015 b), Salen ligand complexes as electrocatalysts for direct electrochemical reduction of gaseous carbon dioxide to value added products, *RSC Advances*, 5, 3581-3589.

Zeng J., Fan H., Wang Y., Zhang S., Xue J., and Zhang C. (2012), Oxidized electroplating zinc-covered carbon fibers as microwave absorption materials, *Journal of Alloys and Compounds*, 524, 59-62.

5

Metal oxides as electrocatalysts for dERC

Chapter 5

Metal oxides as electrocatalysts for dERC

In this chapter, metal oxides were synthesized, characterized, and evaluated for the dERC in terms of amount of product formation, Faradaic efficiency, and selectivity. Four metal oxides, namely, cupric oxide, zinc oxide, cobalt oxide, and nickel oxide have been studied. Some of the synthesized metal oxides showed improved efficiency while others could not be proved better than their corresponding pure metals. This chapter discusses the basic features of metal oxides, syntheses, characterization, and their overall performance for the dERC along with the comparison of the metal oxides with the corresponding metals at the end.

5.1 Background

Metal oxides have always been very interesting in the field of CO_2 adsorption. The reason is that CO_2 possesses soft acidic nature since it is a weak Lewis acid. However, the oxygen anions on the metal oxide surface are Lewis base sites. These oxygen anions of metal oxides exhibit basic, electron donor character. Thus, CO_2 gets attracted to the strong basic sites on the metal oxide surface because of the electropositive nature of the carbon atom. This fact depicts that the presence of strong basicity phases such as oxides can enhance the CO_2 adsorption capacity on the surface, which may eventually enhance the reducing capacity of the catalysts for CO_2. Literature shows various reports on the CO_2 adsorption by metal oxides, such as α-Cr_2O_3 (Abbe *et al.* 2001), La_2O_3-doped Bi_2O_3 (Esaka and Motoike 2006), mesoporous MgO/TiO_2 mixed oxides (Jeon *et al.* 2012), phenolic resin derived carbon (Plaza *et al.* 2013) *etc*. Many researchers have worked over the metal oxides for the electrochemical reduction of CO_2 in liquid phase and reported the formation of methanol, ethanol, methane, CO *etc*. It is reported that Cu_2O exhibits high Faradaic efficiency for CO_2 reduction at considerable low overpotential (Le *et al.* 2011; Keerthiga *et al.* 2012). The major benefit of Cu_2O is its resistivity towards deactivation due to surface changes caused by the oxidation of Cu, which does not allow for the graphite adsorption (Lee and Tak 2001). It is also said that Cu_2O enables easy formation of $\bullet CO_2^-$ intermediate and decreases H^+ reduction (Li and Kanan 2012), which allows Cu_2O to yield hydrocarbons for longer duration without much affected by poisoning. Oxide surfaces of Zn and Ru have also been investigated in aqueous solutions (Ikeda *et al.* 2000; Bandi 1990; Qu *et al.* 2005). However, in none of the studies, reaction was carried out for gas phase CO_2 reduction. Therefore, the oxides of copper, zinc, nickel, and cobalt were synthesized for studying their response for the dERC.

The oxide of copper was synthesized in which the oxidation state of Cu was 2 and called as cupric oxide (CuO). The oxide of Zn and Ni were ZnO and NiO, respectively. However, cobalt oxide (Co_3O_4) was studied instead of CoO, because CoO is metastable in ambient conditions.

Thermodynamically Co_3O_4 is the preferred oxide form of Co at room temperature and oxygen partial pressure (Fierro 2006; Petitto *et al.* 2008) and hence it was synthesized and discussed.

5.2 Experimental

5.2.1 Materials

The oxides have been synthesized using nitrate or sulphate salts of the metals. $Cu(NO_3)_2$, $Zn(NO_3)_2$, $NiSO_4$, $Co(NO_3)_2$, ammonia solution (30%), polyvinyl alcohol, and NaOH were purchased from Merck. Pt/C (40 wt% Pt) was purchased from ElectroChem, Inc. USA. All the chemicals were used without further purification and de-ionized water was used in all the experiments unless stated otherwise. Gas diffusion layer (GDL) from CeTech was used as backing layer for the electrocatalyst film. Nafion membrane (Nafion-117) and solution (5 wt%) were procured from DuPont, USA.

5.2.2 Methods

5.2.2.1 Synthesis of metal oxide electrocatalysts

The CuO and ZnO electrocatalysts were synthesized using aqueous precipitation method (Ikeda *et al.* 2009). $Cu(NO_3)_2$ and $Zn(NO_3)_2$ precursors have been chosen to form CuO and ZnO, respectively and precipitated with appropriate amount of ammonia solution. The resulting mixtures were aged for 5-6 hours and the precipitates were filtered and washed with water. The precipitates were dried and calcined at 360°C for 24 hours to get CuO and ZnO (Singh *et al.* 2012).

Nickel oxide (NiO) was synthesized using sol-gel method. $NiSO_4$ (0.1 M) was reacted with NaOH (0.5 M) at 70°C to form green gel of $Ni(OH)_2$. Precipitate was filtered and washed with distilled water and dried at 100°C for 10 hours. The dried precipitate was further subjected to calcination at 300°C for 3 hours to get NiO (Srivastava and Srivastava 2010).

Cobalt oxide (Co_3O_4) was synthesized using $Co(NO_3)_2$ precursor through polymer combustion route (Jiu *et al.* 2002). Aqueous solution (10% w/w) of polyvinyl alcohol was prepared in water at 90ºC with continuous stirring resulting in viscous gel. An aqueous solution of 0.5 M $Co(NO_3)_2$ was added slowly into the gel with PVA:Co ratio of about 3:1. The solution was kept at 80ºC overnight for drying. It resulted in pink polymer matrix, which was later calcined at 600ºC for 45 min to obtain black color Co_3O_4 catalyst (Singh *et al.* 2015).

5.2.2.2 Characterization techniques

The synthesized electrocatalysts were characterized using X-ray diffraction, Fourier transform infrared spectroscopy, BET surface area studies, field emission scanning electron microscopy, energy dispersive X-ray spectroscopy, and electrochemical half-cell studies as discussed in chapter 3.

5.2.2.3 Preparation of electrodes and membrane electrode assembly

Pt/C (40 wt% Pt) with Nafion dispersion (5 wt%) as binder, was used to prepare the anode electrocatalyst ink. The ink was coated over the gas diffusion layer using spraying technique and dried at 100°C overnight to get the anode. For the cathode (or working electrode), the electrocatalyst ink was prepared by dispersing the metal oxide electrocatalysts in iso-propyl alcohol along with the Nafion dispersion (5 wt%) as binder. The electrocatalyst ink was then coated over the gas diffusion layer followed by drying. The electrocatalyst loading for anode and cathode was kept as 0.5 $mg \cdot cm^{-2}$ and 2 $mg \cdot cm^{-2}$, respectively. The cation exchange membrane (Nafion-117) was treated using the standard procedure as discussed in section 3.3.2.1.1. The membrane electrode assembly was prepared by sandwitching the treated Nafion membrane in between anode and cathode at 110°C and 50 $kg \cdot cm^{-2}$ pressure.

5.2.2.4 Electrochemical tests

The half-cell studies were conducted in three-electrode cell assembly using Ag/AgCl as reference electrode and Pt wire as counter electrode. The working electrode was prepared using 2 $mg \cdot cm^{-2}$ electrocatalyst loading supported over the gas diffusion layer. The half-cell tests were carried out in aqueous as well as non-aqueous electrolytes at the scan rate of 10 $mV \cdot s^{-1}$. In all the half-cell studies, the potential is reported with respect to standard hydrogen electrode (SHE), unless stated otherwise. The full cell studies were carried out in an electrochemical reactor using the developed experimental set-up as described in section 3.3.2.1 and 3.3.2.2 respectively. The experiment was conducted using chronoamperometry technique (pulse width 5 s) at 6 different electrode potentials and the reaction products were collected at the cathode outlet and analyzed by GC. The electrochemical experiments were carried out at 30°C and at atmospheric pressure.

5.3 Results and discussions

5.3.1 Metal oxide characterization

5.3.1.1 Physical characterizations

The synthesized metal oxide electrocatalysts were characterized using XRD, FTIR, BET, FESEM, and EDX techniques.

5.3.1.1.1 XRD studies

XRD pattern of as-prepared metal oxide electrocatalysts is shown in figure 5.1 to 5.4. Figure 5.1 shows the X-ray diffractogram of the CuO nanoparticles. The CuO nanoparticles show single phase monoclinic structure. The intensities and position of peaks are in good agreement with the reported values (JCPDS file No. 05-661). The main peaks appeared at 35.47°, 38.65°, and 48.7°. These three peaks correspond to (002), (111), and (-202) planes, respectively (Wu *et al.* 2002). Estimation of the

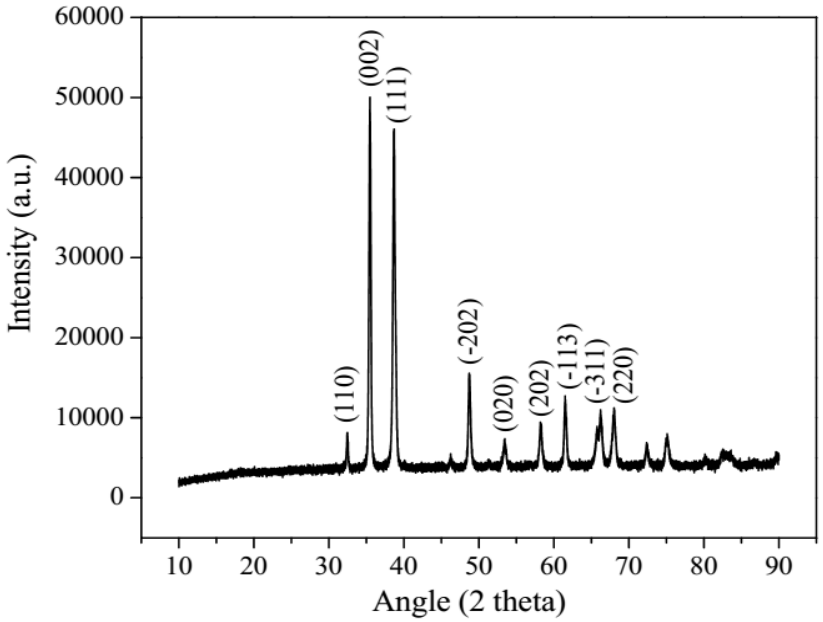

Figure 5.1 XRD pattern of CuO

crystallite size based on X-ray peak broadening was calculated using Debye-Scherrer equation and found to be 52.5 nm.

Figure 5.2 shows the XRD pattern of as-prepared ZnO nanoparticles having hexagonal ZnO phase (wurtzite structure) (Chieng and Loo 2012). The main peaks appeared at 31.9°, 34.6°, 36.4°, and 56.7°. The crystallite size of ZnO was found to be 49.5 nm. The XRD pattern of NiO shows the peaks at 37.12°, 43.09°, 62.62°, 74.96°, and 79.17° representing the NiO planes (111), (200), (220), (311), and (222) respectively (Figure 5.3). All these diffraction peaks can be indexed to face centered cubic (FCC) structure. Presence of broad peaks represents that synthesized particles are quite small. The crystallite size was found to be 2.54 nm. Figure 5.4 shows Co_3O_4 diffraction peaks, which correspond to spinel structure of the cobalt oxide (He *et al.* 2005; Suraja *et al.* 2013). The crystallite size of Co_3O_4 was found to be 29.55 nm. All the XRD patterns show that samples are single phased and pure as no other peaks for any impurity are present and thus confirming the high purity of synthesized electrocatalysts.

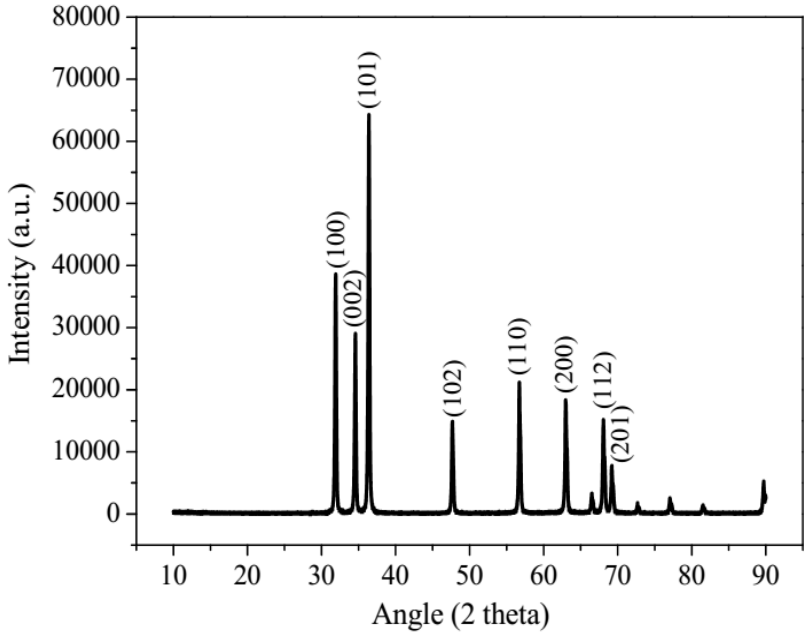

Figure 5.2 XRD pattern of ZnO

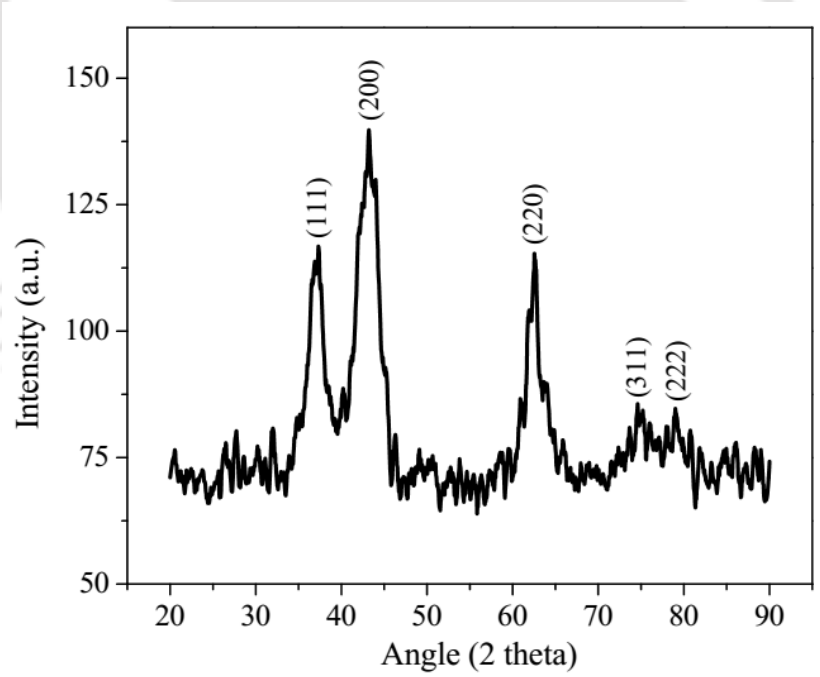

Figure 5.3 XRD pattern of NiO

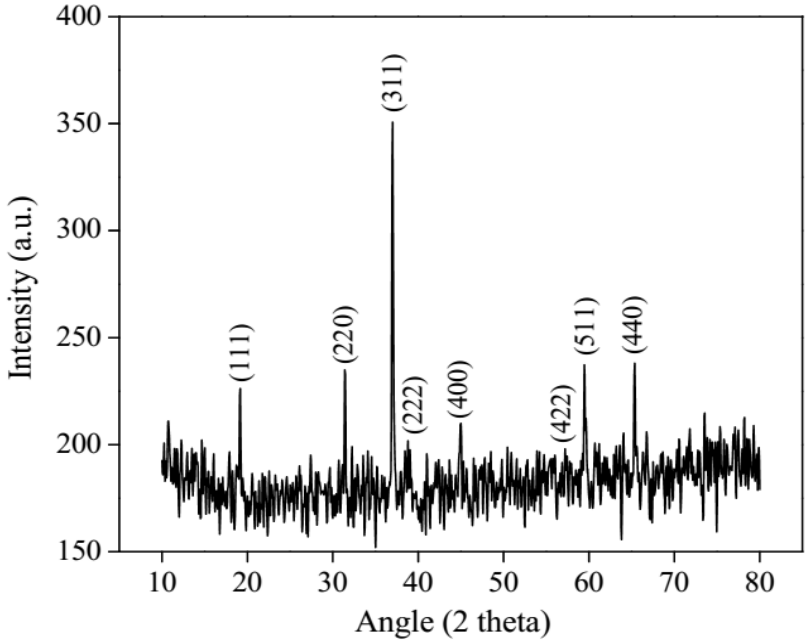

Figure 5.4 XRD pattern of Co_3O_4

5.3.1.1.2 FTIR studies

Figure 5.5 to 5.8 show the FTIR spectra of CuO, ZnO, NiO, and Co_3O_4. FTIR spectra were recorded in the range of 400-4000 cm^{-1}. The FTIR spectrum of CuO nanostructure indicates two signature peaks at 520 and 598 cm^{-1} (Liu *et al.* 2006). In the present case, the spectrum for CuO shows characteristic bands at 497 and 603 cm^{-1} which corroborate the formation of CuO nanostructure (Figure 5.5). No peaks could be observed in the range of 605-660 cm^{-1}, which proved that no other phase, *i.e.*, Cu_2O was present (Singh *et al.* 2015). FTIR spectrum of ZnO shows the characteristic peak at 551 cm^{-1}, which refers to the Zn–O bond stretching vibration (Hassan *et al.* 2014). The bands at 889 cm^{-1} are due to the microstructural features in Zn–O lattice (Figure 5.6). The peak around 3400 cm^{-1} may be due to the O–H stretching vibration of the H_2O molecule present inside ZnO nanoparticles. FTIR spectrum of NiO is shown in figure 5.7. In case of NiO, peak at 418 cm^{-1} represents Ni–O bond. The FTIR spectrum of Co_3O_4 is shown in figure 5.8. It shows two strong absorption bands at 660 and 580 cm^{-1}, which confirm the spinel structure of Co_3O_4 (Figure 5.8). The

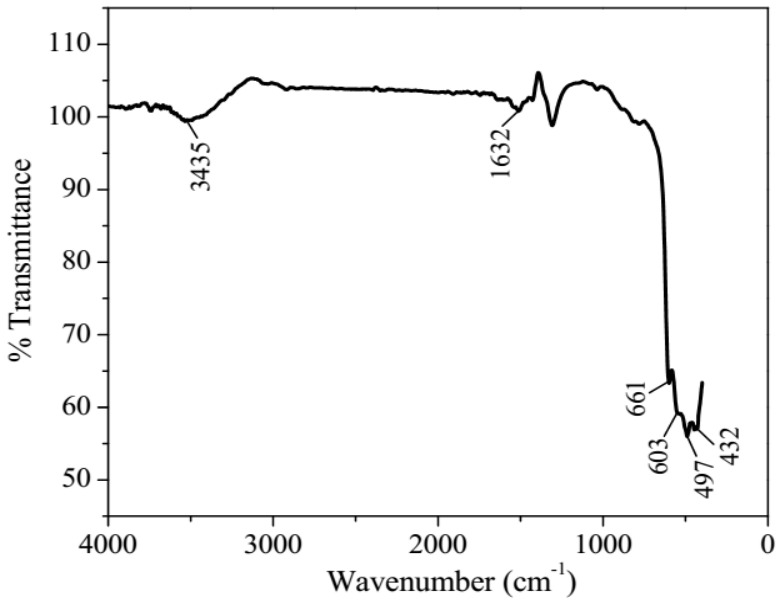

Figure 5.5 FTIR spectrum of CuO

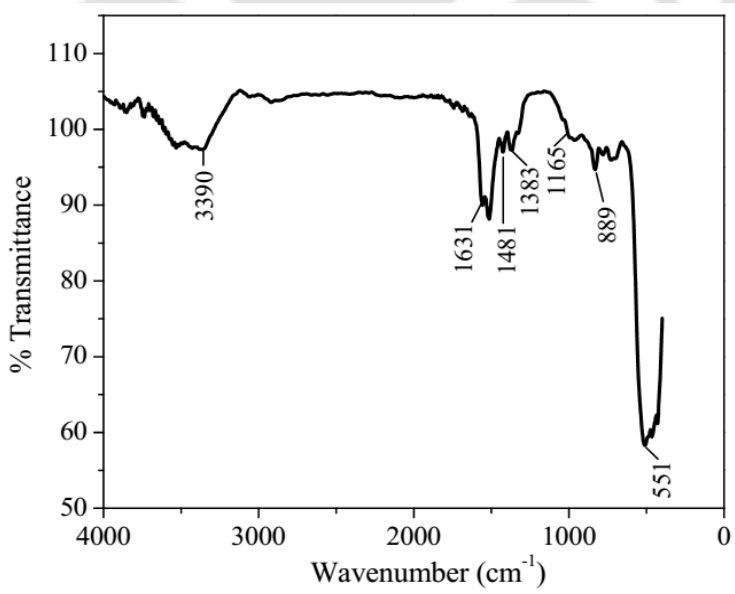

Figure 5.6 FTIR spectrum of ZnO

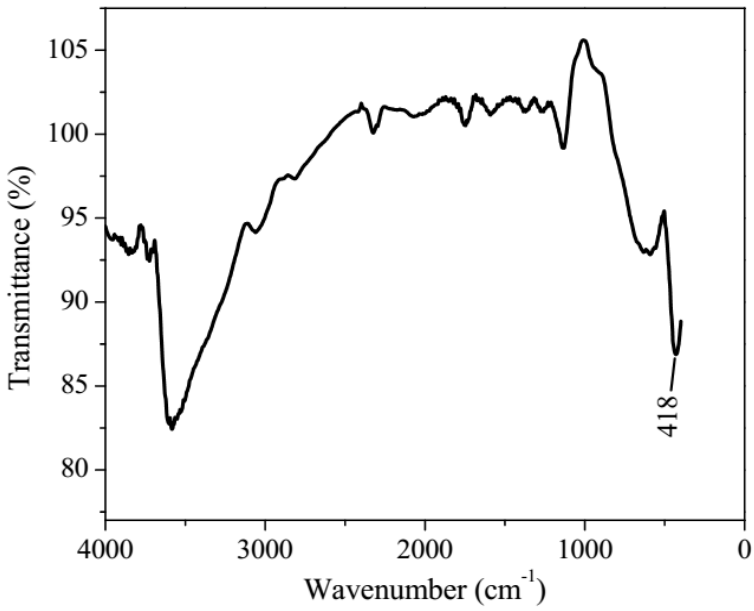

Figure 5.7 FTIR spectrum of NiO

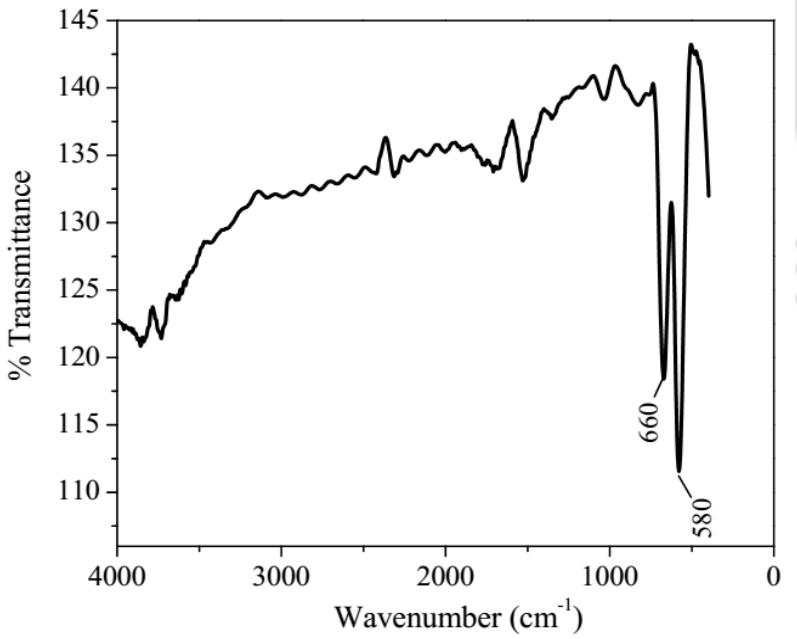

Figure 5.8 FTIR spectrum of Co_3O_4

peak at 660 cm^{-1} is due to the stretching vibration mode of Co–O bond in which oxidation state of Co is +2, and hence coordinated tetrahedrally. The band at 580 cm^{-1} can be assigned to the Co–O bond in which the oxidation state of Co is +3 and thus coordinated octahedrally (Herrero *et al.* 2007; Suraja *et al.* 2013; Singh *et al.* 2015).

5.3.1.1.3 BET surface area studies

The BET surface area measurements were carried out using N_2 adsorption desorption isotherm at -196°C as discussed in section 3.2.3. The surface area of CuO, ZnO, NiO, and Co_3O_4 were found to be 9.9 $m^2 \cdot g^{-1}$, 15.9 $m^2 \cdot g^{-1}$, 143.48 $m^2 \cdot g^{-1}$, and 9.2 $m^2 \cdot g^{-1}$ respectively.

5.3.1.1.4 FESEM studies

To study the morphology of the synthesized electrocatalysts, FESEM analysis, as discussed in section 3.2.5, was done for all the metal oxides. The FESEM images (Figures 5.9 to 5.12) show the morphology of the electrocatalyst particles. The size of the CuO particles ranges from 70 to 300 nm.

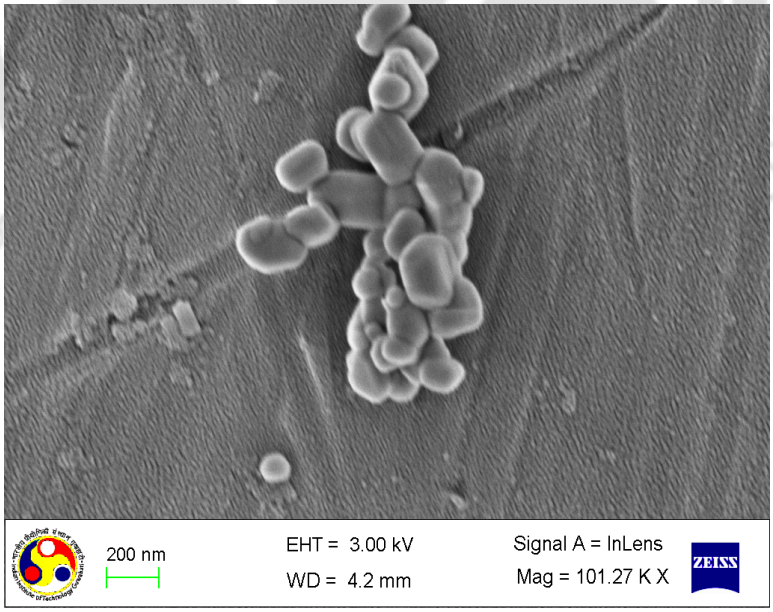

Figure 5.9 FESEM analysis of CuO

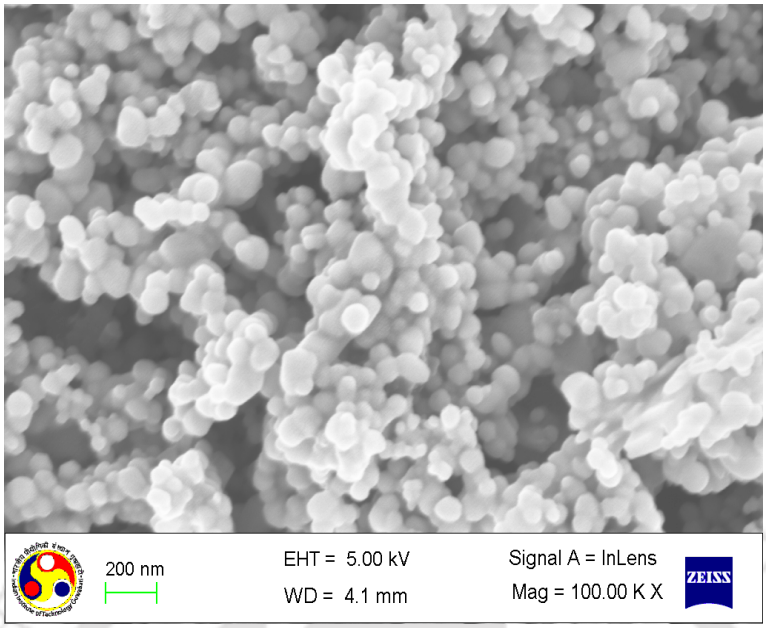

Figure 5.10 FESEM analysis of ZnO

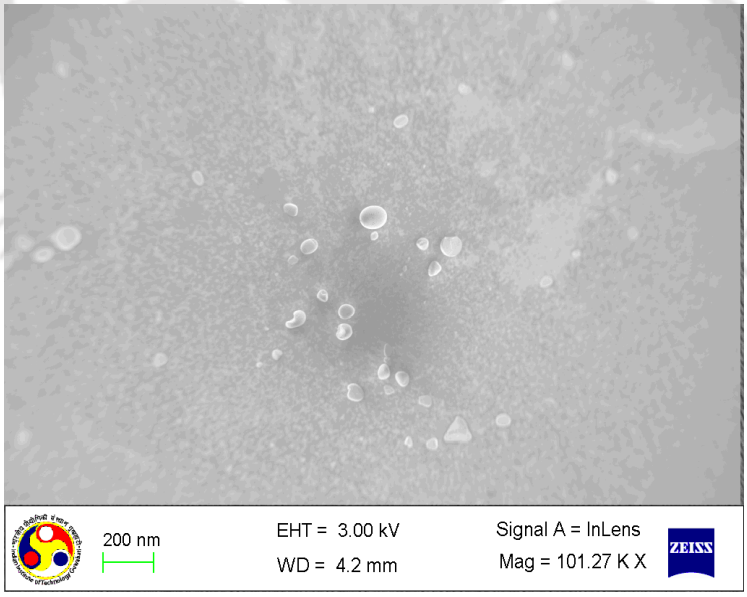

Figure 5.11 FESEM analysis of NiO

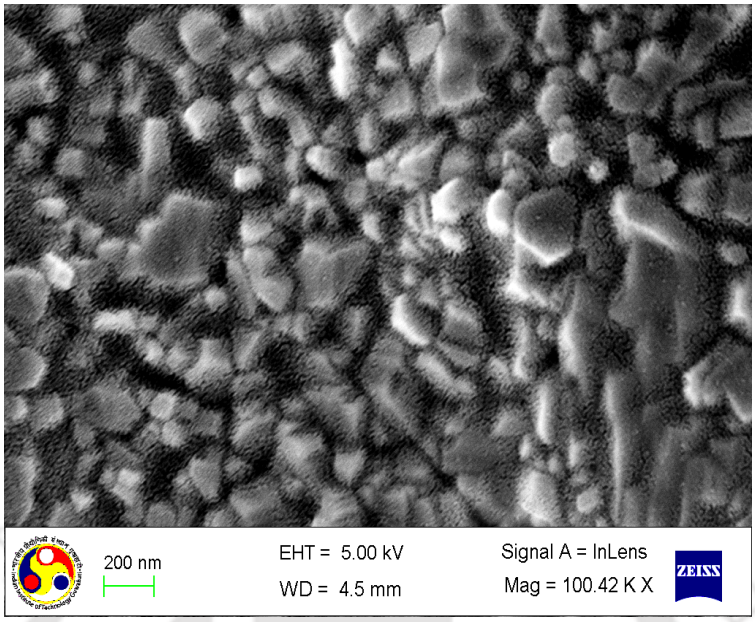

Figure 5.12 FESEM analysis of Co_3O_4

The image of ZnO clearly demonstrates the uniform formation of spherical nanoparticles. The particle size varies from 64 to 77 nm (Figure 5.10). The FESEM image of NiO particles is shown in figure 5.11. The particles of NiO are very small, which was also reflected in its XRD pattern and BET surface area determinations. In case of Co_3O_4, the particles are irregular in shape, ranging from 150 – 300 nm (Figure 5.12) (Singh *et al.* 2015). Small size of particles is preferable as it provides high absorptive surface area.

5.3.1.1.5 EDX studies

The EDX studies were carried out to further confirm the presence of desired species and absense of undesired species in the samples. The EDX spectra of the metal oxide electrocatalysts are shown in figure 5.13. It can be seen that all the samples showed the presence of metal species (Cu, Zn, Ni, and Co) along with oxygen element. It confirms that impurities were not present in the samples and metal oxides were pure.

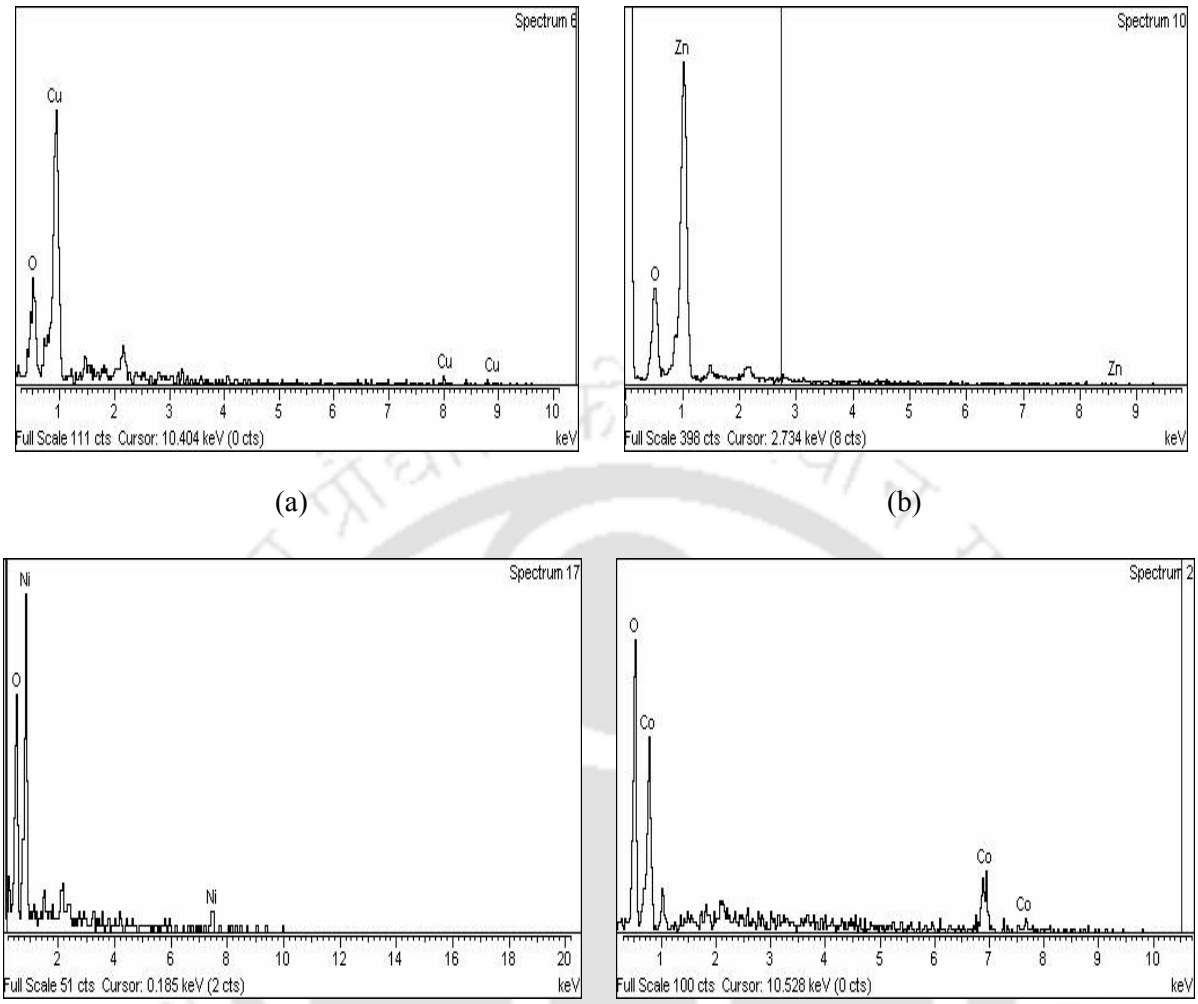

Figure 5.13 EDX spectra of metal oxide electrocatalysts (a) CuO, (b) ZnO, (c) NiO, and (d) Co_3O_4

5.3.1.2 Electrochemical characterizations

The synthesized metal oxides need to be tested for their electrochemical behaviour after the physical characterizations. The powdered metal oxide electrocatalysts were dispersed in a solvent to form the electrocatalyst ink, which was then coated over the electrode surface, as discussed in section 5.2.2.3. However, in case of NiO, no appropriate solvent could be found in which it can be dispersed homogeneously. Therefore, no electrochemical study could be done in case of NiO. Thus, the

electrochemical studies were performed for rest of the three metal oxides, namely CuO, ZnO, and Co_3O_4 in half-cell as well as full cell (dERC reactor).

5.3.1.2.1 Cyclic voltammetry

In order to evaluate the electrocatalyst, first, the cyclic voltammetry was conducted to know the behavior of the electrocatalysts (CuO, ZnO, and Co_3O_4) for CO_2 reduction in inert and CO_2 saturated environment. The cyclic voltammetry test was conducted using 0.5 M $KHCO_3$ solution, which was saturated with N_2 or CO_2 gases, to compare the voltammograms in inert and CO_2 environments, respectively. The pH of the saturated solution with N_2 and CO_2 was 8.5 and 7.5, respectively. The cyclic voltammograms (CVs) of the CuO, ZnO, and Co_3O_4 in the potential range of 0 to 3 V *vs.* SHE are shown in figure 5.14 to 5.16. The cyclic voltammogram of CuO is shown in figure 5.14 (Singh *et al.* 2015). Current density produced in inert environment is due to the reduction of H^+ species which is present in aqueous medium. Moreover, the current density observed in CO_2 environment is due to the reduction of both CO_2 and H^+ species. Onset potential (the potential at which 0.1 $mA{\cdot}cm^{-2}$ current

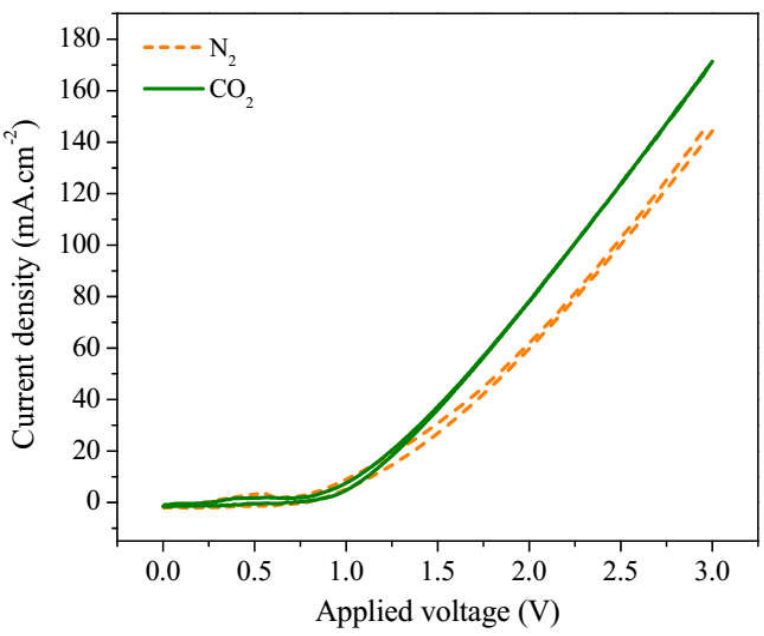

Figure 5.14 Cyclic voltammograms of CuO in N_2 (broken line), and CO_2 (solid line) atmosphere

density is observed) for CuO is 0.4 V. It can be noticed that current density in CO_2 atmosphere is more than in the N_2 environment. It might indicate that electrocatalyst is able to reduce the CO_2. Therefore, further evaluation of the electrochemical activity of the catalyst towards ERC was conducted based on the developed protocol (section 5.3.1.2.2). Similarly, the voltammograms of ZnO are shown in figure 5.15 (Singh *et al.* 2015). It can be seen that there are two broad peaks present at 0.26 V and 1.6 V *vs.* SHE in CO_2 atmosphere. Similar peaks are also present in N_2 atmosphere at 0.13 V and 1.75 V *vs.* SHE. These peaks, however, do not correspond to the CO_2 reduction as these are present in inert atmosphere too. The reason is that the ZnO does not remain stable in aqueous electrochemical system and undergoes 2 electron reduction to form Zn as per the following reaction (equation 5.1)

$$ZnO + H_2O + 2e^- \rightarrow Zn + 2\,OH^- \qquad E° = -1.260\ V \qquad (5.1)$$

This reaction takes place in absence as well as presence of CO_2, hence peaks are observed in both the inert and CO_2 environments. Moreover, the current density produced in both the environments is almost similar and hence no prediction about the activity of ZnO is possible. The cyclic voltammograms of Co_3O_4 is shown in figure 5.16. The current density observed in both inert (N_2 saturated) and CO_2 environment is shown. The onset potential for the CO_2 reduction using Co_3O_4 was calculated to be 0.6 V. It can be seen that current density in CO_2 environment is less than in inert atmosphere. The slight peaks observed in the voltammograms of Co_3O_4 are present in both inert and CO_2 atmosphere, thus confirming that peaks are not because of the reduction of CO_2. These peaks are due to the interconversion of Co^{+2} and Co^{+3} oxidation states of Co_3O_4 (Singh *et al.* 2015).

Thus, in case of all the metal oxide electrocatalysts, cyclic voltammograms have given some insight towards their behaviour in electrochemical environment. To get the substantial information regarding the activity towards CO_2 reduction, these electrocatalysts will be characterized using the developed catalytic activity protocol (Singh *et al.* 2015).

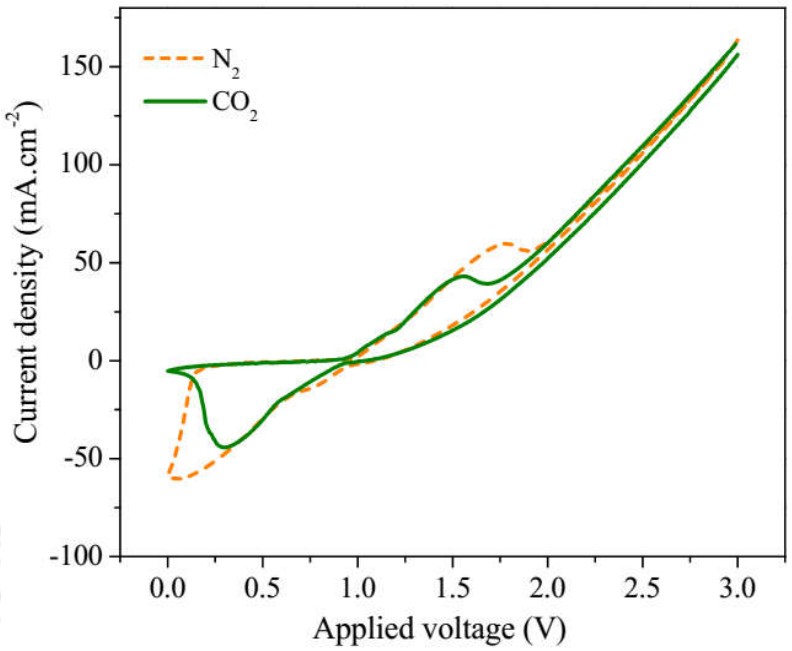

Figure 5.15 Cyclic voltammograms of ZnO in N_2 (broken line), and CO_2 (solid line) atmosphere

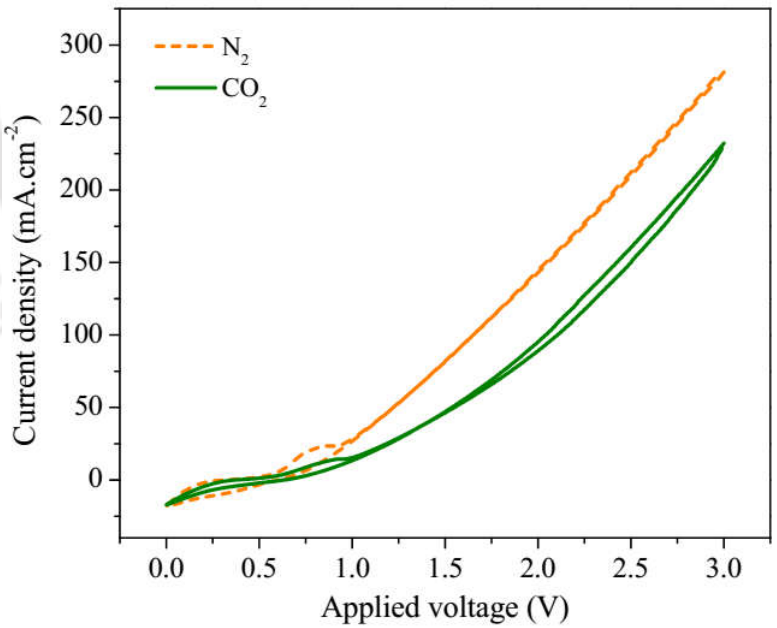

Figure 5.16 Cyclic voltammograms of Co_3O_4 in N_2 (broken line), and CO_2 (solid line) atmosphere

5.3.1.2.2 The developed protocol

According to the protocol (section 4.3.1.2.2), the linear sweep voltammograms (LSVs) were plotted using gas diffusion layer (GDL) without any electrocatalyst coating and then compared with the electrocatalysts coated GDL in three different media. The plots are shown in figure 5.17 to 5.19. It can be seen in the figures that all the metal oxide electrocatalysts show higher current density than the bare GDL in every test. It signifies that the electrocatalysts are active in every media. However, the increased current density in the 3rd test of the protocol clearly proves that electrocatalysts are able to reduce the CO_2. These results depicts that all the three metal oxides are active for CO_2 reduction, although there is the tendency towards competitive H^+ reduction too. The results of 2nd test show that Co_3O_4 is the most active for H^+ reduction, while CuO is the least active. Therefore, it can be predicted that CuO should be the most active for CO_2 reduction and Co_3O_4 should be the least. In figure 5.19, it becomes clear that highest current density difference was found between the CuO electrocatalyst and

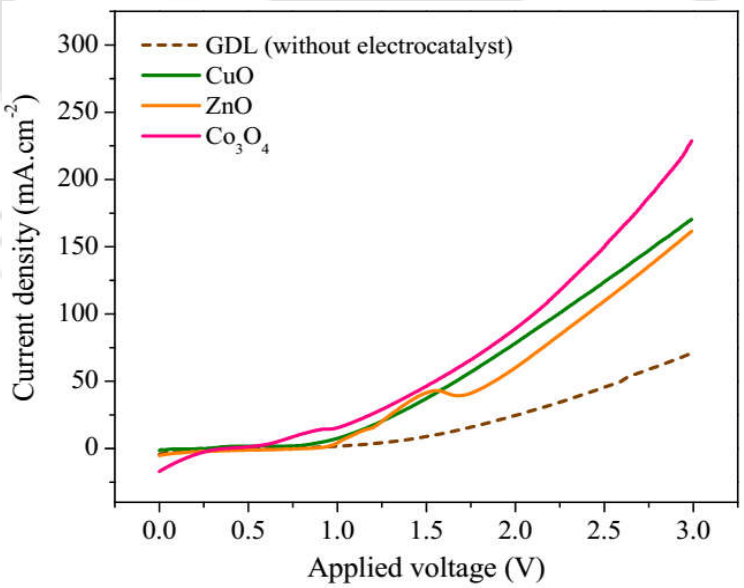

Figure 5.17 Comparison of electrocatalytic activity of metal oxides on GDL (solid lines), and only GDL (broken line) for the 1st test as per the catalytic activity protocol

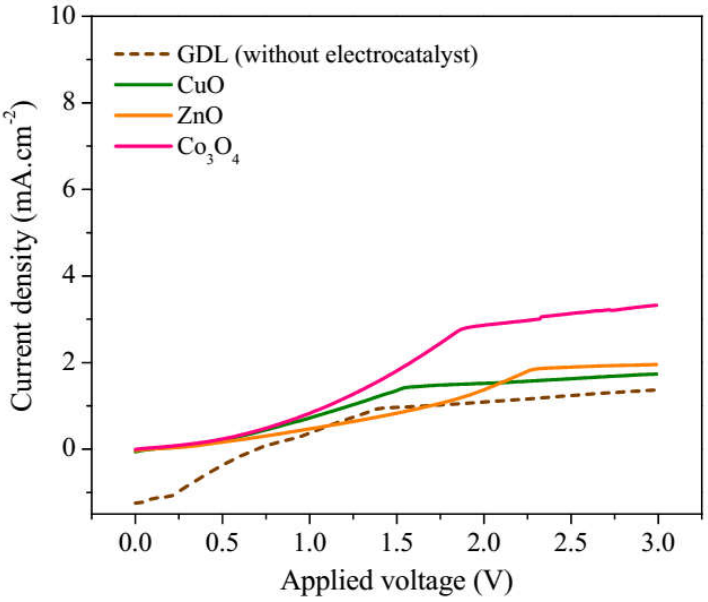

Figure 5.18 Comparison of electrocatalytic activity of metal oxides on GDL (solid lines), and only GDL (broken line) for the 2nd test as per the catalytic activity protocol

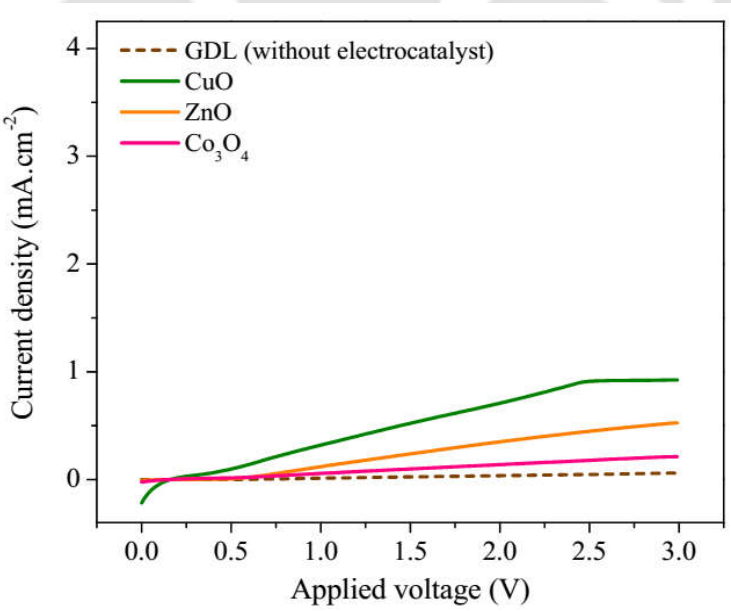

Figure 5.19 Comparison of electrocatalytic activity of metal oxides on GDL (solid lines), and only GDL (broken line) for the 3rd test as per the catalytic activity protocol

GDL, confirming that among all the metal oxide electrocatalysts, CuO is the most active for CO_2 reduction. The minimum current density is found for the Co_3O_4 which suggests that it is the least active electrocatalyst for CO_2 reduction as compared to CuO and ZnO.

5.3.2 dERC studies using metal oxide electrocatalysts

The characterization of metal oxide electrocatalysts through physical and electrochemical means shows that the synthesized metal oxides were able to reduce CO_2 electrochemically. Therefore, further studies were carried out to understand the activity of metal oxides towards product formation and selectivity in dERC. The reactions were carried out above the onset potential range which was determined in CV test. The products formed were collected at the cathode outlet and analyzed using gas chromatography.

5.3.2.1 Effect of applied voltage on current density and Faradaic efficiency towards dERC

Figure 5.20 shows the current density with respect to applied voltages for the metal oxide electrocatalysts. It can be seen that the current density increases with the increasing applied potential values, which refers to various reactions taking place at the electrode surface. These reactions are due to the CO_2 reduction as well as unwanted H^+ reduction. The highest current density can be seen in the case of Co_3O_4. For CuO, the current density at 1.5 V is 0.4 $mA \cdot cm^{-2}$ and reaches 5.1 $mA \cdot cm^{-2}$ at 3 V. The current density obtained corresponds to the formation of various products and by-products at the cathode surface of the electrochemical reactor. In case of ZnO, the current density is less than the CuO. Current density at 3 V is 3.8 $mA \cdot cm^{-2}$ for ZnO. The current density in case of Co_3O_4 is the highest with 12.09 $mA \cdot cm^{-2}$ at 3 V. Moreover, the efficiency of the electrocatalyst towards CO_2 reduction can not be determined only on the basis of current density parameter. The reason being that obtained current density is the result of various electrochemical reactions taking place in the reactor to form products as well as by-products. Therefore, figure 5.21 shows the cumulative Faradaic

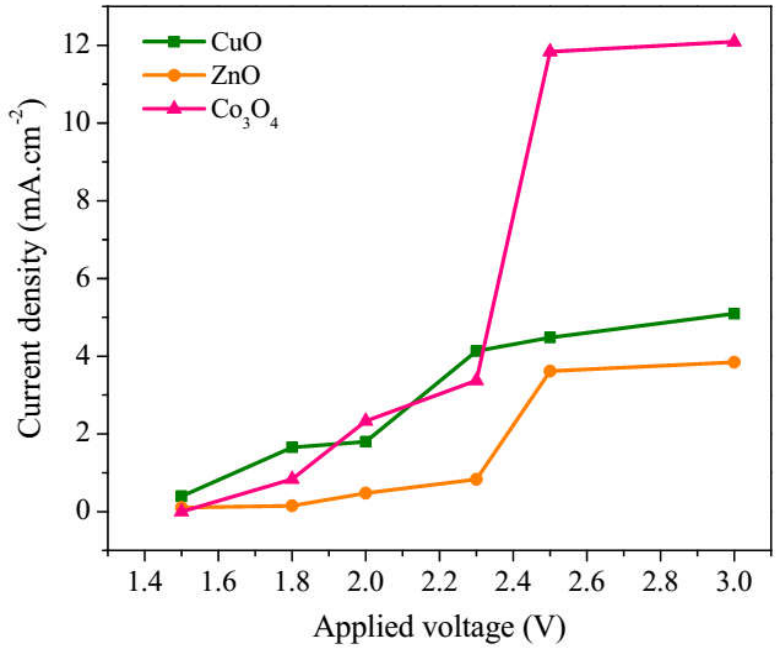

Figure 5.20 Current density as a function of applied voltage for metal oxide electrocatalysts

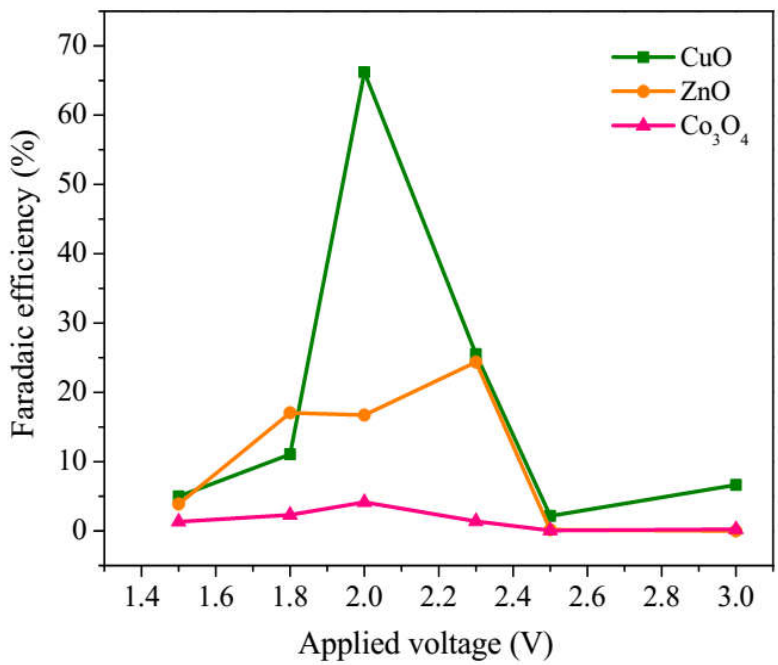

Figure 5.21 Faradaic efficiency as a function of applied voltage for metal oxide electrocatalysts

efficiency of all the electrocatalysts for CO_2 electroreduction reaction products only. Here it can be seen that appreciable Faradaic efficiency has been observed for the metal oxides. CuO shows the highest Faradaic efficiency of 66.2% at 2 V. Co_3O_4 shows the least Faradaic efficiency *viz.* 4.2% at 2 V. ZnO results in intermediate Faradaic efficiency among the three metal oxide electrocatalysts. However, in case of ZnO, the highest Faradaic efficiency was observed at 2.3 V with 24.4%. To determine the energy utilized (Faradaic efficiency) for the various reaction products, it is necessary to quantify the reaction products at the cathode of the electrochemical reactor. Therefore, further results are given for the individual metal oxide electrocatalyst.

5.3.2.2 Performance of metal oxide electrocatalysts for the formation of various dERC products

To know the effectiveness of various metal oxides for different product formation, the amount of the products formed and Faradaic efficiency of individual products were calculated for each of the metal oxide electrocatalyst.

5.3.2.2.1 CuO metal oxide electrocatalyst

Figure 5.22 shows the amount of the products formed in electrochemical reduction of CO_2 using CuO. It can be seen that amount of the methane formation is the highest among all the products. The highest formation of CH_4 (82.4 µmol) was found at 2 V. CO formation was found highest at 1.8 V with 38.6 µmol. C_2H_4 formation was only in trace amount at 3 V. Hydrogen formation is increasing with the increasing applied potential value. It reflects that most of the supplied energy is getting wasted in the formation of hydrogen. Faradaic efficiency was also calculated for the metal oxide electrocatalysts, as discussed in section 3.5.1. Faradaic efficiency is the measure of the amounts of the products formed with respect to the supplied electrical energy. The Faradaic efficiency of CuO is shown in figure 5.23. Similar to the figure 5.22, the highest Faradaic efficiency is reported for the CH_4 (59.91%), followed by the CO (7.63%), and C_2H_4 (0.47%). Excess hydrogen formation at higher applied voltages, as seen in the figure 5.22 is also reflected in figure 5.23. However, it can be said

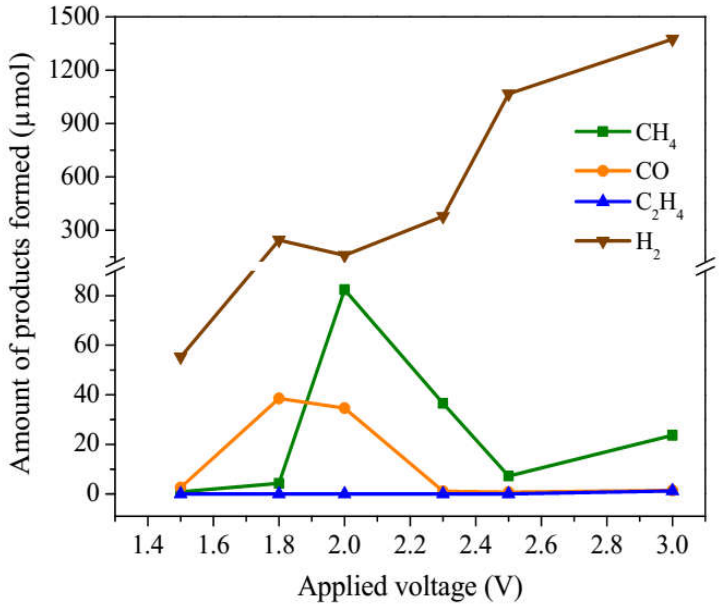

Figure 5.22 Amount of the products formed as a function of applied voltage for electrochemical reduction of CO_2 using CuO

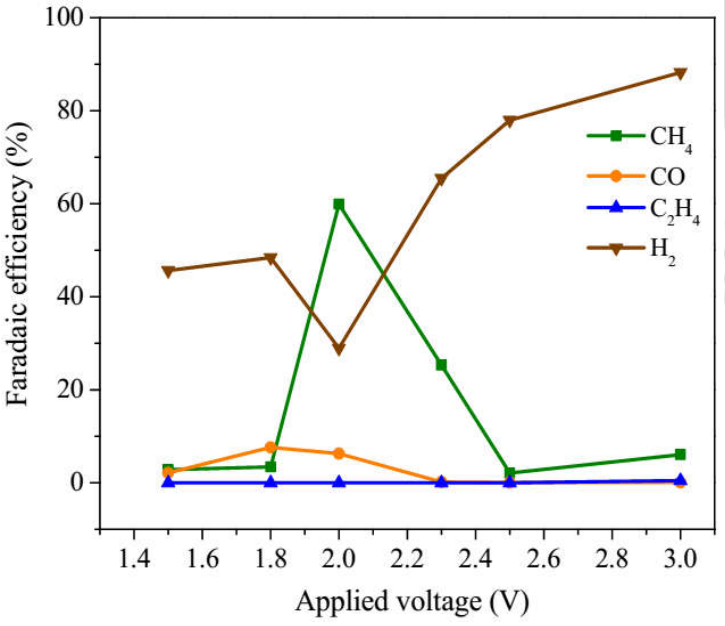

Figure 5.23 Faradaic efficiency as a function of applied voltage for electrochemical reduction of CO_2 using CuO

that Faradaic efficiency achieved in case of CuO is appreciable. Moreover, CuO remains active for CO_2 reduction not only upto 60 minutes but also beyond it. The variation of Faradaic efficiency with time is shown in figure 5.24. It can be seen that hydrocarbon formation takes place significantly in first 40 minutes, after which its formation decreases and approaches <5% Faradaic efficiency. Moreover, CO formation continues upto 90 minutes. It is important to note that with increasing time, the hydrogen formation increases which affects CO_2 reduction negatively. Thus, increased concentration of H^+ at the cathode surface adversely affects the reduction of CO_2.

The better performance of CuO for CO_2 electroreduction can be attributed to the adsorption properties of CuO. Thermodynamically, it is proven that adsorption reaction between CuO and CO_2 is highly favourable with $\Delta G = 4.9$ kJ·mol^{-1} under ambient temperature and pressure conditions (Isahak *et al.* 2013). Thus, although the BET surface area of the as-prepared CuO electrocatalyst was less, the favourable thermodynamics between CuO and CO_2 helped to overcome it and resulted in high

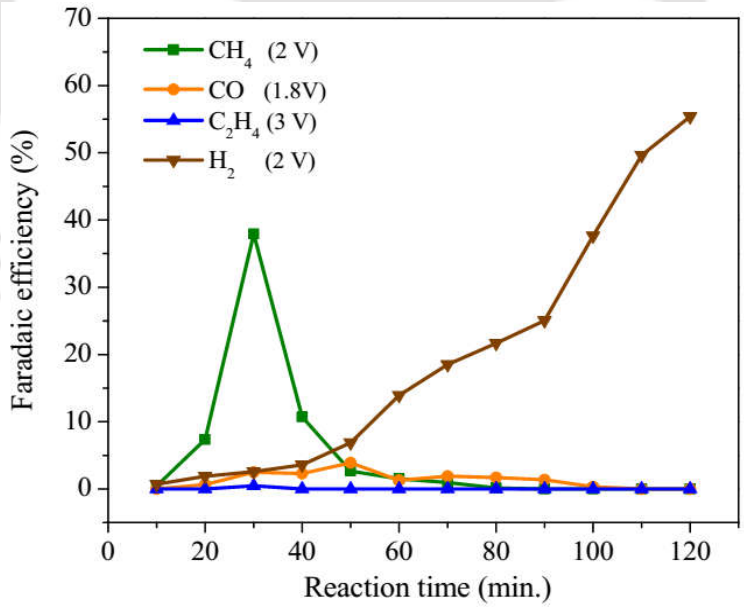

Figure 5.24 Faradaic efficiency variation with time during electrochemical reduction of CO_2 using CuO

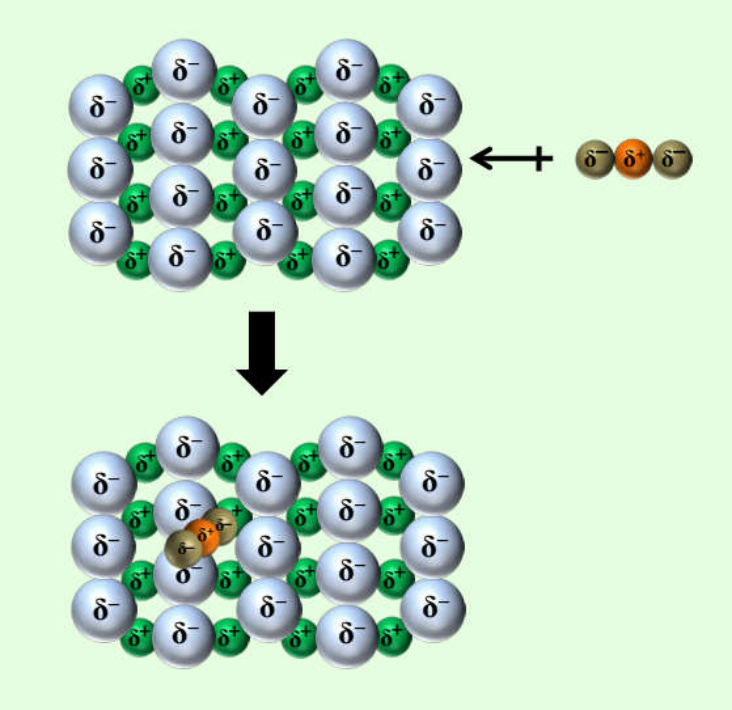

Scheme 5.1 Representation of the acidic and basic character of the CO_2 and metal oxide, respectively, which helps in adsorption of CO_2 over the electrocatalyst surface (Orange and brown spheres represent C and O respectively, while green and blue represent the cations and anions of metal oxide electrocatalyst, respectively).

activity of the electrocatalyst. Moreover, the basic properties of CuO further enhanced the attraction between CuO and CO_2. As shown in the scheme 5.1, the metal oxides are basic due to the electropositive nature of the metals, while CO_2 is Lewis acid. Therefore, cations and anions of the metal oxide possess a partial positive and negative charge, respectively, which has the tendency to adsorb (acidic) CO_2. Thus, most of the sites get occupied by CO_2 leading to better adsorption and hence improved reduction of the CO_2.

5.3.2.2.2 ZnO metal oxide electrocatalyst

The results for the CO_2 reduction using ZnO electrocatalyst are shown in figure 5.25 and figure 5.26. As it was observed in figure 5.20, the current density in case of ZnO is less therefore; the amount of the products formed is also less. The highest formation can be seen in case of CO with 8.25 µmol at 2 V. Another product is CH_4, which was found highest at 2.3 V with 6.56 µmol. Hydrogen formation is also comparatively less than other oxide electrocatalysts, however, its formation is significantly higher than any of the products. The formation of hydrogen follows the same trend as that of current density and it is increasing with the applied potential values. At 3 V, the hydrogen formation is highest with 554.57 µmol. The Faradaic efficiency of the ZnO is shown in figure 5.26. Contrary to figure 5.25, the trends of Faradaic efficiencies are different. It is so because; Faradaic efficiency takes into the account the number of moles of electrons supplied. Therefore, if the same amount of CO and CH_4 is formed, the Faradaic efficiency towards CH_4 would be 4 times higher, since there are 8 electrons involved in the formation of one mole of methane while only 2 in the formation of one mole of CO. Hence, although the number of moles of CH_4 is less at 1.8 V (Figure 5.25), the corresponding Faradaic efficiency at 1.8 V is high (Figure 5.26). Faradaic efficiency for CH_4 formation is more at two potential values *viz.* 1.8 V and 2.3 V with 16.6% and 18.8%, respectively. Moreover, the Faradaic efficiency for CO formation is highest at 2 V with 10.34%. The overall Faradaic efficiency is 24.36% at 2.3 V. High activity at two potential values is a peculiar feature and it is due to the unstable behaviour of ZnO. During the reaction, the ZnO itself undergoes reduction resulting in the formation of Zn according to equation (5.1) (Ikeda *et al.* 2000). The evidence for the self-reduction of ZnO to Zn has also been seen in its cyclic voltammogram, which was discussed in section 5.3.1.2.1. Hence, it was postulated that the formation of CH_4 at 1.8 V is due to the activity of ZnO. On increasing the voltage upto 2.3 V, the conversion of ZnO to Zn takes place (equation 5.1) and thus, the *in-situ* formed Zn results in the formation of CH_4. This notion is also supported by the fact that Zn metal shows its highest Faradaic efficiency for CO_2 reduction at 2.3 V, as was seen in section 4.3.4.2. After

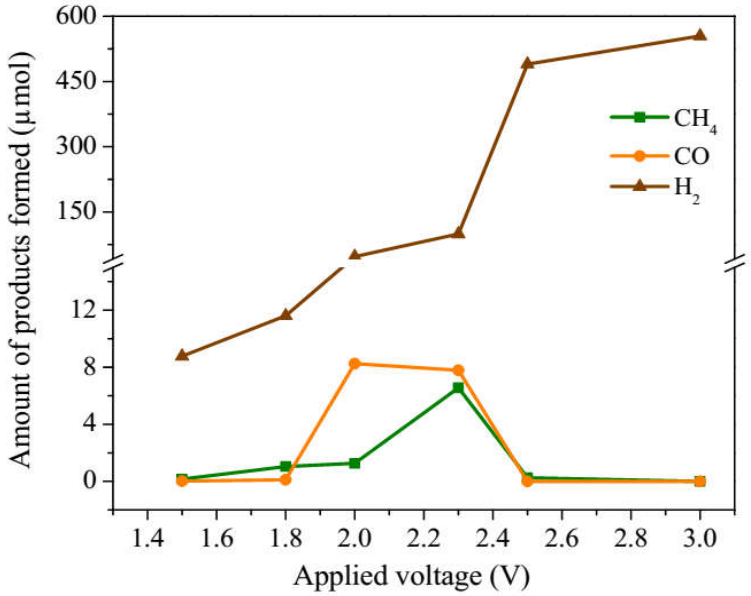

Figure 5.25 Amount of the products formed as a function of applied voltage for electrochemical reduction of CO_2 using ZnO

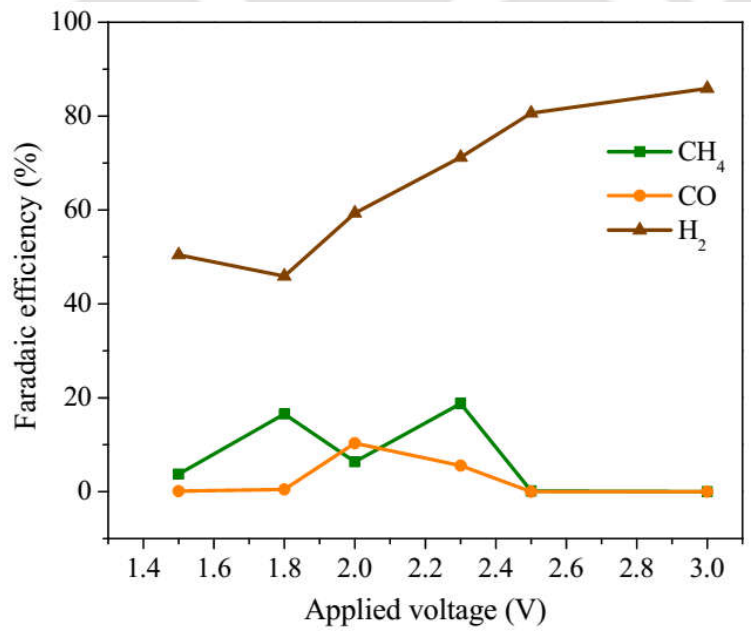

Figure 5.26 Faradaic efficiency as a function of applied voltage for electrochemical reduction of CO_2 using ZnO

2.3 V, both the species lose their catalytic activity for CO_2 reduction and further reaction results only in the formation of H_2. Compared to CuO, the performance of ZnO for CO_2 reduction is far less and it results in only two products. Further, it was also seen that it is not very durable and its activity decreases drastically with time even during 60 minutes of reaction. It happens because despite being an oxide, ZnO is not as favourable for CO_2 adsorption as CuO because the experimental heat of adsorption of CO_2 on ZnO surface is 140 $kJ \cdot mol^{-1}$ (Martins *et al.* 2004). In case of ZnO, there is competition between CO_2 and H_2O molecules for binding to ZnO surface due to the similar energetics of both the species. In CO_2 electroreduction, few H_2O molecules reach upto the cathode along with the CO_2 gas (humidified). Due to the similar energetics, adsorption of H_2O on the ZnO surface displaces the preadsorbed CO_2, which ultimately leads to the decreased efficiency for CO_2 electroreduction (Gouvea *et al.* 2014). Another important fact is that the synthesized ZnO is having very low surface area. This allows very few reaction sites to adsorb CO_2 which is already accompanied with the competitive H_2O. This further adds-up a challenge for ZnO to reduce CO_2. Moreover, amphoteric nature and stability issues of ZnO also pose negative effect over its performance.

5.3.2.2.3 Co_3O_4 metal oxide electrocatalyst

Cobalt oxide (Co_3O_4) is the combination of two interconvertible forms of cobalt, namely, cobalt(II) and cobalt(III) *viz.* CoO and Co_2O_3. The amount of products formed using Co_3O_4 is shown in figure 5.27. Three products were formed namely, CH_4, CO, and C_2H_6. Major product was found to be CO with 9.58 µmol at 2.3 V. CH_4 formation was found highest at 2 V with ~4 µmol. Moreover, C_2H_6 was detected only in trace amounts. As was seen in figure 5.20, the current density obtained in case of Co_3O_4 was the highest with 12 $mA \cdot cm^{-2}$ at 3 V. This current density corresponds to the various reactions taking place at the electrode surface. Figure 5.27 shows that these reactions are not for the reduction of CO_2, rather, unwanted hydrogen formation is taking place. At 3 V, the amount of the hydrogen formed is 3327.11 µmol. Excessive H_2 formation interfere with the reduction of CO_2

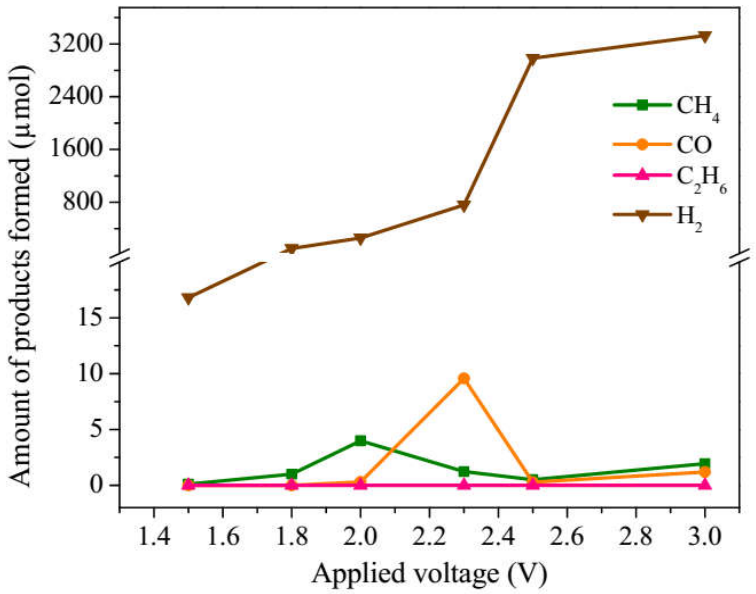

Figure 5.27 Amount of the products formed as a function of applied voltage for electrochemical reduction of CO_2 using Co_3O_4

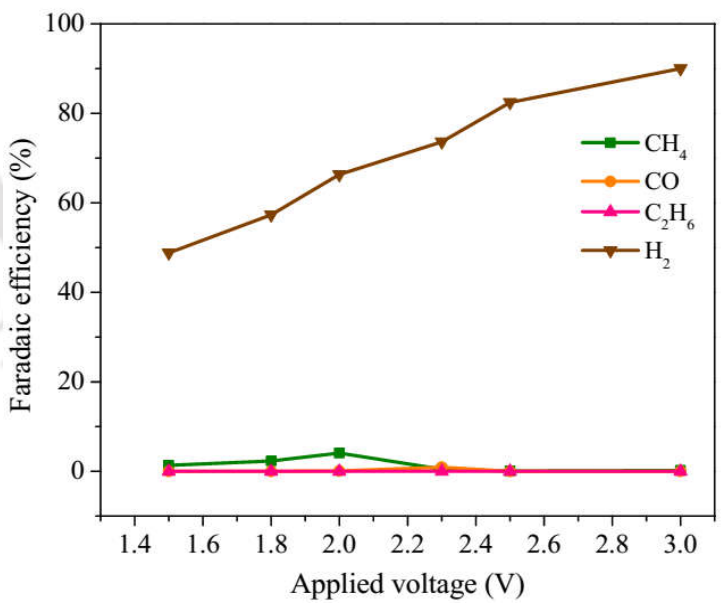

Figure 5.28 Faradaic efficiency as a function of applied voltage for electrochemical reduction of CO_2 using Co_3O_4

and hence the product formation is very less. Faradaic efficiency of various products formed is shown in figure 5.28. The highest Faradaic efficiency was found in case of CH_4, followed by CO, and C_2H_6, respectively. Similar to ZnO (section 5.3.2.2.2), Co_3O_4 also shows contrast results for the Faradaic efficiency as compared to amount of the products formed. CH_4 formation is highest at 2 V with 4% Faradaic efficiency while CO formation is highest at 2.3 V with 0.93%. The overall Faradaic efficiency was found highest at 2 V with 4.16%. In case of CH_4 and CO, it can be seen that after achieving maxima at 2 V and 2.3 V, respectively, the slight increase in amount was again observed at 3 V. The exact reason for this could not be elucidated; however, these variations may be attributed to the variable oxidation states of Co_3O_4. Here, Co^{+2}/Co^{+3} oxidation states interconvert quite readily when imposed to relatively mild variation in oxidizing and reducing ambient conditions (Casella and Gatta 2002; Petitto *et al.* 2008) which might affect the pattern of product formation at variable voltages. Moreover, it can be said that Co_3O_4 is not at all suitable electrocatalyst for CO_2 reduction as it resulted only in meager quantity of products and most of the supplied energy was wasted only in the formation of unwanted H_2 in the dERC reactor.

Table 5.1 shows the rate of the reaction of all the metal oxide electrocatalysts. The rate of the reaction is calculated at the voltage where the highest formation of products was observed for a particular electrocatalyst (Section 3.5.2). It can be seen that the highest rate is recorded in case of CuO, while the lowest rate in case of Co_3O_4.

If the selectivity patterns of all the metal oxide electrocatalysts are seen then, it becomes clear that CuO is selective for CH_4, while ZnO and Co_3O_4 show mixed selectivity pattern for both CH_4 and CO. The selectivity patterns of all the metal oxide electrocatalysts are shown in figures 5.29, 5.30, and 5.31. For CuO, initially CO formation prevails, but after 1.8 V, CH_4 formation increases and continues to be prevalent. For ZnO and Co_3O_4, both CH_4 and CO are selective at different potential values.

Table 5.1 Rate of the reaction of metal oxide electrocatalysts for dERC

Metal electrocatalysts	Applied voltage (V)	Maximum amount of product formed (µmol)		Rate of reaction (10^{-3} g·(g·h^{-1})$^{-1}$)	
		CH_4	CO	CH_4	CO
CuO	2.0	82.41	34.64	73.25	53.88
ZnO	2.3	6.56	7.79	5.83	12.12
Co_3O_4	2.3	1.24	9.58	1.11	14.91

Therefore, for ZnO and Co_3O_4, the applied potential plays an important role in determining selectivity. The variability in the selectivity patterns of ZnO and Co_3O_4 can also be attributed to the unstable nature of ZnO and variable oxidation states of Co_3O_4 as discussed in sections 5.3.2.2.2 and 5.3.2.2.3, respectively.

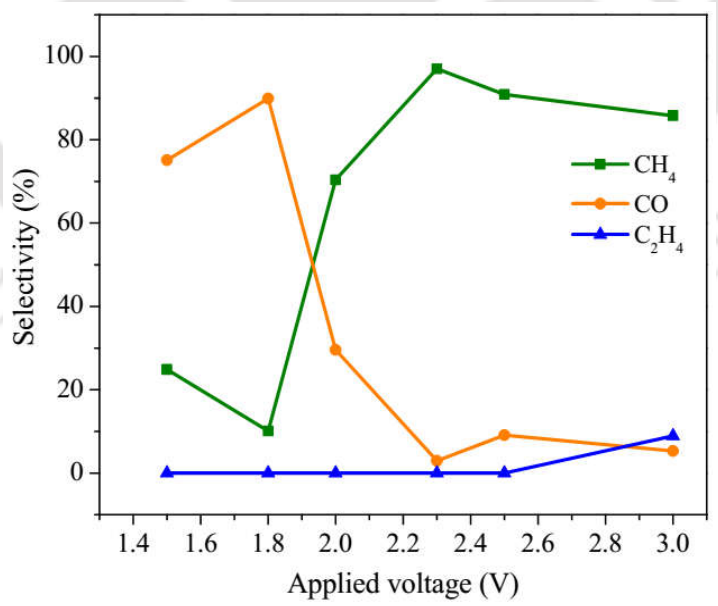

Figure 5.29 Selectivity of products using CuO electrocatalyst for dERC

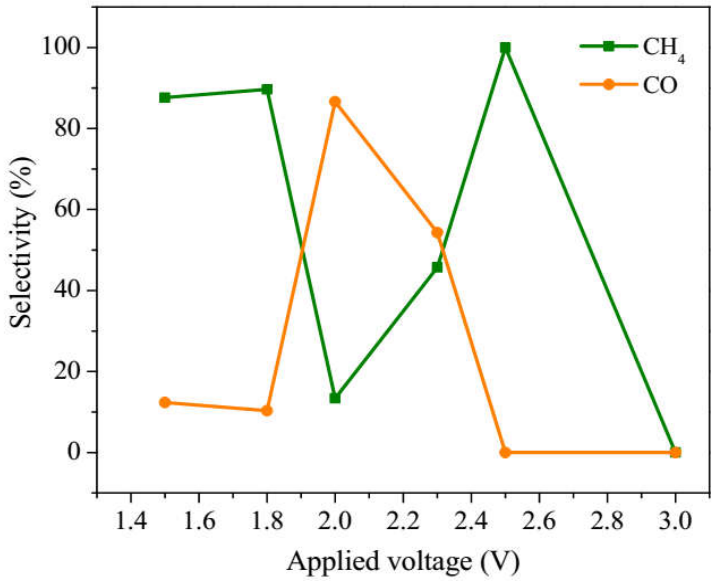

Figure 5.30 Selectivity of products using ZnO electrocatalyst for dERC

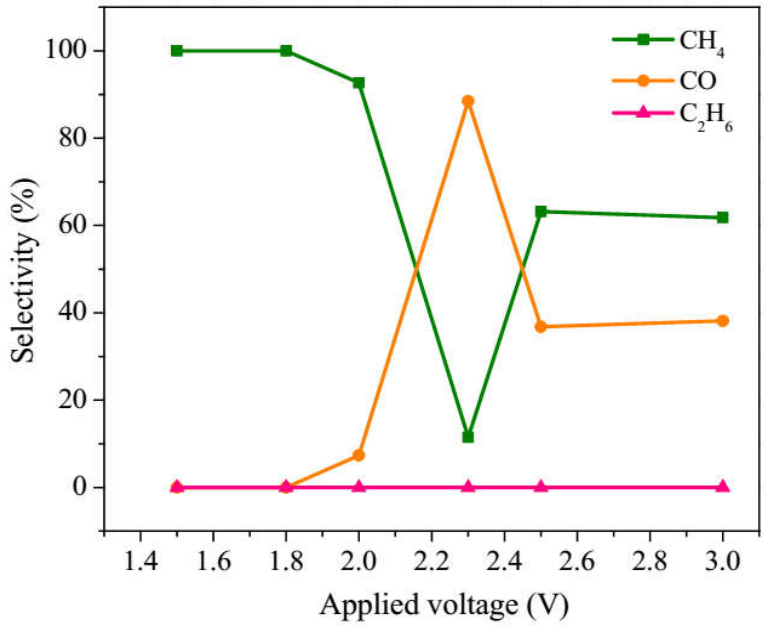

Figure 5.31 Selectivity of products using Co_3O_4 electrocatalyst for dERC

5.4 Metal oxides *vs.* metals

Since, the metal oxides have been synthesized in order to improve the efficiency of CO_2 electroreduction as compared to pure metal electrocatalysts, it becomes necessary to compare the performance of the metals with corresponding metal oxides in terms of the Faradaic efficiency and the overpotential required in the reaction. Figure 5.32, 5.33, and 5.34 show the Faradaic efficiency of the metals and corresponding metal oxides. It can be seen that CuO and ZnO electrocatalysts performed much better in comparison to their pure metal counterparts (Figure 5.32 and 5.33). Where in case of Cu only two products could be obtained, CuO resulted in the formation of C_2 hydrocarbon too. Further, the hydrogen production is also less in case of CuO, which suggests that CuO selectively favoured the CO_2 reduction reaction with Faradaic efficiency as high as 66.2% at 2 V (Figure 5.32). Moreover, in case of CuO, the formation of CO took place at 1.8 V in contrast to 2 V in case of Cu. Thus, 0.2 V decrease in overpotential, increase in total Faradaic efficiency, and formation of C_2 hydrocarbon by using CuO suggests that direct electrochemical reduction of gaseous CO_2 could be

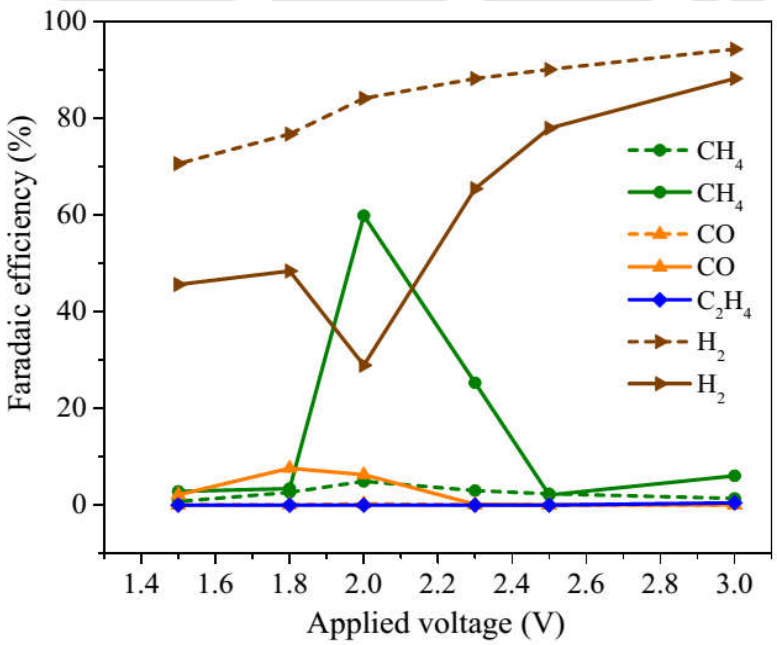

Figure 5.32 Comparison of Faradaic efficiency of CuO (solid line) with Cu (broken line)

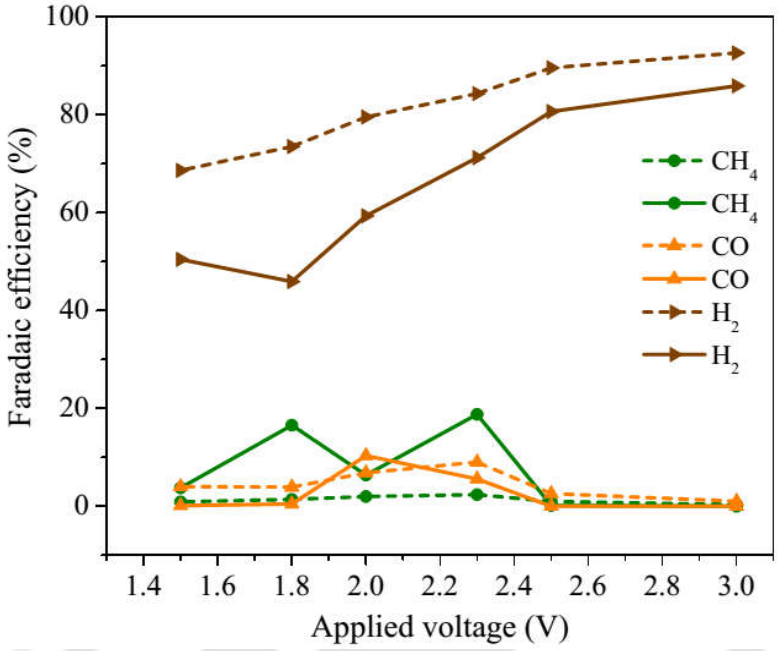

Figure 5.33 Comparison of Faradaic efficiency of ZnO (solid line) with Zn (broken line)

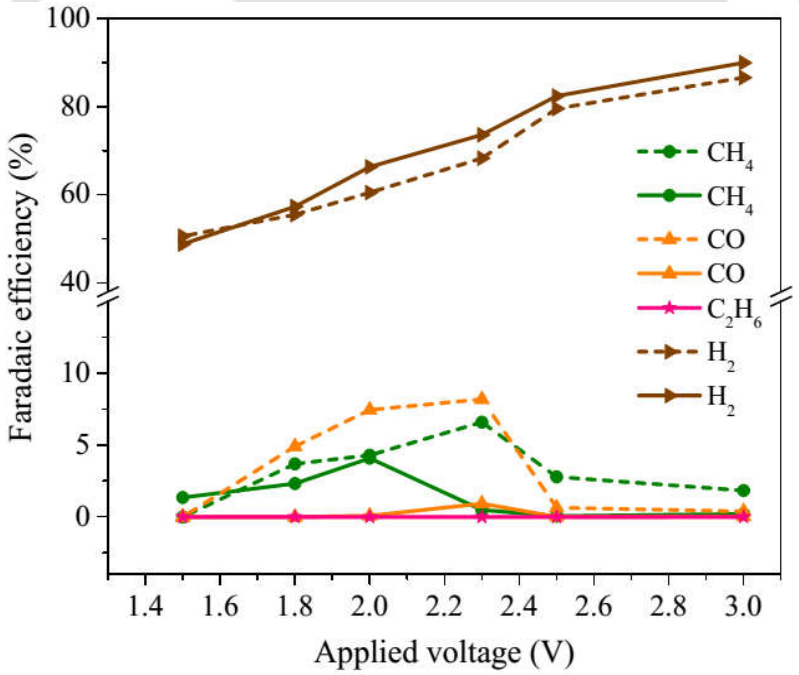

Figure 5.34 Comparison of Faradaic efficiency of Co_3O_4 (solid line) with Co (broken line)

improved by modifying Cu in the form of oxide.

The comparison of ZnO and Zn is shown in figure 5.33. In this case, the types of product formed remained unaltered and both the catalysts resulted in the formation of only CH_4 and CO. However, the product distribution varied. In case of Zn, CO was the major product at each potential value, while ZnO resulted in the CH_4 and CO formation depending upon the applied potential value. The Faradaic efficiency obtained in case of ZnO is better than in case of Zn. Further, it can also be seen in figure 5.33 that the overpotential was reduced when ZnO was used as electrocatalyst and the formation of CH_4 took place at 1.8 V along with at 2.3 V. Thus, improvement in CO_2 electroreduction was also achieved by modifying Zn in the form of oxide. However, the major problem with Zn and ZnO was their unstable nature in ERC reaction conditions which renders them unsuitable for CO_2 electroreduction. As far as Co_3O_4 is concerned, figure 5.34 shows that it did not result in improvement over the pure Co electrocatalyst. Rather, the performance of Co_3O_4 is lesser than the Co. As can be seen, both CH_4 and CO formation diminished (Figure 5.34). Moreover, H_2 formation was also found more in case of Co_3O_4.

To summarize, in this chapter it has been seen that Cu and Zn metals could be improved by converting these metals into their oxide forms for the direct electrochemical reduction of gaseous CO_2. Since, Zn as well as ZnO was found to be quite unstable in the dERC system, Zn metal would not be studied further. However, keeping in mind the appreciable performance of copper after the oxide treatment, another form of Cu as the Cu metal complex will be studied in the next chapter. In case of Ni, since its oxide form could not be studied for electrochemical reactions, hence it was complexed with a ligand to study its performance for CO_2 reduction, as discussed in the next chapter (chapter 6). As far as Co is concerned, its oxide treatment could not be proved suitable at all; therefore a new electrocatalyst was designed by incorporating a second metal into Co (chapter 7).

References

Abee M.W., York S.C., and Cox D.F. (2001), CO_2 adsorption on α–Cr_2O_3 ($10\bar{1}2$) surfaces, *Journal of Physical Chemistry B*, 105, 7755-7761.

Bandi A. (1990), Electrochemical reduction of carbon dioxide on conductive metallic oxides, *Journal of the Electrochemical Society*, 137(7), 2157-2160.

Casella I.G. and Gatta M. (2002), Study of the electrochemical deposition and properties of cobalt oxide species in citrate alkaline solutions, *Journal of Electroanalytical Chemistry*, 534, 31-38.

Chieng B.W. and Loo Y.Y. (2012), Synthesis of ZnO nanoparticles by modified polyol method, *Materials Letters*, 73, 78-82.

Esaka T. and Motoike K. (2006), Adsorption and desorption of carbon dioxide in the rare earth oxide doped Bi_2O_3 powder, *Journal of Alloys and Compounds*, 408-412, 480-483.

Fierro J.L.G. (2006), Metal Oxides – Chemistry and Applications, Taylor & Francis Group, Florida, USA, ISBN: 10: 0-8247-2371-6.

Gouvea D., Ushakov S.V., and Navrotsky A. (2014), Energetics of CO_2 and H_2O adsorption on Zinc Oxide, *Langmuir*, 30, 9091-9097.

Hassan H.S., Elkady M.F., El-Shazly A.H., and Bamufleh H.S. (2014), Formulation of synthesized zinc oxide nanopowder into hybrid beads for dye separation, *Journal of Nanomaterials*, Article ID 967492, doi: 10.1155/2014/967492.

He T., Chen D., Jiao X., Wang Y., and Duan Y. (2005), Solubility controlled synthesis of high quality Co_3O_4 nanocrystals, *Chemistry of Materials*, 17, 4023-4030.

Herrero M., Benito P., Labajos F.M., and Rives V. (2007), Nanosize cobalt oxide containing electrocatalysts obtained through microwave assisted methods, *Catalysis Today*, 128, 129-137.

Ikeda S., Hattori A., Maeda M., Ito K., and Noda H. (2000), Electrochemical reduction behavior of carbon dioxide on sintered zinc oxide electrode in aqueous solution, *Electrochemistry*, 68, 257.

Ikeda S., Ito K., and Noda H. (2009), Electrochemical reduction of carbon dioxide using gas diffusion electrodes loaded with fine electrocatalysts, *Proceedings of International Conference on Nanoscience and Nanotechnology*, CP1136, 108-113.

Isahak W.N.R.W., Ramli Z.A.C., Ismail M.W., Ismail K., Yusop R.M., Hisham M.W.M., and Yarmo M.A. (2013), Adsorption-desorption of CO_2 on different type of copper oxides surfaces: Physical and chemical attractions studies, *Journal of CO_2 Utilization*, 2, 8-15.

Jeon H., Min Y.J., Ahn S.H., Hong S.M., Shin J.S., Kim J.H., and Lee K.B. (2012), Graft copolymer templated synthesis of mesoporous MgO/TiO_2 mixed oxide nanoparticles and their CO_2 adsorption capacities, *Colloids and Surfaces A: Physicochemical and Engineering Aspects*, 414, 75-81.

Jiu J., Ge Y., Li X., and Nie L. (2002), Preparation of Co_3O_4 nanoparticles by a polymer combustion route, *Materials Letters*, 54, 260-263.

Keerthiga G., Viswanathan B., Pulikottil C.A., and Chetty R. (2012), Electrochemical reduction of carbon dioxide at surface oxidized copper electrodes, *Bonfring International Journal of Industrial Engineering and Management Science*, 2(1), 41-43.

Le M., Ren M., Zhang Z., Sprunger P.T., Kurtz R.L., and Flake J.C. (2011), Electrochemical reduction of CO_2 to CH_3OH at copper oxide surfaces, *Journal of the Electrochemical Society*, 158(5), E45-E49.

Lee J. and Tak Y. (2001), Electrocatalytic activity of Cu electrode in electroreduction of CO_2, *Electrochimica Acta*, 46, 3015-3022.

Li C.W. and Kanan M.W. (2012), CO_2 reduction at low overpotential on Cu electrodes resulting from the reduction of thick Cu_2O films, *Journal of the American Chemical Society*, 134, 7231-7234.

Liu J., Huang X., Li Y., Sulieman K.M., He X., and Sun F. (2006), Hierarchical nanostructures of cupric oxide on a copper substrate: controllable morphology and wettability, *Journal of Materials Chemistry*, 16, 4427-4434.

Martins J.B.L., Longo E., Salmon O.D.R., Espinoza V.A.A., and Taft C.A. (2004), The interaction of H_2, CO, CO_2, H_2O, and NH_3 on ZnO surfaces: an Onium study, *Chemical Physics Letters*, 400, 481-486.

Petitto S.C., Marsh E.M., Carson G.A., and Langell M.A. (2008), Cobalt oxide surface chemistry: The interaction of CoO(100), Co_3O_4(110), and Co_3O_4(111) with oxygen and water, *Journal of Molecular Catalysis A: Chemical*, 281(1-2), 49-58.

Plaza M.G., Thurecht K.J., Pevida C., Rubiera F., Pis J.J., Snape C.E., and Drage T.C. (2013), Influence of oxidation upon the CO_2 capture performance of a phenolic-resin-derived carbon, *Fuel Processing Technology*, 110, 53-60.

Qu J., Zhang X., Wang Y., and Xie C. (2005), Electrochemical reduction of CO_2 on RuO_2/TiO_2 nanotubes composite modified Pt electrode, *Electrochimica Acta*, 50, 3576-3580.

Singh S., Aeshala L.M., and Verma A. (2012), Sustainable production of fuel from electrochemical reduction of carbon dioxide, *International Journal of Innovative Research and Development*, 1(7), 155-160.

Singh S., Mukherjee C., and Verma A. (2015), Development of catalytic activity protocol for electrochemical reduction of carbon dioxide to value added products, *Clean Technologies and Environmental Policy*, 17(2), 533-540.

Srivastava N. and Srivastava P.C. (2010), Realizing NiO nanocrystals from a simple chemical method, *Bulletin of Materials Science*, 33(6), 653-656.

Suraja P.V., Yaakob Z., Binitha N.N., Triwahyono S., and Silija P.P. (2013), Co_3O_4 doped over SBA 15: excellent adsorbent materials for the removal of methyleneblue dye pollutant, *Clean Technologies & Environmental Policy*, 15(6), 967-975.

Wu H.Q., Wei X.W., Shao M.W., Gu J.S., and Qu M.Z. (2002), Synthesis of copper oxide nanoparticles using carbon nanotubes as templates, *Chemical Physics Letters*, 364, 152-156.

6

Salen ligand metal complexes as electrocatalysts for dERC

Chapter 6

Salen ligand metal complexes as electrocatalysts for dERC

Metal complex consists of an organic moiety, called as ligand, in which metal is incorporated. This chapter describes the potential evaluation of salen metal complexes for the direct electrochemical reduction of gaseous CO_2. The synthesized metal complexes were characterized by various methods to ascertain their composition and performance towards dERC. After the confirmation of the activity of metal complexes, full cell reactions were carried out and obtained products were analyzed. Performance shows that metal complexes are quite efficient for the electrochemical reduction of CO_2, giving rise to products having high calorific values. Based on the products formed, a reaction mechanism is also proposed for electrochemical reduction of CO_2 using metal complexes.

6.1 Background

It has been found in the literature that a number of metal complexes have been studied in order to reduce the activation overpotential of the CO_2 electroreduction reaction with well designed ligand and central metal atoms (Benson *et al.* 2009; Cole and Bocarsly 2010; Finn *et al.* 2012). Macrocyclic metal complexes, such as Fe porphyrins; Mn, Cu, Zn phthalocyanins; and Ru bipyridines *etc.* have been extensively studied for CO_2 electroreduction (Mahmood *et al.* 1987; Hammouche *et al.* 1991; Bhugan *et al.* 1996; Appel *et al.* 2013; Inglis *et al.* 2012; Ishida *et al.* 1987; Laitar *et al.* 2005). Most of these systems resulted in the two-electron reduction of CO_2, forming CO and/or $HCOO^-$. A few of the workers also reported six and eight-electron reduction mechanism of ERC resulting in CH_3OH and CH_4 formation using Mn, Zn porphyrins; and Cu, Ga, and Ti phthalocyanines, respectively (Garcia *et al.* 2014; Furuya and Matsui 1989; Magdesieva *et al.* 2002). Thus, the synergetics of suitable metal and ligand in metal complex may have greater role in the formation of high calorific value products as well as lowering down the overpotential. Therefore, in the present study, salen ligand metal complexes have been studied as the electrocatalysts for direct electrochemical reduction of the gaseous CO_2.

Salen ligand complexes are well known for their ability to chemically catalyze various reactions (Cozzi 2004; Darensbourg *et al.* 2004; Cohen and Coates 2006; Skljarevski *et al.* 2011). Therefore, Gambarotta *et al.* (1982) studied the bifunctional salen ligand complex containing nucleophilic cobalt (I) and an alkali cation for CO_2 capture. They have found very encouraging results, where acidic-basic (bifunctional) sites present in the metal complex played a role in binding the CO_2. Infact, this inculcated the idea to bind the CO_2 at the site and simultaneously reduce it at the electrode. Moreover, there is no study on such complexes for CO_2 electroreduction. Hence, the potential of salen complexes was explored in the field of dERC. In this effort, the primary objective of the work was to evaluate the salen metal complexes in the electrochemical reduction of CO_2 for the formation of value added products. To establish and evaluate the dERC, Ni and Cu were used to form salen metal

complex electrocatalysts. As stated in the previous chapter, Cu was chosen to ascertain its activity for dERC in the complexed form, while selection of Ni was aimed to improve its performance for dERC. It has been seen that Ni mostly results in undesired H_2 production with meager formation of CO and CH_4 during dERC (Section 4.3.4.3), and the same has also been reported by other workers in aqueous ERC (Hori *et al.* 1986, 1989, 1994). Therefore, these metals were chosen to understand the effect of salen metal complex over dERC.

6.2 Experimental

6.2.1 Materials

The 4-nitro-*o*-phenylenediamine was procured from Alfa Aesar. Potassium bicarbonate ($KHCO_3$), and *N*,*N*-dimethylformamide (DMF) were purchased from Loba Chemie. Acetonitrile (CH_3CN), $NiCl_2{\cdot}6H_2O$, $CuCl_2{\cdot}2H_2O$, triethylamine (Et_3N), ethanol (EtOH), and salicylaldehyde were procured from Merck. $CDCl_3$ for NMR spectroscopy was purchased from Sigma Aldrich. Pt/C (40 wt% Pt) was purchased from ElectroChem, Inc. USA. All the chemicals were used without further purification and de-ionized water was used in all the experiments unless stated otherwise. Gas diffusion layer (GDL) from CeTech was used as backing layer for electrocatalyst film to form electrodes. Nafion membrane (Nafion-117) and solution (5 wt%) were procured from DuPont, USA.

6.2.2 Methods

6.2.2.1 Synthesis of the ligand ($H_2L^{NO}{}_2$) and corresponding complexes

4-Nitro-*o*-phenylenediamine (**A**) contains a highly electron withdrawing $–NO_2$ group at the *–para* position of one of the two amine groups (Scheme 6.1) and hence, the $–NO_2$ group reduces the nucleophilic character of the amine group. Therefore, the ligand, $H_2L^{NO}{}_2$, was synthesized by reacting large excess (6 equivalents) of salicylaldehyde with **A** in ethanol under refluxing condition. The ligand upon reacting with equivalent amounts of $NiCl_2{\cdot}6H_2O$/$CuCl_2{\cdot}2H_2O$ in acetonitrile in the

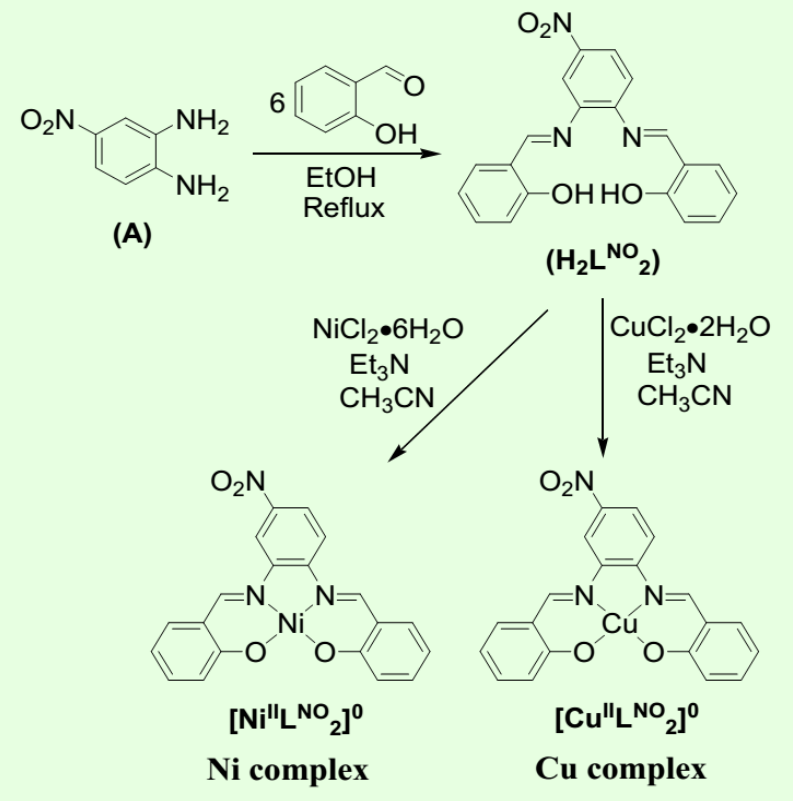

Scheme 6.1 Synthesis route to formation of the salen ligand and corresponding Ni(II) and Cu(II) complexes (**A** = 4-Nitro-*o*-phenylenediamine)

presence of Et_3N provided Ni complex/ Cu complex, respectively. The synthesis route of the ligand and the metal complexes is shown in the scheme 6.1.

6.2.2.1.1 Synthesis of salen ligand ($H_2L^{NO_2}$)

A suspension of 4-Nitro-*o*-phenylenediamine (1.53 g, 10 mmol) was prepared in ethanol solution (20 mL). Salicylaldehyde (7.33 g, 60 mmol) was added dropwise into the prepared suspension to form a mixture. The resulting mixture was heated to reflux for 20 hours. A yellow precipitate appeared after cooling the mixture at 30°C. The precipitate was filtered, washed thoroughly with EtOH, and finally air dried to get $H_2L^{NO_2}$. The yield of the synthesized ligand was 78% (Singh *et al.* 2015 a).

6.2.2.1.2 Synthesis of metal complexes [$Ni^{II}L^{NO_2}$ and $Cu^{II}L^{NO_2}$]

In CH_3CN solution (10 mL) of $H_2L^{NO_2}$ (0.180 g, 0.5 mmol), $NiCl_2{\cdot}6H_2O$ (0.120 g, 0.50 mmol)/$CuCl_2{\cdot}2H_2O$ (0.090 g, 0.50 mmol) and triethylamine (0.2 mL) were added and the resulting solution was stirred at 30°C for five hours. During this time the colour of the solution changed to reddish-brown (for Ni complex)/yellowish-brown (for Cu complex) with concomitant precipitation of the solid with the said colour. Further, the solid was filtered, washed thoroughly with CH_3CN, and air dried. The yield of the Ni complex and Cu complex was found to be 80% and 82%, respectively (Singh *et al.* 2015 a).

6.2.2.2 Characterization techniques

The synthesized ligand and metal complexes were characterized using Fourier transform infrared spectroscopy (FTIR), nuclear magnetic resonance spectroscopy (NMR), high-resolution mass spectrometry (HR-MS), elemental (CHN) analysis, and electrochemical half-cell studies as discussed in chapter 3.

6.2.2.3 Preparation of electrodes and membrane electrode assembly

Pt/C (40 wt% Pt) with Nafion dispersion (5 wt%) as binder, was used to prepare the anode electrocatalyst ink. The ink was coated over the gas diffusion layer using spraying technique and dried to get the anode. For the cathode (or working electrode), the ink was prepared by dispersing the metal complex electrocatalyst in appropriate solvent along with Nafion dispersion. The electrocatalyst ink was then coated over the gas diffusion layer followed by drying. The electrocatalyst loading for anode and cathode was kept as 0.5 $mg{\cdot}cm^{-2}$ and 2 $mg{\cdot}cm^{-2}$, respectively. The cation exchange membrane (Nafion-117) was treated using the standard procedure as discussed in section 3.3.2.1.1. The membrane electrode assembly was prepared by sandwitching the Nafion membrane in between anode and cathode at 60°C and 50 $kg{\cdot}cm^{-2}$ pressure.

6.2.2.4 Electrochemical tests

The half-cell studies were conducted in three-electrode cell assembly using Ag/AgCl as reference electrode and Pt wire as counter electrode. The working electrode was prepared by using 2 $mg \cdot cm^{-2}$ electrocatalyst loading supported over the gas diffusion layer. The cyclic voltammetry test was carried out in aqueous (0.5 M $KHCO_3$) and non-aqueous (dimethylformamide, DMF) electrolytes at the scan rate of 10 $mV \cdot s^{-1}$. In all the half-cell studies, the potential is reported with respect to standard hydrogen electrode (SHE), unless stated otherwise. The full cell studies were carried out in an electrochemical reactor using the experimental set-up described in section 3.3.2.1 and 3.3.2.2, respectively. The experiment was conducted using chronoamperometry technique (pulse width 5 s) at 8 different electrode potentials and the reaction products were collected at the cathode outlet and analyzed using gas chromatography (GC). The electrochemical experiments were carried out at 30°C and at atmospheric pressure.

6.3 Results and discussions

6.3.1 Metal complex electrocatalyst characterization

6.3.1.1 Physical characterizations

The salen ligand and metal complexes were characterized using FTIR spectroscopy along with other characterization techniques as described in section 6.2.2.2. However, ESI-MS measurement for the complexes was not possible due to insoluble nature of the complexes in the measurement friendly solvents.

6.3.1.1.1 FTIR studies

The FTIR spectrum of the synthesized ligand is shown in figure 6.1. The infrared spectrum of ligand $H_2L^{NO_2}$ showed a number of characteristic peaks at 3447, 1615, 1566, 1511, 1478, 1341, 1277, 1194,

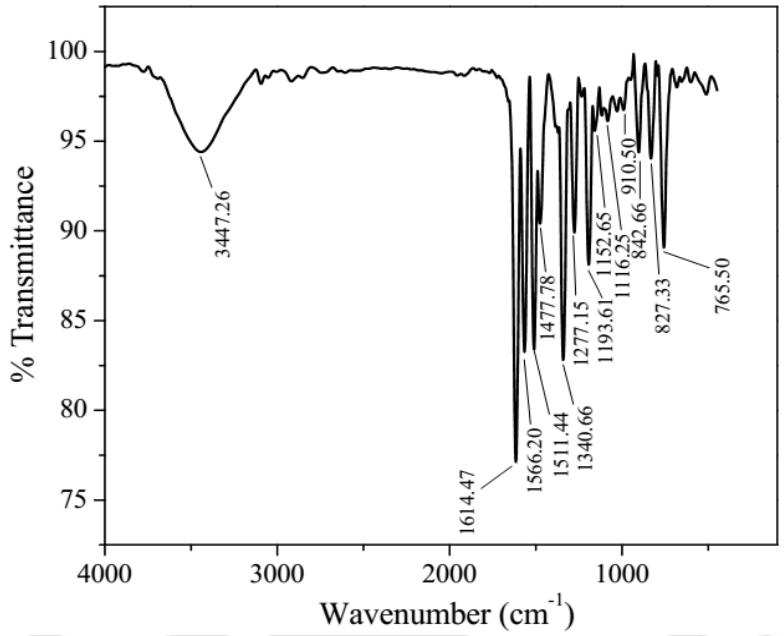

Figure 6.1 FTIR spectrum of salen ligand

1153, 910, 843, and at 765 cm^{-1}. The broad band centered at 3447 cm^{-1} is due to ν(O–H) stretching of two –OH groups. The broadness of the band implied hydrogen bonding in the ligand. The aldamine C=N stretch appeared at 1615 cm^{-1}. A sharp band at 1566 cm^{-1} was found because of phenyl asymmetric ν(C=C) stretch. The existence of bands at 1511 cm^{-1} and 1341 cm^{-1} consolidated the presence of $–NO_2$ functional group in the ligand. The phenolic ν(C–O) band appeared at 1277 cm^{-1}.

The FTIR spectra were also recorded for Ni and Cu complexes and shown in figure 6.2 and 6.3. In the FTIR spectra of complexes, prominent shift in peaks was observed as compared to ligand. In Ni and Cu complexes, the aldamine C=N stretch shifted slightly to lower value and appeared at 1610 cm^{-1} and 1612 cm^{-1}, respectively. After complexation, asymmetric ν(C=C) stretching band for phenyl ring appeared at 1576 cm^{-1} and 1575 cm^{-1} for Ni complex and Cu complex, respectively, and the value was ~10 cm^{-1} higher compared to the value observed in the free ligand. This indicated more aromatic character inside the phenyl rings in the complexes compared to the ligand. Additionally, lower phenolic ν(C–O) stretching value in the complexes (1248 cm^{-1} in Ni complex and 1259 cm^{-1} in Cu

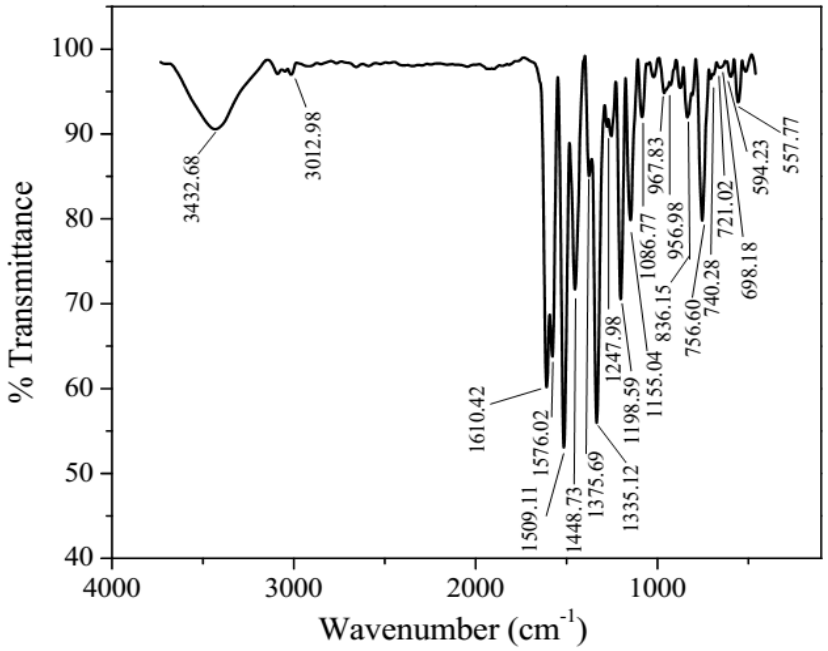

Figure 6.2 FTIR spectrum of Ni salen complex

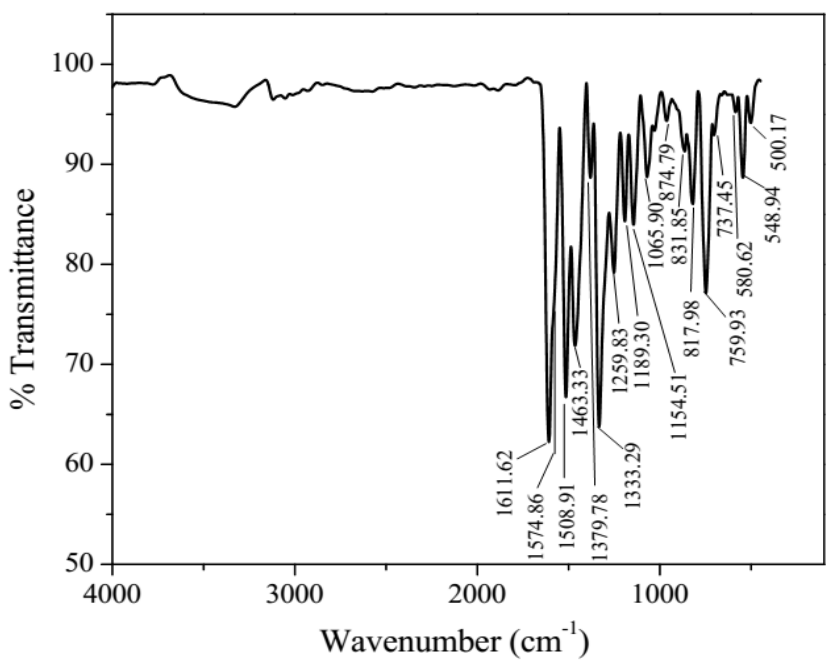

Figure 6.3 FTIR spectrum of Cu salen complex

complex) compared to free ligand (1277 cm^{-1}) supported further the higher aromatic character of the phenolate moiety. In the IR spectra of both the complexes, no appreciable changes were observed in 1511 cm^{-1} and 1341 cm^{-1} stretching bands. This indicated undisturbed and non-interacting nature of the $–NO_2$ group in both Ni and Cu complexes. Interestingly, in Cu complex a relatively weak and broad band appeared at 3321 cm^{-1} (Figure 6.3). The band is attributed to ν(O–H) stretching of H-bonded lattice water. Microanalysis data (section 6.3.1.1.4) further supported the presence of lattice water.

6.3.1.1.2 NMR studies

NMR studies were carried out to discover the structure of the salen ligand. These studies were done using proton NMR spectroscope at the frequency of 400 MHz as detailed in section 3.2.8. The obtained NMR spectrum of salen ligand is shown in figure 6.4. The various peaks obtained show the position of hydrogen atoms which are bonded to C and/or O atoms. The position of the peaks in increasing order of concentration can be written as: δ 6.97 (td, J = 7.6 Hz, 1.2 Hz, 2H), 7.05 (t, J = 8.0 Hz, 2H), 7.33 (d, J = 8.8 Hz, 1H), 7.41-7.46 (m, 4H), 8.15 (d, J = 2.4 Hz, 1H), 8.18 (dd, J = 8.8 Hz, 2.4 Hz, 1H), 8.65 (s, 1H), 8.73 (s, 1H), 12.50 (s, 1H), 12.56 (s, 1H) (Singh *et al.* 2015 a). The H-atoms in the hydroxyl groups are reflected at the position of 12.50 and 12.56 ppm. Rests of the H-atoms are bonded to C atoms through doublet, triplet, or multiplet bonds, as shown in figure 6.4.

6.3.1.1.3 High resolution mass spectroscopy (HR-MS) analysis

HR-MS analysis, as discussed in section 3.2.9, was done to find the molecular weight of the salen ligand. The spectrum obtained is shown in figure 6.5. Theoretically calculated weight of salen ligand was 362.1135 g, while the spectroscopic analysis revealed it to be 362.1115 g (Figure 6.5). These two values are almost similar, thus proving that ligand was synthesized successfully.

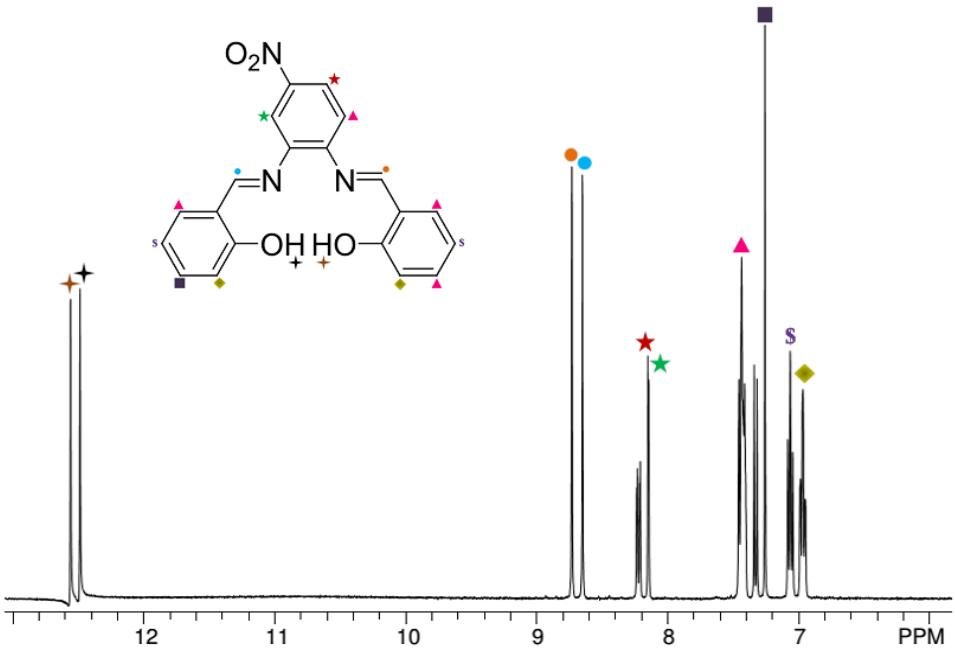

Figure 6.4 NMR spectrum of salen ligand

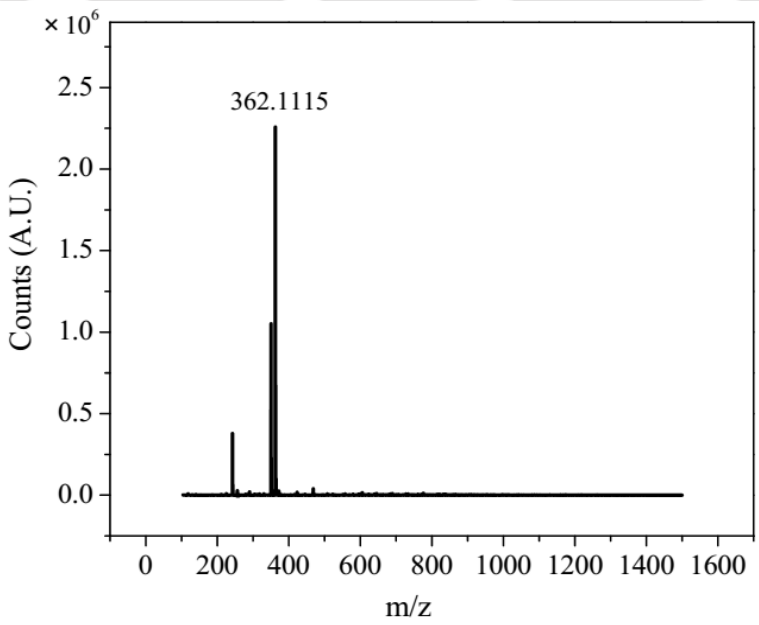

Figure 6.5 HR-MS of salen ligand

6.3.1.1.4 Elemental analysis

Since, the ESI-MS studies were not possible to conduct for Ni and Cu complexes, hence elemental (CHN) analysis, as described in section 3.2.10, was done to determine the elemental formula of the metal complexes. On the basis of theoretical calculations, the percentage amount of C, H, and N was found to be 57.55%, 3.14%, and 10.07%, respectively, for Ni complex. Moreover, the experimental data revealed the percentage amount of C, H, and N as 59.46%, 3.14%, and 9.66%, respectively. Thus, the elemental formula of Ni complex was found to be $C_{20}H_{13}N_3O_4Ni$. In case of Cu complex, the percentage amount of C, H, and N was found to be 55.93%, 3.63%, and 11.87% on the basis of theoretical calculations, while on the basis of experimental analysis it was 56.04%, 3.26%, and 11.92%. Therefore, the presence of lattice bound water and acetonitrile was found to be associated with the Cu complex. Hence, its elemental formula was given as $C_{20}H_{13}N_3O_4Cu{\cdot}CH_3CN{\cdot}0.5H_2O$ (Singh *et al.* 2015 a).

6.3.1.2 Electrochemical characterizations

6.3.1.2.1 Cyclic Voltammetry

To find out the feasibility of the synthesized metal complexes as heterogeneous electrocatalysts for electrochemical reduction of CO_2, half-cell studies were carried out. Metal complexes were studied using the conventional cyclic voltammetry test as well as the prototcol test. The cyclic voltammograms (CVs) of the Ni and Cu complexes in the potential range of 0 to 3 V *vs.* SHE are shown in figure 6.6 and 6.7. The CVs were recorded in inert (N_2) as well as CO_2 environment for both the complexes. It can be seen that significant amount of current density is observed in both the environments. However, the current density in CO_2 saturated system is higher than the corresponding current density in N_2 saturated system for both the complexes. The onset potential (the potential at which 0.1 $mA{\cdot}cm^{-2}$ current density is observed) was found to be ~1 V for both the complexes. It can be seen that with the increase in the applied voltage beyond onset potential, the current density

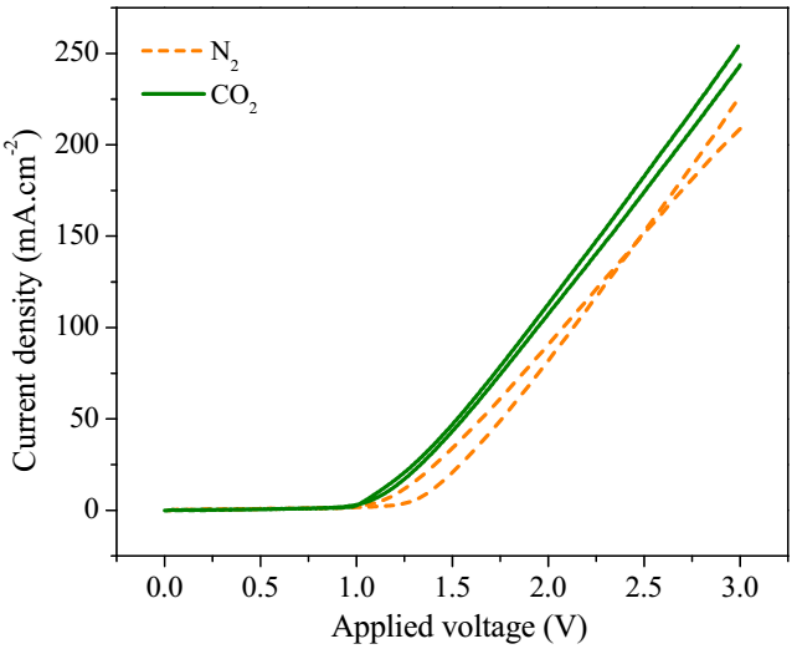

Figure 6.6 Cyclic voltammograms of Ni salen complex in N_2 (broken line), and CO_2 (solid line) atmosphere

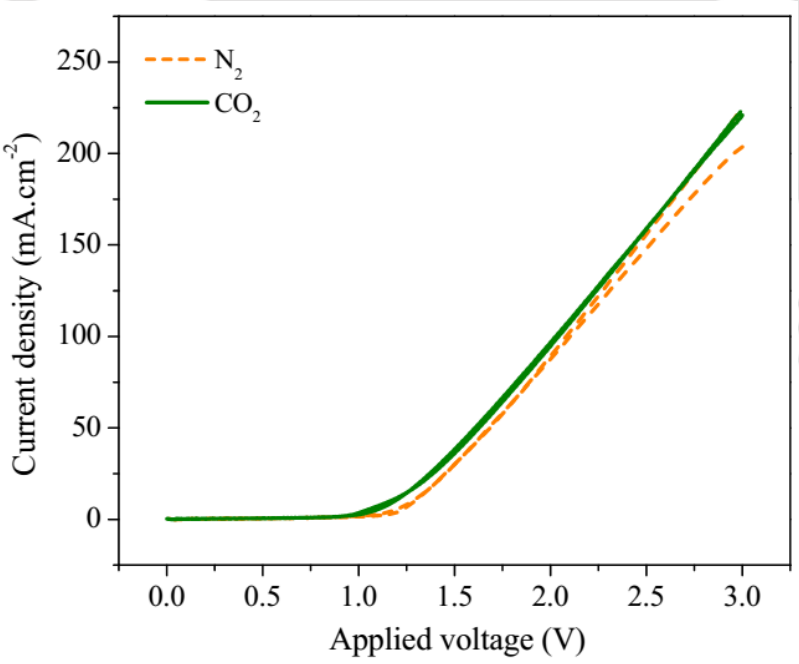

Figure 6.7 Cyclic voltammograms of Cu salen complex in N_2 (broken line), and CO_2 (solid line) atmosphere

increases (Figure 6.6 and 6.7). It can also be seen that the current density was found to be more, upto some extent, in CO_2 environment as compared to inert environment for both the complexes. The higher current density in CO_2 saturated environment may signify that electrocatalysts are able to reduce the CO_2. However, the actual determination of the electrocatalytic activity for CO_2 reduction can be done on the basis of protocol tests. Hence, the electrocatalysts were also tested as per the catalytic activity protocol.

6.3.1.2.2 The developed protocol

To further confirm the electrocatalytic activity of complexes towards CO_2 reduction, the protocol test was performed. As per the catalytic activity protocol (Singh *et al.* 2015 b), an electrocatalyst is judged for its performance on the basis of current density for CO_2 reduction in presence and absense of electrocatalyst. The comparative graphs for all the tests are shown in figure 6.8 to figure 6.10. It can

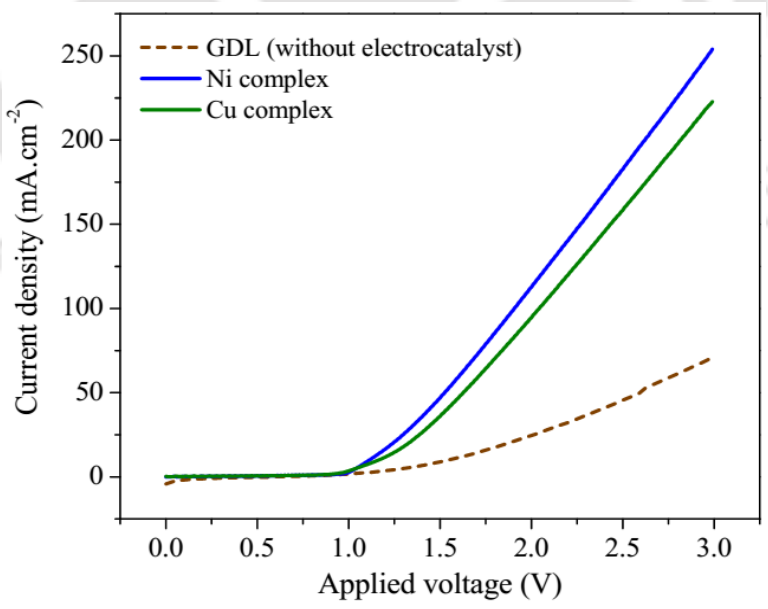

Figure 6.8 Comparison of electrocatalytic activity of metal complexes on GDL (solid lines), and only GDL (broken line) for the 1st test as per the catalytic activity protocol

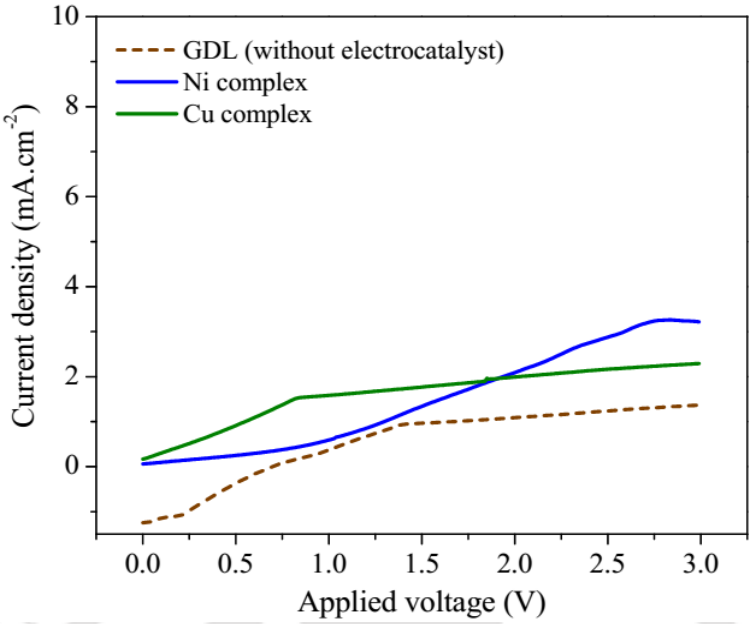

Figure 6.9 Comparison of electrocatalytic activity of metal complexes on GDL (solid lines), and only GDL (broken line) for the 2nd test as per the catalytic activity protocol

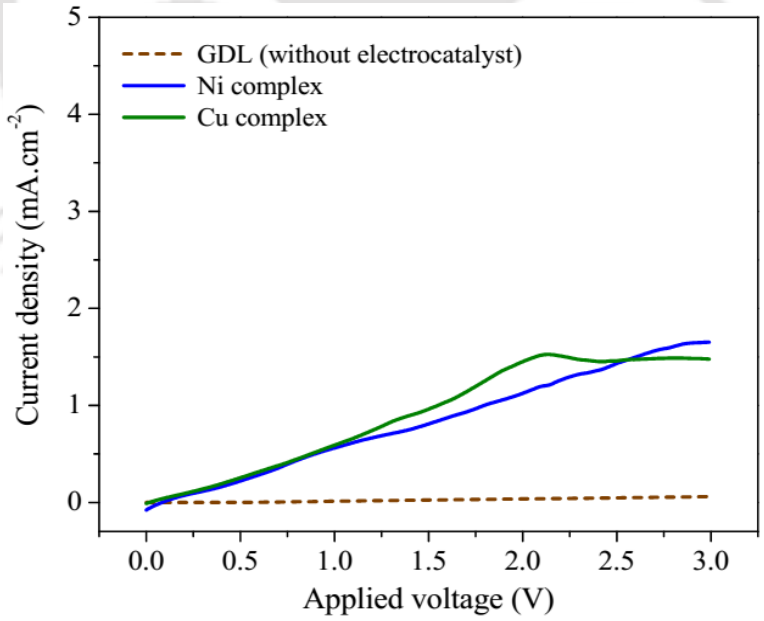

Figure 6.10 Comparison of electrocatalytic activity of metal complexes on GDL (solid lines), and only GDL (broken line) for the 3rd test as per the catalytic activity protocol

be seen that both the metal complexes resulted in higher current density compared to GDL in all the three media. This current density is due to the reactions occuring at the electrode surface. High current density in presence of electrocatalysts shows that electrocatalysts are responding in electrochemical environment. Increased current density in presence of electrocatalysts as compared to GDL in 3rd test confirms that electrocatalysts are able to reduce the CO_2; however, the unwanted H^+ reduction also takes place to some extent in presence of the salen ligand complex electrocatalysts. It was also seen in figure 6.10 that, there is no increment in current density after 2.8 V *vs.* SHE and 2.6 V *vs.* SHE in LSV of Ni complex and Cu complex, respectively. Moreover, on comparing the corresponding current densities in figure 6.8 and 6.10, it can be seen that the magnitude of current density is significantly low in case of figure 6.10. In case of CO_2 saturated aqueous system (Figure 6.8) a significant amount of current density was due to the reduction of H^+ into hydrogen gas at the cathode apart from the CO_2 reduction. In case of DMF (Figure 6.10), however, the CO_2 was bubbled only upto a certain level to maintain the pH instead of CO_2 saturation in the DMF. Moreover, the electroreduction might not be completed due to absence of other reactants to combine with the reduced or activated CO_2. In turn, the low level of CO_2 in the electrolyte along with increased mass transfer resistance and scarcity of co-reactant reduces the current density, which does not increase even with the increase in the applied voltage. Apart from the other reasons, the difference (in the order of 10^3) in electrical conductivities of the media ($mS \cdot cm^{-1}$ in case of $KHCO_3$, while $\mu S \cdot cm^{-1}$ in case of DMF) also affect the performance (Singh *et al.* 2015 a, b). Therefore, these studies confirm qualitatively the efficacy of the metal complexes, however, can not be used for quantifying the role of the electrocatalysts. Therefore, further study was conducted to evaluate and quantify the products obtained out of the dERC using Ni and Cu complexes.

6.3.2 dERC studies using metal complex electrocatalysts

Once the activity of the synthesized metal complexes was proved for the electrochemical reduction of CO_2 in preliminary half-cell studies, the full cell studies were attempted for the qualitative and

quantitative information regarding the products formed in dERC using the complexes. The reactions were carried out above the onset potential range, which is ~1 V in both the cases. The products formed were collected at definite time intervals from the cathode outlet and analyzed using gas chromatography.

6.3.2.1 Effect of applied voltage on current density and Faradaic efficiency

For both the metal complex electrocatalysts, the experimental results obtained are presented in figure 6.11 and 6.12. Figure 6.11 shows the current density corresponding to various applied voltages at the terminals of the electrochemical reactor. It can be seen that the current density increases with the increase in the applied voltage for both the complexes, which in turn signifies the increased rate of various electrochemical reactions including H_2 gas generation (undesired) at the electrode surface.

Figure 6.12 shows the Faradaic efficiency for electrochemical reduction of CO_2 using metal complexes. It can be seen that the Faradaic efficiency for Ni complex is quite high *viz.* 74% at 1.5 V. On further increasing the voltage, the Faradaic efficiency decreases sharply. The Faradaic efficiency for the Cu complex increases initially, attains maxima at 1.8 V, and then subsides gradually with the increase in the voltage. The highest Faradaic efficiency of 25% is achieved at 1.8 V for the Cu complex electrocatalyst. It may be noted that the Faradaic efficiency using the complexes is the result of cumulative efficiencies for the formation of various products from electroreduction of CO_2. To determine the energy utilized (Faradaic efficiency) for the individual reaction products, it is necessary to quantify the reaction products at the cathode of the electrochemical reactor.

6.3.2.2 Performance of metal complex electrocatalysts for the formation of various dERC products

To get more insight of the performance of metal complexes for the formation of various products, the studies were conducted to find the Faradaic efficiencies of individual products of dERC as well as hydrogen production.

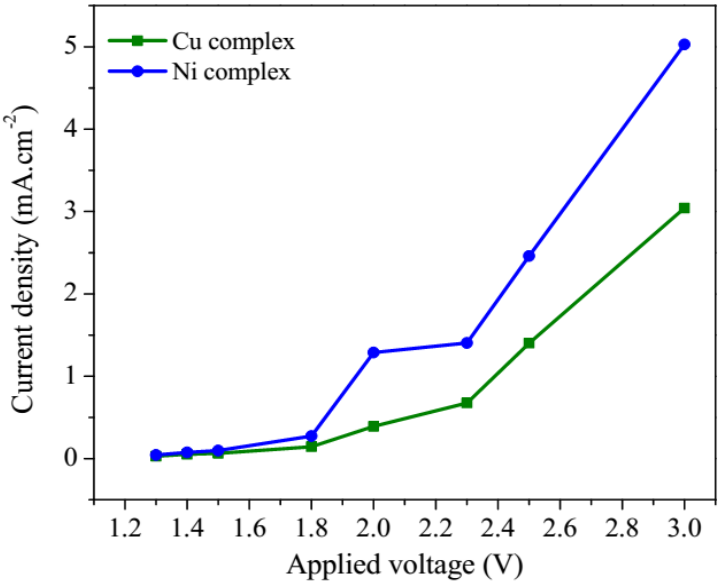

Figure 6.11 Current density as a function of applied voltage for metal complex electrocatalysts

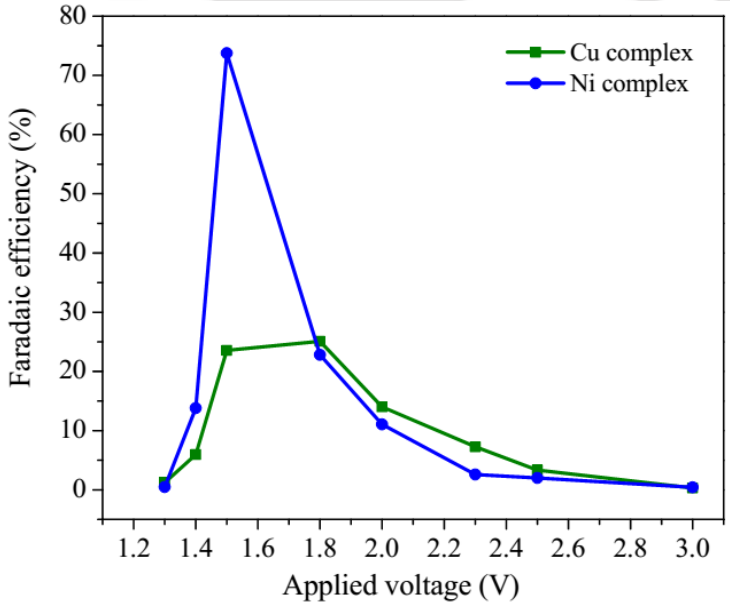

Figure 6.12 Faradaic efficiency as a function of applied voltage for metal complex electrocatalysts

6.3.2.2.1 Ni salen complex electrocatalyst

Figure 6.13 shows the amount of the products formed using Ni salen complex as an electrocatalyst for the electrochemical reduction of gaseous CO_2. It can be seen that major product formed is CO, along with the other products such as CH_4, C_2H_4, C_2H_6, and by-product H_2. The highest amount of CO was found to be 17.74 µmol at 2 V. Moreover, 12.32 µmol was formed at 1.5 V. The decrease in the CO formation at 1.8 V is due to simultaneous increment in the formation of CH_4. Highest number of moles of CH_4 (2.22 µmol) was found at 1.8 V. The formation of C_2H_4 and C_2H_6 appears to be in trace amount with maximum number of moles of 0.03 µmol and 0.71 µmol, at 1.4 V and 1.5 V, respectively. Hydrogen formation was found to be increasing with the applied voltage resulting into 1438.98 µmol at 3 V. The amount of the products formed is an outcome of the applied voltage at the terminals of the electrochemical reactor. Therefore, to have a clear picture of the efficiency of the system, it is necessary to analyze both these parameters together. Determination of Faradaic efficiency serves this purpose and hence, figure 6.14 shows the Faradaic efficiency of various products as a function of applied voltage. It can be seen in the figure 6.14 that main products of dERC are hydrocarbons and carbon monoxide using Ni salen complex. In case of Ni complex, Faradaic efficiency for CH_4 (16.6%) and C_2H_6 (16.35%) is considerably high with maximum for CO formation (40.8%) (Figure 6.14). It is to be noticed that CO, CH_4, and C_2H_6 show highest Faradaic efficiency at 1.5 V. However, C_2H_4, which was minor, formed at 1.4 V with Faradaic efficiency of 2.1%. Along with the products resulting from CO_2 reduction, H_2 formation was also found, which approximately compensate for rest of the Faradaic efficiency at any particular voltage (Singh *et al.* 2015 a). Apart from the formation of hydrocarbons (C_1 and C_2), another important attribute of Ni salen complex is that its performance was found to be well even after 60 minutes of reaction. When the reaction was continued after 60 minutes, it was seen that CO formation took place in appreciable quantities. The Faradaic efficiency variation with time using Ni salen complex is shown in figure 6.15. It can be seen that although hydrocarbons formation was significant only upto initial 40 minutes, the CO formation

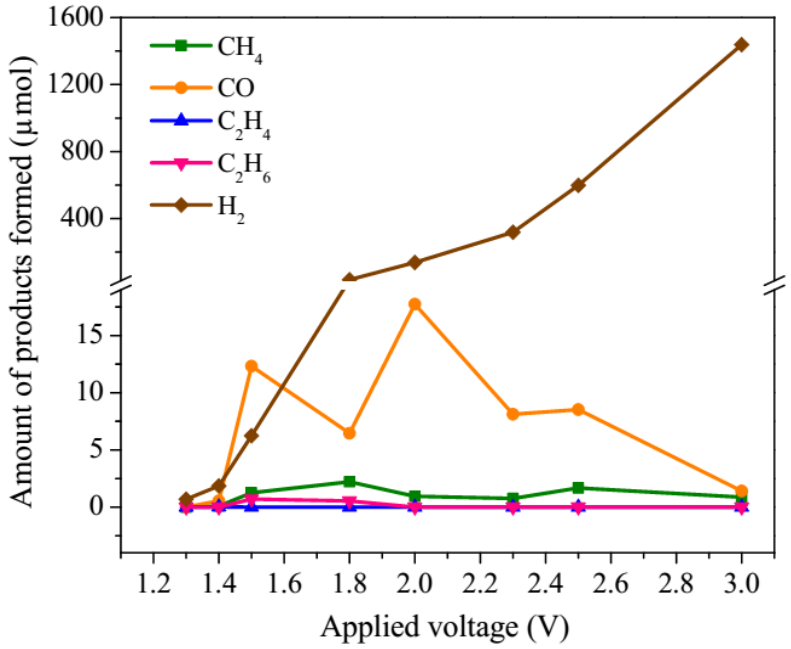

Figure 6.13 Amount of the products formed as a function of applied voltage for electrochemical reduction of CO_2 using Ni salen complex

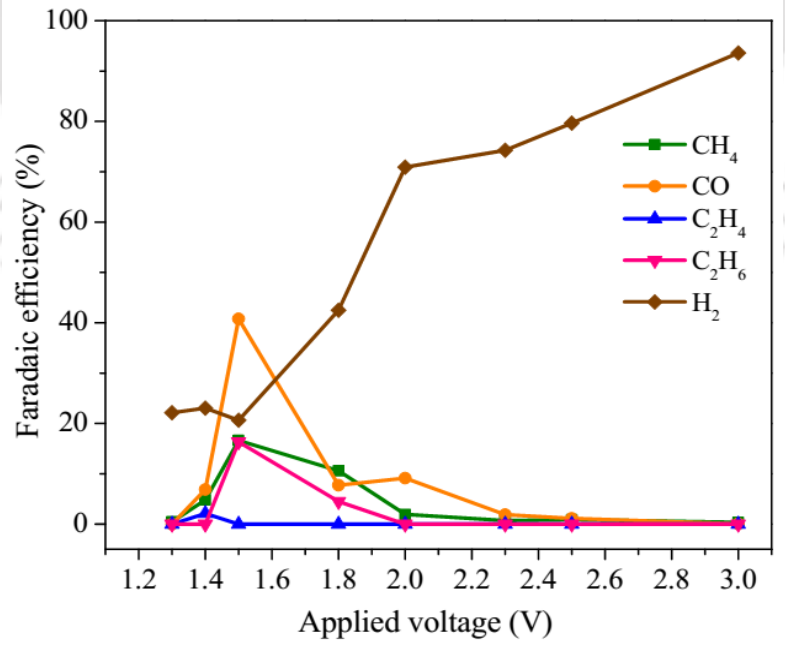

Figure 6.14 Faradaic efficiency as a function of applied voltage for electrochemical reduction of CO_2 using Ni salen complex

was continued even after 60 minutes with appreciable Faradaic efficiency (Figure 6.15). It should be noted that the Faradaic efficiency variation with time has been considered at the voltage where the maximum Faradaic efficiency for a particular product was observed (Figure 6.14). Moreover, for comparison, the hydrogen formation is also shown at the same voltage. With increasing time, the hydrogen formation was found to be increasing continuously. The possible reason for this can be that, with increasing time, the hydrogen ions accumulation takes place at the cathode surface which results in lowering down the pH. This low pH favours the H_2 formation, which ultimately renders CO_2 electroreduction to decrease. After 80 minutes, the electrocatalytic activity of Ni salen complex seizes completely as no product from CO_2 electroreduction could be observed and all the supplied energy was wasted in the formation of unwanted hydrogen formation.

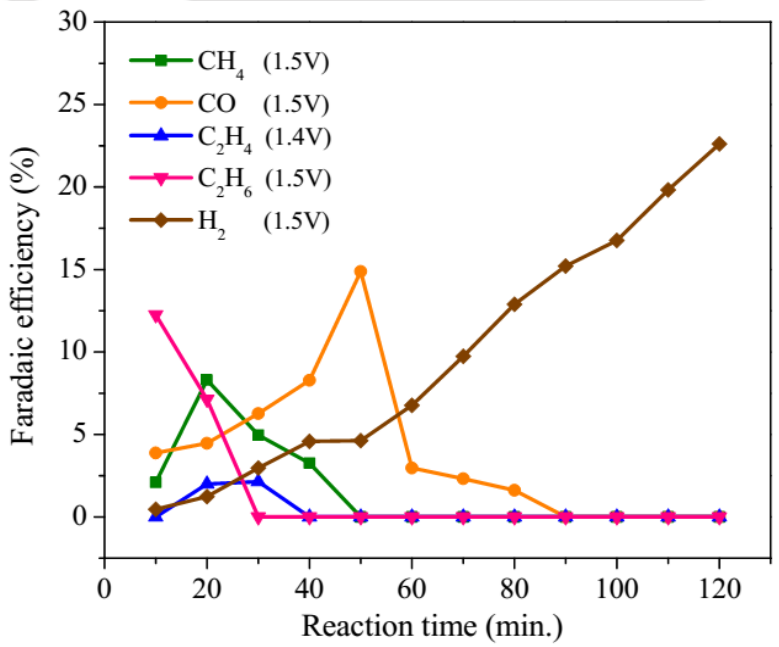

Figure 6.15 Faradaic efficiency variation with time during electrochemical reduction of CO_2 using Ni salen complex

6.3.2.2.2 Cu salen complex electrocatalyst

Similar with the case of Ni salen complex, the amount of the products formed was also determined for Cu salen complex and shown in figure 6.16. Contrary to the case of Ni salen complex, Cu salen complex resulted in the highest formation of CH_4 with ~30 µmol at 2.3 V. Second major product is the CO with 6.3 µmol at 2.5 V. C_2H_4 was formed only in trace amounts. However, a large amount of the supplied energy was wasted in the formation of undesired H_2 formation with 826.97 µmol at 3 V. One important thing to note is that the amount of hydrogen formed is far less than in case of Ni salen complex, which was also reflected in figure 6.9. However, this does not enhance the reduction of CO_2. This is due to the less current density obtained in case of Cu salen complex (Figure 6.11).

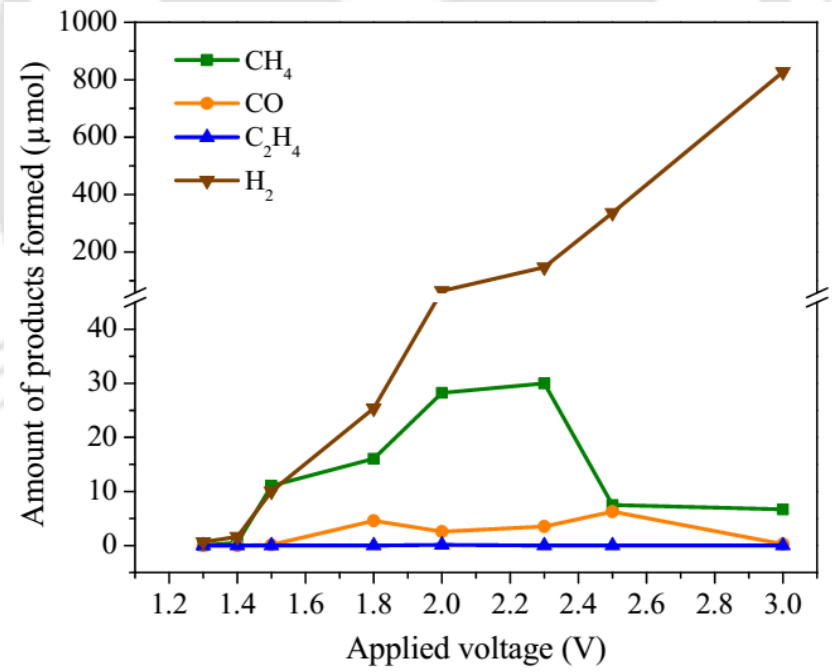

Figure 6.16 Amount of the products formed as a function of applied voltage for electrochemical reduction of CO_2 using Cu salen complex

Figure 6.17 shows the Faradaic efficiency for the Cu salen complex. In this case, CH_4 was the major product along with considerable Faradaic efficiency of CO (Figure 6.17). Moreover, C_2H_4 was formed feebly with Faradaic efficiency of 1%. It can be seen that the Faradaic efficiency for CH_4 (23%) is highest at 1.5 V; however, CO attains its maxima at 1.8 V with Faradaic efficiency of 10.5%. Apart from the products resulting from CO_2 reduction, H_2 formation was also found which, similar to Ni salen complex, approximately compensate for rest of the Faradaic efficiency at any particular voltage. It is important to note for both the complexes that the voltage, at which the highest amount of product formation was observed, does not correspond to the voltage at which highest Faradaic efficiency was observed (Figure 6.13 *vs.* 6.14 and Figure 6.16 *vs.* 6.17). It is due to the fact that Faradaic efficiency takes into the account the number of moles of electrons supplied. Therefore, if the same amount of CO and CH_4 is formed, then the Faradaic efficiency towards CH_4 would be 4 times higher, since there are 8 electrons involved in the formation of one mole of CH_4 while only 2 in the formation of one mole of CO. Similar explanation is also valid for C_2H_4 and C_2H_6 where 12 and 14 electrons are utilized, respectively.

Another similarity between Cu and Ni salen complex is that the Cu salen complex is also stable even after 60 minutes of reaction in contrast to the pure copper metal which loses its catalytic activity in the same duration (Hori *et al.* 2005; Li and Kanan 2012). The variation of Faradaic efficiency with time for Cu salen complex is shown in figure 6.18. Similar to Ni salen complex, in case of Cu salen complex too, the hydrocarbons formation takes place in initial 20-40 minutes, while CO formation stops only after 90 minutes. This shows improvement over the pure Cu metal. The continuously increasing hydrogen formation indicates the same cause as discussed in case of Ni salen complex, which finally results in obstruction of CO_2 electroreduction.

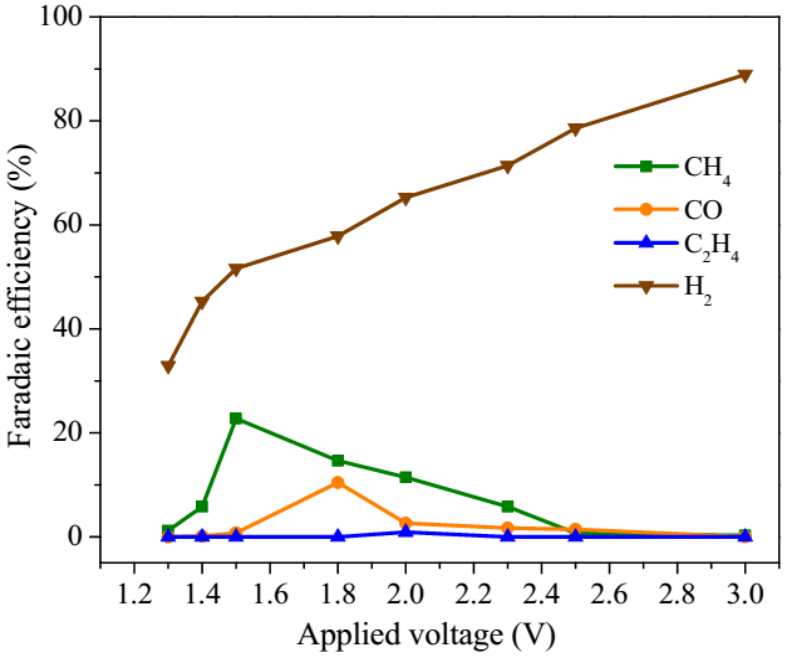

Figure 6.17 Faradaic efficiency as a function of applied voltage for electrochemical reduction of CO_2 using Cu salen complex

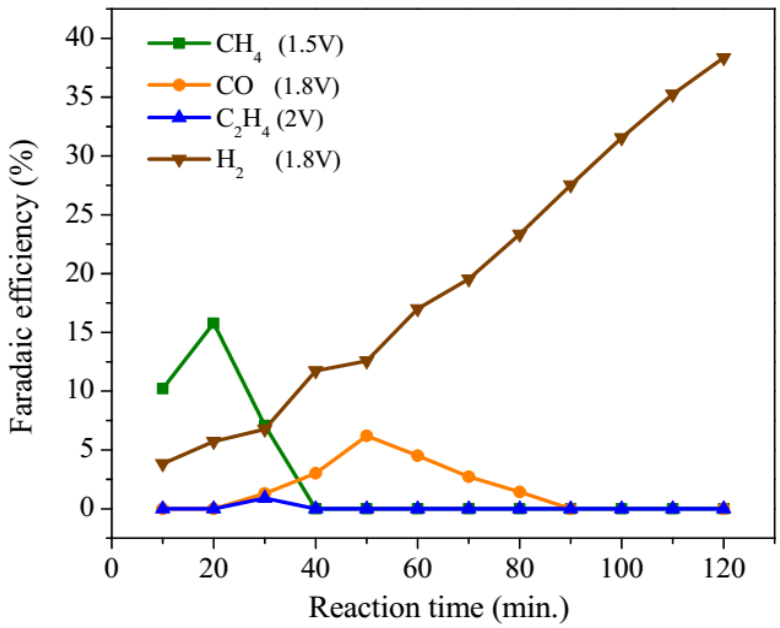

Figure 6.18 Faradaic efficiency variation with time during electrochemical reduction of CO_2 using Cu salen complex

It is evident that both the Ni and Cu complexes were active towards CO_2 reduction and underwent multi-electron reduction of CO_2 resulting in C_1 and C_2 hydrocarbons, which is usually rare in case of other metal complexes. It happened because incorporation of anchoring -NO_2 group in the ligand ($H_2L^{NO_2}$) backbone provides better interaction of salen complexes to the electrode material and hence, facilitate an efficient electron transfer during the conversion of CO_2 to the products. Additionally, during the conversion process, when M^{n+} reduces to $M^{(n-1)+}$ state (M stands for metal), the decrease in Lewis basicity of the central metal ion due to increase in metal-to-ligand(imine) π-back donation is compensated by two strong σ donations by two phenolate donors as shown in scheme 6.2. This is due to more aromatic character inside the phenyl rings of the complexes, which was depicted in FTIR spectra.

Overall, Ni complex was found to perform much better than Cu complex at relatively low overpotential, as it is also evident from Table 6.1. The better performance of the Ni complex can be explained in terms of the stability of the Ni(I) and Cu(I) intermediate species. As it is known that the optimum stability or binding of metal-CO_2 bond is crucial for multi-electron reduction during dERC.

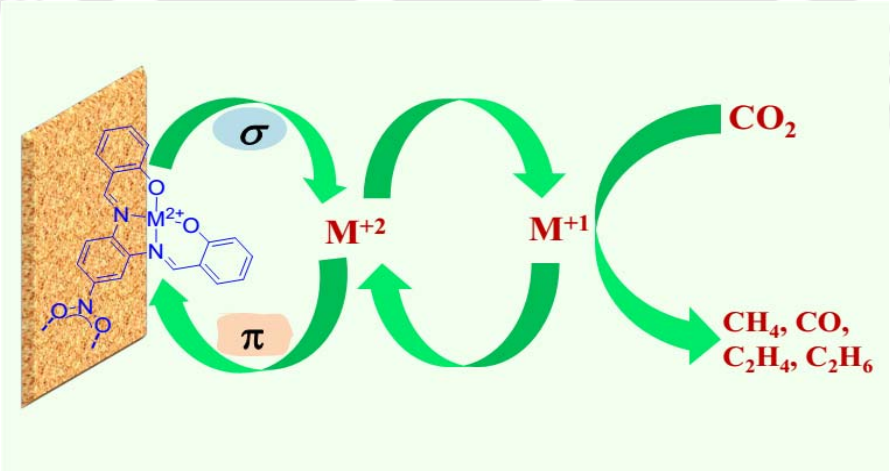

Scheme 6.2 Representation of redox behaviour of salen ligand complex ('M' represents metal) (Singh *et al.* 2015 a)

Table 6.1 Rate of the reaction of metal complex electrocatalysts for dERC

Metal complex electrocatalysts	Applied voltage (V)	Maximum amount of product formed (μmol)		Rate of reaction (10^{-3} g·(g·h^{-1})$^{-1}$)	
		CH_4	CO	CH_4	CO
Ni salen complex	2.0	0.94	17.75	0.84	27.60
Cu salen complex	2.3	30	3.53	26.67	5.49

The strong binding of metal-CO_2 may poison the electrocatalyst, whereas weak bonding may result in higher overpotential for the reaction along with dissociation of product from the reaction site by utilizing only a few electrons. During the CO_2 reduction process, Ni(II) and Cu(II) converts to Ni(I) and Cu(I) species, respectively. Ni(I) being less stable, coordinates with CO_2 yielding stable Ni-CO_2 complex (Costamagna *et al.* 1996) thus resulting in effective multi-electron reduction of CO_2 with high efficiency, however, Cu(I) is comparatively more stable and hence does not bind with CO_2 with the same efficacy, which in turn results in lower performance. Based on the products formed, an elementary reaction mechanism is proposed for the formation of hydrocarbons and CO as shown in scheme 6.3. The scheme 6.3 shows that initially the metal complexed to the salen ligand is in +2 state and it gets reduced to +1 state by taking up an electron from the electrode. The addition of CO_2 in the system receives the electron from the reduced metal, which was in +1 state, and binds with it. Moreover, the stability of the system was maintained by the phenolate group of the ligand. Simultaneously, H^+ ions were transported through membrane from the anode side to the cathode during the full cell reaction and reacted with the metal complex-CO_2 along with some internal rearrangements in the complex to form either the adsorbed CO (CO_{ad}) or free CO, which escapes from the cathode. The CO_{ad} may further participate in the reaction to form hydrocarbons (Schouten *et al.* 2011; Aeshala *et al.* 2014) as shown in the scheme 6.3. Ultimately, the metal in the complex reverts to its previous oxidation state (+2). Thus, the redox behaviour of the salen metal complex

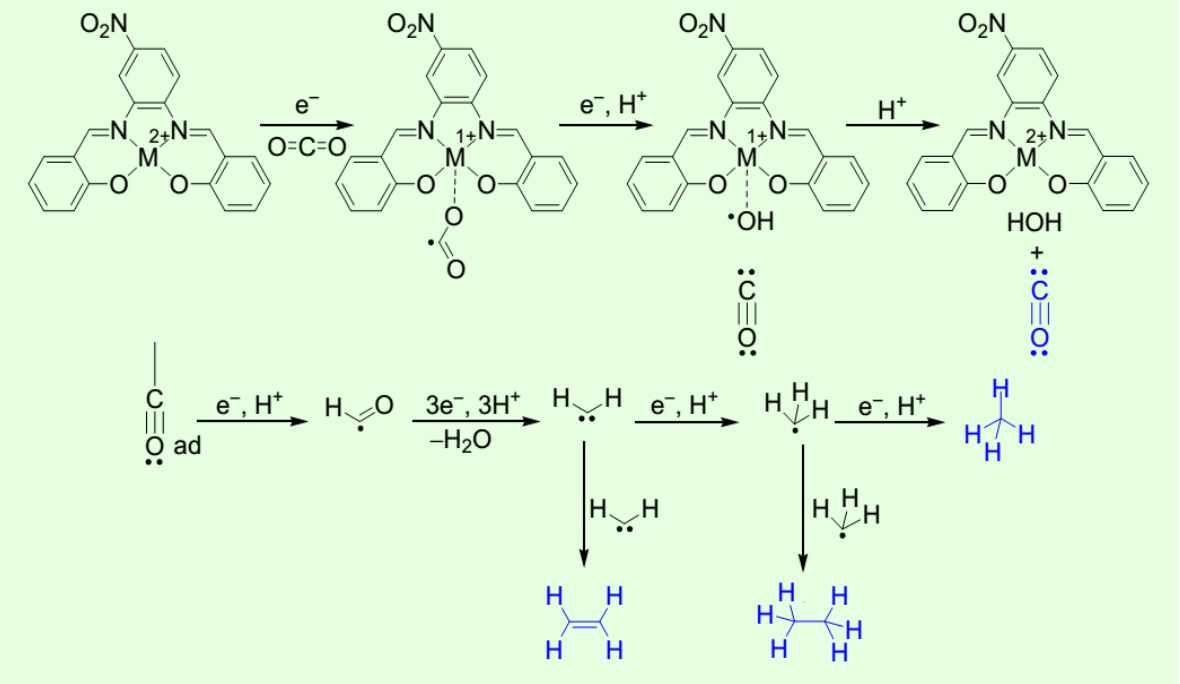

Scheme 6.3 Proposed elementary mechanism for the formation of reaction products using salen metal complexes (Singh *et al.* 2015 a)

helps in efficient electron transfer between itself and CO_2 and, therefore, results in variety of products with high efficiency (Singh *et al.* 2015 a).

The selectivity of these metal complexes is shown in figure 6.19and 6.20. It can be seen that Ni salen complex is highly selective for CO formation while Cu salen complex is selective for CH_4. This trend proves that although the efficiency of the complexes for CO_2 reduction is remarkably affected by the ligand moiety, but the selectivity is largely determined by the metal ion present at the centre of the ligand, as it has been witnessed in earlier chapters that Ni is selective for CO while Cu is selective for CH_4. The ups and downs in the selectivity patterns may be due to the variety of factors, a major factor being the stability of intermediates. At any particular voltage, the stability of various intermediate species varies and that affects the formation of the products. Apart from the stability, the adsorption tendency of different intermediates and their orientation at the electrode/electrocatalyst surface

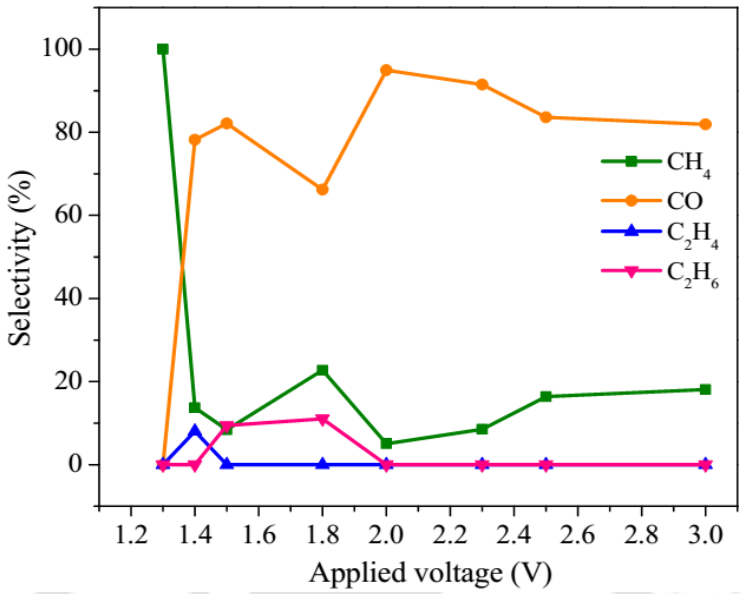

Figure 6.19 Selectivity of products using Ni salen complex electrocatalyst for dERC

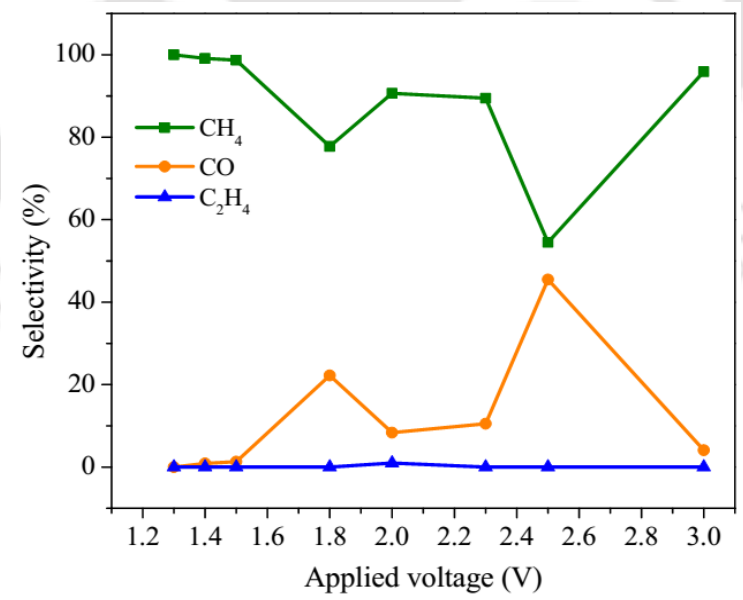

Figure 6.20 Selectivity of products using Cu salen complex electrocatalyst for dERC

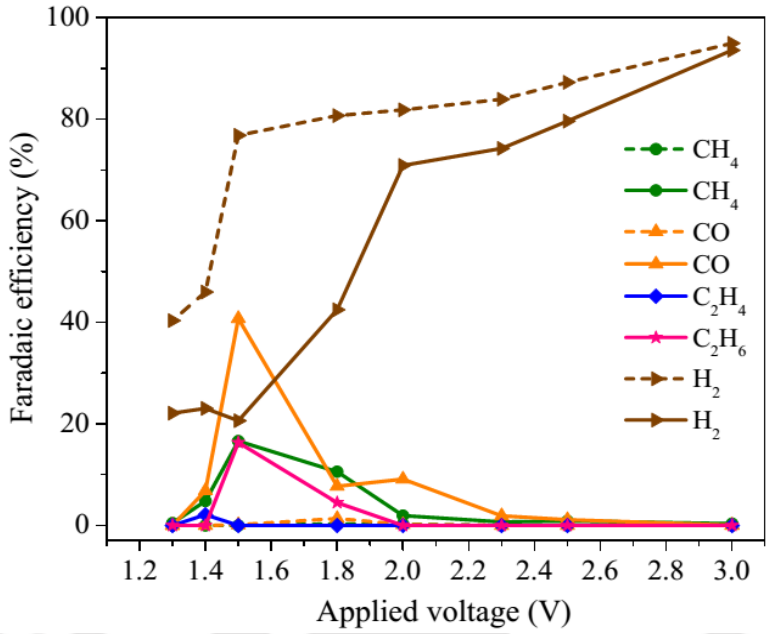

Figure 6.21 Comparison of Faradaic efficiency of Ni salen complex (solid line) with Ni (broken line)

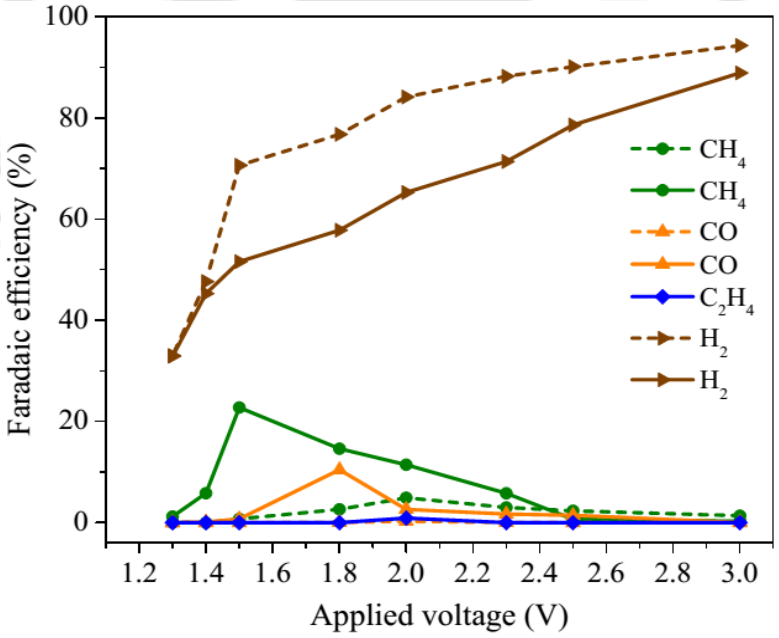

Figure 6.22 Comparison of Faradaic efficiency of Cu salen complex (solid line) with Cu (broken line)

largely determines the product formation. Therefore, interplay of all these factors renders one unable to trace the exact reason for the non-linear nature shown in the selectivity patterns.

6.4 Metal complexes *vs.* metals

The synthesis of metal complexes was aimed to improve the electrocatalytic performance of the Ni and Cu metals for the reduction of CO_2. It has been seen in section 6.3 that the performance of the metal complexes was appreciable for the dERC. To get more insight into the performance, the Faradaic efficiency of metal complexes was compared with metals and shown in figure 6.21 and 6.22. It can be seen that Faradaic efficiency for all the products was increased in case of metal complexes. Moreover, hydrogen production was also decreased as compared to metals. It can be seen in figure 6.21 that Ni metal resulted only in CH_4 and CO; however, Ni complex was able to produce CH_4, C_2H_4, C_2H_6, and CO. It shows that efficiency was improved to a great extent after incorporating metal with the ligand moiety (Singh *et al.* 2015 a).

Figure 6.22 shows the comparison between Cu metal complex and Cu pure metal. Where, Cu metal resulted only in CH_4 and CO, Cu metal complex was also able to form C_2H_4. It can be seen that CH_4 formation was increased from 4.93% (2 V) in case of Cu to 22.77% (1.5 V) for Cu metal complex. Significant improvement was also seen in CO formation, where Faradaic efficiency was increased from 0.27% (2 V) to 10.47% (1.8 V) by using Cu metal complex. By-product, H_2, was also found less in case of metal complex electrocatalyst. Apart from the better Faradaic efficiency, the metal complexes also proved to be helpful in reducing overpotential. The overpotential required for the reaction was quite low for both the metal complexes as compared to pure metals as can be seen in Table 6.2. It is because of the initial reduction of metal complex itself (M^{n+} to $M^{(n-1)+}$), and subsequent reaction with CO_2. Thus, metal complexes acted as redox couple, which help in reducing the overpotential for the CO_2 electroreduction as well as in multielectron transfer resulting in C_1 and C_2 hydrocarbons (Sullivan *et al.* 1993). Thus, it can be said that salen ligand complexes of both the

Table 6.2 Reduction in overpotential for a few representative reaction products using the metal (Ni or Cu) and metal complexes (Singh *et al.* 2015 a)

Electrocatalysts	**Applied voltage (V) corresponding to maximum Faradaic efficiency of the product**		
	CH_4	**CO**	**C_2H_6**
Ni	2	1.8	-
Ni-complex	1.5	1.5	1.5
Reduction in overpotential (V)	**0.5**	**0.3**	-
Cu	2	2	-
Cu-complex	1.5	1.8	-
Reduction in overpotential (V)	**0.5**	**0.2**	-

metals (Ni and Cu) were found to be much better than their pure metal counterparts in terms of energy efficiency as well as catalytic efficiency (Singh *et al.* 2015 a). It fulfilled the aim of enhancing the efficiency of Ni and Cu metals for the formation of fuel kind of products. Next chapter discusses another strategy to improve the performance of Co metal by incorporating second metal into it.

References

Aeshala L.M., Uppaluri R.G., and Verma A. (2014), Electrochemical conversion of CO_2 to fuels: Tuning of reaction zone using suitable functional group in solid polymer electrolyte, *Physical Chemistry Chemical Physics*, 16, 17588-17594.

Appel A.M., Bercaw J.E., Bocarsly A.B., Dobbek H., DuBois D.L., Dupuis M., Ferry J.G., Fujita E., Hille R., Kenis P.J.A., Kerfeld C.A., Morris R.H., Peden C.H.F., Portis A.R., Ragsdale S.W., Rauchfuss T.B., Reek J.N.H., Seefeldt L.C., Thauer R.K., and Waldrop G.L. (2013), Frontiers, opportunities, and challenges in biochemical and chemical catalysis of CO_2 fixation, *Chemical Reviews*, 113, 6621-6658.

Benson E.E., Kubiak C.P., Sathrum A.J., and Smieja J.M. (2009), Electrocatalytic and homogeneous approaches to conversion of CO_2 to liquid fuels, *Chemical Society Reviews*, 38, 89-99.

Bhugun I., Lexa D., and Saveant J.M. (1996), Catalysis of the electrochemical reduction of carbon dioxide by iron(0) porphyrins: Synergystic effect of weak Bronsted acids, *Journal of American Chemical Society*, 118, 1769-1776.

Cohen C.T. and Coates G.W. (2006), Alternating copolymerization of propylene oxide and carbon dioxide with highly efficient and selective (Salen)Co(III) catalysts: Effect of ligand and cocatalyst variation, *Journal of Polymer Science: Part A: Polymer Chemistry*, 44, 5182-5191.

Cole E.B. and Bocarsly A.B. (2010), Photochemical, electrochemical, and photoelectrochemical reduction of carbon dioxide, In: Aresta M. (ed) 'Carbon dioxide as chemical feedstock', Ch. 11, Wiley-VCH Verlag GmbH & Co., Weinheim, Germany, pp. 291-316.

Costamagna J., Ferraudi G., Canales J., and Vargas J. (1996), Carbon dioxide activation by aza-macrocyclic complexes, *Coordination Chemistry Reviews*, 148, 221-248.

Cozzi P.G. (2004), Metal-Salen Schiff base complexes in catalysis: practical aspects, *Chemical Society Reviews*, 33, 410-421.

Darensbourg D.J., Mackiewicz R.M., Phelps A.L., and Billodeaux D.R. (2004), Copolymerization of CO_2 and epoxides catalyzed by metal salen complexes, *Accounts of Chemical Research*, 37(11), 836-844.

Finn C., Schnittger S., Yellowlees L.J., and Love J.B. (2012), Molecular approaches to the electrochemical reduction of carbon dioxide, *Chemical Communications*, 48, 1392-1399.

Furuya N. and Matsui K. (1989), Electroreduction of carbon dioxide on gas-diffusion electrodes modified by metal phthalocyanines, *Journal of Electroanalytical Chemistry and Interfacial Electrochemistry*, 271(1-2), 181-191.

Gambarotta S., Arena F., Floriani C., and Zanazzi F. (1982), Carbon dioxide fixation: Bifunctional complexes containing acidic and basic sites working as reversible carriers, *Journal of American Chemical Society*, 104, 5082-5092.

Garcia M., Aguirre M.J., Canzi G., Kubiak C.P., Ohlbaum M., and Isaacs M. (2014), Electro and photoelectrochemical reduction of carbon dioxide on multimetallic porphyrins/polyoxotungstate modified electrodes, *Electrochimica Acta*, 115, 146-154.

Hammouche M., Lexa D., Momenteau M., and Saveant J.M. (1991), Chemical catalysis of electrochemical reactions. Homogeneous catalysis of the electrochemical reduction of carbon dioxide by iron(“0”) porphyrins. Role of the addition of magnesium cations, *Journal of American Chemical Society*, 113, 8455-8466.

Hori Y., Kikuchi K., Murata A., and Suzuki S. (1986), Production of methane and ethylene in electrochemical reduction of carbon dioxide at copper electrode in aqueous hydrogencarbonate solution, *Chemistry Letters*, 897-898.

Hori Y., Konishi H., Futamura T., Murata A., Koga O., Sakurai H., and Oguma K. (2005), Deactivation of copper electrode in electrochemical reduction of CO_2, *Electrochimica Acta*, 50, 5354-5369.

Hori Y., Murata A., and Takahashi R. (1989), Formation of hydrocarbons in the electrochemical reduction of carbon dioxide at a copper electrode in aqueous solution, *Journal of Chemical Society, Faraday Transactions 1*, 85, 2309-2326.

Hori Y., Wakebe H., Tsukamoto T., and Koga O. (1994), Electrocatalytic process of CO selectivity in electrochemical reduction of CO_2 at metal electrodes in aqueous media, *Electrochimica Acta*, 39, 1833-1839.

Inglis J.L., MacLean B.J., Pryce M.T., and Vos J.G. (2012), Electrocatalytic pathways towards sustainable fuel production from water and CO_2, *Coordination Chemistry Reviews*, 256, 2571-2600.

Ishida H., Tanaka K., and Tanaka T. (1987), Electrochemical CO_2 reduction catalyzed by $[Ru(bpy)_2(CO)_2]^{2+}$ and $[Ru(bpy)_2(CO)Cl)^{+}$. The effect of pH on the formation of CO and $HCOO^{-}$, *Organometallics*, 6, 181-186.

Laitar D.S., Muller P., and Sadighi J.P. (2005), Efficient homogeneous catalysis in the reduction of CO_2 to CO, *Journal of American Chemical Society*, 127, 17196-17197.

Li C.W. and Kanan M.W. (2012), CO_2 reduction at low overpotential on Cu electrodes resulting from the reduction of thick Cu_2O films, *Journal of the American Chemical Society*, 134, 7231-7234.

Magdesieva T.V., Zhukov I.V., Kravchuk D.N., Semenikhin O.A., Tomilova L.G., and Butin K.P. (2002), Electrocatalytic CO_2 reduction in methanol catalyzed by mono-, di-, and

electropolymerized phthalocyanin complexes, *Russian Chemical Bulletin, International Edition*, 51(5), 805-812.

Mahmood M.N., Masheder D., and Harty C.J. (1987), Use of gas-diffusion electrodes for high rate electrochemical reduction of carbon dioxide. II. Reduction at metal phthalocyanine-impregnated electrodes, *Journal of Applied Electrochemistry*, 17, 1223-1227.

Schouten K.J.P., Kwon Y., Ham C.J.M.V., Qin Z., and Koper M.T.M. (2011), A new mechanism for the selectivity to C_1 and C_2 species in the electrochemical reduction of carbon dioxide on copper electrodes, *Chemical Science*, 2, 1902-1909.

Singh S., Mukherjee C., and Verma A. (2015 b), Development of catalytic activity protocol for electrochemical reduction of carbon dioxide to value added products, *Clean Technologies and Environmental Policy*, 17(2), 533-540.

Singh S., Phukan B., Mukherjee C., and Verma A. (2015 a), Salen ligand complexes as electrocatalysts for direct electrochemical reduction of gaseous carbon dioxide to value added products, *RSC Advances*, 5, 3581-3589.

Skljarevski S., Peverly A.A., and Peters D.G. (2011), Cyclic voltammetric and spectrophotometric investigation of the catalytic reduction of 1,1,2-trichloro-1,2,2-trifluoroethane (CFC-113) by electrogenerated cobalt(I) salen in dimethylformamide saturated with carbon dioxide, *Journal of Electroanalytical Chemistry*, 661, 39-43.

Sullivan B.P., Krist K., and Guard H.E. (1993), Electrochemical and electrocatalytic reactions of carbon dioxide, Elsevier, Amsterdam, ISBN: 0-444-88316-9.

7

Bimetallic electrocatalyst for dERC

7.1 Background

7.2 Experimental

7.3 Results and discussions

7.4 Bimetallic electrocatalyst *vs.* metal

Chapter 7

Bimetallic electrocatalyst for dERC

To understand the effect of combination of two metals over the electrochemical reduction of gaseous carbon dioxide, the synthesis of bimetallic electrocatalyst was carried out. Bimetallic electrocatalyst offers opportunity to tune the physical properties of the involved metals and thus affects the efficiency and selectivity for the reaction products. This chapter discusses the evaluation of bimetallic electrocatalyst for the dERC. The bimetallic electrocatalyst was synthesized and characterized by various methods to ascertain its composition, and purity followed by activity towards dERC. After confirming the activity of synthesized bimetallic electrocatalyst, the reactions were carried out in full cell and the obtained products were analyzed. Performance shows that bimetallic electrocatalyst has marked influence over the selectivity, and energy efficiency of the reaction products. The improvement over the pure metal could also be achieved.

7.1 Background

Bimetallic electrocatalysts may be the potential candidates for dERC as the addition of second metal may impart potentially unique catalytic properties to the system. Though only a couple of recent studies on bimetallic electrocatalysts for ERC are available (Christophe *et al.* 2012; Kim *et al.* 2014; Rasul *et al.* 2015), there are many studies available on bimetallic catalysts for CO or CO_2 hydrogenation (Ishihara *et al.* 1987; Cao *et al.* 1988; Duvenhage and Coville 1997; Mirzaei *et al.* 2010; Satthawong *et al.* 2013), where it was shown that bimetallic catalyst formation resulted in the improved activity and selectivity along with the formation of C_2 hydrocarbons. The improved results were reportedly due to the change in chemisorption properties of the involved metals. Recently, a few studies suggested that adjustment of binding energies of the intermediate with the electrocatalyst may promote the formation of a particular product (Christophe *et al.* 2012; Kim *et al.* 2014). It has been found that *d*-orbital of the transition metals plays a crucial role in determining the binding strength by interacting with the adsorbate (Nørskov *et al.* 2009). The basic reason for the change in binding strength is the charge (electron) transfer in these bimetallic systems (Rodriguez 1996). These preliminary studies have opened up an avenue to investigate the effect of bimetallic electrocatalysts for the electrochemical reduction of CO_2 to synthesize fuel kind of products. It has been seen that most of the studies in the past were based on Cu as one of the metals in bimetallic system (Christophe *et al.* 2012; Kim *et al.* 2014; Rasul *et al.* 2015). In the present study, Co and Ag are chosen to investigate the effect of their combination for the electrochemical reduction of CO_2. The rationale to choose Co is that it is a transition metal having incompletely filled *d*-orbital. On the other hand, Ag possesses only incompletely filled *s*-orbital in its outermost shell. Therefore, these two metals have been chosen with the hypothesis that the combination of Ag and Co might trigger a change in the binding energy of the bimetal with CO_2 due to the electron transfer, as suggested by Rodriguez and Goodman (1992, 1996) and Kuhn *et al.* (1993). This change in binding energy may lead to modified physical and chemical properties of the bimetal–CO_2 system and in-turn influence the CO_2 reduction

reaction. Therefore, Co-Ag electrocatalyst was synthesized and thoroughly characterized to understand the role of bimetals for the gaseous CO_2 electroreduction instead of solubilized CO_2 in a liquid electrolyte. Bimetallic electrocatalyst is evaluated in half-cell as well as in the full electrochemical reactor (full cell).

7.2 Experimental

7.2.1 Materials

Nitrate compounds of Co and Ag were used as the metal precursors. $Co(NO_3)_2$ was purchased from Qualigens and $AgNO_3$ was procured from Merck. Sodium borohydride, which was used as the reducing agent, was purchased from LobaChemie. Potassium bicarbonate ($KHCO_3$) and *N*,*N*-dimethylformamide (DMF) were also procured from Loba Chemie. Pt/C (40 wt% Pt) was purchased from ElectroChem, Inc. USA. All the chemicals were used without further purification and de-ionized water was used in all the experiments unless stated otherwise. Gas diffusion layer from CeTech was used as backing layer for electrode preparation. Nafion membrane (Nafion-117) and Nafion dispersion (5 wt%) were procured from DuPont, USA.

7.2.2 Methods

7.2.2.1 Synthesis of bimetallic electrocatalyst

The bimetallic Co-Ag electrocatalyst was prepared by simultaneous reduction of nitrate precursors of Co and Ag metals *viz.* $Co(NO_3)_2$ and $AgNO_3$, respectively. Sodium borohydride ($NaBH_4$) was used as the reducing agent for metal precursors. The equimolar solution of both the metal salts was prepared and reduced by using $NaBH_4$ with dropwise addition of the former. The reaction was carried out in ice bath to avoid secondary reactions of $NaBH_4$. The reaction mixture was agitated continuously during the reaction. The resulting precipitate was filtered, washed, and dried at 60°C to get the equimolar mixture of Co-Ag electrocatalyst (Lima *et al.* 2006).

7.2.2.2 Physical methods

The synthesized electrocatalyst was characterized using X-ray diffractometer (XRD), BET surface area studies, field emission scanning electron microscopy (FESEM), transmission electron microscopy (TEM), energy dispersive X-ray spectroscopy (EDX), and electrochemical tests as discussed in chapter 3.

7.2.2.3 Preparation of electrodes and membrane electrode assembly

Catalyst ink for cathode (or working electrode) was prepared by dispersing the bimetallic electrocatalyst in appropriate solvent along with Nafion dispersion. The electrocatalyst ink was then coated over the gas diffusion layer followed by drying. Pt/C (40 wt% Pt), and Nafion dispersion (5 wt%) as binder, were used to prepare the anode electrocatalyst ink. This ink was coated over the gas diffusion layer using spraying technique which was then dried to get the anode. The electrocatalyst loading for anode and cathode was kept as 0.5 $mg \cdot cm^{-2}$ and 2 $mg \cdot cm^{-2}$, respectively. The cation exchange membrane (Nafion-117) was treated as per the standard procedure discussed in section 3.3.2.1.1. The membrane electrode assembly was prepared by sandwiching the Nafion membrane in between anode and cathode at 110°C and 50 $kg \cdot cm^{-2}$ pressure.

7.2.2.4 Electrochemical tests

The half-cell studies were conducted in three-electrode cell assembly using Ag/AgCl as reference electrode and Pt wire as counter electrode. The working electrode (0.5 cm^2) was prepared using 2 $mg \cdot cm^{-2}$ electrocatalyst loading supported over gas diffusion layer. The cyclic voltammetry test was carried out in aqueous (0.5 M $KHCO_3$) and non-aqueous (DMF) electrolyte at the scan rate of 10 $mV \cdot s^{-1}$. In all the half-cell studies, the potential is reported with respect to standard hydrogen electrode (SHE), unless stated otherwise. For full cell studies, the electrochemical reactor and experimental set-up was used as discussed in section 3.3.2.1 and 3.3.2.2, respectively. The experiment was conducted using chronoamperometry technique (pulse width 5 s) at 6 different electrode

potentials and the reaction products were collected at the cathode outlet and analyzed using gas chromatograph. The reaction was carried out for an hour and the Faradaic efficiency is reported in terms of total charge passed in an hour at particular voltage. The electrochemical experiments were carried out at 30°C and at atmospheric pressure.

7.3 Results and discussions

7.3.1 Characterization of Co-Ag bimetallic electrocatalyst

7.3.1.1 Physical characterizations

The bimetallic electrocatalyst was characterized by using XRD, BET surface area analysis, FESEM, TEM, and EDX analyses as discussed in section 3.2.

7.3.1.1.1 XRD analysis

The X-ray diffractogram of the synthesized Co-Ag bimetallic electrocatalyst is shown in figure 7.1. It shows distinct peaks of Co and Ag metals. The XRD pattern indicates the face centered cubic (FCC) structure of silver and hexagonal closed packed (HCP) structure of cobalt. The main peaks appeared at 38.13°, 44.32°, 44.53°, 48.75°, 64.39°, 77.46°, and 81.60° corresponding to Ag (111), Ag (200), Co (002), Co (101), Ag (220), Ag (311), and Ag (222) planes, respectively (Figure 7.1). Moreover, it can be seen that the synthesized electrocatalyst is pure and hardly show any peak related to impurity. The presence of characteristic peaks of both the metals in the XRD pattern indicates that the synthesized electrocatalyst is a kind of mixture or heterostructure, where Co and Ag atoms are mixed randomly.

7.3.1.1.2 BET surface area analysis

The BET surface area analysis of the synthesized Co-Ag electrocatalyst was carried out as per the procedure described in section 3.2.3. The specific surface area based on N_2 adsorption and desorption

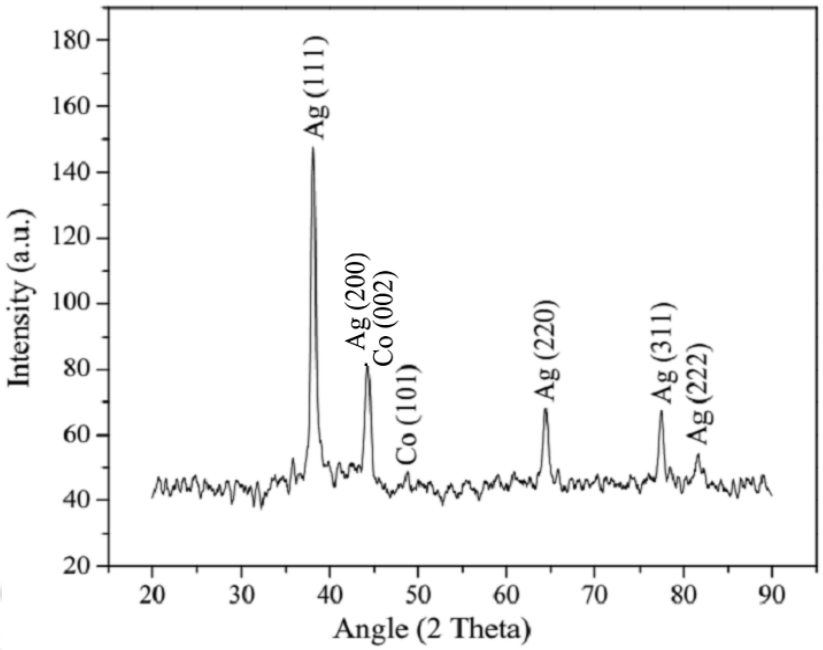

Figure 7.1 XRD pattern of Co-Ag bimetallic electrocatalyst

method was found to be 67.45 $m^2 \cdot g^{-1}$. The BET surface area of the bimetallic electrocatalyst was found to be much higher than the surface area of either Co (15.89 $m^2 \cdot g^{-1}$) (Hongzhen *et al.* 2008) or Ag (23.81 $m^2 \cdot g^{-1}$) (Zhou *et al.* 2009). This indicates that synthesized particles are quite small and will be good for electrocatalysis application.

7.3.1.1.3 Morphological analyses

The morphological features were identified using field emission scanning electron microscopy (FESEM) and transmission electron microscopy (TEM) as discussed in section 3.2.5 and 3.2.6, respectively. The images are shown in figure 7.2 and 7.3. The FESEM image (Figure 7.2) reveals that the synthesized particles are spherical and size ranges from 32-65 nm. Some of the particles are also seen in agglomerated form. TEM image in figure 7.3 gives clear morphology showing spherical particles of varying sizes and agglomerates.

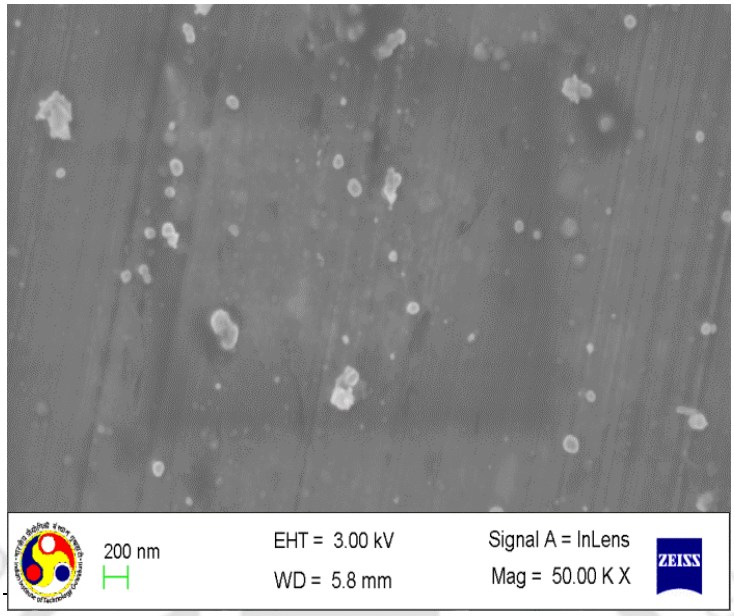

Figure 7.2 FESEM analysis of Co-Ag bimetallic electrocatalyst

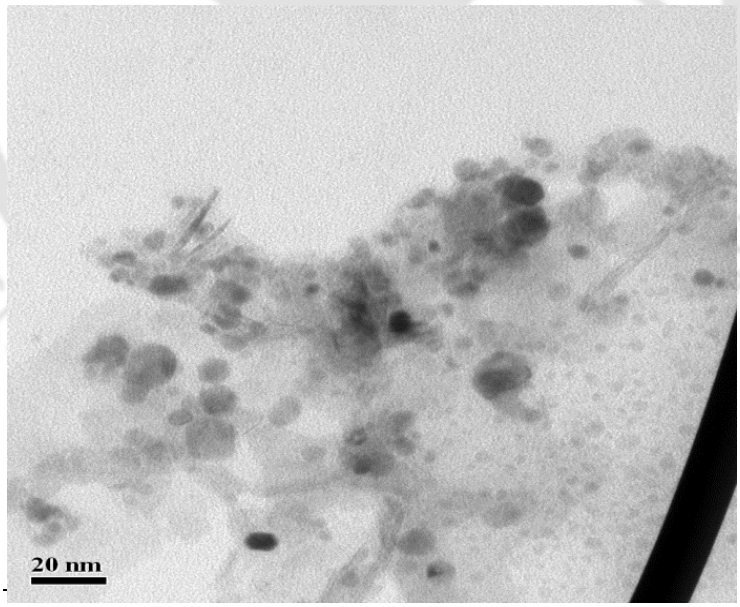

Figure 7.3 TEM analysis of Co-Ag bimetallic electrocatalyst

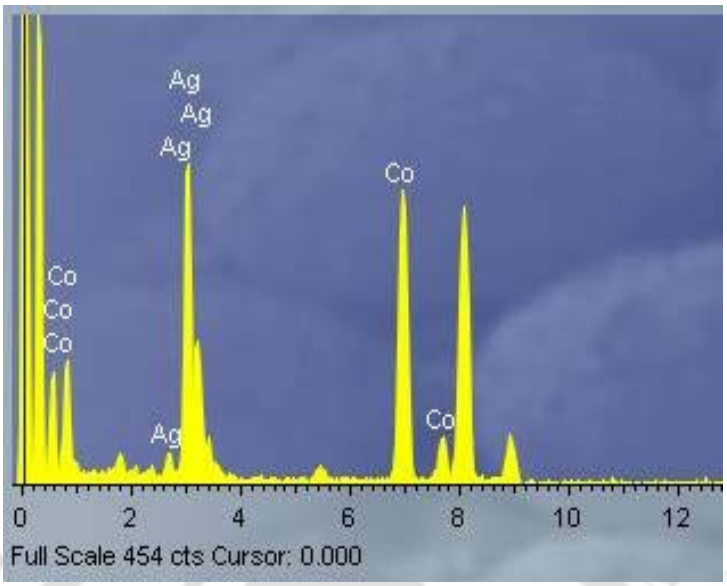

Figure 7.4 EDX spectrum of Co-Ag bimetallic electrocatalyst

7.3.1.1.4 EDX analysis

In XRD spectrum, there were only two weak peaks at 44.53° and 48.75° for Co. However, an inherent peak of Co(100) was not clearly seen as it was superimposed by Ag. Hence EDX was carried out to confirm the presence of Co in the sample. Figure 7.4 shows the EDX spectrum for Co-Ag bimetallic electrocatalyst, which shows the marked presence of Co and Ag atoms in the sample. Moreover, absence of any peak of impurity suggests that the synthesized electrocatalyst is pure. Thus, all these characterizations reveal that the bimetallic (Co-Ag) electrocatalyst was synthesized successfully.

7.3.1.2 Electrochemical characterization

7.3.1.2.1 Cyclic voltammetry

Before performing the protocol test for Co-Ag bimetallic electrocatalyst, the cyclic voltammetry (CV) studies were carried out to gather the basic information about Co-Ag bimetallic electrocatalyst. As mentioned before, the CV test was conducted in 0.5 M $KHCO_3$ solution saturated with N_2 or CO_2 gas,

to compare the voltammograms in inert and CO_2 environments, respectively, as shown in Figure 7.5. It can be seen that significantly high current densities are observed in both the environments. However, the current density obtained in CO_2 saturated system is lower than the corresponding current density in N_2 saturated system for Co-Ag electrocatalyst. It can be seen that the onset potential (the potential at which 0.1 $mA{\cdot}cm^{-2}$ current density is observed) for Co-Ag is 0.35 V. This reflects that activation overvoltage required in case of Co-Ag bimetallic electrocatalyst is significantly less as compared to Co where it was found to be 0.95 V (section 4.3.1.2.1). Interestingly, figure 7.5 shows that the current density is lower in CO_2 saturated atmosphere as compared to inert atmosphere for Co-Ag electrocatalyst. Thus, the determination of the activity of Co-Ag will be done on the basis of protocol test, as discussed in section 7.3.1.2.2.

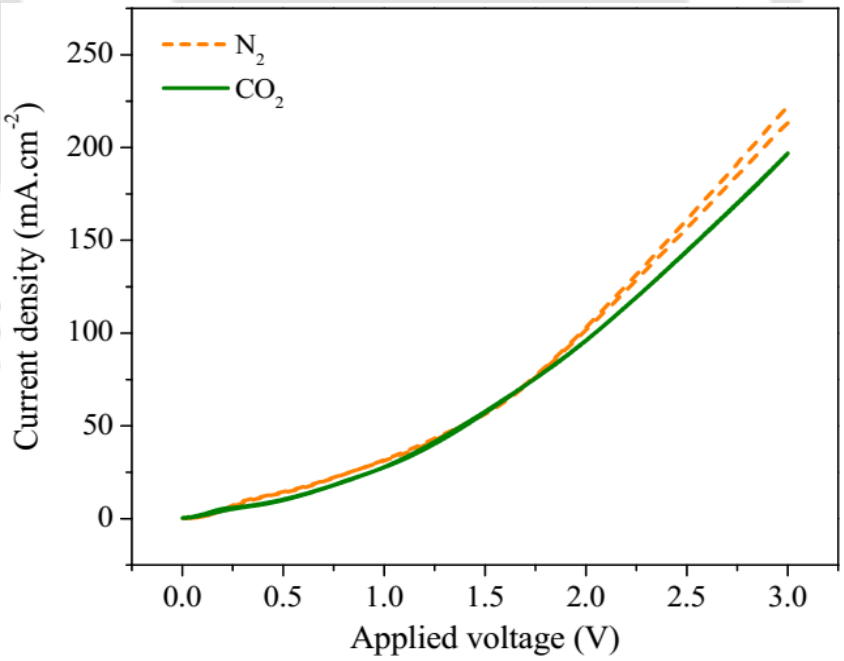

Figure 7.5 Cyclic voltammograms of Co-Ag bimetallic electrocatalyst in N_2 (broken line), and CO_2 (solid line) atmosphere

7.3.1.2.2 The developed protocol

As discussed in earlier chapters and section 4.3.1.2.2, the protocol test was performed by plotting the linear sweep voltammograms (LSVs) using gas diffusion layer (GDL) without any electrocatalyst coating and then compared with the Co-Ag electrocatalyst coated GDL in three different media (Singh *et al.* 2015 a). The plots are shown in figure 7.6 to 7.8. It can be seen in the figures that the bimetallic electrocatalyst shows higher current density than the bare GDL in every test. This signifies that the electrocatalyst is active in every media. However, the increased current density in the 3rd test of the protocol (Figure 7.8) clearly proves that Co-Ag is able to reduce the CO_2, although there is the tendency towards competitive H^+ reduction too (Figure 7.7). It is to be noted that in 3rd test, higher applied voltage beyond 1.5 V results in depletion of CO_2 at the electrode surface, and hence plateau of current density is formed with further increase in the applied voltage.

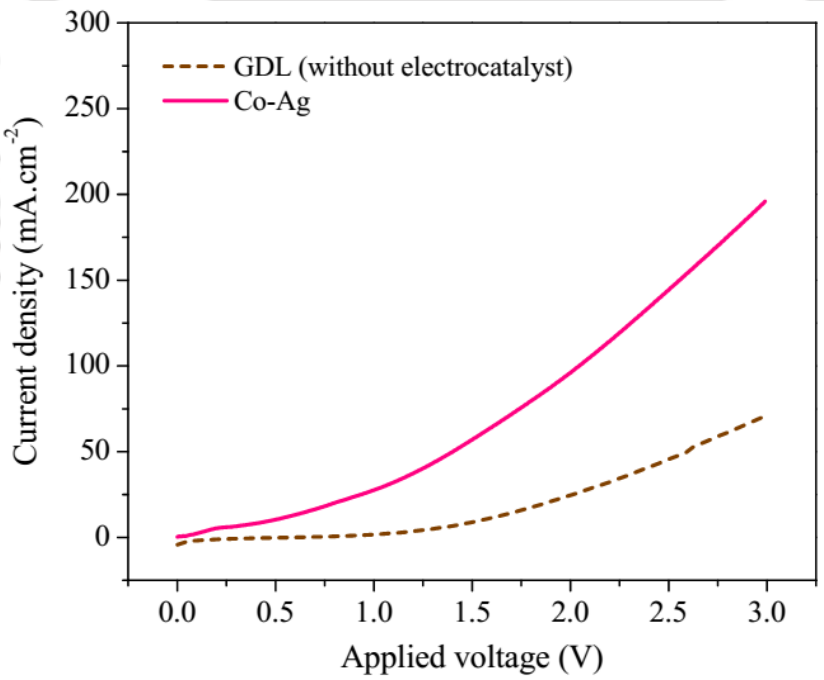

Figure 7.6 Comparison of electrocatalytic activity of Co-Ag bimetal on GDL (solid line), and only GDL (broken line) for the 1st test as per the catalytic activity protocol

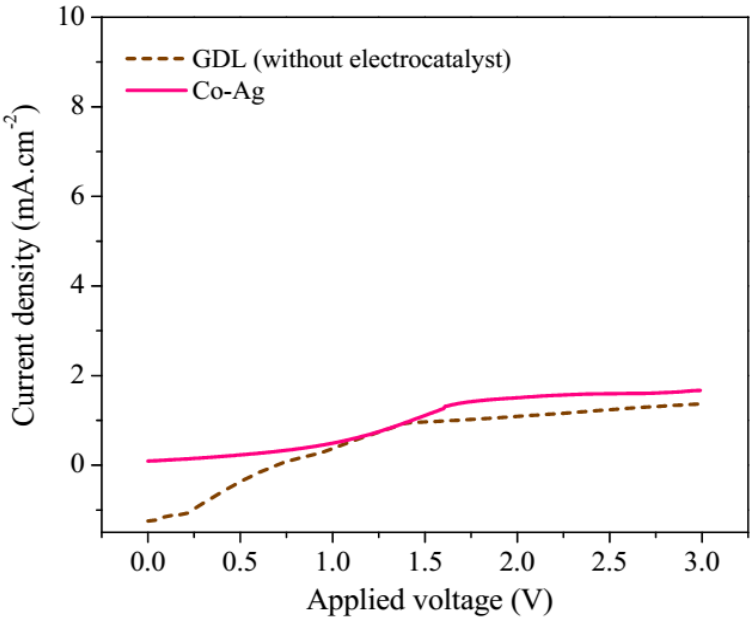

Figure 7.7 Comparison of electrocatalytic activity of Co-Ag bimetal on GDL (solid line), and only GDL (broken line) for the 2nd test as per the catalytic activity protocol

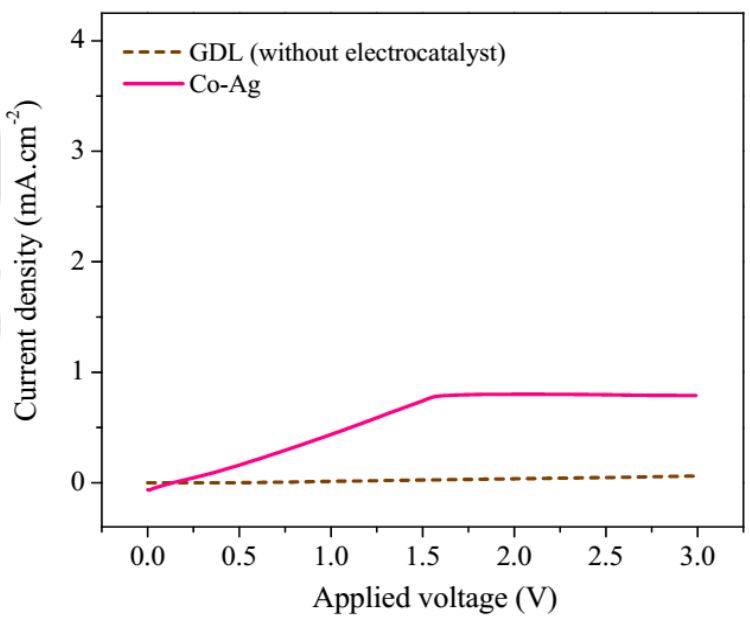

Figure 7.8 Comparison of electrocatalytic activity of Co-Ag bimetal on GDL (solid line), and only GDL (broken line) for the 3rd test as per the catalytic activity protocol

7.3.2 dERC studies for Co-Ag bimetallic electrocatalyst

The dERC study in full electrochemical reactor was conducted to identify the products formed from electrochemical reduction of gaseous CO_2 using Co-Ag electrocatalyst. Figure 7.9 represents the current density in electrochemical reactor using Co-Ag electrocatalyst at different applied voltages in the range of 1.5 V to 3 V. It can be seen in figure 7.9 that on increasing the applied voltage, the current density increases gradually because of the increased rate of the reactions occurring at the cathode of the reactor.

Figure 7.10 shows the amount of the products formed in full cell reactions using Co-Ag bimetallic electrocatalyst. The products formed at various voltages are hydrocarbons and CO. Hydrocarbons include CH_4 and meager quantity of C_2H_4. Along with these products, hydrogen formation also took place which is a by-product of the process. It can be seen in figure 7.10 that the highest amount was formed in case of CO with 16.6 µmol at 2 V. CH_4 was formed with 10.4 µmol while C_2H_4 was formed only in trace amounts (0.29 µmol) at 2 V. Hydrogen formation was found to be increasing with increasing applied potential values and reaches maxima at 3 V with 2020 µmol.

Faradaic efficiency of the products formed as a result of the dERC using Co-Ag bimetallic electrocatalyst was calculated and shown in the figure 7.11. CH_4 was found as the major product with Faradaic efficiency of 19.5% at 2 V. CO formed with highest Faradaic efficiency of 7.8% at 2 V. C_2H_4 formation was quite meager with only 0.8% Faradaic efficiency at 2 V. Overall, around 28% Faradaic efficiency (at 2 V) was found for the CO_2 electroreduction using Co-Ag electrocatalyst. The Faradaic efficiency of hydrogen formation, a by-product, was high at every applied voltage and found to be increased with increasing applied voltage. Another important thing to note here is that the trend of Faradaic efficiency is different from that observed for the amount of products. It can be seen that the highest amount of the product formed is of CO (Figure 7.10), however the Faradaic efficiency is highest for CH_4 (Figure 7.11). This is due to the fact that Faradaic efficiency takes into account the

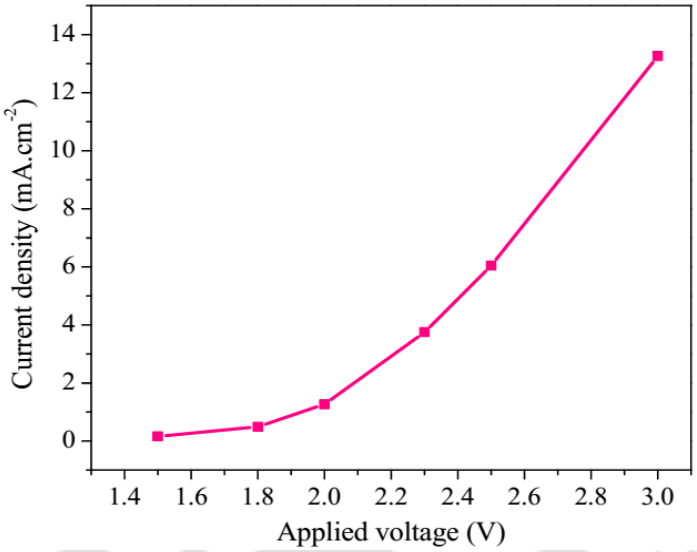

Figure 7.9 Current density as a function of applied voltage for Co-Ag bimetallic electrocatalyst

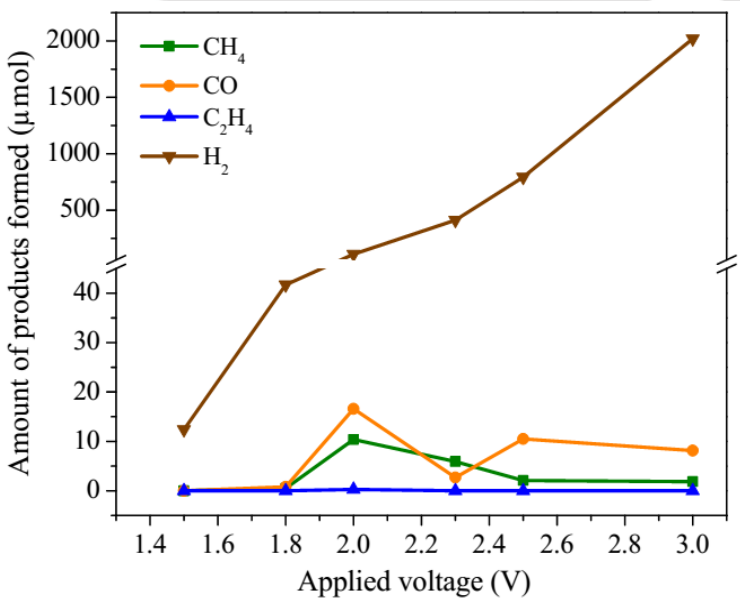

Figure 7.10 Amount of the products formed as a function of applied voltage for electrochemical reduction of CO_2 using Co-Ag bimetallic electrocatalyst

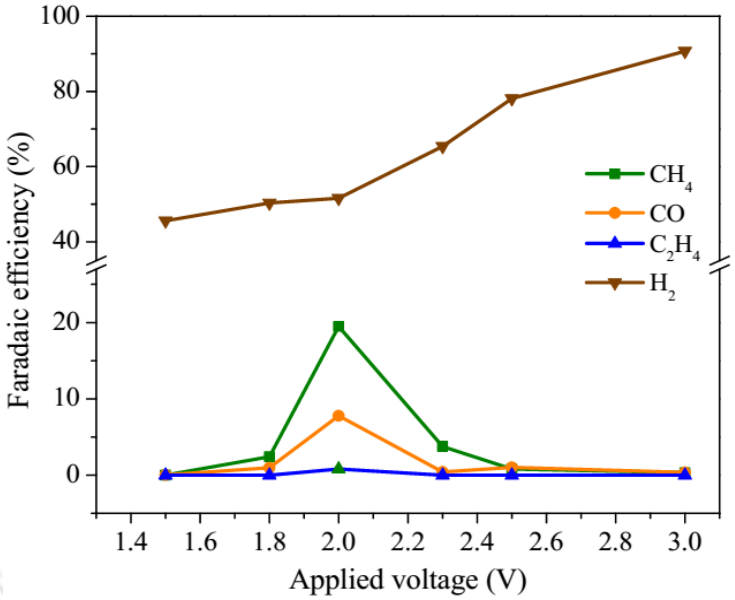

Figure 7.11 Faradaic efficiency as a function of applied voltage for electrochemical reduction of CO_2 using Co-Ag bimetallic electrocatalyst

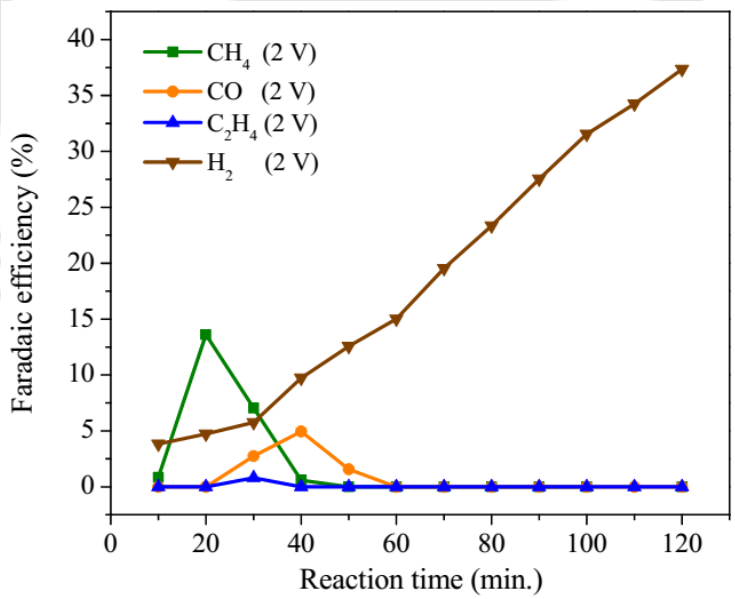

Figure 7.12 Faradaic efficiency variation with time during electrochemical reduction of CO_2 using Co-Ag bimetallic electrocatalyst

number of moles of electrons supplied. Therefore, if the same amount of CO and CH_4 is formed, then the Faradaic efficiency towards CH_4 would be 4 times higher, since there are 8 electrons involved in the formation of one mole of CH_4 while only 2 in the formation of one mole of CO. Based on these results, it can be said that Co-Ag is able to electrocatalyze the CO_2 for the formation of fuel kind of products. Moreover, it was also observed that Co-Ag results in the product formation only upto 60 minutes of the reaction, and beyond this period only H_2 evolution took place. The variation of Faradaic efficiency with time is shown in figure 7.12. The variation of Faradaic efficiency with time is shown at the applied voltage where the highest Faradaic efficiency was observed for a particular product.

Table 7.1 shows the kinetic data in terms of reaction rate as discussed in section 3.5.2. This data further supports that electrocatalyst is able to effectively reduce CO_2 into hydrocarbons and CO. It is found that 2 V is the favourable potential value for Co-Ag electrocatalyst, where the highest conversion takes place under the experimental conditions. On further increase in applied voltage, the rate of formation of the products decreases as at higher voltage the formation of H_2 is favoured more (Figure 7.10 and 7.11).

It is known that Ag alone is exclusively selective for CO formation (Hori *et al.* 1985, 1994; Hara *et al.* 1995; Kaneco *et al.* 1998) and Co alone predominantly results in the formation of unwanted H_2 with little formation of CO and HCOOH in CO_2 electroreduction reactions (Hara *et al.* 1995). In case

Table 7.1 Rate of the reaction of bimetallic electrocatalyst for dERC

Applied voltage (V)	**Amount of the products (μmol)**			**Rate of the reaction (10^{-3} g·(g·h^{-1})$^{-1}$)**		
	CH_4	**CO**	**C_2H_4**	**CH_4**	**CO**	**C_2H_4**
2.0	10.4	16.6	0.288	9.244	25.822	0.449

of Co, the CO_2 gets converted to adsorbed CO (CO_{ad}) over the surface and this presorbed CO_{ad} causes enhancement of H_2 adsorption (Sastri and Viswanathan 1955) which ultimately reduces the CO_2 protonation. Therefore, the CO_2 electrocatalytic reduction efficiency of Co is poor. However, the reduction of CO_2 catalyzed by Co-Ag shows a striking feature, *viz.* the formation of hydrocarbons. It suggests that during synthesis, the Co and Ag metal centers are put in contact and form a dinuclear compound in which the atoms can be united by a multiple metal-metal bond (Rodriguez and Goodman 1992). Typically, Ag^+ with low reduction potential reduces first and serves as seed for the growth of the Co-Ag electrocatalyst. Because of the large surface mismatch of Ag and the Co (3*d* transition metal) irregular shale morphology of the clusters may be formed (Guo *et al.* 2012). This atomic level internal re-arrangement in Co-Ag clusters somehow affects the binding strength of the intermediate products, rendering the formation of hydrocarbons. It is believed that during CO_2 electroreduction, the formation of hydrocarbons takes place through the adsorbed CO (CO_{ad}) (Schouten *et al.* 2011; Nie *et al.* 2014; Singh *et al.* 2015 b). Therefore, it can be speculated that Ag has very low binding strength with CO_{ad}, hence, CO desorbs quickly after its formation over the Ag surface, resulting the exclusive formation of CO, whereas Co has strong binding strength with CO_{ad}. However, on mixing Co and Ag, the transfer of electron cloud takes place from Co to Ag, according to the model suggested by Kuhn *et al.* (1993) resulting in the formation of metal-metal bond. It is well established that formation of metal-metal bond in bimetallic systems induces large changes in the electron density of the metals (Rodriguez and Goodman 1992). It is shown earlier in XRD pattern that Co-Ag electrocatalyst is a heterostructure of the two metals and in such structures electronic interactions occur very well. These changes in electronic structure affect the binding strength of the bimetallic electrocatalyst with intermediate species, as well as the chemical properties of the metals. Thus, the altered binding energy improves the binding strength of the Co-Ag with CO_{ad} and promotes the formation of hydrocarbons.

Figure 7.13 shows the selectivity of different products at various applied voltages. Since the dERC process is carried out for the generation of fuel, the selectivity is one of the important parameters of concern. The selectivity is defined as the amount of desired product to the amount of total CO_2 reduction products obtained (based on the carbon content) (Ogura *et al.* 2004; Aeshala *et al.* 2014). The selectivity of Co-Ag for CH_4 formation was highest at 2.3 V, and the maximum rate of the reaction and Faradaic efficiency was at 2 V (Table 7.1; Fig. 7.11). It is proven that the chemisorption properties were tailored over bimetallic surface for facilitating carbon-carbon bond formation, resulting into higher hydrocarbons (Satthawong *et al.* 2013). It may be the reason for the formation of C_2H_4 in the present study, though in low quantity.

Based on the understanding, a scheme has been proposed (Scheme 7.1) for the reaction mechanism as well as binding strength of the electrocatalysts for dERC. It can be seen that the electron transfer between the two metals synchronizes in such a way that Co-Ag achieves favorable binding strength with CO_{ad}, resulting in fuel kind of products. Such changes bring significant effect in the reactivity and selectivity of the dERC process.

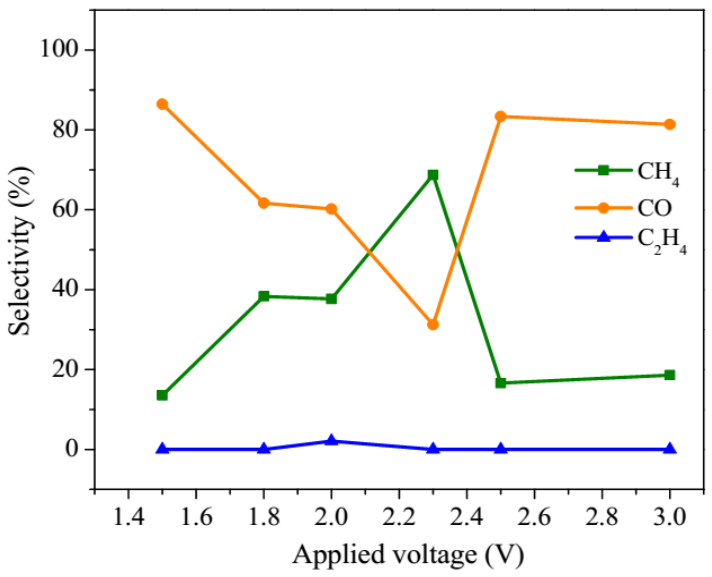

Figure 7.13 Selectivity of products using Co-Ag bimetallic electrocatalyst for dERC

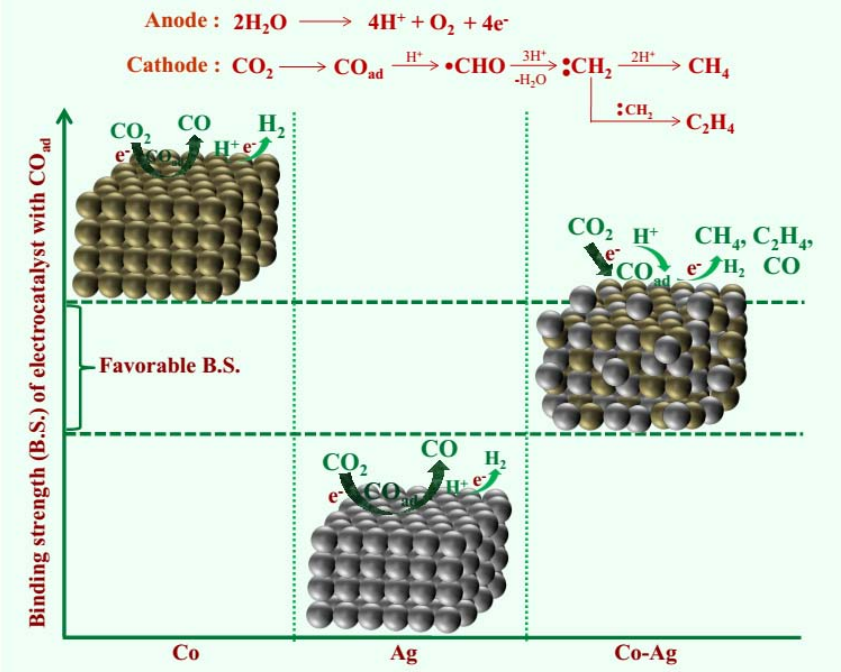

Scheme 7.1 Representative binding strength of CO_{ad} with Co-Ag electrocatalyst (Brown and grey spheres represent Co and Ag, respectively)

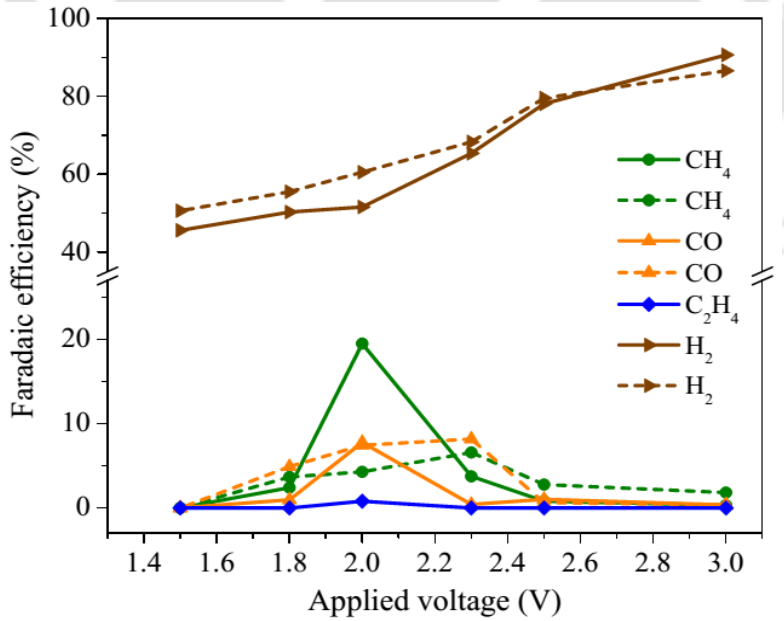

Figure 7.14 Comparison of Faradaic efficiency of Co-Ag bimetallic electrocatalyst (solid line) with Co (broken line)

7.4 Bimetal *vs.* metal

To ascertain the superiority of Co-Ag bimetallic electrocatalyst over Co metal, the comparison of Faradaic efficiency of both the electrocatalysts was done, and shown in figure 7.14. It can be seen that Co-Ag is better in performance than Co. Here, two important parameters need to be focussed. First, the formation of hydrocarbons has increased approximately 3 times in case of Co-Ag than in Co, which is appreciable in view of the formation of fuel kind of products. Second, the optimum voltage required for the formation of highest amount of product was 2 V for Co-Ag, in spite of 2.3 V in case of Co. This makes Co-Ag more energy efficient than Co. It is due to the high surface area of the as-prepared Co-Ag electrocatalyst which provided more CO_2 adsorption sites, as well as due to the synergistic effect of the involved metals (Co and Ag). Owing to electron transfer between the Co and Ag, binding strength variation resulted in the improved efficiency and selectivity in case of bimetallic electrocatalyst. Thus, bimetallic electrocatalyst was found to be better than Co.

The next chapter provides the conclusion of the research work carried out and reported in the thesis.

References

Aeshala L.M., Uppaluri R.G., and Verma A. (2014), Electrochemical conversion of CO_2 to fuels: Tuning of reaction zone using suitable functional group in solid polymer electrolyte, *Physical Chemistry Chemical Physics*, 16, 17588-17594.

Cao R., Pan W.X., and Griffin G.L. (1988), Direct synthesis of higher alcohols using bimetallic copper/cobalt catalysts, *Langmuir*, 4(5), 1108-1112.

Christophe J., Doneux Th., and Buess-Herman C. (2012), Electroreduction of carbon dioxide on copper based electrodes: Activity of copper single crystals and copper-gold alloys, *Electrocatalysis*, 3, 139-146.

Duvenhage D.J. and Coville N.J. (1997), Fe:Co/TiO_2 bimetallic catalysts for the Fischer-Tropsch reaction I. Characterization and reactor studies, *Applied Catalysis A: General*, 153, 43-67.

Guo H., Chen Y., Chen X., Wang L., Ping H., and Peng D.L. (2012), Preparation of bimetallic core-shell nanoparticles with magnetically recyclable and high catalytic abilities, *Procedia Engineering*, 36, 504-509.

Hara K., Kudo A., and Sakata T. (1995), Electrochemical reduction of carbon dioxide under high pressure on various electrodes in an aqueous electrolyte, *Journal of Electroanalytical Chemistry*, 391, 141-147.

Hongzhen D., Xiangyang L., Guanpeng L., Lei X., and Fengsheng L. (2008), Synthesis of Co nanoparticles and their catalytic effect on the decomposition of ammonium perchlorate, *Chinese Journal of Chemical Engineering*, 16, 325-328.

Hori Y., Kikuchi K., and Suzuki S. (1985), Production of CO and CH_4 in electrochemical reduction of CO_2 at metal electrodes in aqueous hydrogencarbonate solution, *Chemistry Letters*, 1695-1698.

Hori Y., Wakebe H., Tsukamoto T., and Koga O. (1994), Electrocatalytic process of CO selectivity in electrochemical reduction of CO_2 at metal electrodes in aqueous media, *Electrochimica Acta*, 39(11/12), 1833-1839.

Ishihara T., Eguchi K., and Arai H. (1987), Hydrogenation of carbon monoxide over SiO_2 supported Fe-Co, Co-Ni, and Ni-Fe bimetallic catalysts, *Applied Catalysis*, 30, 225-238.

Kaneco S., Iiba K., Ohta K., Mizuno T., and Saji A. (1998), Electrochemical reduction of CO_2 at an Ag electrode in KOH-methanol at low temperature, *Electrochimica Acta*, 44, 573-578.

Kim D., Resasco J., Yu Y., Asiri A.M., and Yang P. (2014), Synergistic geometric and electronic effects for electrochemical reduction of carbon dioxide using gold-copper bimetallic nanoparticles, *Nature Communications*, 5, 4948-4955.

Kuhn W.K., Campbell R.A., and Goodman D.W. (1993), Adsorption on Bimetallic surfaces, In King D.A. (ed.) 'The chemical physics of solid surfaces', Ch. 5, Elsevier, Amsterdam, pp. 157-183.

Lima F.H.B., de Castro J.F.R., and Ticianelli E.A. (2006), Silver-cobalt bimetallic particles for oxygen reduction in alkaline media, *Journal of Power Sources*, 161, 806-812.

Mirzaei A.A., Beig babaei A., Galavy M., and Youssefi A. (2010), A silica supported Fe-Co bimetallic catalyst prepared by the sol/gel technique: Operating conditions, catalytic properties and characterization, *Fuel Processing Technology*, 91, 335-347.

Nie X., Luo W., Janik M.J., and Asthagiri A. (2014) Reaction mechanisms of CO_2 electrochemical reduction on Cu(111) determined with density functional theory, *Journal of Catalysis*, 312, 108-122.

Nørskov J.K., Bligaard T., Rossmeisl J., and Christensen C.H. (2009), Towards the computational design of solid catalysts, *Nature Chemistry*, 1, 37-46.

Ogura K., Yano H., and Tanaka T. (2004), Selective formation of ethylene from CO_2 by catalytic electrolysis at a three phase interface, *Catalysis Today*, 98, 515-521.

Rasul S., Anjum D.H., Jedidi A., Minenkov Y., Cavallo L., and Takanabe K. (2015), A highly selective copper-indium bimetallic electrocatalyst for the electrochemical reduction of aqueous CO_2 to CO, *Angewandte Chemie*, 54, 2146-2150.

Rodriguez J.A. and Goodman D.W. (1992), The nature of the metal-metal bond in bimetallic surfaces, *Science*, 257(5072), 897-903.

Rodriguez J.A. (1996), Physical and chemical properties of bimetallic surfaces, *Surface Science Reports*, 24, 223-287.

Sastri M.V.C. and Viswanathan T.S. (1955), Adsorption of carbon monoxide and hydrogen on cobalt: Presorption experiments, *Journal of the American Chemical Society*, 77, 3967-3971.

Satthawong R., Koizumi N., Song C., and Prasassarakich P. (2013), Bimetallic Fe-Co catalysts for CO_2 hydrogenation to higher hydrocarbons, *Journal of CO_2 Utilization*, 3-4, 102-106.

Schouten K.J.P., Kwon Y., Ham C.J.M., Qin Z., and Koper M.T.M. (2011), A new mechanism for the selectivity to C_1 and C_2 species in the electrochemical reduction of carbon dioxide on copper electrodes, *Chemical Science*, 2, 1902-1909.

Singh S., Mukherjee C., and Verma A. (2015 a), Development of catalytic activity protocol for electrochemical reduction of carbon dioxide to value added products, *Clean Technologies and Environmental Policy*, 17(2), 533-540.

Singh S., Phukan B., Mukherjee C., and Verma A. (2015 b), Salen ligand complexes as electrocatalysts for direct electrochemical reduction of gaseous carbon dioxide to value added products, *RSC Advances*, 5, 3581-3589.

Zhou M., Wei Z., Qiao H., Zhu L., Yang H., and Xia T. (2009), Particle size and pore structure characterization of silver nanoparticles prepared by confined arc plasma, *Journal of Nanomaterials*, Article Id 968058, doi: 10.1155/2009/968058.

8

Conclusions and future scope

8.1 Conclusions

8.2 Future scope

Chapter 8

Conclusions and future scope

The overall results for the investigations which have been discussed in previous chapters are given in this chapter. Along with this, the chapter also tries to formulate some new ideas based on the current research work and the same has been given under the future scope.

8.1 Conclusions

In the present work, the electrocatalysts have been synthesized for direct electrochemical reduction of gaseous CO_2 (dERC) to fuel kind of products. All the electrocatalysts developed were tested in half-cell and full cell electrochemical reactor. The major outcomes of the entire study are further discussed below in detail.

To judge the applicability of any electrocatalyst for electrochemical reduction of CO_2 becomes challanging as the process itself is too cumbersome and time consuming. Hence, a catalytic activity protocol was developed which could help to access the appropriateness of the synthesized electrocatalyst in the initial stage. The protocol was based on the fact that the increased current density in presence of electrocatalyst reflects that electrocatalyst was able to catalyze the reaction. As per the protocol, the electrocatalyst required to undergo 3 different tests in 3 different media *viz.* CO_2 saturated aqueous $KHCO_3$, KOH solution, and CO_2 bubbled DMF. If the current density is found to be increasing in both 1^{st} and 2^{nd} test, then it infered that the electrocatalyst was catalyzing both the CO_2 (desired) as well as H^+ reduction (undesired). Hence, 3^{rd} test helped to decide the applicability of the electrocatalyst specifically for CO_2 reduction, since, being a non-aqueous solvent; it does not contain any H^+ ions. Thus, it becomes evident at the end of the 3^{rd} test whether a particular electrocatalyst can be used for the full cell dERC reactions or not. This protocol has been applied for all the electrocatalysts synthesized in the present work, and found to be quite useful and simple method to screen qualitatively the useful electrocatalysts among many, without undergoing the full cell reaction.

Further, to study the effect of pure metals over the dERC, copper, zinc, nickel, and cobalt metal electrocatalysts have been developed through electroplating process and used as cathode (or working electrode). The electrocatalysts have been characterized using XRD, SEM, and EDX techniques to ascertain their quality. The characterization results confirmed that the developed metal

electrocatalysts were suitable for use in dERC. After performing the half-cell tests (cyclic voltammetry and protocol test) over these metal electrocatalysts, each and every individual electrocatalyst has been tested in full cell reactor for the identification and quantification of the products obtained after CO_2 reduction. It has been seen that all the 4 metal electrocatalysts have resulted in the formation of only two products, namely, CH_4 and CO. However, the total Faradaic efficiency at any particular voltage in case of all the metal electrocatalysts was quite low *viz.* 5.20%, 11.37%, 1.70%, and 14.78% for copper, zinc, nickel, and cobalt, respectively. Moreover, the selectivity towards different products was also varied. The copper was selective for hydrocarbon, while the zinc was found to be selective for CO only. Nickel and cobalt were found to alter their selectivity depending on the applied voltage. Thus, it could be concluded that to enhance the performance of these electrocatalysts, there is need of some kind of treatment which can enhance their activity towards CO_2 electroreduction.

It has been devised that if in place of metals, the oxides of metals could be used, then the basic nature of metal oxide can help to attract CO_2 which is a Lewis acid, and it will eventually help to enhance the adsorption over the electrocatalyst surface leading to better reactivity. Based on this idea, the metal oxide of all the metals *viz.* CuO, ZnO, NiO, and Co_3O_4 have been synthesized and characterized. The aqueous precipitation method was used for the synthesis of CuO and ZnO, sol-gel method was chosen for NiO, and Co_3O_4 was synthesized using polymer combustion route. The developed electrocatalysts were characterized using XRD, FTIR, BET, FESEM, and EDX techniques. The characterization results depicted about the various physio-chemical features of the electrocatalysts. Thereafter, the electrocatalysts were tested using the cyclic voltammetry test as well as the protocol tests and it was found that CuO might prove to be an efficient electrocatalyst for CO_2 electroreduction, while ZnO is unstable during the reaction. The Co_3O_4 has shown its ability for CO_2 electroreduction but it was also found to favour H^+ reduction to a great extent. Moreover, NiO could not be tested for dERC as no suitable solvent was found to prepare the catalyst ink of NiO. The full cell studies were conducted

using these electrocatalysts, and product formation was observed in all the cases. CuO was proved to be quite efficient for the CO_2 electroreduction with Faradaic efficiency as high as 66.2% at 2 V. Moreover, the CuO was found to be selective for CH_4 formation, although the formation of CO, and C_2H_4 took place in little amounts. In case of ZnO, as the half-cell studies indicated, it was found to be unstable during the reaction and converted to Zn. Therefore, in this case, the high Faradaic efficiency for CH_4 was found at two potential values *viz.* 1.8 V (16.6%) and 2.3 V (18.8%). However, the formation of CO was also found with Faradaic efficiency of 10.34% (2 V). No other product could be obtained using ZnO electrocatalyst. These two oxides were found to be superior over their pure metals (Cu and Zn). As far as Co_3O_4 is concerned, it could not be proved better than Co as very meager formation of CH_4, CO, and C_2H_6 was found with total Faradaic efficiency of 4.16% (2 V), and most of the supplied energy was wasted in the formation of unwanted H_2. Therefore, further improvement of the efficiency of Co metal was envisaged along with Ni metal treatment as oxide of nickel could not be tested for the CO_2 electroreduction.

The metal complexes have always been proved to be quite active for CO_2 electroreduction reactions. Therefore, a new class of metal complexes, namely, salen ligand complexes was synthesized, in which Cu and Ni metals were incorporated. The ligand as well as metal complexes were characterized using FTIR, NMR, HR-MS, and elemental analysis. The calculated mass of the ligand matched with the mass spectroscopic data, which confirmed that the salen ligand was synthesized successfully. The NMR spectrum further enhanced the clarity about the structure of the salen ligand. The elemental analysis revealed the formula for Ni and Cu complexes as $C_{20}H_{13}N_3O_4Ni$ and $C_{20}H_{13}N_3O_4Cu{\cdot}CH_3CN{\cdot}0.5H_2O$, respectively. These two metal complexes were tested in half-cell using both cyclic voltammetry and protocol test, where it could be confirmed that the metal complexes were able to reduce the CO_2. The full electrochemical reactor studies revealed the appreciable performance of both the metal complexes. Ni complex was able to form CH_4, CO, C_2H_4, and C_2H_6; and Cu complex resulted in the formation of CH_4, CO, and C_2H_4. The total Faradaic

efficiency was found to be 74% (1.5 V) and 25% (1.8 V) for Ni complex and Cu complex, respectively. Second benefit using these metal complexes was found in the reduction of overpotential. A maximum of 0.5 V reduction in overpotential could be achieved using these metal complexes. All these results proved that Ni and Cu complexes are very efficient electrocatalysts for the CO_2 reduction reaction. Based on the results, CO_2 reduction mechanism was also proposed. It has been formulated that the redox behaviour of the salen ligand complexes, *viz.* conversion of Ni(II)/Cu(II) to Ni(I)/Cu(I), was responsible for the reduction in overpotential and for the efficient formation of hydrocarbons and CO. Further, low stability of Ni(I) resulted in the stronger interaction with CO_2 as compared to Cu(I), and hence Ni complex was found to be better performer as compared to Cu complex.

To investigate the role of bimetallic electrocatalyst in the field of direct electrochemical reduction of gaseous CO_2, and to enhance the performance of the cobalt metal; second metal, *viz.* silver, has been introduced. The Co-Ag bimetallic electrocatalyst has been synthesized using borohydride reduction method and characterized using XRD, BET, FESEM, TEM, and EDX techniques. The results made it clear that the synthesized electrocatalyst is a mixture or heterostructure of Co and Ag metals. Half-cell studies confirmed that the synthesized electrocatalyst is able to reduce CO_2; hence, the further reactions were carried out in full cell reactor. Product analysis revealed the striking results as the formation of CH_4, CO, and C_2H_4 took place, although none of the chosen metal was selective for hydrocarbons formation in individual state. This result has been attributed to the metal-metal bond formation, which helped in the electron transfer from Co to Ag. This electron transfer resulted in change in binding strength of the Co-Ag mixture towards the intermediate products of the reaction, and hence, altered the expected formation of products. Further, the Faradaic efficiency was found to be almost double in case of Co-Ag (28.1%) as compared to Co (14.8%). Reduction in operating potential from 2.3 V in case of Co, to 2 V in case of Co-Ag is another remarkable feature. Thus, it can be said that inclusion of second metal to the cobalt proved to be beneficial as it resulted not only in

enhanced Faradaic efficiency and reduction in overpotential, but also in the formation of hydrocarbons, which are more desirable as far as generation of fuel kind of products is concerned.

All these results concluded above states that the thesis has been able to achieve its aim, which was to study the metals and the various treatments applied to them, for improving the efficiency of the direct electrochemical reduction of gaseous CO_2 at low overpotentials along with the formation of fuel kind of products. Although the electrocatalyst stability and deactivation could not be dealt in detail as the emphasis was to explore the technical know-how of the process. However, in almost all the cases, the synthesized electrocatalysts have been found to perform longer than their pure metal counterparts. The work contained in the thesis investigated the performance of various electrocatalysts for the direct electrochemical reduction of gaseous CO_2, which was not reported earlier. Further, thesis compiles the synthesis, physio-chemical properties, and performance of different classes of electrocatalysts, starting from pure metals, to their oxides, complexes, and bimetal. In order to make the selection of useful electrocatalysts from the group of many, in quick and effective manner, a protocol has also been developed and validated in the thesis. Therefore, it is expected that this research would be beneficial for the upcoming researchers to deal with the problem of increasing atmospheric CO_2 concentration and decreasing fossil fuel reserves using dERC.

8.2 Future scope

Further research in this field should be done for improving the overall efficiency, selectivity, and durability of the electrocatalysts. Moreover, in order to understand the dERC further, the investigations can also be made in other related fields too. The prospective areas for the future research can be summarized as follows:

- Deactivation studies for the electrocatalysts in half-cell as well as full cell can be done, and accordingly an effective strategy can be formulated to minimize it.

- To better understand the performance of electrocatalysts at each step of the CO_2 electroreduction, kinetic studies are crucial. Kinetic studies will surely help to focus on the mass transfer limitations of CO_2 at the interface of electrode and electrolyte. Density functional theory (DFT) can also be applied to find the exact mechanism of the reaction, especially in case of bimetallic electrocatalysts.
- The discussed catalytic activity protocol would be helpful to screen the useful electrocatalysts. To further enhance the effectiveness, the studies on the exchange current density and related parameters can be done.
- In this study, the focus has been only over the cathode electrocatalyst. To maximize the performance, investigations can also be made over the anode electrocatalysts.
- To make the process more practical and effective, development of photoelectrodes can also be undertaken.

RESEARCH OUTPUT

Publications in peer reviewed journals

1. **Singh S.**, Phukan B., Mukherjee C., Verma A., "Salen ligand complexes as electrocatalysts for direct electrochemical reduction of gaseous carbon dioxide to value added products", *RSC Advances*, Vol. 5, 2015, pp. 3581 – 3589.
2. **Singh S.**, Mukherjee C., Verma A., "Development of catalytic activity protocol for electrochemical reduction of carbon dioxide to value added products", *Clean Technologies and Environmental Policy*, Vol. 17(2), 2015, pp. 533 – 540.
3. **Singh S.**, Aeshala L.M., Verma A., "Sustainable production of fuel from electrochemical reduction of carbon dioxide", *International Journal of Innovative Research and Development*, Vol. 1(7), 2012, pp. 155 – 160.

Manuscript under preparation

1. **Singh S.**, Verma A. "Bimetallic Co-Ag electrocatalyst for electrochemical conversion of CO_2 to CH_4".

Publications from related work

1. Butti S.K., Velvizhi G., Sulonen M.L.K., Haavisto J.M., Koroglu E.O., Cetinkaya A.Y., **Singh S.**, Arya D., Modestra J.A., Krishna K.V., Verma A., Ozkaya B., Lakaniemi A.M., Puhakka J.A., Venkata Mohan S. "Microbial electrochemical technologies with the perspective of harnessing bioenergy: Maneuvering towards upscaling", *Renewable & Sustainable Energy Reviews*, Vol. 53, 2016, pp. 462 – 476.
2. **Singh S.**, Verma A., Basu S. "Oxygen reduction non-PGM electrocatalysts for PEM fuel cells – Recent Advances", *Chapter 16* in "Electrochemical Energy: Advanced Materials and

Technologies" edited by Shen P.K., Wang C.Y., Jiang S.P., Sun X., Zhang J., *Taylor & Francis*, CRC Press, ISBN 9781482227277, 2015, pp. 385 – 403.

Papers and posters in conferences/seminars

1. **Singh S.**[*], Verma A., "National Conference on Challenges in Environmental Research (NCOCER)", organized by Centre for the Environment, IIT Guwahati, Assam during Jun. 4-6, 2015.
2. Malik K. [*], Gautam R.K., **Singh S.**, Verma A., "XI Open House 2015", organized by IIT Delhi, New Delhi on Apr. 18, 2015.
3. **Singh S.**[*], Verma A., "National Conference on Sustainable Development of Environmental Systems (NCOSDOES)", organized by Centre for the Environment, IIT Guwahati, Assam during Jun. 20-21, 2014.
4. Yadav V.S.K. [*], **Singh S.**, Verma A., "Reflux 2.0 – Annual Chemical Engineering Symposium", organized by Department of Chemical Engineering, IIT Guwahati, Assam during Mar. 29-30, 2014.
5. **Singh S.** [*], Mukherjee C., Verma A., "International Conference on Harnessing Natural Resources for Sustainable Development: Global Trends", organized by Cotton College, Guwahati, Assam during Jan. 29-31, 2014.
6. **Singh S.** [*], Mukherjee C., Verma A., "4th International Conference on Advances in Energy Research (ICAER)" organized by Department of Energy Science & Engineering, IIT Bombay, Mumbai during Dec. 10-12, 2013.
7. **Singh S.** [*], Aeshala L.M., Verma A., "International Seminar and Workshop on Energy, Sustainability and Development (ISWESD)" organized by Sibsagar College, Joysagar, Assam during Oct. 12-14, 2012.

8. **Singh S.** *, Verma A., "One Day Symposium on Environment and Us" organized by Centre for the Environment, IIT Guwahati, Assam on Jun. 5, 2012.

Awards

1. **1st Prize** for presenting the paper entitled, "Study on electrocatalysts for electrochemical reduction of CO_2 to value added products" on the occasion of "Research Scholars Day - 2015" organized by Centre for the Environment, IIT Guwahati, Assam on Jan. 19, 2015.
2. **Best Paper Award** (2nd Runner-up) from **Springer** for presenting the paper entitled, "Development of catalytic activity protocol for electrochemical reduction of carbon dioxide" at 4th International Conference on Advances in Energy Research (ICAER)" organized by Department of Energy Science & Engineering, IIT Bombay, Mumbai during Dec. 10-12, 2013.
3. **Best Poster Award** in "One day Symposium on Environment and Us" organized by Centre for the Environment, IIT Guwahati, Assam on Jun. 5, 2012.

BIOGRAPHY

Surya Singh was born and brought up in Raebareli, Uttar Pradesh, India. She completed her secondary (2001) and senior secondary (2003) education from Government Girls Inter College, Raebareli. She completed her graduation (B.Sc.) from University of Allahabad in 2006 with the subjects Botany & Zoology. She was the 6th rank holder among all the successful candidates. She obtained Master's degree (M.Sc.) in Environmental Sciences from University of Allahabad in 2009. She was ranked 1st among all the successful candidates in M.Sc. She also obtained Master's degree (M.Tech.) in Environmental Science & Engineering from Birla Institute of Technology, Mesra, Ranchi in 2011 where she was ranked 1st among all the successful candidates.

She qualified UGC-NET (Environmental Sciences) in 2010 and CSIR-NET (Earth, Atmospheric, Ocean, and Planetary Sciences) in 2011. She has also been selected for the INSPIRE fellowship sponsored by Department of Science & Technology (DST), New Delhi. She joined Centre for the Environment, IIT Guwahati as a Doctoral student in July 2011 under the joint supervision of Dr. Anil Verma and Dr. Chandan Mukherjee. Her Ph.D. work is focussed over the investigations on electrocatalysts for the process of electrochemical conversion of gaseous CO_2 to fuel kind of products. She has published research papers in peer reviewed high impact factor international journals. She has also published a book chapter and presented several scientific and technical research papers in various international and national conferences. She was felicitated by Springer with the best paper award (2nd runner-up) in 2013, and she has also won the best presentation awards in 2012 and 2015. Moreover, she is working as 'Programme Officer' in ENVIS Centre of the Central Pollution Control Board (CPCB), Delhi under the Ministry of Environment, Forests, and Climate Change (MoEF&CC) since October 2015.